U.PORTO
FACULDADE DE CIÊNCIAS
UNIVERSIDADE DO PORTO

Ciências ULisboa
Faculdade de Ciências da Universidade de Lisboa

PhD

3rd CYCLE

FCUP
FCUL
2026

U.PORTO

A comprehensive approach to integrated phenotypic evolution: deciphering the diversification of a transcontinental lizard radiation

Pablo Vicent-Castelló

FC

U.PORTO
FACULDADE DE CIÊNCIAS
UNIVERSIDADE DO PORTO

Ciências ULisboa
Faculdade de Ciências da Universidade de Lisboa

A comprehensive approach to integrated phenotypic evolution: deciphering the diversification of a transcontinental lizard radiation

Pablo Vicent-Castelló

Doctoral Programme in Biodiversity, Genetics and Evolution

Faculty of Sciences of the University of Porto and Faculty of Sciences of the University of Lisbon

2026

PhD

A comprehensive approach to integrated phenotypic evolution: deciphering the diversification of a transcontinental lizard radiation

Pablo Vicent - Castelló

Thesis carried out as part of the Doctoral Programme in Biodiversity, Genetics and Evolution

Faculty of Sciences of the University of Porto, Department of Biology

2026

Supervisor
Antigoni Kaliontzopoulou, Associate Professor,
BEECA, IRBio, Facultat de Biologia, Universitat de Barcelona

Co-supervisors
D. James Harris, Researcher, CIBIO-InBIO, BIOPOLIS

Anthony Herrel, Researcher, C.N.R. S/M.N.H.N, Ghent University, University of Antwerp, Naturhistorisches Museum Bern

All the corrections determined by the jury, and only those, were made.

The Supervisor,

Porto, _____/_____/_____

Note: This page should only be included **in the final version after defence and only if the jury approves the thesis with a recommendation for the student to correct errors, inaccuracies or formal inaccuracies** identified and expressly mentioned during the tests. **This page must be deleted from the version to be submitted as part of the thesis submission prior to the defence.**

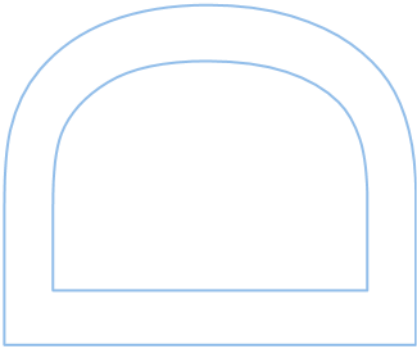

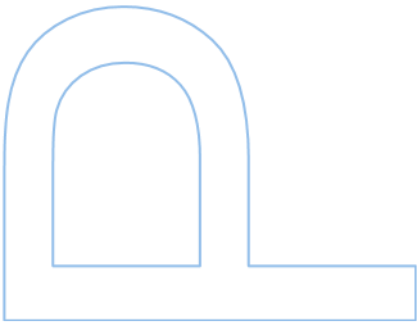

Declaration of Honor

I, Pablo Vicent Castelló, of Spanish nationality, born in Valencia, residing in Barcelona, holder of Identification Document (DNI) nº 23825468K, enrolled in the Doctoral Programme in Biodiversity, Genetics and Evolution at the Faculty of Sciences of the University of Porto, declare, in accordance with the provisions of point a) of article 14 of the Academic Code of Ethical Conduct of U.Porto, that the content of this thesis reflects my perspectives, research work, and interpretations at the time of its submission.

Upon submitting this thesis, I also declare that it is the result of my own research work and includes contributions that have not been previously used in other works submitted to this or any other institution.

Furthermore, I declare that all references to other authors strictly comply with attribution rules, being properly cited within the text and listed in the references section. This thesis does not disclose any content whose reproduction is restricted by copyright.

I am aware that the practice of plagiarism and self-plagiarism constitutes an academic offence.

Foreword

Two scientific articles were published, and one is in press, in peer-reviewed international journals as a result of the work developed within the scope of this thesis. These articles are listed below, in which the candidate appears as the first author in collaboration with other authors, having actively participated in their conception, data collection and analysis, discussion of results, and preparation of the published versions.

Vicent-Castelló, P., Herrel, A., Harris, D. J., & Kaliontzopoulou, A. 2025. Walking or hanging: the role of habitat use for body shape evolution in lacertid lizards. J. Evol. Biol., 38(3): 353–366. https://doi.org/10.1093/jeb/voaf003

Vicent-Castelló, P., Enriquez-Urzelai, U., Martínez-Freíria, F., Garcia-Porta, J., & Kaliontzopoulou, A. 2025. Context-dependent body size evolution in lacertid lizards: differential role of structural habitat and climate across radiations. Evolution, 79(10): 2023–2034. https://doi.org/10.1093/evolut/qpaf130

Vicent-Castelló, P., Adams, D., Sicilia-Cebrián, C-A., Herrel, A., & Kaliontzopoulou, A. 2026. Variable yet ubiquitous: Hierarchical scaling of head functional morphology in lizards. Evolution, *in press*

This thesis was developed with BIOPOLIS-CIBIO, Research Centre in Biodiversity and Genetic Resources, Vairão, Portugal, as the main host institution, and the Department of Evolutionary Biology, Ecology and Environmental Sciences (BEECA), Institute for Biodiversity Research (IRBio), University of Barcelona, Barcelona, Spain, as the secondary institution. The Faculty of Sciences of the University of Porto was the degree-awarding institution. The work was supervised by Dr. Antigoni Kaliontzopoulou, and co-supervised by Dr. James Harris and Dr. Anthony Herrel.

This work was supported by the Fundação para a Ciência e a Tecnologia (FCT) through the award of the doctoral scholarship SFRH/BD/07368/2021, it was also supported by the SYNTHESYS + Project https://www.synthesys.info/ that is financed by European Community Research Infrastructure Action under the H2020 Integrating Activities Programme, Project number 823827, Project acronym GB-TAF-TA4-030. A.K. is supported by a Ramón y Cajal research grant cofounded by the Spanish State Research Agency and the European Social Fund (RYC2019-026688-I/AEI/10.13039/501100011033) and by Research Group of Generalitat de Catalunya

“GRC Zoological Systematics and Evolution,” ZooSysEvo (2021-SGR-00689). J.G.P. is supported by the program “Atracción de talento investigador a la Comunidad de Madrid en centros de I+D, modalidad 1” (2022-T1/AMB-24171).

Acknowledgements

I would like to express my deepest gratitude to Antigoni for her guidance, patience, and humanity throughout the supervision of this thesis. She has shown me that it is possible to supervise with presence, respect, and a genuine commitment to teaching and helping students grow exponentially. She has stood by my side during every stage of this journey, allowing me the space to make mistakes when necessary and to learn from them. Her mentorship has not only shaped this thesis but has also made these four years a period of time that I will truly miss.

I am also sincerely grateful to my co-supervisors, James Harris and Anthony Herrel, for their continuous support, encouragement, and critical insights. Their perspectives greatly enriched this research and helped me refine my ideas. Science is a collective journey, and I am deeply grateful to my collaborators, Joan García-Porta, Fernando Martinez-Freiria and Dean Adams, whose support, ideas, and teamwork made this work possible.

I am deeply grateful to the fieldwork team in Morocco: Helen, Antigoni, Fernando, Ana, Frederico, Ionna and Ale for their enthusiasm and tireless efforts. Working together in the field was not only fundamental to this project but also an unforgettable experience. I will always carry those days — the challenges, the shared efforts, and the moments of laughter — close to my heart.

To my coworkers during these years — Valeria, Claudia, and Helen — thank you for always being there, not only sharing the work but also congresses, trips and life experiences along the way, also to the entire Phenevol group for listen my endless congress presentations. Special mention to Helen: sharing both a home and an office with you made this journey truly unique. This project would have been far less special (and probably much more boring) without you. Thank you for being by my side for three years, basically 24/7.

To the people who saw me begin this project in Porto — the OG *estrellas* — thank you for being there from the very start. Pedro, Javi, Sara, Xabi, Gabri, Prem, Inês, Diogo, Clarinha, Alessia, Kate and all the *estrellas* who laughed, worked, celebrated, and grew alongside me during one of the most special years of my life — that period of time will always mean so much to me because of you.

Finally, to my family — thank you for always giving me the opportunity to grow, to study, and to pursue whatever I wanted in life. Thank you for supporting me unconditionally and for holding me up whenever I could not do it on my own. And last but not least, to the love of my life, Valeria, thank you for your endless support during these years, which at times became very, very tough. You have shown me that I can always count on you, no matter what.

Resumo

Compreender a evolução de fenótipos complexos requer a integração entre morfologia, desempenho e ecologia em múltiplas escalas biológicas. No âmbito do paradigma ecomorfológico, espera-se que os caracteres fenotípicos respondam a constrangimentos ecológicos através dos seus efeitos no desempenho funcional; contudo, estas relações podem variar consoante a escala filogenética e organizacional considerada. Nesta tese, investigo a forma como o tamanho corporal, a forma do corpo e o desempenho evoluem em resposta ao uso do habitat estrutural e ao clima, bem como a forma como as relações forma–função se estruturam desde o nível individual até ao nível de espécie numa grande radiação de répteis. Utilizando os lagartos da família Lacertidae como sistema modelo, combino dados extensivos de morfologia, desempenho, ecologia e filogenia num enquadramento comparativo. Em primeiro lugar, analiso a evolução do tamanho corporal à escala da família, demonstrando que o habitat estrutural e as variáveis climáticas influenciam as trajectórias e taxas evolutivas de forma fortemente dependente do contexto, variando entre grupos filogenéticos e escalas de análise. Em segundo lugar, avalio o efeito do uso do eixo vertical versus horizontal do habitat na evolução da forma corporal, revelando respostas específicas por caracter, com padrões claros na morfologia da cabeça e respostas mais complexas nos caracteres locomotores. Por fim, examino a relação entre a forma da cabeça e a força de mordida em diferentes níveis biológicos, mostrando que as associações forma–função persistem entre escalas, mas seguem trajectórias evolutivas distintas, consistentes com um cenário de mapeamento many-to-one entre morfologia e desempenho. No conjunto, estes resultados demonstram que a integração fenotípica pode coexistir com desacoplamento evolutivo e que os efeitos ecológicos na evolução fenotípica são dependentes da escala de análise.

Abstract

Understanding how complex phenotypes evolve requires integrating morphology, performance, and ecology across multiple biological scales. Within the ecomorphological paradigm, phenotypic traits are expected to respond to ecological constraints through their effects on functional performance; however, these relationships may vary across phylogenetic and organizational levels. In this thesis, I investigate how body size, body shape, and performance evolve in response to structural habitat use and climate, and how form–function relationships scale from individuals to species across a major reptile radiation. Using lacertid lizards as a model system, I combine extensive morphological, performance, ecological, and phylogenetic data within a comparative framework. First, I examine body size evolution across the family, showing that structural habitat and climatic variables influence evolutionary rates and trajectories in a strongly context-dependent manner, with patterns differing among phylogenetic groups and across scales. Second, I assess how vertical versus horizontal habitat use shapes body form, revealing trait-specific responses: head morphology shows clear habitat-associated evolutionary trends, whereas locomotor traits exhibit more complex and weakly constrained patterns. Finally, I analyze the relationship between head shape and bite force across hierarchical biological levels, demonstrating that form–function associations persist from individuals to the family level but follow different evolutionary directions, consistent with many-to-one mapping between morphology and performance. Together, these results highlight that phenotypic integration can coexist with evolutionary decoupling, and that ecological effects on phenotypic evolution are scale-dependent. This thesis emphasizes the importance of multilevel approaches for understanding how complex phenotypes diversify under interacting ecological constraints.

Table of Contents

List of Tables

List of Figures

List of Abbreviations

FCUP	FACULTY OF SCIENCES OF THE UNIVERSITY OF PORTO
UP	UNIVERSITY OF PORTO
BEECA	DEPARTMENT OF EVOLUTIONARY BIOLOGY, ECOLOGY AND ENVIRONMENTAL SCIENCES
IRBIO	INSTITUTE FOR BIODIVERSITY RESEARCH
FCT	FUNDAÇÃO PARA A CIÊNCIA E A TECNOLOGIA
ZOOSYSEVO	ZOOLOGICAL SYSTEMATICS AND EVOLUTION
GD	GROUND-DWELLING
CL	CLIMBERS
IUCN	INTERNATIONAL UNION FOR CONSERVATION OF NATURE
GBIF	GLOBAL BIODIVERSITY INFORMATION FACILITY
SVL	SNOUT-VENT LENGTH
BAMM	BAYESIAN ANALYSIS OF MACROEVOLUTIONARY MIXTURES
ARD	ALL-RATES-DIFFERENT

Chapter 1:

General introduction

1.1. Ecomorphological paradigm

Ecomorphology, or ecological morphology, refers to the study of an organism's physical shape (morphology) in relation to its ecological roles within the environment (Klaauw, 1948; Schwenk, 2000). This conceptual foundation underlies the ecomorphological paradigm established by Arnold (1983), where performance is proposed as a link between morphology and ecology, to explain how morphological traits that enhance functional performance ultimately enhance fitness and promote survival in specific environments (Arnold, 1983). The paradigm proposes that species adapt to their environments through morphological modifications that improve performance in ecologically relevant tasks) (Huey & Stevenson, 1979)—such as locomotion, bite force, escape behavior, foraging, etc. Enhanced performance, in turn, increases fitness by improving survival and reproductive success (Figure 1.1). This feedback reinforces the morphological and performance traits that confer advantages, establishing a causal framework that interconnects all elements of the paradigm (Irschick et al. 2008; Kingsolver & Huey, 2003). In recent years, additional components have been integrated into the traditional definition to account for other biological aspects that influence the morphology–performance relationship, as Kingsolver and Huey, 2003 suggested in their revision of the ecomorphological paradigm. These include physiology, behavior, life-history traits, and the trade-offs among them (Lailvaux & Husak, 2014). As a result, whole-organism performance is understood as part of an integrated group of phenotypic traits that can be predicted to evolve together. Although the ecomorphological paradigm was originally formulated to explain individual fitness within populations and focused to aid intraspecific studies, it has proven highly valuable for macroevolutionary research, as it not only explains how traits relate to ecological function at the organismal level but it also provides a framework for interpreting large-scale evolutionary patterns (Baken & Adams, 2019). By linking morphology and performance to ecological demands, this approach helps clarify how adaptive radiation unfolds, why unrelated lineages may converge on similar morphologies in response to shared ecological pressures (Edwards, 2011; Edwards et al. 2012) or how niche partitioning allows closely related species to coexist (Elstrott & Irschick, 2004), among other evolutionary questions. These macroevolutionary implications have made ecomorphology a central tool for connecting microevolutionary processes observed within populations to the diversification of clades across ecological space over different timescales (Taverne et al. 2021).

Thus, determining whether morphological differences translate into performance differences among organisms in different environments is essential for unravelling the complex interactions among phenotypic traits contributing to fitness. This understanding ultimately increases our knowledge of the mechanisms driving integrated phenotypic evolution (Irschick & Garland, 2001; Miles, 2014; Vanhooydonck & Van Damme, 2001).

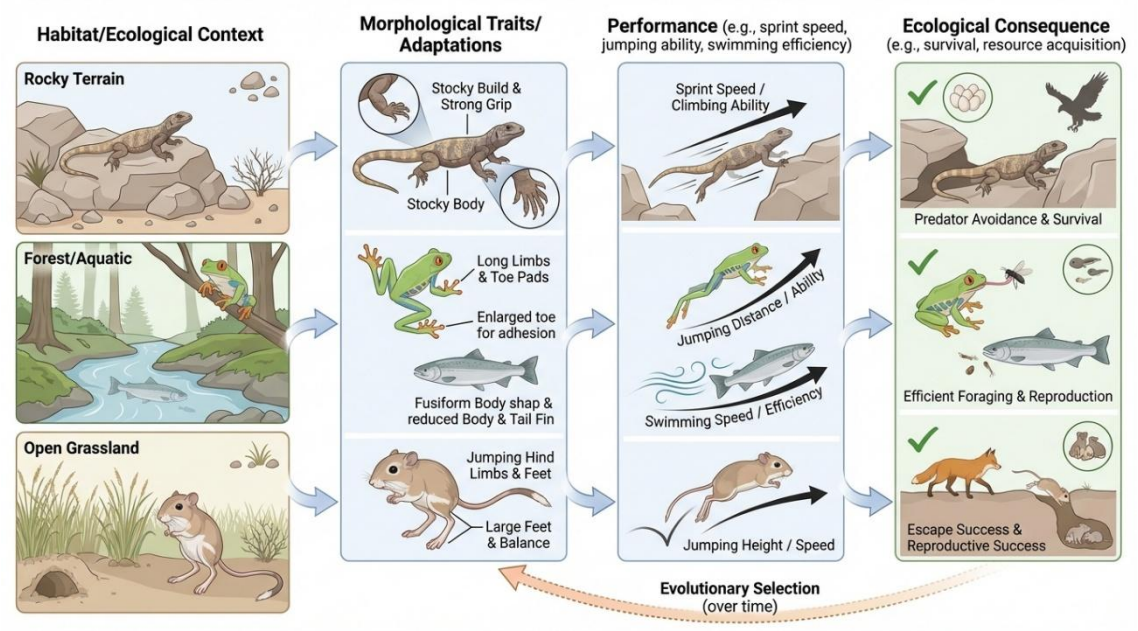

Figure 1.1. Graphical representation of the ecomorphological paradigm, modified from Arnold (1983), illustrating the causal pathway linking habitat or ecological context to morphological traits and adaptations, which in turn influence performance capacities (e.g., sprint speed, climbing ability, swimming efficiency). These performance outcomes affect ecological consequences such as survival, predator avoidance, foraging efficiency, and reproductive success. Natural selection acts on these ecological consequences over time, feeding back to shape morphology through evolutionary processes.

1.2. Morphological evolution as a response to ecology in reptiles

Morphological evolution in reptiles is strongly shaped by ecological factors, since both body size and body shape play critical roles in survival and reproduction, and are therefore expected to be subject to natural selection (Goodman et al. 2008; Goodman & Isaac, 2008; Vitt et al. 1997). Size and shape influence a range of biological activities, including locomotion (Irschick & Garland, 2001; Vanhooydonck & Van Damme, 2001),

thermoregulation (Kingsolver & Huey, 2008), feeding efficiency (Verwaijen et al. 2002), predator avoidance (Goodman, 2009; Vanhooydonck & Van Damme, 2003), and reproductive success (Lappin & Husak, 2005). In addition, size also affects how shape changes in the context of the allometric growth (Klingenberg, 2016; Tejero-Cicuéndez et al. 2023). Since morphology is known to be the one of the intermediate elements between the environment and the organisms, variation if these traits is often tightly linked to ecological preferences among species and populations (Goodman et al. 2008).

A key ecological driver of morphological diversification is structural habitat (Goodman et al. 2008; Vicent-Castelló, Herrel, et al. 2025). Reptiles that exploit different habitat types often evolve distinct morphologies that enhance performance in ecologically relevant tasks. For example, *Anolis* lizards have repeatedly evolved ecomorphs in the Caribbean that differ in limb length, body size, shape morphology, among others, depending on whether they live on tree trunks, grass, twigs, or ground surfaces (Elstrott & Irschick, 2004; Losos, 1992; Losos & Mahler, 2010). Arboreal and climbing species often possess elongated limbs, slender and dorsoventrally depressed bodies, as well as flattened heads, to maintain the gravity center close to the surface and to be able to use crevices to escape from predators (Goodman et al. 2008). In contrast, ground-dwelling lizards often evolve more robust bodies and relatively shorter limbs, which are advantageous for sprinting across open ground and for rapid predator escape (Collar et al. 2010, 2011; Vanhooydonck & Van Damme, 2001). According to this, it is evident that size and shape respond jointly, or at different levels, to adaptation to specific structural habitats (Arnold, 1983).

On the other hand, climatic conditions also exert a strong influence on reptile morphology. Temperature, humidity, seasonality and resource availability impose physiological and energetic constraints that affect both body size and shape (Angilletta & Dunham, 2003; Atkinson, 1994; Bergmann, 1847; Blackburn et al. 1999; Gouveia & Correia, 2016; Kingsolver & Huey, 2008). A widely recognized pattern is the heat conservation hypothesis (Bergman's rule for endotherms), which predicts larger body sizes in cooler environments due to the thermal inertia provided by a low surface area–to–volume ratio (Bergmann, 1847). This trend has been reported in some reptile groups, including *Liolaemus* lizards (Pincheira-Donoso et al. 2008) and turtles (Ashton & Feldman, 2003). Conversely, smaller, more gracile morphologies may be advantageous

in hot or arid regions, where efficient heat dissipation and water conservation are critical, as it is the example of lizards from the tribe Eremiadini of the Lacertidae family (Vicent-Castelló, Enriquez-Urzelai, et al. 2025).

Together, ecological variables such as structural habitat and climatic conditions play a central role in shaping the evolutionary trajectories of reptile morphology. By mediating the relationship between morphology, performance, and fitness, these factors promote adaptation to diverse ecological niches and contribute to the remarkable morphological diversity observed across reptile lineages.

1.3. Evolution of functional morphology in reptiles

Performance can be defined as a relevant task that organisms carry out in order to obtain resources, survive, and reproduce (Irschick et al. 2008; Le Galliard et al. 2004). Its evolutionary importance lies in the fact that performance represents the intermediate link between morphology and the environment, shaping how organisms interact with their surroundings (Anderson et al. 2008). Moreover, performance is likely the actual target of selection, being the morphological output adjusted to improvements in performance traits, which in turn enhance fitness (Arnold, 1983). In this sense, performance provides a mechanistic framework for understanding how variation in shape translates into ecological outcomes, and ultimately, into evolutionary trajectories.

In reptiles (and other groups such as mammals and birds), one of the most relevant performance traits is bite force (Deeming, 2022; Herrel et al. 1999, 2001, 2002). Bite force plays a central role in feeding, territory defence, male–male combat, mating success, prey handling, and foraging. Because of this wide functional relevance, bite force can influence both survival and reproductive success, positioning it at the intersection of ecological and sexual selection pressures. Such constraints may also generate trade-offs among performance traits—for example, between burrowing ability and prey handling (Le Guilloux et al. 2020) or song production and feeding in Darwin's finches (Herrel et al. 2009) where improving one function could come at the expense of the other.

Bite force is strongly correlated with body size, a relationship repeatedly demonstrated across biological levels, both within and among species (Isip et al. 2022). However, when

controlling for size and the allometric scaling of bite force, biting performance also shows direct associations with other morphological features, such as head width, head height, and muscle architecture (Anderson et al. 2008; Cruz et al. 2021; De Meyer et al. 2019; Deeming, 2022; Herrel et al. 2008; Verwaijen et al. 2002). This indicates that head morphology provides the structural framework within which performance evolves, with musculature and skeletal dimensions jointly determining the magnitude of bite force. This suggests that, although the relationship between form and function in this system is not entirely straightforward (Cruz et al. 2021), there is usually a morphological component that explains variation in bite force. Importantly, the production of bite force relies on a combination of interacting elements, which not only contribute to this function but are also embedded in a broader network of traits simultaneously exposed to diverse selective pressures. Such functional networks imply that changes in one trait (e.g., jaw muscle size) can affect other elements through the head system, affecting performance and potentially generating correlated evolutionary responses in other traits.

1.4. Phylogenetic Comparative Methods for studying macroevolution

Because morphological traits and functional performance often covary across species due to ecological pressures, direct comparisons can be misleading—closely related species tend to resemble each other simply because of shared ancestry (Cornwell & Nakagawa, 2017; Felsenstein, 1985; Martins & Garland, 1991). Phylogenetic comparative methods (PCMs) were developed to account for this statistical non-independence and allow more accurate evolutionary inferences (Felsenstein, 1985). Since then, PMCs have been extremely expanded to address different evolutionary patterns and processes, which include the study of evolutionary rates and drivers, the tempo and mode of evolution of specific characters, coevolutionary patterns and models of speciation and extinction (Kaliontzopoulou & Adams, 2016). In those methods the covariance matrix, which nests the relationship between species from phylogeny, is used to correct the analyses and obtain the results accepting the non-independence assumption (Kaliontzopoulou & Adams, 2016).

These methods have become essential for understanding the evolution of complex traits such as morphology and performance, as they allow researchers to disentangle the

effects of shared ancestry from adaptive responses to ecological pressures. In ecomorphological and allometric studies, PCMs provide a powerful framework to test whether trait variation among species reflects adaptive evolution, phylogenetic inertia, or a combination of both. For example, methods such as phylogenetic generalize least squares (PGLS) and phylogenetic regressions (Grafen, 1989; Martins & Garland, 1991), have been developed to test evolutionary hypothesis and investigate how the phenotypes diversify over time (Rohlf, 2001). Moreover, approaches such as model fitting are incredible useful to study the tempo and mode of evolution of phenotypic traits (Kaliontzopoulou & Adams, 2016), understanding if those traits are following a diversifying selection and adaptation, or on the other hand are dependent on the cladogenesis. These methods can also help identify cases of convergent or divergent evolution in specific lineages (Losos, 2011; Stayton, 2006).

By integrating information on species relationships, ecological variables, and phenotypic data, these methods enable the identification of evolutionary correlations, the estimation of ancestral states, and the comparison of evolutionary rates across lineages or environments. Consequently, PCMs are powerful tools for investigating macroevolutionary patterns and for testing how functional traits vary in relation to ecological and selective gradients across species.

1.5. The Lacertidae family as a model system

Lacertid lizards constitute a highly diverse and widely distributed Old-World family, that comprises over 360 species distributed through Europe, Asia and Africa (Uetz, 2023). They are the predominant lizard family in Europe and they have been extensively studied in terms of several biological and evolutionary aspects, making them a perfect model to approach macroevolutionary questions. The most recent and complete phylogeny for the family employed both genomic and genetic data, solving the relationships between big lacertid groups (Garcia-Porta et al. 2019). Possessing a well-resolved phylogeny represents the first and most essential step for performing robust comparative phylogenetic analyses and for addressing complex evolutionary questions.

This family is divided into two major subfamilies: Gallotinae and Lacertinae. Gallotinae is a relatively small, insular clade primarily restricted to the Canary Islands and parts of

Iberia and North Africa (Cox et al. 2010), whereas Lacertinae represents the majority of the diversity within the family. Lacertinae is further divided into two monophyletic tribes: Lacertini and Eremiadini. The Lacertini tribe (140 species) radiated across mesic (moderately humid) Eurasian habitats, adapting to a variety of forested, rocky, and scrubby environments, while Eremiadini (211 species) is primarily composed of species that dominate arid regions of Africa and the Middle East, with adaptations suited to survival in hot, dry climates (Arnold et al. 2007). Their ability to occupy and adapt to such varied environments makes them a perfect model to study how the adaptational process to specific structural habitat and climatic conditions has shaped their morphology, behaviour and physiological characteristics.

Despite their success in the occupation in such amount of different habitats, lacertid lizards generally maintain a relatively conserved body plan (Arnold, 1998; Vanhooydonck & Van Damme, 1999). However, several ecomorphological adaptations at macro and microscale have been previously shown across lacertid lizards, such as adaptations to structural habitat both in morphology and performance. For example, some lacertid species differed in sprint speed and climbing ability, but these differences do not translate into morphological differences at limb level (Van Damme et al. 1998; Van Damme & Vanhooydonck, 2002; Vanhooydonck et al. 2002; Vanhooydonck & Van Damme, 2001). On the other hand, bite force and head shape was also investigated in *Podarcis* lizards, showing differences between sexes but no direct relationship between head shape, performance and habitat occupation (Kaliontzopoulou et al. 2015; Taverne et al. 2020). However, a direct relationship between head shape and habitat occupation was demonstrated for lacertid lizards (Arnold, 1998; Gomes et al. 2016; Kaliontzopoulou, 2012; Kaliontzopoulou et al. 2010; Urošević et al. 2013) All this hints at the complex relationship between phenotypic traits across this family. For that reason, a deeper understanding of how phenotypic traits evolve altogether is essential.

References

Anderson, R. A., L. D. McBrayer, and A. Herrel. 2008. Bite force in vertebrates: opportunities and caveats for use of a nonpareil whole-animal performance measure. Biol. J. Linn. Soc. 93:709–720.

Angilletta, M. J., and A. E. Dunham. 2003. The temperature-size rule in ectotherms: simple evolutionary explanations may not be general. Am. Nat. 162:332–342.

Arnold, E. N. 1998. Structural niche, limb morphology and locomotion in lacertid lizards (Squamata, Lacertidae); a preliminary survey. Bull. Nat. Hist. Mus., Zool 64:63–90.

Arnold, S. 1983. Morphology, Performance and Fitness. Am. Zool. 23:347–361.

Ashton, K. G., and C. R. Feldman. 2003. Bergmann's rule in nonavian reptiles: turtles follow it, lizards and snakes reverse it. Evolution 57:1151–1163.

Atkinson, D. 1994. Temperature and Organism Size—A Biological Law for Ectotherms? Pp. 1–58 in. Elsevier.

Baken, E. K., and D. C. Adams. 2019. Macroevolution of arboreality in salamanders. Ecol. Evol. 9:7005–7016.

Bergmann, K. G. 1847. On the relations of the heat economy of animals to their size. Göttinger Studien 3:595–708.

Blackburn, T. M., K. J. Gaston, and N. Loder. 1999. Geographic gradients in body size: a clarification of Bergmann's rule. Divers. Distrib. 5:165–174.

Collar, D. C., J. A. Schulte II, and J. B. Losos. 2011. Evolution of extreme body size disparity in monitor lizards (*Varanus*). Evolution 65:2664–2680. Blackwell Publishing Inc Malden, USA.

Collar, D. C., J. A. Schulte, B. C. O'Meara, and J. B. Losos. 2010. Habitat use affects morphological diversification in dragon lizards. J. Evol. Biol. 23:1033–1049.

Cornwell, W., and S. Nakagawa. 2017. Phylogenetic comparative methods. Current Biology 27:R333–R336.

Cox, S. C., S. Carranza, and R. P. Brown. 2010. Divergence times and colonization of the Canary Islands by *Gallotia* lizards. Mol. Phylogenet. Evol. 56:747–757.

Cruz, F. B., D. L. Moreno Azocar, B. Vanhooydonck, J. A. Schulte, C. S. Abdala, and A. Herrel. 2021. Drivers and patterns of bite force evolution in liolaemid lizards. Biol. J. Linn. Soc.134:126–140.

De Meyer, J., D. J. Irschick, B. Vanhooydonck, J. B. Losos, D. Adriaens, and A. Herrel. 2019. The role of bite force in the evolution of head shape and head shape dimorphism in *Anolis* lizards. Funct. Ecol. 33:2191–2202.

Deeming, D. C. 2022. Inter-relationships among body mass, body dimensions, jaw musculature and bite force in reptiles. J. Zool. 318:23–33.

Edwards, S. 2011. Convergence in Morphology is Preceded by Convergence in Performance in Lizards. P. in Lizards: Thermal ecology, genetic diversity and functional role in ecosystems. Nova Science Publishers.

Edwards, S., B. Vanhooydonck, A. Herrel, G. J. Measey, and K. A. Tolley. 2012. Convergent Evolution Associated with Habitat Decouples Phenotype from Phylogeny in a Clade of Lizards. PLOS ONE 7:e51636. Public Library of Science.

Elstrott, J., and D. J. Irschick. 2004. Evolutionary correlations among morphology, habitat use and clinging performance in Caribbean *Anolis* lizards: COMPARATIVE CLINGING. Biol. J. Linn. Soc.83:389–398.

Felsenstein, J. 1985. Phylogenies and the Comparative Method. Am. Nat. 125:1–15. [The University of Chicago Press, The American Society of Naturalists].

Garcia-Porta, J., I. Irisarri, M. Kirchner, A. Rodríguez, S. Kirchhof, J. L. Brown, A. MacLeod, A. P. Turner, F. Ahmadzadeh, G. Albaladejo, J. Crnobrnja-Isailovic, I. De La Riva, A. Fawzi, P. Galán, B. Göçmen, D. J. Harris, O. Jiménez-Robles, U. Joger, O. Jovanović Glavaš, M. Karış, G. Koziel, S. Künzel, M. Lyra, D. Miles, M. Nogales, M. A. Oğuz, P. Pafilis, L. Rancilhac, N. Rodríguez, B. Rodríguez Concepción, E. Sanchez, D. Salvi, T. Slimani, A. S'khifa, A. T. Qashqaei, A. Žagar, A. Lemmon, E. Moriarty Lemmon, M. A. Carretero, S. Carranza, H. Philippe, B. Sinervo, J. Müller, M. Vences, and K. C. Wollenberg Valero. 2019. Environmental temperatures shape thermal physiology as well as diversification and genome-wide substitution rates in lizards. Nat. Commun. 10:4077.

Gomes, V., M. A. Carretero, and A. Kaliontzopoulou. 2016. The relevance of morphology for habitat use and locomotion in two species of wall lizards. Acta Oecologica 70:87–95.

Goodman, B. A. 2009. Nowhere to run: the role of habitat openness and refuge use in defining patterns of morphological and performance evolution in tropical lizards. J. Evol. Biol. 22:1535–1544.

Goodman, B. A., and J. L. Isaac. 2008. Convergent body flattening in a clade of tropical rock-using lizards (Scincidae: Lygosominae). Biol. J. Linn. Soc.94:399–411.

Goodman, B. A., D. B. Miles, and L. Schwarzkopf. 2008. Life on the rocks: habitat use drives morphological and performance evolution in lizards. Ecology 89:3462–3471.

Gouveia, S. F., and I. Correia. 2016. Geographical clines of body size in terrestrial amphibians: water conservation hypothesis revisited. J. Biogeogr. 43:2075–2084.

Grafen, A. 1989. The Phylogenetic Regression. Philosophical Transactions of the Royal Society of London. Series B, Biological Sciences 326:119–157. Royal Society.

Herrel, A., E. De Grauw, and J. A. Lemos-Espinal. 2001. Head shape and bite performance in xenosaurid lizards. J. Exp. Biol.290:101–107.

Herrel, A., A. De Smet, L. F. Aguirre, and P. Aerts. 2008. Morphological and mechanical determinants of bite force in bats: do muscles matter? J. Exp. Biol. 211:86–91.

Herrel, A., J. C. O'Reilly, and A. M. Richmond. 2002. Evolution of bite performance in turtles. 15:1083–1094.

Herrel, A., J. Podos, B. Vanhooydonck, and A. P. Hendry. 2009. Force–velocity trade-off in Darwin's finch jaw function: a biomechanical basis for ecological speciation? Funct. Ecol.23:119–125.

Herrel, A., L. Spithoven, R. Van Damme, and F. DE Vree. 1999. Sexual dimorphism of head size in *Gallotia galloti*: testing the niche divergence hypothesis by functional analyses. Funct. Ecol. 13:289–297.

Huey, R., and R. D. Stevenson. 1979. Integrating Thermal Physiology and Ecology of Ectotherms: A Discussion of Approaches. Am. Zool. 19:357–366.

Irschick, D., and T. Garland. 2001. Integrating Function and Ecology in Studies of Adaptation: Investigations of Locomotor Capacity as a Model System. Annu. Rev. Ecol. Syst. 32:367–396. Annual Reviews.

Irschick, D., J. Meyers, J. Husak, and J. Le Galliard. 2008. How does selection operate on whole-organism functional performance capacities? A review and synthesis. doi: 10.7275/R58G8HX6. University of Massachusetts Amherst Libraries.

Isip, J. E., M. E. H. Jones, and N. Cooper. 2022. Clade-wide variation in bite-force performance is determined primarily by size, not ecology. Proc. R. Soc. B. 289:20212493. Royal Society.

Kaliontzopoulou, A. 2012. Relationships between head morphology, bite performance and ecology in two species of *Podarcis* wall lizards. Evol. Ecol. doi: 10.1007/s10682-011-9538-y.

Kaliontzopoulou, A., and D. C. Adams. 2016. Phylogenies, the Comparative Method, and the Conflation of Tempo and Mode. Syst, Biol, 65:1–15.

Kaliontzopoulou, A., M. A. Carretero, and D. C. Adams. 2015. Ecomorphological variation in male and female wall lizards and the macroevolution of sexual dimorphism in relation to habitat use. J. Evol. Biol. 28:80–94.

Kaliontzopoulou, A., M. A. Carretero, and G. A. Llorente. 2010. Intraspecific ecomorphological variation: linear and geometric morphometrics reveal habitat-related patterns within *Podarcis* bocagei wall lizards. J. Evol. Biol. 23:1234–1244.

Kingsolver, J. G., and R. B. Huey. 2003. Introduction: The Evolution of Morphology, Performance, and Fitness. Integr. Comp. Biol. 43:361–366.

Kingsolver, J. G., and R. B. Huey. 2008. Size, temperature, and fitness: three rules. Evol. Ecol. Res. 10:251–268.

Klaauw, C. J. van der. 1948. Ecological Morphology. E.J. Brill.

Klingenberg, C. P. 2016. Size, shape, and form: concepts of allometry in geometric morphometrics. Dev. Genes. Evol. 226:113–137.

Lailvaux, S. P., and J. F. Husak. 2014. The life history of whole-organism performance. Q. Rev. Biol. 89:285–318.

Lappin, A. K., and J. F. Husak. 2005. Weapon performance, not size, determines mating success and potential reproductive output in the collared lizard (*Crotaphytus collaris*). Am. Nat. 166:426–436.

Le Galliard, J.-F., J. Clobert, and R. Ferrière. 2004. Physical performance and Darwinian fitness in lizards. Nature. 432:502–505.

Le Guilloux, M., A. Miralles, J. Measey, B. Vanhooydonck, J. C. O'Reilly, A. Lowie, and A. Herrel. 2020. Trade-offs between burrowing and biting force in fossorial scincid lizards? Biol. J. Linn. Soc.130:310–319.

Losos, J. B. 2011. Convergence, adaptation, and constraint. Evolution. 65:1827–1840.

Losos, J. B. 1992. The Evolution of Convergent Structure in Caribbean *Anolis* Communities. Syst. Biol. 41:403–420.

Losos, J. B., and L. D. Mahler. 2010. Adaptive Radiation: The Interaction of Ecological Opportunity, Adaptation, and Speciation. Pp. 381–420 in Evolution Since Darwin: The First 150 Year.

Martins, E. P., and T. Garland. 1991. Phylogenetic analysis of the correlated evolution of continuous characters: a simulation study. Evolution. 45:534–557.

Miles, D. B. 2014. Covariation between morphology and locomotor performance in sceloporine lizards. Pp. 207–236 in L. J. Vitt and E. R. Pianka, eds. Lizard ecology: historical and experimental perspectives. Princeton University Press.

Pincheira-Donoso, D., D. J. Hodgson, and T. Tregenza. 2008. The evolution of body size under environmental gradients in ectotherms: why should Bergmann's rule apply to lizards? BMC Evol. Biol. 8:68.

Rohlf, F. J. 2001. Comparative methods for the analysis of continuous variables: geometric interpretations. Evolution. 55:2143–2160.

Schwenk, K. 2000. CHAPTER 1 - Tetrapod Feeding in the Context of Vertebrate Morphology. Pp. 3–20 in K. Schwenk, ed. Feeding. Academic Press, San Diego.

Stayton, C. T. 2006. Testing Hypotheses of Convergence with Multivariate Data: Morphological and Functional Convergence Among Herbivorous Lizards. Evolution. 60:824–841.

Taverne, M., H. Dutel, M. Fagan, A. Štambuk, D. Lisičić, Z. Tadić, A.-C. Fabre, and A. Herrel. 2021. From micro to macroevolution: drivers of shape variation in an island radiation of *Podarcis* lizards. Evolution. 75:2685–2707.

Taverne, M., N. King-Gillies, M. Krajnović, D. Lisičić, Ó. Mira, D. Petricioli, I. Sabolić, A. Štambuk, Z. Tadić, C. Vigliotti, B. Wehrle, and A. Herrel. 2020. Proximate and ultimate drivers of variation in bite force in the insular lizards *Podarcis melisellensis* and *Podarcis sicula*. Biol. J. Linn. Soc.131:88–108.

Tejero-Cicuéndez, H., I. Menéndez, A. Talavera, G. Mochales-Riaño, B. Burriel-Carranza, M. Simó-Riudalbas, S. Carranza, and D. C. Adams. 2023. Evolution along allometric lines of least resistance: morphological differentiation in *Pristurus* geckos. Evolution. 77:2547–2560.

Uetz. 2023. The Reptile Database.

Urošević, A., K. Ljubisavljević, and A. Ivanović. 2013. Patterns of cranial ontogeny in lacertid lizards: morphological and allometric disparity. J. Evol. Biol. 26:399–415.

Van Damme, R., P. Aerts, and B. Vanhooydonck. 1998. Variation in morphology, gait characteristics and speed of locomotion in two populations of lizards. Biol. J. Linn. Soc.63:409–427.

Van Damme, R., and B. Vanhooydonck. 2002. Speed versus manoeuvrability: association between vertebral number and habitat structure in lacertid lizards. J. Zool. 258:327–334.

Vanhooydonck, B., and R. Van Damme. 1999. Evolutionary relationships between body shape and habitat use in lacertid lizards. Evol. Ecol. Res. 1:785–803.

Vanhooydonck, B., and R. Van Damme. 2001. Evolutionary trade-offs in locomotor capacities in lacertid lizards: are splendid sprinters clumsy climbers? J. Evol. Biol. 14:46–54.

Vanhooydonck, B., and R. Van Damme. 2003. Relationships between locomotor performance, microhabitat use and antipredator behaviour in lacertid lizards. Funct. Ecol. 17:160–169.

Vanhooydonck, B., R. Van Damme, and P. Aerts. 2002. Variation in speed, gait characteristics and microhabitat use in lacertid lizards. J. Exp. Biol. 205:1037–1046.

Verwaijen, D., R. Van Damme, and A. Herrel. 2002. Relationships between head size, bite force, prey handling efficiency and diet in two sympatric lacertid lizards. Funct. Ecol.16:842–850.

Vicent-Castelló, P., U. Enriquez-Urzelai, F. Martínez-Freíria, J. Garcia-Porta, and A. Kaliontzopoulou. 2025a. Context-dependent body size evolution in lacertid lizards: differential role of structural habitat and climate across radiations. Evolution qpaf130.

Vicent-Castelló, P., A. Herrel, D. J. Harris, and A. Kaliontzopoulou. 2025b. Walking or hanging: the role of habitat use for body shape evolution in lacertid lizards. J. Evol. Biol. voaf003.

Vitt, L. J., J. P. Caldwell, P. A. Zani, and T. A. Titus. 1997. The role of habitat shift in the evolution of lizard morphology: evidence from tropical *Tropidurus*. PNAS. 94:3828–3832.

Chapter 2:

Objectives and thesis outline

2.1. Objectives

The overarching objective of this PhD thesis is to investigate how phenotypic traits evolve in response to ecological constraints, and how the relationships among morphology, performance, and body size are structured across different biological and phylogenetic scales. Using lacertid lizards as a model system, this thesis aims to disentangle how ecological factors such as structural habitat use and climate shape phenotypic diversification, and to assess how integrated trait systems respond to selection in a context-dependent and scale-dependent manner.

More specifically, this thesis seeks to:

Assess how body size evolution is influenced by ecological factors across phylogenetic scales.

This objective focuses on evaluating the relative role of structural habitat use and broad-scale climatic variables in shaping body size evolution across the Lacertidae family, and on determining whether evolutionary patterns observed at finer phylogenetic levels (e.g., tribes or subfamilies) are maintained or obscured when analyses are conducted at broader scales.

Examine the role of structural habitat use in shaping body shape evolution.

This objective aims to test whether the use of predominantly vertical versus horizontal habitat axes has driven consistent morphological differentiation in lacertid lizards, to identify which body regions are most responsive to habitat-related selective pressures, and to evaluate whether these pressures promote morphological convergence or diversification.

Investigate the relationship between morphology and performance across hierarchical biological levels.

Focusing on head shape and bite force, this objective seeks to determine how form–function relationships are expressed at the individual, species, and family levels, and to assess whether these relationships scale predictably across levels of biological organization.

Evaluate the role of body size and allometry in mediating phenotypic integration.

This objective aims to quantify the contribution of body size to the relationships between morphology and performance, and to determine whether size-independent shape variation retains functional relevance once allometric effects are accounted for.

Explore the extent to which phenotypic integration coexists with evolutionary decoupling.

By combining macroevolutionary and multilevel approaches, this objective seeks to test whether integrated phenotypic systems exhibit conserved evolutionary trajectories, or whether different components of the phenotype respond semi-independently to ecological and selective pressures, consistent with many-to-one mapping between form and function.

Together, these objectives provide a comprehensive framework for understanding how complex phenotypes evolve under multiple, interacting ecological constraints, and how evolutionary patterns depend on both the biological scale of analysis and the evolutionary context in which diversification occurs.

2.2. Thesis outline

This dissertation is structured into six chapters.

Chapter 1 presents a general introduction, offering essential background information to facilitate a comprehensive understanding of the thesis. It begins by discussing key concepts such as phenotypic evolution, the ecomorphological paradigm, and the form–function relationship, and explains how these processes contribute to the emergence of evolutionary patterns across species. Additionally, this chapter introduces lacertid lizards as both a biological family and a model system for addressing the evolutionary questions posed throughout the thesis.

Chapter 2, which serves as the conceptual foundation of the dissertation, outlines the main objectives, specific research questions, and the motivations that guided this work.

Chapter 3 explores the evolution of body size across broader phylogenetic scales, including the tribal and family levels, examining how this morphological trait has evolved under the influence of various environmental factors, such as climatic conditions and structural habitat. Phylogenetic comparative methods were employed to account for

evolutionary relationships and to investigate the tempo and mode of body size evolution. The findings of this study were published in:

- Vicent-Castelló, P., Enriquez-Urzelai, U., Martínez-Freíria, F., Garcia-Porta, J., & Kaliontzopoulou, A. 2025. Context-dependent body size evolution in lacertid lizards: differential role of structural habitat and climate across radiations. Evolution, 79(10): 2023–2034. https://doi.org/10.1093/evolut/qpaf130

Chapter 4 investigates the influence of structural habitat use (climbing versus ground-dwelling) on the evolution of body shape in lacertid lizards. It further examines whether the strength of this evolutionary trend has been sufficient to drive morphological convergence between these two ecological groups. This work was published in:

- Vicent-Castelló, P., Herrel, A., Harris, D. J., & Kaliontzopoulou, A. 2025. Walking or hanging: the role of habitat use for body shape evolution in lacertid lizards. J. Evol. Biol., 38(3): 353–366. https://doi.org/10.1093/jeb/voaf003

Chapter 5 investigates how form–function relationships scale across hierarchical biological levels, from individuals to species and across the family Lacertidae. Using head shape and bite force as a model system, this chapter examines whether morphological variation translates into consistent performance differences at the intraspecific, interspecific, and family levels. By explicitly accounting for body size and allometry, it evaluates whether size-independent shape variation remains functionally relevant and whether phenotypic integration is conserved or decoupled across evolutionary scales. This paper was published in:

- Vicent-Castelló, P., Adams, D., Sicilia-Cebrián, C-A., Herrel, A., & Kaliontzopoulou, A. 2026. Variable yet ubiquitous: Hierarchical scaling of head functional morphology in lizards. Evolution, in press

In Chapter 6 a comprehensive discussion of the central topics and interpretations addressed in this thesis is provided, with particular emphasis on the principal findings and the prospective challenges for future research.

Chapter 3:

Context-dependent body size evolution in lacertid lizards: differential role of structural habitat and climate across radiations

3.1. Introduction

Body size is a prominent phenotypic trait that modulates how species interact with their natural environment and dramatically affects major organismal features such as performance, physiology, and ecology (LaBarbera, 1989; Meiri, 2008; Peters, 1986; Wilson, 1975; Womack & Bell, 2020). Every aspect that body size influences is cornerstone to the survival of individuals and is, therefore, subject to the action of natural selection. As such, understanding how body size evolves under the influence of the environment where organisms live and across different phylogenetic scales (Klompmaker et al. 2015; Slavenko et al. 2019; Smith & Lyons, 2013) is relevant for understanding speciation and diversification (Cardillo et al. 2005; Etienne et al. 2012; Stanley, 1973).

The structural habitat and climatic niche, understood respectively as the physical features, individuals interact with (i.e., microhabitat), and the range of climatic conditions in which populations persist (i.e., the Hutchinsonian niche [Hutchinson,1957 , 1978]), have been identified as key factors influencing body size evolution in a wide diversity of ectotherms, including ants (Cushman et al.1993), flies (Kubota et al.2007), amphibians (Johnson et al. 2023; Olalla-Tárraga & Rodríguez, 2007), and reptiles (Collar et al. 2011; Garcia-Porta et al. 2016; Velasco et al. 2020). Squamates in particular constitute an optimal model system to address questions in ecomorphology. On the one hand, how reptiles utilize their structural habitat (e.g., performing as ground-dwelling, arboreal, aquatic, and saxicolous) is closely linked to their morphological traits, which translate into different morphological adaptations to it (Arnold,1983; Collar et al. 2010, 2011; Goodman et al. 2008; Kaliontzopoulou et al. 2010; Vanhooydonck & Van Damme, 1999; Vervust et al. 2007; Vicent-Castelló et al. 2025). Variation in body size is predominant in such ecomorphological patterns, where arboreal and saxicolous species tend to be smaller in body size, while ground-dwelling species tend to be larger (Collar et al. 2011; Goodman et al. 2008; Kaliontzopoulou et al. 2010; Revell et al. 2007). Another habitat-related factor that plays a major role in body size evolution is insularity, with remarkable examples of both gigantism and dwarfism in islands occurring in several groups, including reptiles (Benítez-López et al. 2021). Insularity and habitat-driven factors have been shown to in- fluence both average body size and the pace of its evolution, as seen

in accelerated rates during island colonization (Garcia-Porta & Ord, 2013; Millien, 2006; Raia & Meiri, 2011) or adaptive radiation into different habitats (Thomas et al. 2009).

On the other hand, large-scale climatic variation is also considered central in shaping body size evolution (Johnson et al. 2023; Olalla-Tárraga et al. 2006; Terribile et al. 2009). Since the formulation of Bergman's rule (Bergmann, 1848)—which is the most noteworthy ecogeographical rule focused on body size variation and predicts bigger forms in colder environments— several hypotheses have been proposed to explain large-scale, climate-driven evolutionary trends of body size variation. Frameworks such as the "heat conservation hypothesis" (Olalla-Tárraga et al. 2006), "heat balance hypothesis" (Olalla-Tárraga et al. 2006), "water conservation hypothesis" (Gouveia & Correia, 2016), "primary productivity hypothesis" (Huston & Wolverton, 2011; Yom-Tov & Geffen, 2006), "starvation resistance hypothesis" (Troost et al. 2009), and "seasonality hypothesis" (Slavenko et al. 2019) explain variation in body size as a response to broad climatic conditions, such as temperature, precipitation, productivity, and seasonality. These hypotheses are not mutually exclusive, and different drivers could have affected body size evolution at different phylogenetic, geographic, and evolutionary scales (i.e., individuals, populations, and species) (Henry et al. 2023).

Among ectotherms, squamates show no clear relationship between body size and geography or broad-scale climatic conditions across the entire order (Slavenko et al. 2019). Nevertheless, at smaller scales, environmental conditions have been shown to affect body size evolution in coherent taxonomic groups, such as at the family (Liang et al. 2021), genus (Velasco et al. 2020), and intraspecific levels (Zamora-Camacho et al. 2014). This highlights the lack of consistency in the patterns and processes of body size evolution across phylogenetic and geographic scales (Hawkins & Lawton, 1995; Olalla-Tárraga & Rodríguez, 2007; Olalla- Tárraga et al. 2006; Slavenko et al. 2019; Terribile et al. 2009). This could be because at broad phylogenetic scales there is typically also a high amount of clade-specific variation in life history and other basic biological traits (e.g., body form and limb presence/absence), which could blur evolutionary patterns at lower taxonomic scales. Furthermore, body size is shaped by multiple selective pressures—ecological, sexual, reproductive, and historical—acting simultaneously. At broader scales, conflicting pressures may obscure environmental influence at the family level (Johnson et al. 2023). This observation opens an important question regarding

macroevolution, and specifically body size evolution: does the phylogenetic/geographic scale of the study affect the evolutionary trends found in specific and coherent groups? Or can the patterns found at finer geographic or phylogenetic scales be generalized to broader scales?

Here, we used the Old-World lizard family Lacertidae to study body size evolution across different phylogenetic scales and with respect to distinct aspects of the environment. Lacertid lizards are an ideal model for studying body size evolution in an eco-phylogenetic framework. They have diversified into a considerable range of body sizes (30–240 mm), and they occupy a great diversity of environments across their wide global distribution range across Eurasia and Africa. Interestingly, this family is composed of two subfamilies of quite different ecogeographic and phylogenetic characteristics, the Gallotinae and the Lacertinae. The Gallotinae are relatively species-poor (14 species), and they have quite a limited current distribution, being restricted mostly to the Canary Islands (genus *Gallotia*), with four additional species in the Iberian Peninsula and North of Africa (genus *Psammodromus*) (Cox et al. 2010). By contrast, the Lacertinae encompasses the vast diversity of the family, and they are further divided into two monophyletic tribes, which have diversified along largely non-overlapping distributions, under different ecogeographical conditions and different evolutionary histories (Arnold et al. 2007). The Lacertini tribe (140 species) has diversified throughout Eurasia, while Eremiadini species (211 species) are predominant through Africa and the Middle East (Arnold et al. 2007). Adaptation to varied climatic conditions has been demonstrated to exert disparate wide-scale selective pressures (Hipsley et al. 2014), where the Eremiadini have diversified into a great variety of arid-adapted species mostly specialized in ground microhabitats, while the Lacertini underwent their diversification in mesic conditions occupying mostly elevated microhabitats that require climbing (Arnold, 1998). All these historical differences between the three main phylogenetic groups of lacertids (i.e., Gallotinae, and the two tribes within Lacertinae: Lacertini and Eremiadini) may have provided substantially different contexts for body size evolution.

As such, this study aims to understand the evolution of body size in the Lacertidae family across geographic and phylogenetic scales. We investigate the effect of structural and climatic environment and assess whether evolutionary patterns at fine phylogenetic and geographic scales (i.e., tribe and subfamily) are mirrored at broader scales (i.e., family).

Then, we examine how these environmental axes have influenced the tempo and mode of body size evolution, all within coherent phylogenetic groups. If structural habitat is a predominant driver of body size evolution, we expect ground-dwelling species to be larger than climbing ones, as has been reported for other lizard groups (Collar et al. 2011). Therefore, we anticipate body size evolution to exhibit different evolutionary optima for climbers and ground- dwellers in both Eremiadini and Lacertini, and for ground- dwellers in Gallotinae (since there are no climbing species in this subfamily). In addition to trends in body size evolution, we also anticipate differences in the tempo of phenotypic evolution. Specifically, we expect highly specialized species to exhibit lower evolutionary rates, as selective pressures would drive body size toward similar values. In contrast, generalist species are likely to exhibit higher evolutionary rates. Accordingly, we predict that climbing species (which are in principle more specialized) from both tribes will display low evolutionary rates. Similarly, members of the subfamily Gallotinae are expected to show high evolutionary rates, driven by a major shift to insularity. Moreover, we also predict that broad climatic conditions have affected the three groups differently, leading to distinct evolutionary pathways. As a result, we expect the patterns observable at lower phylogenetic scales not to be trace- able at the family level, since the contrasting effects be- tween groups would blur clade-specific climatic effects on body size evolution. Finally, due to the limited distribution range and habitat-use homogeneity observed across the species in this subfamily, we anticipate body size evolution in the Gallotinae to be driven by local climatic conditions alone.

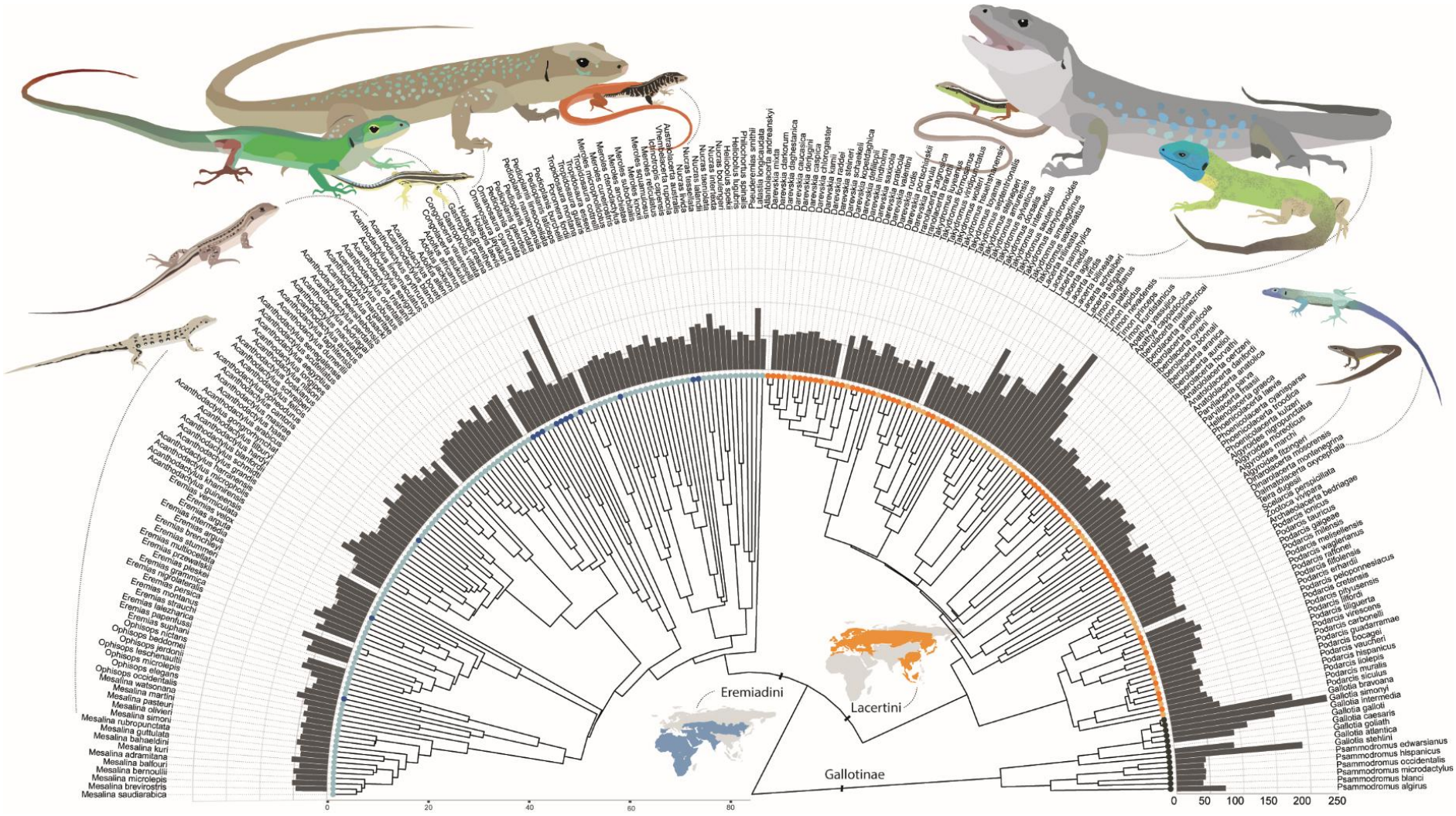

Figure 3.1. Body size variation across lacertid species (grey bars) and corresponding structural habitat and phylogenetic group regimes next to phylogeny tips. Colors indicate phylogenetic group: blue palette for Eremiadini, orange palette for Lacertini, and black for Gallotinae. Intensities indicate structural habitat use, with lighter colors for ground-dwelling (GD) species and dark colors for climbing (CL) species. Scale for snout-vent length in mm in the bottom-right corner of the tree. Temporal scale in millions of years is shown in the bottom-left corner. Phylogenetic tree from García-Porta et al. (2019). Illustrations are scaled to the relative size between selected species. Illustrations by P. Vicent-Castelló.

3.2. Material and methods

3.2.1. Data collection

Body size

We used snout-vent length (SVL) as the measure of body size. SVL was chosen over body mass to mitigate the influence of body condition and the potential effects of long-term ethanol preservation on the analyses (Vervust et al. 2007). Data for 234 species were collected, covering ~60% of the family, and including at least one species per genus (Figure 3.1). Morphological information was obtained from museum collections and field campaigns (1374 individuals) and supplemented with previously published measurements for specific species (64 species) (Table S3.1 and Figure 3.1). Only adult males were measured to control for the effects of sexual dimorphism and age. Measurements were recorded to the nearest 0.01 mm using electronic calipers. The mean SVL per species was calculated and the data were ln-transformed for downstream analyses to facilitate the interpretation of relative body size variation across evolutionary scales (Kerkhoff & Enquist, 2009).

Structural habitat

To explore how the structural habitat affects body size evolution, we divided species into two different groups: climbing and ground-dwelling, following the classification in Vicent-Castelló et al. (2025). These two categories describe the vertical vs. horizontal use of the habitat, regardless of the substrate that forms it. To classify species into one of the two structural habitat groups, we conducted an extensive qualitative bibliographic review, consulting specific articles as well as general sources such as the Reptile database (Uetz, 2023) and the Internation Union for Conservation of Nature (IUCN) (IUCN, 2022) (Table S3.2). For more details about the classification, see Vicent-Castelló et al. (2025).

Climatic variation

To characterize the climatic conditions where species live, we first derived distributional ranges for 233 species by overlapping polygons from the IUCN Red List (IUCN, 2022), and records compiled from specific publications (e.g., Baha El Din, 2007; Caeiro-Dias et al. 2018) and obtained from public repositories, such as Global Biodiversity Information Facility, https://www.gbif.org/, using the function *sp_occurrence* implemented in geodata (Hijmans et al. 2024) (Table S3.3). We estimated the distribution ranges at 10 arcminutes

of resolution (0.17 degrees) in the World Geodetic System 1984 datum. Then, we obtained different climatic and topographic variables to characterize the climatic conditions experienced by each species across their ranges (Table S3.2). We used the maximum and minimum values of each variable, in addition to the mean, as we expect species to adapt to extreme climatic conditions. A detailed description of the procedures used to obtain species environmental descriptors is provided by Martínez-Freiría et al. (2020). We selected coherent climatic variables to answer the previously presented large-scale ecogeographic hypotheses (Figure 3.2). These variables included (1) maximum, mean, and minimum of the average annual precipitation across each species' distribution (Pmax, Pavg, and Pmin), which correspond to the water conservation hypothesis; (2) maximum, mean, and minimum of the average annual temperature (Tmax, Tavg and Tmin), maximum and minimum of the maximum annual temperature (Tmax- Max and TminMax), and maximum and minimum of the minimum annual temperature (TmaxMin and TminMin), which correspond to the heat balance and the heat conservation hypothesis; (3) maximum, mean, and minimum normalized difference vegetation index (NDVImax, NDVIavg, and NDVImin), which correspond to the primary productivity hypothesis; and (4) maximum, mean, and minimum temperature (TseasonMax, TseasonAvg, and TseasonMin) seasonality and precipitation (PseasonMax, PseaonAvg, and PseasonMin), which correspond to the seasonality and the starvation resistance hypothesis. We then assessed Pearson correlations between variables and removed those with correlation coefficients greater than 0.7, aiming to retain at least one variable relevant to the hypothesis mentioned above. When possible, we prioritized keeping maximum and minimum values, as we believe that environmental adaptation is most evident in responses to climatic extremes. After this filtering, we retained for analyses the maximum and minimum of average annual precipitation (Pmax and Pmin), maximum of the maximum annual temperature and minimum of the minimum annual temperature (TmaxMax and TminMin), maximum and minimum of NDVI (NDVImax and NDVImin), and minimum precipitation seasonality (PseasonMin). Temperature and precipitation data to construct our variables were downloaded from WorldClim v.2.1 database (https://www.worldclim.org; Fick & Hijmans, 2017) at a spatial resolution of 10 arcminutes and for the period 1970–2000. NDVI data were downloaded from the NASA Earth Observatory portal (https:// earthobservatory.nasa.gov/) at a spatial resolution of 10 min and for the period 2001–2023. We performed all the calculations in

ArcGis v.10.5 (ESRI, 2017) and R v.4.2.2 (R Core Team, 2021) using the packages "raster" (Hijmans et al. 2023) and "ncdf4" (Pierce, 2024). For further information on the procedure, see Enríquez-Urzelai et al. (2022) and Martínez-Freiría et al. (2020).

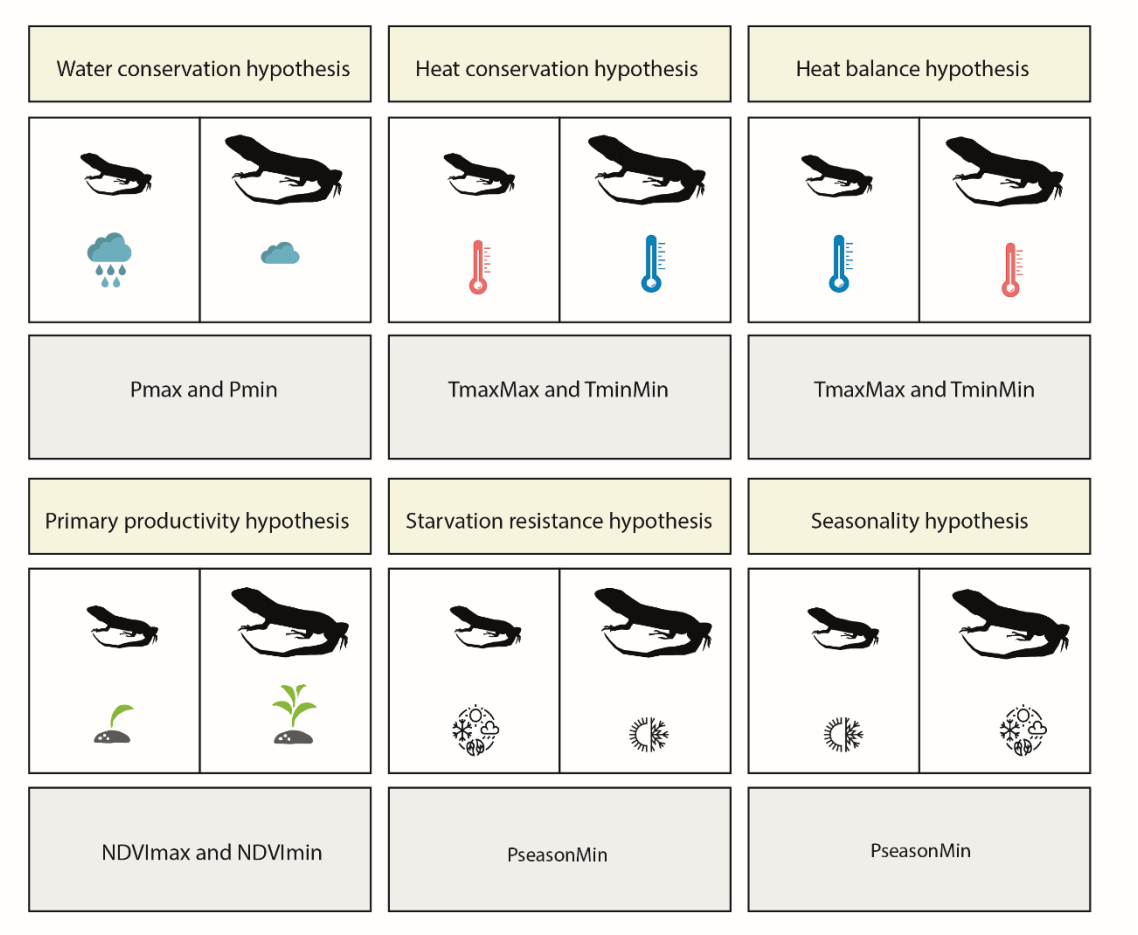

Figure 3.2. Ecogeographic hypotheses considered and predicted relationships between body size and climatic variables associated with each of them.

Phylogeny

To investigate the evolution of body size, we implemented phylogenetic comparative methods using the most complete phylogeny of the family Lacertidae (Garcia-Porta et al. 2019), a time-calibrated phylogenomic tree comprising 246 species. We trimmed the phylogeny to the species for which we had morphological, structural habitat, and climatic data for downstream analyses (but see further on for how habitat use was reconstructed using the full phylogeny).

3.2.1. Comparative analyses

Phylogenetic signal

To explore patterns of body size evolution, we first evaluated the degree of phylogenetic signal of log-transformed SVL at different phylogenetic scales. We first obtained the phylogenetic signal at the family level using the complete phylogeny. Then, we trimmed the phylogeny to obtain specific trees for Gallotinae, Lacertini, and Eremiadini, and we performed analyses separately. We used the *phylosig* function in the R package "phytools" (Revell, 2010) to calculate Blomberg K statistic (Blomberg et al. 2003) and test whether those are statistically different from what is expected under a case of phenotypic evolution proportional to the phylogeny, considering a Brownian motion (BM) model of evolution. Then, to test whether *K* values were significantly different from 1, we used custom code to compare empirical vs. simulated values generated under BM (where $K = 1$ is expected). The code to perform the comparison is available in the Dryad repository and it was obtained from "https:// blog.phytools.org/ 2011/ 12/testing- for-phylogenetic- signal- k.html."

Shifts in body size evolution

To identify which groups or clades are particularly relevant for studying ecomorphology and environmental variables, we conducted preliminary analyses to detect shifts in body size evolution along the Lacertidae phylogeny without predefined groupings. First, we applied the *PhyloEM* function implemented in the R package "PhylogeneticEM" which identifies trait shifts (Bastide et al. 2017), under a BM model of evolution. Second, we used Bayesian analysis of macroevolutionary mixtures (BAMM) to identify changes in the rates of body size evolution. This analysis was conducted using one rjMCMC run, consisting of four chains, with a thinning interval of 10^5 generations and a total chain length of 10^6 generations to ensure the Markov Chain Monte Carlo (MCMC)

convergence. Settings priors were established with the *setBAMMpriors* function from the "BAMMtools" package. We deleted the first 10% of generations as a "burn-in" and then determined the best-fitting configuration using the *getBestShiftConfiguration* function from the "BAMMtools" package (Rabosky et al. 2014).

Influence of structural and climatic niche on body size

To investigate whether structural and climatic habitats affected the diversification of body size in lacertid lizards, we conducted a series of phylogenetic analyses of variance for the structural habitat variable and phylogenetic generalized least squares for climatic predictors. These analyses were performed at family, subfamily, and tribe levels for each group of structural and climatic habitat variables. To account for phylogenetic relationships, we employed the trimmed phylogeny for each group to obtain the variance-covariance matrix. As predictors, we used the structural habitat classification and climatic variables to test large-scale geographic hypotheses (Figure 3.2). We compared the fit of linear models (SVL~climatic variable) using two different models with the *phylolm* function from the "phylolm" package (Ho et al. 2024). The models used for the error term included BM and Ornstein–Uhlenbeck (OU) processes, with the ancestral state estimated at the root ("OUfixedRoot"). To evaluate which model best explained the data, we compared the two approaches using the Akaike information criterion (AIC), selecting the model with the lowest AIC score. We applied a threshold of 4 AIC points, selecting the simpler model (BM) if the difference was less than 4. Finally, to estimate the amount of variance explained by the predictors we calculated the R^2_{pred} using the function *R2_pred* from the R package "rr2" and making the comparison with the predictor equals 1, to obtain the isolated effect of the predictor (Ives, 2019).

Tempo and mode of body size evolution

To investigate how structural habitats have affected the tempo and mode of body size evolution, we employed the stochastic character histories derived from Vicent-Castelló et al. (2025) for habitat use across the complete phylogeny (Garcia-Porta et al. 2019), trimmed down to match our morphological dataset. Next, we fitted and compared different evolutionary models using 100 randomly selected simmaps out of the 1000 simulations obtained in Vicent-Castelló et al. (2025). We considered 14 models representing different hypotheses about body size evolution. First, we fitted a white noise model, where the phylogeny does not affect body size evolution at all, which could be

taken as a null hypothesis. Then, we fitted six models to describe potential effects of the structural habitat and seven to describe that of the environment (paleotemperature, see below) on body size evolution. A single-rate BM (BM1) represented non-directional body size evolution under a single evolutionary rate (σ2), in proportion to evolutionary relatedness. We also fitted a multiple- rate BM model (BMS), which allows for different evolutionary rates for each of the structural habitat states (climbing vs. ground-dwelling). Furthermore, we examined OU models, which encompass directionality in body size evolution, including a single-optimum model (OU1), with the same evolutionary peak (θ) for both habitats and a multiple-optima model (OUM), that allows for different evolutionary peaks for ground-dwellers and climbers. To test whether different phylogenetic groups (Gallotinae, Lacertini, and Eremiadini) evolved under different evolutionary tempos/modes, we first classified the data based on clade composition to isolate and assess the clade's effect on body size evolution. Then, we addressed the effect of structural habitat with respect to the clade. To do so, we considered the same 100 randomly selected simmaps and manually modified the structural habitat reconstruction (Figure S3.1) (Butler & King,2004), in order to account for different states of structural habitat depending on the phylogenetic group. All simmaps were thus reclassified to reflect whether the branches, internal and terminal nodes belonged to the Gallotinae, Lacertini, or Eremiadini, in addition to the underlying structural habitat reconstruction (Butler & King, 2004). The intermediate node separating the Lacertini and Eremiadini tribes were randomly assigned to one phylogenetic group or the other in a 50/50 proportion across all considered simmaps. This approach allowed us to fit multi-rate BM and multi-optima OU models, which allow for different rates and optima for each structural habitat in each radiation (i.e., ground-dwellers in the subfamily Gallotinae, ground-dwellers and climbers in Eremiadini, and ground- dwellers and climbers in Lacertini). All evolutionary models were fitted using the "Ouwie" package (Beaulieu et al. 2012), except for the white noise model, which was fitted using *fitContinuous* function in "geiger" package (Pennell et al. 2014).

Finally, in order to model the possible effect of paleoenvironment on the tempo and mode of body size evolution, we fit different temperature-dependent models using the functions *fit-t-env* (Clavel & Morlon, 2017) and *fit_t_env_ou* (Clavel & Morlon, 2017; Goswami & Clavel, 2024; Troyer et al. 2022) implemented in the package "RPANDA" (Morlon et al.

2016). These models extend the “classical” BM and OU models, to incorporate variation in evolutionary rates (σ2) and optima (θ) depending on an environmental variable. We implemented two approaches available in the function, one with an exponential and another with a linear association between the environmental variable and the rate/optimum parameters (Clavel & Morlon, 2017). We tested three degrees of increasing data smoothing using cubic splines (Velasco et al. 2020). Paleotemperature data registered from sea temperature, which is a reflection of environmental temperature, were obtained from Cramer et al. (2011), which encompasses the last 108 million years. After fitting the models, we discarded model runs that presented negative eigenvalues, and which produced unrealistic estimates (Beaulieu et al. 2012; Kolmann et al. 2020; Price & Hopkins, 2015). Then, to compare model fit, we used the modified AIC (AICc), selecting the model with the lowest value. If more than one model were equally supported (AICc < 4), we chose the simplest one as the best supported model.

3.3. Results

We found that SVL exhibited significant phylogenetic signal in all examined phylogenetic levels (Table S3.4). Across Lacertidae, Gallotinae, and Lacertini, values ranged from 0.72 to 1.36 and were all not statistically distinguishable from 1 (Table S3.4). However, the Eremiadini exhibited a value of K = 0.614, which was statistically different from 1 (Table S3.4).

Before defining a priori groupings based on habitat and clade, "phylogeneticEM" detected six shifts in body size evolution (Figure S3.2). Three occurred within the subfamily Gallotinae, specifically in the *Gallotia* genus. Three more were identified in the Lacertini tribe — one within the *Timon- Lacerta* clade and another on the terminal branch leading to *Anatololacerta oertzeni*. The final shift was found in Eremiadini, corresponding to the terminal branch leading to *Omanosaura jayakari*. BAMM identified five shifts in evolutionary rates as the best shift configuration (Figure S3.3). One occurred at the root of the *Gallotia* genus. In the Lacertini tribe, two shifts were detected—one before the *Anatololacerta* clade and another in the *Timon-Lacerta* clade. Finally, two shifts were found in Eremiadini — one at the base of *Omanosaura* clade and another within *Acanthodactylus*.

Phylogenetic ANOVAs conducted at various phylogenetic levels revealed no significant variation in present-time body size depending on structural habitat at the family, subfamily, or tribe levels (Table S3.5). However, when investigating the effect of climatic variables on body size evolution, we found that results differed according to different phylogenetic scales (Tables S3.6). At the family level, all phylogenetic regression models of SVL on different climatic variables followed an OU model, but none of those relationships were significant (Table S6). A BM model was the best fit for all variables in the subfamily Gallotinae, but here the association between SVL and climatic variables was also non-significant (Table S6). Finally, in both the Eremiadini and Lacertini tribes BM was the best-fitting model for all SVL–climate relationships. The Lacertini exhibited a negative significant relationship between body size and precipitation seasonality minima, explaining 3% of variance (PseasonMin) (Table S3.6 and Figure 3.3). Instead, in the tribe Eremiadini we found a negative significant relationship between body size and minimum of the minimum temperature, explaining 1.55% of variance (TminMin) (Table S3.6 and Figure 3.3). Finally, an examination of evolutionary models for body size and structural habitat evolution indicated that the best-fitting model was a multiple-rate BM with different rates for each structural habitat in each phylogenetic group (Table S3.7). The evolutionary rates from the best-selected model revealed that the Gallotinae (all ground-dwelling species) exhibited rates an order of magnitude higher than those of the two tribes of the Lacertinae. Among Eremiadini species, climbers evolved at higher rates than ground-dwellers, while among Lacertini species, ground-dwellers exhibited higher evolutionary rates than climbers (Figure 3.4 and Table S3.8).

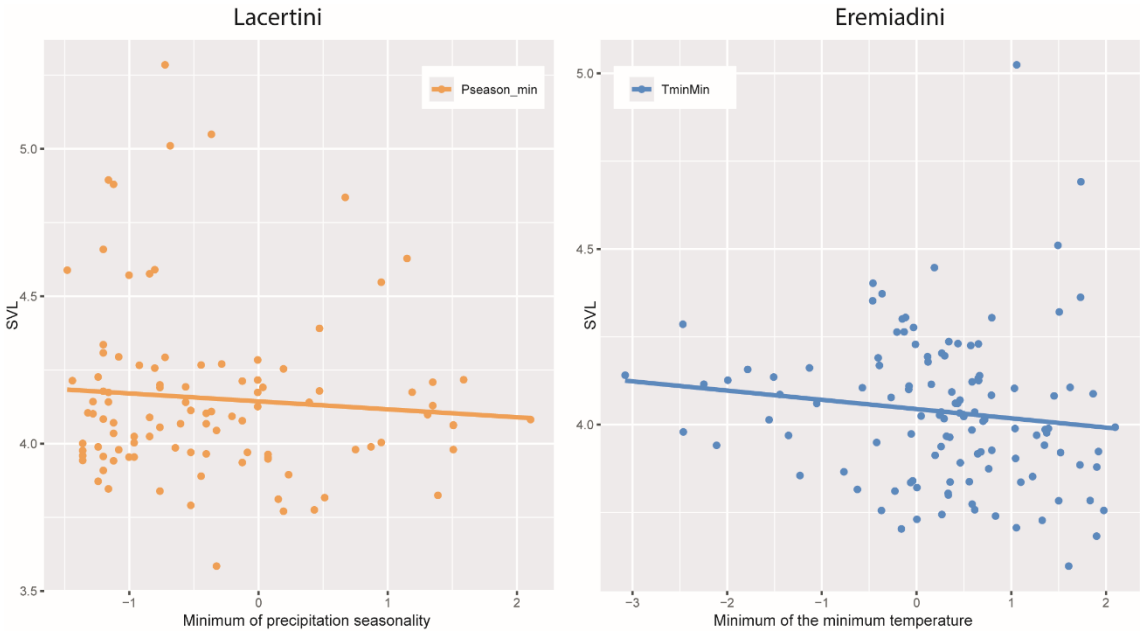

Figure 3.3. Significant scaled predictors' (climatic variables) effects on logarithmic body size for the Lacertini and Eremiadini tribes.

3.4. Discussion

The study of body size evolution is central to evolutionary biology, as this morphological trait has a profound influence on numerous biological traits (Brown et al. 1993; Meiri, 2008; Schmidt-Nielsen, 1984), which affect fitness. An evolutionary approach to studying body size provides important insights into the mechanisms driving adaptation and speciation (Cardillo et al. 2005; Etienne et al. ,2012; Stanley, 1973). Our results provide a comprehensive view on the effect of habitat use and climatic variation on body size evolution, and on how this effect varies across phylogenetic and geographic scales. While average body size did not vary across structural habitats at any phylogenetic scale in lacertids, evolutionary shifts were identified in different phylogenetic clades (Figures S3.2 and S3.3), indicating that rather than following a general trend, specific clades are evolving independently. After establishing ecological and phylogenetic groups, we also found that the rate of body size evolution differs between structural habitats (ground-dwelling vs. climbing) and it does so under different rules across phylogenetic groups (Gallotinae, Eremiadini, and Lacertini). In addition, as predicted, we found that different climatic variables are involved in explaining variation in body size depending on the phylogenetic group under consideration. This means that the evolution of body size

follows different ecogeographical rules depending on the phylogenetic level examined, which highlights the importance of phylogenetic scale in macroevolutionary inferences.

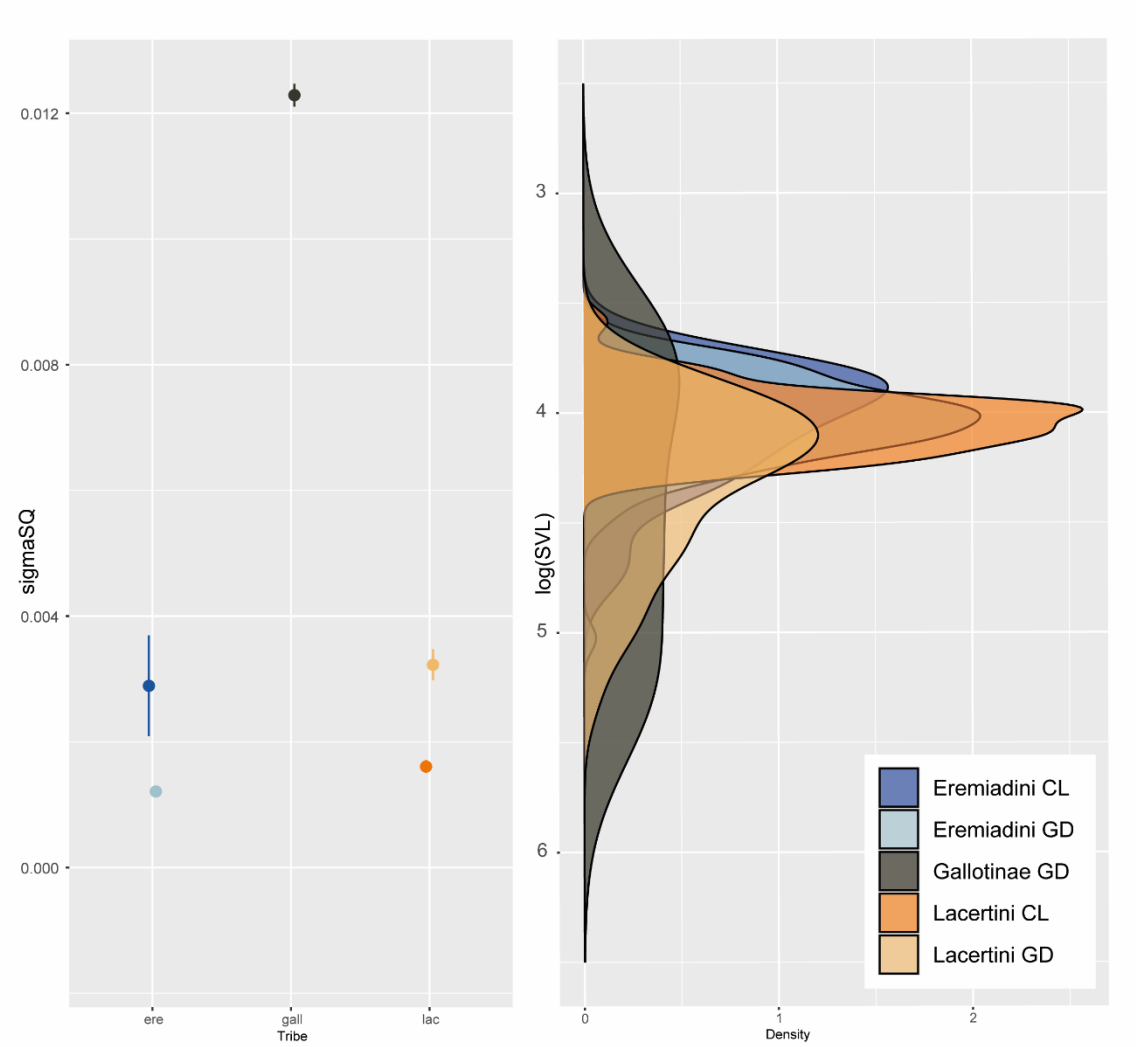

Figure 3.4. Evolutionary rates (σ^2) from the multi-rate Brownian motion, selected as the best-fitting model (Tables S3.7 and S3.8) (left), and density of log(SVL) of the different phylogenetic and structural habitat groups (right). Colors indicate phylogenetic group: blue palette for Eremiadini, orange palette for Lacertini, and black for Gallotinae. Intensities indicate structural habitat use, with lighter colors for ground-dwelling (GD) species and dark colors for climbing (CL) species. For Gallotinae, no differentiation is presented because no CL species exist in this group.

Structural habitat can influence morphological evolution in different ways. In some cases, it may promote adaptation toward a narrow, specific morphological outcome, leading to convergence (Collar et al. 2010; Goodman et al. 2008) or it can foster morphological diversification, by creating opportunities for species to exploit diverse niches or by relaxing selective pressures (Alfaro et al. 2007; Collar et al. 2011; Simpson, 2019). Our results clearly demonstrate that structural habitat promotes diversification rather than adaptation toward habitat-specific optima in lacertid lizards. This is supported by the absence of significant differences in average body size between climbers and ground-dwellers, which, nonetheless, have been observed in other reptile groups (Collar et al. 2011), and by our best-fitting model of body size evolution. Lacertid lizards evolve under a multi-rate BM model (Table S3.7), which does not align with the hypothesis of directional adaptation toward optima specific to structural habitat (Cressler et al. 2015). Instead, different evolutionary rates are presented by climbers and ground-dwellers, as well as across phylogenetic groups (Table S3.8). First, the subfamily Gallotinae is clearly distinguishable in evolving more than three times faster than either of the two Lacertinae tribes in terms of body size (Table S3.8). This highlights the remarkably broad range of body size diversification within this group, which includes both some of the largest (e.g., *Gallotia simonyi*, SVL = 235.31 mm) and smallest (e.g., *Psammodromus microdactylus*, SVL = 43.43 mm) species of lacertids. This pattern may be at least partially driven by the island syndrome being expressed in *Gallotia* lizards of the Canary archipelago, which is a known promoter of higher evolutionary rates due to the distinctive evolutionary pressures that act on body size in island environments (Novosolov et al. 2013), although a more thorough study would be necessary to confirm this hypothesis. The miniaturization of some *Psammodromus* that occur in North Africa is more intriguing but could be related to climatic effects (see further on).

While insularity is a known driver of body size diversification rates, our results also pinpoint a clade-specific effect of habitat, previously unsuspected (Vanhooydonck & Van Damme, 1999), that accentuates the importance of putting ecologically driven variation in the context of coherent evolutionary groups. Among the Eremiadini, climbing species exhibit higher evolutionary rates than ground-dwelling ones, while this pattern is reversed among the Lacertini (Table S8). Here, contrasting patterns of species' diversification and a distinct evolutionary history between the two tribes may be at play. The Eremiadini are

arid-adapted species, which underwent fast radiation (Harris et al. 1998; Hipsley et al. 2014; Makokha et al. 2007) and are predominantly ground-dwelling (Figure 3.1). Here, climbing species are derived from several evolutionary events, which combine descendants of a climbing ancestor for the entire family (Figure S3.1, and see Vicent-Castelló et al. 2025 for a detailed treatment on Lacertid habitat evolution) and more recent shifts in certain branches. Such shifts were then probably accompanied by species-specific body size modifications, resulting in a greater range of body sizes, and higher evolutionary rates for the climbing species of Eremiadini. These evolutionary events are largely reversed in the Lacertini: here, most species maintain the ancestral climbing habitat use state and relatively uniform body sizes. Instead, recurrent instances of shifting toward ground-dwelling habits in different phylogenetic groups of very different ecological and biogeographical contexts most probably promoted diversification into a wide range of sizes, with the observable effects for body size evolution. These patterns suggest that, rather than following a consistent trend across the phylogeny, body size evolution is rather shaped by the specific conditions that underlay the diversification of habitat utilization. Depending on the evolutionary context, species end up utilizing the same microhabitat differently, resulting in discrepant ecological adaptations that promote high rates of size diversification and high levels of size disparity in the same habitat (Collar et al. 2011).

The importance of the evolutionary background for identifying ecological effects on morphological evolution is further exemplified in our system by different responses to climatic factors across phylogenetic clades. For the subfamily Gallotinae, we found no effect of climatic variables on body size variation, which is rather potentially driven by the distinctiveness of *Gallotia* lizards due to the island syndrome and their evolution toward herbivory (Barahona et al. 2000; Čerňanský al., 2016; Van Damme, 1999). On the other hand, we found contrasting patterns for the two Lacertinae tribes. Within the Lacertini, we found a significant, negative association between body size and precipitation seasonality (Table S3.6 and Figure 3.3), under a BM evolutionary model (Table S3.6). These results lend support to the “seasonality hypothesis” (Slavenko et al. 2019) for body size evolution in the Lacertini, though such an association seems to be occurring in a non-adaptive manner, as suggested by an underlying BM evolutionary model. As such, given the non-phylogenetic distribution of environmental factors it may rather be driven

by more recent, ecological-scale factors. The distribution of Lacertini species spans primarily temperate regions, with most of its diversity concentrated in the Mediterranean Basin (Arnold et al. 2007), which present marked wet and dry seasons. In such environments, fluctuations in precipitation and resource availability seem to exert a strong selective pressure on body size in these lizards. Therefore, the seasonality hypothesis emerges naturally in this context, resulting in smaller sizes due to short periods of growth (Slavenko et al. 2019), which will be beneficial to synchronize their activities, such as reproductive cycles and foraging, with favorable environmental conditions (Bauwens & Díaz-Uriarte, 1997; Sibly & Brown, 2007; Yom-Tov & Geffen, 2006).

The Eremiadini tribe presents a totally different trend from Lacertini. Eremiadini species seem to evolve smaller body sizes toward hotter environments, supporting the “heat conservation hypothesis,” as has been found in other ectotherms (Pincheira-Donoso et al. 2008; Zamora-Camacho et al. 2014). Again, this trend occurs under a BM evolutionary model, which suggests a recent association rather than deep-time adaptation to the environment. Responses to temperature seem to be the main driver leading body size evolution in Eremiadini. This tribe’s distribution across desert and semi-desertic regions (Harris et al. 1998) highlights the critical role of temperature as a selective pressure. In these arid environments, the extreme thermal variability will favor sizes that optimize fitness under such conditions. For example, in hotter and drier lowlands, smaller sizes would dominate as they would confer advantages in thermoregulation (fast thermoregulation and reduced risk of overheating) and activity patterns (Olalla-Tárraga & Rodríguez, 2007). In contrast, populations inhabiting colder or high-altitude environments exhibit larger body sizes, reflecting adaptations to low temperatures that facilitate the heat conservation (Blackburn et al. 1999). These patterns underscore how climatic gradients have shaped the morphological diversity and ecological specialization of Eremiadini, linking body size variation directly to the environmental challenges of their habitats. Although those patterns are significant across the two tribes, the percentage of variation explained by the model is quite limited (~3%), suggesting that other factors also contribute to the evolution of this morphological trait across phylogenetic scales, as we observed in the case of structural habitat for this family.

Our results highlight the importance of focusing on coherent taxonomic groups, understood as phylogenetically independent sets, for macroevolutionary studies, and how analyses at broad scales can misidentify evolutionary patterns (Henry et al. 2023; Slavenko et al. 2019). Our results indicate that no climatic variables significantly influence body size evolution at the family level. Similarly, the structural approach reveals a clear effect of this environmental axis in body size diversification within coherent, finer scale, taxonomic groups, but this effect is not observed at the family level. However, when digging into finer taxonomic groups, such as genus or intraspecific level, patterns different than the ones observed in this study are present within Lacertidae family, which in last instance are not mirrored at higher taxonomic scales (Liang et al. 2021; Volynchik, 2014). These findings suggest that the absence of general patterns in body size evolution does not negate the role of climate as an important driver of body size evolution (Collar et al. 2011; Olalla-Tárraga & Rodríguez, 2007). Instead, our analyses highlight the complex interplay of climatic variables across tribes, indicating that body size evolution in ectotherms is likely governed by context-dependent eco-evolutionary dynamics that vary with taxonomic and geographic scales. The pursuit of generalizing climate-driven patterns at broad taxonomic scales has posed considerable challenges in various studies (Johnson et al. 2023; Slavenko & Meiri, 2015; Slavenko et al. 2019). However, our findings suggest that instead of seeking broad-scale generalizations in evolutionary patterns of body size, focusing on evolutionary independent sets of species provides deeper insights into the evolutionary processes shaping these groups.

References

Alfaro, M. E., F. Santini, and C. D. Brock. 2007. Do reefs drive diversification in marine teleosts? evidence from the pufferfish and their allies (Order Tetraodontiformes). Evolution 61:2104–2126.

Arnold, E. N. 1998. Structural niche, limb morphology and locomotion in lacertid lizards (Squamata, Lacertidae); a preliminary survey. Bull. Nat. Hist. Mus., Zool 64:63–90.

Arnold, E. N., O. Arribas, and S. Carranza. 2007. Systematics of the Palaearctic and Oriental lizard tribe Lacertini (Squamata: Lacertidae: Lacertinae), with descriptions of eight new genera. Zootaxa 1430:1–86.

Arnold, S. 1983. Morphology, Performance and Fitness. Am. Zool. 23:347–361.

Baha El Din, S. M. 2007. A new lizard of the *Acanthodactylus scutellatus* group (Squamata: Lacertidae) from Egypt. Zool. Middle East. 40:21–32. Taylor & Francis.

Barahona, F., S. E. Evans, J. A. Mateo, M. García-Márquez, and L. F. López-Jurado. 2000. Endemism, gigantism and extinction in island lizards: the genus *Gallotia* on the Canary Islands. J. Zool. 250:373–388.

Bastide, P., M. Mariadassou, and S. Robin. 2017. Detection of Adaptive Shifts on Phylogenies by using Shifted Stochastic Processes on a Tree. J. R. Stat. Soc. Ser. B Stat. Method. 79:1067–1093.

Bauwens, D., and R. Díaz-Uriarte. 1997. Covariation of Life-History Traits in Lacertid Lizards: A Comparative Study. Am. Nat. 149:91–111. [The University of Chicago Press, The American Society of Naturalists].

Beaulieu, J. M., D.-C. Jhwueng, C. Boettiger, and B. C. O'Meara. 2012. Modeling Stabilizing Selection: Expanding the Ornstein–Uhlenbeck Model of Adaptive Evolution. Evolution 66:2369–2383.

Benítez-López, A., L. Santini, J. Gallego-Zamorano, B. Milá, P. Walkden, M. A. J. Huijbregts, and J. A. Tobias. 2021. The island rule explains consistent patterns of body size evolution in terrestrial vertebrates. Nat. Ecol. Evol. 5:768–786.

Bergmann, C. 1848. Über die Verhältnisse der Wärmeökonomie der Thiere zu ihrer Größe. Vandenhoeck und Ruprecht.

Blackburn, T. M., K. J. Gaston, and N. Loder. 1999. Geographic gradients in body size: a clarification of Bergmann's rule. Divers. Distrib. 5:165–174.

Blomberg, S. P., T. Garland, and A. R. Ives. 2003. Testing for phylogenetic signal in comparative data: behavioral traits are more labile. Evolution. 57:717–745.

Brown, J. H., P. A. Marquet, and M. L. Taper. 1993. Evolution of body size: consequences of an energetic definition of fitness. Am. Nat. 142:573–584.

Butler, M. A., and A. A. King. 2004. Phylogenetic Comparative Analysis: A Modeling Approach for Adaptive Evolution. Am. Nat. 164:683–695. The University of Chicago Press.

Caeiro-Dias, G., C. Luís, C. Pinho, P.-A. Crochet, N. Sillero, and A. Kaliontzopoulou. 2018. Lack of congruence of genetic and niche divergence in *Podarcis hispanicus* complex. J. Zool. Syst. Evol. Res. 56:479–492.

Cardillo, M., K. Jones, J. Bielby, O. Bininda-Emonds, W. Sechrest, D. Orme, and A. Purvis. 2005. Multiple Causes of High Extinction Risk in Large Mammal Species. Science (New York, N.Y.) 309:1239–41.

Čerňanský, A., J. Klembara, and K. T. Smith. 2016. Fossil lizard from central Europe resolves the origin of large body size and herbivory in giant Canary Island lacertids. Zool. J. Linn. Soc. 176:861–877.

Clavel, J., and H. Morlon. 2017. Accelerated body size evolution during cold climatic periods in the Cenozoic. PNAS. 114:4183–4188.

Collar, D. C., J. A. Schulte II, and J. B. Losos. 2011. Evolution of extreme body size disparity in monitor lizards (*Varanus*). Evolution. 65:2664–2680. Blackwell Publishing Inc Malden, USA.

Collar, D. C., J. A. Schulte, B. C. O'Meara, and J. B. Losos. 2010. Habitat use affects morphological diversification in dragon lizards. J. Evol. Biol. 23:1033–1049.

Cox, S. C., S. Carranza, and R. P. Brown. 2010. Divergence times and colonization of the Canary Islands by *Gallotia* lizards. Mol. Phylogenet. Evol. 56:747–757.

Cramer, B. S., K. G. Miller, P. J. Barrett, and J. D. Wright. 2011. Late Cretaceous–Neogene trends in deep ocean temperature and continental ice volume: Reconciling records of benthic foraminiferal geochemistry (δ18O and Mg/Ca) with sea level history. J. Geophys. Res.: Oceans 116.

Cressler, C. E., M. A. Butler, and A. A. King. 2015. Detecting adaptive evolution in Phylogenetic Comparative Analysis using the Ornstein–Uhlenbeck Model. Syst Biol 64:953–968.

Cushman, J. H., J. H. Lawton, and B. F. J. Manly. 1993. Latitudinal patterns in European ant assemblages: variation in species richness and body size. Oecologia 95:30–37.

Enríquez-Urzelai, U., F. Martínez-Freiría, I. Freitas, A. Perera, Í. Martínez-Solano, D. Salvi, G. Velo-Antón, and A. Kaliontzopoulou. 2022. Allopatric speciation, niche conservatism and gradual phenotypic change in the evolution of European green lizards. doi: 10.1111/jbi.14497. John Wiley & Sons.

ESRI. 2017. ArcGIS 10.5.1, ArcGIS Pro 2.0, and ArcGIS Earth 1.5 Enterprise Deployment. ESRI, California.

Etienne, R., S. Visser, T. Janzen, J. Olsen, H. Olff, and J. Rosindell. 2012. Can clade age alone explain the relationship between body size and diversity? Interface focus 2:170–9.

Fick, S. E., and R. J. Hijmans. 2017. WorldClim 2 New 1-km Spatial Resolution Climate Surfaces for Global Land Areas. Int. J. Climatol. 37, 4302-4315. Scientific Research Publishing.

Garcia-Porta, J., I. Irisarri, M. Kirchner, A. Rodríguez, S. Kirchhof, J. L. Brown, A. MacLeod, A. P. Turner, F. Ahmadzadeh, G. Albaladejo, J. Crnobrnja-Isailovic, I. De La Riva, A. Fawzi, P. Galán, B. Göçmen, D. J. Harris, O. Jiménez-Robles, U. Joger, O. Jovanović Glavaš, M. Karış, G. Koziel, S. Künzel, M. Lyra, D. Miles, M. Nogales, M. A. Oğuz, P. Pafilis, L. Rancilhac, N. Rodríguez, B. Rodríguez Concepción, E. Sanchez, D. Salvi, T. Slimani, A. S'khifa, A. T. Qashqaei, A. Žagar, A. Lemmon, E. Moriarty Lemmon, M. A. Carretero, S. Carranza, H. Philippe, B. Sinervo, J. Müller, M. Vences, and K. C. Wollenberg Valero. 2019. Environmental temperatures shape thermal physiology as well as diversification and genome-wide substitution rates in lizards. Nat. Commun. 10:4077.

Garcia-Porta, J., H. E. Morales, E. Gómez-Díaz, R. Sindaco, and S. Carranza. 2016. Patterns of diversification in islands: A comparative study across three gecko genera in the Socotra Archipelago. Mol. Phylogenet. Evol. 98:288–299.

Garcia-Porta, J., and T. J. Ord. 2013. Key innovations and island colonization as engines of evolutionary diversification: a comparative test with the Australasian diplodactyloid geckos. J. Evol. Biol. 26:2662–2680.

Goodman, B. A., D. B. Miles, and L. Schwarzkopf. 2008. Life on the rocks: habitat use drives morphological and performance evolution in lizards. Ecology. 89:3462–3471.

Goswami, A., and J. Clavel. 2024. Morphological evolution in a time of Phenomics. EcoEvoRxiv.

Gouveia, S. F., and I. Correia. 2016. Geographical clines of body size in terrestrial amphibians: water conservation hypothesis revisited. J. Biogeogr. 43:2075–2084.

Harris, D. J., E. N. Arnold, and R. H. Thomas. 1998. Rapid speciation, morphological evolution, and adaptation to extreme environments in South African sand lizards (Meroles) as revealed by mitochondrial gene sequences. Mol. Phylogenet. Evol. 10:37–48.

Hawkins, B. A., and J. H. Lawton. 1995. Latitudinal gradients in butterfly body sizes: is there a general pattern? Oecologia 102:31–36.

Henry, E., L. Santini, M. A. J. Huijbregts, and A. Benítez-López. 2023. Unveiling the environmental drivers of intraspecific body size variation in terrestrial vertebrates. Glob. Ecol. Biogeogr. 32:267–280.

Hijmans, R. J., M. Barbosa, A. Ghosh, and A. Mandel. 2024. geodata: Download Geographic Data.

Hijmans, R. J., J. van Etten, M. Sumner, J. Cheng, D. Baston, A. Bevan, R. Bivand, L. Busetto, M. Canty, B. Fasoli, D. Forrest, A. Ghosh, D. Golicher, J. Gray, J. A. Greenberg, P. Hiemstra, K. Hingee, A. Ilich, I. for M. A. Geosciences, C. Karney, M. Mattiuzzi, S. Mosher, B. Naimi, J. Nowosad, E. Pebesma, O. P. Lamigueiro,

E. B. Racine, B. Rowlingson, A. Shortridge, B. Venables, and R. Wueest. 2023. raster: Geographic Data Analysis and Modeling.

Hipsley, C. A., D. B. Miles, and J. Müller. 2014. Morphological disparity opposes latitudinal diversity gradient in lacertid lizards. Biol. Lett. 10:20140101. Royal Society.

Ho, L. S. T., C. Ane, R. Lachlan, K. Tarpinian, R. Feldman, Q. Yu, W. van der Bijl, J. Maspons, R. Vos, and P. Bastide. 2024. phylolm: Phylogenetic Linear Regression.

Huston, M. A., and S. Wolverton. 2011. Regulation of animal size by eNPP, Bergmann's rule and related phenomena. Ecol. Monogr. 81:349–405.

Hutchinson, G. E. 1978. An Introduction to Population Ecology. Yale University Press.

Hutchinson, G. E. 1957. Concluding Remarks. Cold Spring Harb Symp Quant Biol 22:415–427. Cold Spring Harbor Laboratory Press.

IUCN. 2022. The IUCN Red List of Threatened Species.

Ives, A. R. 2019. R^{2}s for Correlated Data: Phylogenetic Models, LMMs, and GLMMs. Syst. Biol. 68:234–251.

Johnson, J. V., C. Finn, J. Guirguis, L. E. B. Goodyear, L. P. Harvey, R. Magee, S. Ron, and D. Pincheira-Donoso. 2023. What drives the evolution of body size in ectotherms? A global analysis across the amphibian tree of life. Glob. Ecol. Biogeogr. 32:1311–1322.

Kaliontzopoulou, A., M. A. Carretero, and G. A. Llorente. 2010. Intraspecific ecomorphological variation: linear and geometric morphometrics reveal habitat-related patterns within *Podarcis bocagei* wall lizards. J. Evol. Biol. 23:1234–1244.

Kerkhoff, A. J., and B. J. Enquist. 2009. Multiplicative by nature: Why logarithmic transformation is necessary in allometry. J. Theor. Biol. 257:519–521.

Klompmaker, A. A., C. E. Schweitzer, R. M. Feldmann, and M. Kowalewski. 2015. Environmental and scale-dependent evolutionary trends in the body size of crustaceans. Proc. R. Soc. B. 282:20150440. Royal Society.

Kolmann, M. A., M. D. Burns, J. Y. K. Ng, N. R. Lovejoy, and D. D. Bloom. 2020. Habitat transitions alter the adaptive landscape and shape phenotypic evolution in needlefishes (Belonidae). Ecol. Evol. 10:3769–3783.

Kubota, U., R. D. Loyola, A. M. Almeida, D. A. Carvalho, and T. M. Lewinsohn. 2018. Body size and host range co-determine the altitudinal distribution of Neotropical tephritid flies. Web of Science. Blackwell Publishing.

LaBarbera, M. 1989. Analyzing Body Size as a Factor in Ecology and Evolution. Annual Review of Ecology, Evolution, and Systematics 20:97–117. Annual Reviews.

Liang, T., Z. Zhang, W. Dai, L. Shi, and C. Lu. 2021. Spatial patterns in the size of Chinese lizards are driven by multiple factors. Ecol. Evol. 11:9621–9630.

Makokha, J. S., A. M. Bauer, W. Mayer, and C. A. Matthee. 2007. Nuclear and mtDNA-based phylogeny of southern African sand lizards, Pedioplanis (Sauria: Lacertidae). Mol. Phylogenet. Evol. 44:622–633.

Martínez-Freiría, F., K. S. Toyama, I. Freitas, and A. Kaliontzopoulou. 2020. Thermal melanism explains macroevolutionary variation of dorsal pigmentation in Eurasian vipers. Sci Rep 10:16122. Nature Publishing Group.

Meiri, S. 2008. Evolution and ecology of lizard body sizes. Glob. Ecol. Biogeogr. 17:724–734.

Millien, V. 2006. Morphological evolution is accelerated among island mammals. PLoS Biol 4:e321.

Morlon, H., E. Lewitus, F. L. Condamine, M. Manceau, J. Clavel, and J. Drury. 2016. RPANDA: an R package for macroevolutionary analyses on phylogenetic trees. Methods in Ecol. Evol. 7:589–597.

Novosolov, M., P. Raia, and S. Meiri. 2013. The island syndrome in lizards. Glob. Ecol. Biogeogr. 22:184–191.

Olalla-Tárraga, M. Á., and M. Á. Rodríguez. 2007. Energy and interspecific body size patterns of amphibian faunas in Europe and North America: anurans follow Bergmann's rule, urodeles its converse. Glob. Ecol. Biogeogr. 16:606–617.

Olalla-Tárraga, M. Á., M. Á. Rodríguez, and B. A. Hawkins. 2006. Broad-scale patterns of body size in squamate reptiles of Europe and North America. J. Biogeogr. 33:781–793.

Pennell, M. W., J. M. Eastman, G. J. Slater, J. W. Brown, J. C. Uyeda, R. G. FitzJohn, M. E. Alfaro, and L. J. Harmon. 2014. geiger v2.0: an expanded suite of methods for fitting macroevolutionary models to phylogenetic trees. Bioinformatics 30:2216–2218.

Peters, R. H. 1986. The Ecological Implications of Body Size. Cambridge University Press.

Pierce, D. 2024. ncdf4: Interface to Unidata netCDF (Version 4 or Earlier) Format Data Files.

Pincheira-Donoso, D., D. J. Hodgson, and T. Tregenza. 2008. The evolution of body size under environmental gradients in ectotherms: why should Bergmann's rule apply to lizards? BMC Evol. Biol. 8:68.

Price, S. A., and S. S. B. Hopkins. 2015. The macroevolutionary relationship between diet and body mass across mammals. Biol. J. Linn. Soc. , doi: 10.1111/bij.12495.

R Core Team. 2021. R: A Language and Environment for Statistical Computing. R Foundation for Statistical Computing, Vienna. https://www.R-project.org.

Rabosky, D. L., M. Grundler, C. Anderson, P. Title, J. J. Shi, J. W. Brown, H. Huang, and J. G. Larson. 2014. BAMMtools: an R package for the analysis of evolutionary dynamics on phylogenetic trees. Methods in Ecol. Evol. 5:701–707.

Raia, P., and S. Meiri. 2011. The tempo and mode of evolution: body sizes of island mammals. Evolution. 65:1927–1934.

Revell, L. J. 2010. Phylogenetic signal and linear regression on species data. Methods in Ecol. Evol. 1:319–329.

Revell, L. J., M. A. Johnson, J. A. Schulte, J. J. Kolbe, and J. B. Losos. 2007. A Phylogenetic Test for Adaptive Convergence in Rock-Dwelling Lizards. Evolution. 61:2898–2912. [Society for the Study of Evolution, Wiley].

Schmidt-Nielsen, K. 1984. Scaling: Why is Animal Size So Important? Cambridge University Press.

Sibly, R. M., and J. H. Brown. 2007. Effects of body size and lifestyle on evolution of mammal life histories. PNAS. 104:17707–17712.

Simpson, G. G. 2019. The Major Features of Evolution. Columbia University Press.

Slavenko, A., A. Feldman, A. Allison, A. Bauer, M. Böhm, L. Chirio, G. Colli, I. Das, T. Doan, M. LeBreton, M. Martins, D. Meirte, Z. Nagy, C. Nogueira, O. Pauwels, D. Pincheira-Donoso, U. Roll, P. Wagner, Y. Wang, and S. Meiri. 2019. Global patterns of body size evolution in squamate reptiles are not driven by climate. Glob. Ecol. Biogeogr. doi: 10.1111/geb.12868.

Slavenko, A., and S. Meiri. 2015. Mean body sizes of amphibian species are poorly predicted by climate. J. Biogeogr. 42:1246–1254.

Smith, F. A., and S. K. Lyons (eds). 2013. Animal Body Size: Linking Pattern and Process across Space, Time, and Taxonomic Group. University of Chicago Press, Chicago, IL.

Stanley, S. M. 1973. An Explanation for Cope's Rule. Evolution 27:1–26. [Society for the Study of Evolution, Wiley].

Terribile, L. C., M. Á. Olalla-Tárraga, J. A. F. Diniz-Filho, and M. Á. Rodríguez. 2009. Ecological and evolutionary components of body size: geographic variation of venomous snakes at the global scale: snake body size variation. Biol. J. Linn. Soc.98:94–109.

Thomas, G. H., S. Meiri, and A. B. Phillimore. 2009. Body size diversification in *Anolis*: novel environment and island effects. Evolution. 63:2017–2030.

Troost, T. A., J. A. van Dam, B. W. Kooi, and E. Tuenter. 2009. Seasonality, Climate Cycles and Body Size Evolution. Math. Model. Nat. Phenom. 4:135–155.

Troyer, E. M., R. Betancur-R, L. C. Hughes, M. Westneat, G. Carnevale, W. T. White, J. J. Pogonoski, J. C. Tyler, C. C. Baldwin, G. Ortí, A. Brinkworth, J. Clavel, and D. Arcila. 2022. The impact of paleoclimatic changes on body size evolution in marine fishes. Proc. Natl. Acad. Sci. U S A. 119:e2122486119.

Uetz. 2023. The Reptile Database.

Van Damme, R. 1999. Evolution of Herbivory in Lacertid Lizards: Effects of Insularity and Body Size. Journal of Herpetology 33:663–674. SSAR. .

Vanhooydonck, B., and R. Van Damme. 1999. Evolutionary relationships between body shape and habitat use in lacertid lizards. Evol. Ecol. Res. 1:785–803.

Velasco, J. A., F. Villalobos, J. A. F. Diniz-Filho, S. Poe, and O. Flores-Villela. 2020. Macroecology and macroevolution of body size in *Anolis* lizards. Ecography 43:812–822.

Vervust, B., I. Grbac, and R. Van Damme. 2007. Differences in morphology, performance and behaviour between recently diverged populations of *Podarcis sicula* mirror differences in predation pressure. Oikos 116:1343–1352.

Vicent-Castelló, P., A. Herrel, D. J. Harris, and A. Kaliontzopoulou. 2025. Walking or hanging: the role of habitat use for body shape evolution in lacertid lizards. J. Evol. Biol. voaf003.

Volynchik, S. 2014. Climate-Related Variation in Body Dimensions within Four Lacertid Species. International J. Zool. 2014:795387.

Wilson, D. S. 1975. The Adequacy of Body Size as a Niche Difference. Am. Nat. 109:769–784. [University of Chicago Press, American Society of Naturalists].

Womack, M. C., and R. C. Bell. 2020. Two-hundred million years of anuran body-size evolution in relation to geography, ecology and life history. J. Evol. Biol. 33:1417–1432.

Yom-Tov, Y., and E. Geffen. 2006. Geographic variation in body size: the effects of ambient temperature and precipitation. Oecologia 148:213–218.

Zamora-Camacho, F. J., S. Reguera, and G. Moreno-Rueda. 2014. Bergmann's Rule rules body size in an ectotherm: heat conservation in a lizard along a 2200-metre elevational gradient. J. Evol. Biol. 27:2820–2828.

Chapter 4:

Walking or hanging: the role of habitat use for body shape evolution in lacertid lizards

4.1. Introduction

Understanding how species respond and adapt to their environment is central in evolutionary biology (Arnold, 1998; Collar et al. 2010; Elstrott & Irschick, 2004; Irschick & Garland, 2001; Kaliontzopoulou et al. 2010; Openshaw & Keogh, 2014; Outomuro et al. 2013). Habitat use imposes ecological restrictions and demands that may drive morphological and performance adaptations. Consequently, adaptation to similar environmental niches can result in evolutionary convergence (Collar et al. 2014; Stayton, 2006), as seen in exemplary evolutionary cases such as cichlid fishes of East African lakes (Muschick et al. 2012) or spider ecomorphs along the Hawaiian Islands (Blackledge & Gillespie, 2004). Convergence, examined under the ecomorphological paradigm (Aguilar-Puntriano et al. 2018; Collar et al. 2014; Friedman et al. 2016; Stayton, 2015)—where form and function (i.e., whole-organism performance, physiology) are the reflection of the adaptation to a specific ecological niche (Arnold, 1983)—, underscores the close relationship between functional performance, body size and shape, which reflects adaptation to specific ecological niches and environmental pressures (Herrel et al. 2002).

In particular, the shape of the body plays an essential role in the way organisms interact and survive in their environment. As such, body shape adaptations to the habitat have been recorded in various animal groups, including fishes (Friedman et al. 2020, 2021; Kolmann et al. 2020; Larouche et al. 2020; Martinez et al. 2021), dragonflies (Outomuro et al. 2013), frogs (Moen et al. 2016; Stepanova & Womack, 2020), salamanders (Baken & Adams, 2019), and lizards (Bedford & Christian, 1996; Thompson & Withers, 2005; Gray et al. 2019). Among these, lizards have been extensively used as model organisms in ecomorphology because they are very widespread and they utilize a great diversity of habitats (e.g., terrestrial, aquatic, semiaquatic, arboreal, fossorial, and desertic). Remarkably, among all the habitats that lizards occupy, there is a recurrent trend whereby ground-dwelling species transit and adapt to a type of habitat that requires extensive climbing (arboreal or saxicolous) (Collar et al. 2010, 2011; Melville & Swain, 2003; Revell et al. 2007). In this new habitat, selection on functional performance results in convergent evolution (Revell et al. 2007). The contrast between ground-dwelling and climbing environments revolves around how species navigate the structural dimension of the habitat. Saxicolous and tree-climbing species navigate upright and exploit the

vertical axis of the habitat, whereas ground-dwellers predominantly use the horizontal axis of the habitat. Differences in habitat exploitation imply different biomechanical requirements species need to fulfil. Species that move vertically need to cope with the effect of gravity, jump between adjacent rocks or trees, move along vertical surfaces with sufficient efficiency to escape from predators or use small crevices and tree cavities to hide from them (Arnold, 1998; Revell et al. 2007; Vanhooydonck & Van Damme, 1999). By contrast, species that move horizontally, tend to favour speed to escape from predators or to feed on prey in open areas, as well as a large visual field to better notice their surroundings when moving close to the ground (Herrel et al. 2002; Losos, 1990; Vanhooydonck & Van Damme, 2003). These functional requirements are expected to be reflected in the corresponding morphological traits (Goodman et al. 2008; Herrel et al. 2002). Indeed, many climbing lizards present shallower heads (Openshaw & Keogh, 2014; Paluh & Bauer, 2017; Revell et al. 2007) and shorter limbs, both beneficial in maintaining the centre of mass close to the substrate (Huie et al. 2021; Vanhooydonck & Van Damme, 1999, 2001). However, opposite patterns are also observed in some lizard groups regarding limb (Goodman et al. 2008; Revell et al. 2007) and head proportions (Kohlsdorf et al. 2001; Kulyomina et al. 2019; Miles, 2014; Zaaf & Van Damme, 2001). This discrepancy may arise because factors beyond habitat verticality, like substrate type or element broadness, could have influenced limb and head evolution (Aerts et al. 2000; Revell et al. 2007).

Ground-dwelling species, which occupy relatively simple and more open environments, generally present more robust heads and longer hindlimbs to favour sprint and speed over manoeuvrability (Herrel et al. 2002; Losos, 1990), as well as differences in fore to—hindlimb ratios (Goodman et al. 2008), but once again exceptions also exist (Jaksić et al. 1980; Kohlsdorf et al. 2008). Together, these contrasting patterns suggest that maybe there is no overarching trend in morphological adaptations to the use of vertical relative to horizontal substrates in lizards. Furthermore, these findings emphasize that the overall body shape does not always uniformly adapt in response to specific habitats. Different body components, such as the head, limbs, and trunk, serve distinct functional roles in ecological tasks and biomechanical functions, responding variably to environmental factors including habitat use but also, feeding, mating, and territory defence (Edwards et al. 2013; Herrel et al. 2002). Among lizards, the family Lacertidae, with over 360 species

(Uetz, 2023), is a particularly suitable system to investigate the morphological implications of differential habitat-axis utilization. Through this transcontinental radiation, Lacertids have colonized an extraordinary number of ecosystems throughout the Old World. Even though they present a highly conservative morphology (Arnold, 1987, 1989), several macro- and micro-evolutionary studies have examined functional performance and morphology to understand phenotypic evolution in this group. Although the single study that investigated the consequence of habitat use on general body shape at the macroscale in lacertid lizards, could not establish an evolutionary effect (Vanhooydonck & Van Damme, 1999), other findings hint at the complexity of the relationship between morphological diversity and habitat use. Indeed, climbing and ground-dwelling lacertids present discrepancies in terms of locomotor performance (Van Damme et al. 1998; Vanhooydonck & Van Damme, 2003; Vanhooydonck et al. 2000), the tactics to boost speed (stride length vs. stride frequency) (Vanhooydonck et al. 2002), and the number of vertebrae and their function in manoeuvring (Van Damme & Vanhooydonck, 2002). However, those differences do not translate into limb proportion differences or a trade-off between horizontal-running and climbing abilities (Aerts et al. 2000; Vanhooydonck & Van Damme, 1999, 2001). Nevertheless, a recent study found differences in claw morphology between ground-dwelling and vertical-climbing lacertid species (Baeckens et al. 2020). This supports the hypothesis of limb adaptations to habitat in this group and provides further evidence that the use of vertical surfaces may favour the evolution of morphological traits associated with climbing (Hipsley et al. 2014). In contrast with these mixed patterns of limb shape evolution, several studies have established evolutionary links between head shape and microhabitat both within and across lacertid species, where climbers present flatter and narrower heads (Arnold, 1998; Gomes et al. 2016; Kaliontzopoulou et al. 2010, 2012, 2015; Urošević et al. 2013). Furthermore, species inhabiting arid environments have been shown to exhibit convergent evolution of cranial structures (Edwards et al. 2012; Harris et al. 1998; Hipsley & Müller, 2017). These results highlight the need for a comprehensive approach to clarify how the contrast between using predominantly vertical versus horizontal habitats has contributed to body shape evolution in lacertid lizards. Here, we use the most complete Lacertidae phylogeny to date (Garcia-Porta et al. 2019), a comprehensive morphological dataset and state-of-the-art phylogenetic comparative tools to investigate the tempo and mode of body shape evolution as a response to these two structural habitat use axes, as well as adaptation

trends using a comparison between Ornstein–Uhlenbeck (OU) vs Brownian motion models of evolution (Cressler et al. 2015). The implementation of appropriate phylogenetic comparative methods is imperative in untangling the unknowns of body shape evolution in the family Lacertidae, as well as significantly updating the existing background on this topic. To this end, we divide species into two categories: ground-dwelling and climbing. We expect climbing species to have evolved towards having shorter limbs and longer trunks on the one hand, and flattened, longer, and narrower heads on the other, to cope with the functional demands that vertical habitat imposes. We also predict that ground-dwelling species will present longer hindlimbs and a lower forelimb over hindlimb ratio, which are advantageous for sprinting in open areas. In addition, we expect a more robust body with taller heads as it is expected to be favourable in ground-dwelling habitats. We also anticipate ground-dwelling species to exhibit a higher diversity of forms, since they are adapted to a more diverse habitat what are expected to have less evolutionary constraints in comparison to habitats occupied by climbing species. Finally, we test for convergent evolution within each of the two habitats, with the prediction of a lower level of convergence in ground-dwelling species. Assuming that climbing habitat imposes high selective pressures on morphological evolution, we predict a convergent pattern for species that move vertically.

4.2. Material and methods

4.2.1. Morphology and habitat use

We collected linear measurements of a total of 956 adult male specimens for 186 lacertid species, using different datasets (specimens from collections and field campaigns) covering 52.2% of the described species and including at least one species per genus of the family (Uetz, 2023). We measured eight ecologically and evolutionarily relevant linear features in order to capture general body shape, understood as the relative proportions of different body parts. Those measurements are: snout-vent length, head length, head width, head height, mouth length, hindlimb length, forelimb length, and trunk length (Figure 4.1). All measurements were taken to the closest 0.01 mm, employing electronic callipers and following the protocol in (Kaliontzopoulou et al. 2007), and we computed the mean value of each morphological trait per species (Supplementary Table S4.1). For downstream analyses, we log10-transformed all data and used snout-vent length as a measure of body size to obtain size-corrected linear biometric measurements

as the residuals from a phylogenetic regression using all species (Revell, 2009), as implemented in the function *phyl.resid* in the package “phytools” (Revell, 2012). This method allows to correct by size morphological data while accounting for species relatedness, which has been shown to avoid downstream type I error when working with phylogenetic comparative methods (Revell, 2009).

To explore the role of habitat use in the evolution of body shape, we divided the species into two groups: ground-dwellers and climbers. To classify species into one of the two habitat use groups, we conducted an extensive qualitative analysis, employing bibliographic review, consulting specific articles as well as general sources such as the reptile database (Uetz, 2023) and the IUCN red list (IUCN, 2022), among others (Supplementary Table S4.2). We classified as ground-dwelling lacertid species that spend most of their time on the ground, utilizing the horizontal axis of their habitat, independently of the type of substrate. The majority of *Acanthodactylus*, *Eremias*, *Lacerta*, and *Timon* species, among others, were placed in this category. This group also includes species that may use other structures such as rocks or shrubs on occasion, but not predominantly. The second type, climbers, refers to species that mainly employ the vertical axis of the habitat. Climbers are lizards that spend most of their time climbing and moving over vertical surfaces such as trees, shrubs, and rocky surfaces. We collapse all types of habitats that imply movements in the vertical axis, including both saxicolous and tree-climbing species, since lacertid species mainly use trunks rather than branches, which means that species primarily use broader surfaces. Therefore, both types of climbing structures are predicted to impose similar functional demands on lacertid morphologies (Foster et al. 2018; Tulli et al. 2011). These animals can use the ground in some circumstances, such as when escaping from predators, but it is not their preferred habitat. Species of the genera *Gastropholis*, *Takydromus*, *Algyroides*, *Dalmatolacerta*, some *Podarcis*, and others were considered as members of this category.

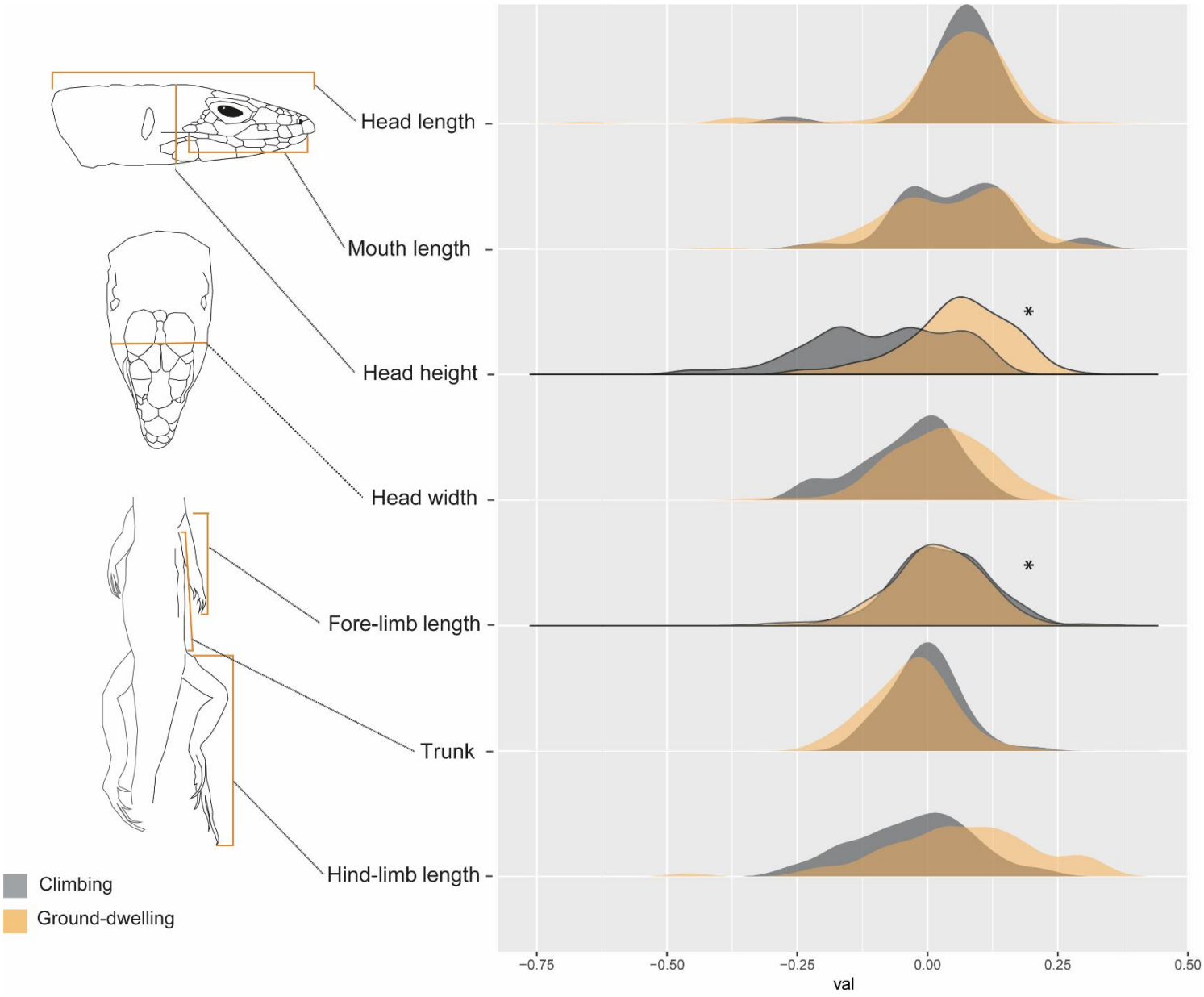

Figure 4.1. Generalized lacertid lizard outline (left) illustrating the seven morphological measurements considered and distribution of the log-transformed and size-corrected data coloured by habitat use category. The density curves with black outlines and asterisk are those that differed significantly in the phylogenetic ANOVAs.

4.2.2. Comparative analyses

To perform comparative analyses, we used the most complete and dated phylogeny of lacertid lizards published to date (Garcia-Porta et al. 2019) (Supplementary Figure S4.1). This dated phylogeny combines genomic and genetic data and reconstructs the evolutionary relationships of 246 species (see Garcia-Porta et al. 2019 for further information). We discarded the tips for which we had no morphological data for downstream morphological analyses (but see further on for how habitat use was reconstructed using the full phylogeny).

Phylogenetic signal

To explore morphological patterns of body shape evolution, we first evaluated the degree of phylogenetic signal in size-corrected morphological traits, by calculating Pagel's λ statistic (Pagel, 1999) using the *phylosig* function in the R package "phytools" (Revell, 2010). This parameter is a measure of the scaling of the phylogeny that is necessary to better fit the data to a Brownian motion model. We opted for this statistic due to its good performance and low level of type I error (Münkemüller et al. 2012). Values near 0 represent phylogenetic independence, whereas values closer to 1 indicate that traits are as similar as expected under a Brownian motion model of evolution. To test if the λ values were significantly different from 1, we performed a likelihood ratio test between the lambda model and a Brownian motion model. We would expect to find lower phylogenetic signal values for putative convergent traits, since high levels of phylogenetic signal would mean species resemble each other more because of their shared ancestral history rather than other external factors.

Morphospace occupancy

In order to describe morphological variation and morphospace occupancy across species we performed two principal component analyses (PCAs), where we separately considered two functional blocks of traits: head relative dimensions and body-limb shape (i.e., considering size-corrected traits of low collinearity, as described above). Then, we plotted the first and second components and projected the phylogeny onto PC space to form a phylomorphospace (Sidlauskas, 2008) using the function *geom_phylomorpho* implemented in the "deeptime" package (Gearty, 2023). Posteriorly, convex polygons were created for climbers and ground dwellers and for both PCAs using the *chull* function of the same R-package. To evaluate whether morphological disparity differed between

habitat groups, as expected if ground dwellers are under less restrictive selective pressures in comparison to climbers, and therefore displaying higher morphological disparity, we used the function *morphol.disparity* in the package "geomorph" (v.4.0.5) (Adams et al. 2022; Baken et al. 2021) and we tested its significance using a permutation procedure of 999 iterations.

Phylogenetic analyses of variance

To investigate if habitat use had an effect on the diversification of body shape in lacertid lizards, we first performed two phylogenetic multivariate analyses of variance (pMANOVA) to examine the effect of habitat use on head shape and the shape of the locomotor apparatus. We fitted linear models using the corresponding morphological traits per functional groups using the function *lm.rrpp* and *manova.update* implemented in the package "RRPP" (Collyer & Adams, 2018, 2023). Subsequently, in order to investigate whether habitat use has an effect on individual morphological traits, and whether significant differences exist in the fore-hind limb ratio between climbers and ground dwellers, we performed phylogenetic analysis of variance (pANOVA). We used each of the morphological traits separately as the dependent variable and habitat use as a predictor in the first case; and we compared forelimb length vs hindlimb length, with habitat use as an interactive effect in the second case. We fitted linear models and evaluated their significance using residual randomization (RRPP), as implemented in the function *lm.rrpp* of the R package "RRPP" (Collyer & Adams, 2018, 2023).

Mode of evolution

To investigate how habitat use has influenced the tempo and mode of shape evolution, we first used stochastic character mapping as implemented in the function *make.simmaps* of the package "phytools" (Revell, 2012) to reconstruct the ancestral states of habitat preference across the phylogeny. Here, we used the complete phylogeny (before trimming it down to the species for which morphological data were available) to obtain a more accurate reconstruction. We fitted discrete trait evolutionary models based on two unordered state transition matrices (Supplementary Table S4.3). The first assumes transitions of equal frequency between trait states (equal rates: ER), while the second allows a different rate for each transition (all-rates-different: ARD). Based on the log-likelihoods of these models, we identified ARD as the best model to describe habitat use evolution in lacertids (Supplementary Table S4.4; see also *Results*

section). Using this model, we produced 1,000 simmaps to explore transitions between states and infer which state was the most probable ancestral habitat use for this lizard family.

Subsequently, we used the "OUwie" package (Beaulieu et al. 2012) and 100 simmaps randomly selected out of the 1,000 simulations to fit and compare different evolutionary models. First, we fitted a single-rate Brownian motion (BM1) that represents the null hypothesis of non-directional morphological evolution under a single evolutionary rate (σ^2), we also fitted a multiple rate Brownian motion (BMS), which allows for different evolutionary rates for ground-dwellers and climbers. Then, we fitted a second group of models that included a new parameter, θ. This parameter indicates the evolutionary tendency or optima of the data and has been used as evidence of adaptation (Cressler et al. 2015). We fitted a single-optimum OU, which has the same evolutionary peak (θ) for both habitats categories (OU1); a multiple optima Ornstein–Uhlenbeck (OUM), that allows for different evolutionary peaks for ground-dwellers and climbers; and finally, a multiple optima and multiple rate Ornstein–Uhlenbeck (OUMV), which allows both the optima and the evolutionary rate to vary depending on habitat use. Among OU-variant of the models, there is a parameter α, which represents the strength of the pull towards the evolutionary peak, that can be allowed to vary. We decided not to consider models that encompass variation in this parameter (i.e., OUMA and OUMVA) as the estimation of this parameter can affect others parameter estimations and can lead to model non-identifiability (Cooper et al. 2016; Friedman et al. 2021; Kaliontzopoulou & Adams, 2016). After fitting the models, we discarded model runs that presented negative eigenvalues, as these produce unreliable estimates (Beaulieu et al. 2012; Kolmann et al. 2020; Price & Hopkins, 2015). To compare model fit, we used the modified Akaike information criterion (AICc). When more than one model was equally supported (ΔAICc < 2), we chose the model with the least number of parameters as the best-supported model. Note that models with similar AICc values often provide qualitatively similar results because the same mode of evolution can be characterized by different sets of parameters (Grabowski et al. 2023). Finally, we generated 97.5% confidence intervals for all model parameters of the best-fit model using parametric bootstrapping as implemented in the *OUwie.boot* function in "OUwie" package (Beaulieu et al. 2012). Due to computational limitations, we selected 10 random simmaps and performed 10 bootstrap replicates for

OUMV and OUM models, while we performed 100 bootstrap replicates for BM1 and OU1 models.

Convergence

Finally, to test for convergent evolution among species belonging to each habitat type, we used pattern-based estimates to quantify the number of lineages that evolved independently towards the same phenotypic space. We used the package "convevol" (Stayton, 2015) to obtain different statistics which measure phenotypic similarity using distance-based approaches and we employed the statistics Ct1, Ct2, Ct3, and Ct4. This method is an updated version of the previous C1-4 (Stayton, 2015), to detect convergent patterns, but in this case, accounting for the time between tips. This method measures the phenotypic distance between species in specific moments in a time-scaled phylogeny. Ct1 measures the distance between two lineages in a specific time, as a proportion of the distance between the tips and the longest distance between the shared evolutionary trajectory. Ct2 captures the absolute magnitude of convergent change. Ct3 and Ct4 are standardized versions of Ct2, which divide this value by the total amount of phenotypic change in the convergence group (Ct3) or the total amount of phenotypic change in the entire clade (Ct4). We ran the analyses separately for each trait and in a multivariate manner for the two functional blocks (e.g., head and limbs) and both for ground-dwelling and climbing species. We created coherent groups by collapsing species to account only for the independent instances of the appearance of the character of interest (e.g., climbing and ground-dwelling), in order to avoid pairwise comparisons between sister taxa with the same state, as recommended by the authors (Grossnickle et al. 2024). We performed the analyses with 50 simulations using BM as an evolutionary model to test if each of the calculated Ct values was greater than expected by chance. The values of this parameter can range from negative to positive values, indicating divergence or convergence respectively (Grossnickle et al. 2024).

4.3. Results

We found that all morphological variables presented significant values of phylogenetic signal (Supplementary Table S4.5). Values for all variables ranged from 0.7 to 0.9, with

all of them significantly different from 1, except for hindlimb length, which was not statistically distinguishable from 1.

The PCA performed with the head relative dimensions accounted for 74.75% of morphological variation in the first two PC axes (Figure 4.2A, Supplementary Table S4.6a). The first principal component (PC1) is related to head relative size, since the magnitude and direction of the components are very similar, with head width being the most strongly correlated. The second principal component (PC2) captured a contrast between head length and mouth length, on one side, and head height and head width, on the other. The second PCA, focusing on the locomotor apparatus (limbs and trunk) (Figure 4.2B, Supplementary Table S4.6b), accounted for 89.2% of the variance in the first two PC axes. The first component (PC1), captured a negative correlation between trunk and limb relative lengths, correlating positively with the limbs and negatively with the trunk (Supplementary Table S4.6b). Across both trait morphospaces, the multivariate morphological disparity did not differ significantly between ground-dwellers and climbers (Supplementary Table S4.7).

The phylogenetic MANOVAs on functional shape blocks (head vs. body) showed that climbing and ground-dwelling species differed when considering the multivariate set of head morphological traits, but not the locomotor apparatus (Supplementary Table S4.8). When investigating the effect of habitat use on individual morphological traits, we found that head height and forelimb length were significantly different between climbers and ground-dwellers (Table 4.1). Climbers present flatter heads and longer forelimbs than ground-dwellers. Finally, we observed no significant difference between habitat groups in forelimb to hindlimb ratio.

The ancestral state reconstruction of habitat occupation indicated that the most probable ancestral state for the root of the family Lacertidae was a climber, being reconstructed in 86% of the stochastic character maps (Figure 4.3). Accordingly, we found that the most common transition was from climbing habitat to ground-dwelling habitat. Regarding the mean total time spent in each state, we observed that the ground-dwelling state

Table 4.1. Results of the phylogenetic ANOVAs conducted to test for differences across habitats in size-corrected morphological variables and to examine if the relationship between fore and hindlimb lengths varied between climbers and ground-dwellers (fore-limb ratio). d.f.: degrees of

freedom; R2: R squared; F: F-value; Z: Z-score. P-values are based on 1000 residual permutations and significant p-values (at α = 0.05) are highlighted in bold.

		d.f	SS	MS	R^2	F	Z	p-val
Head length	Habitat	1	0.001	0.001	0.009	1.599	0.927	0.182
	Residuals	184	0.165	0.001	0.991			
	Total	185	0.166					
Head width	Habitat	1	0.001	0.001	0.019	3.488	1.442	0.074
	Residuals	184	0.066	0.000	0.981			
	Total	185	0.067					
Head height	Habitat	1	0.012	0.012	0.109	22.469	3.314	**0.001**
	Residuals	184	0.100	0.001	0.891			
	Total	185	0.112					
Mouth length	Habitat	1	0.000	0.000	0.002	0.396	-0.019	0.522
	Residuals	184	0.061	0.000	0.998			
	Total	185	0.061					
Forelimb length	Habitat	1	0.001	0.001	0.027	5.131	1.851	**0.024**
	Residuals	184	0.049	0.000	0.973			
	Total	185	0.050					
Hindlimb length	Habitat	1	0.000	0.000	0.005	0.860	0.424	0.360
	Residuals	184	0.087	0.000	0.995			
	Total	185	0.088					
Trunk	Habitat	1	8.69E-05	8.69E-05	0.002	0.427	-0.001	0.515
	Residuals	184	0.037	0	0.998			
	Total	185	0.038					
Fore-hind limb ratio	HLL * Habitat	1	0.000	0.000	0.006	1.862	0.978	0.170
	Residuals	182	0.028	0.000	0.562			
	Total	185	0.050					

Table 4.2. Estimated parameters and confidence intervals (2.5%,97.5%) of the best evolutionary model (see Table S4.10) fitted to each of the seven morphological traits examined. θ: evolutionary optima; α: pull towards the evolutionary optima; σ2: evolutionary rates. Different parameters for

climbers (CL) and ground-dwellers (GD) are included when the model allows the parameters to change between habitat use categories.

Morphological trait	Best model	$\theta_{(CL)}$	$\theta_{(GD)}$	α	$\sigma^2_{(CL)}$	$\sigma^2_{(GD)}$
Head length	OUMV	0.0551 (0.0331,0.0665)	0.0533 (0.0254,0.0672)	0.1930 (0.1071,0.3503)	3.39E-03 (1.71E-03,4.74E-03)	5.45E-03 (3.12E-03,1.21E-02)
Head width	OUM	-0.0245 (-0.0823, -0.0200)	0.0190 (0.0109, 0.0873)	0.0324 (0.0221,0.0433)	6.41E-04 (4.26E-04,8.38E-04)	
Head height	OUM	-0.0883 (-0.2017, -0.0591)	0.0413 (0.0403-0.1719)	0.0391 (0.0221,0.0528)	1.08E-03 (7.20E-04,1.44E-03)	
Mouth length	BM1	-		-	3.27E-04 (2.57E-04,3.98E-04)	
Forelimb length	OU1	0.0070 (-0.0667, 0.0653)		0.0184 (0.0083,0.0399)	3.90E-04 (2.84E-04,5.63E-04)	
Hindlimb length	BM1	-		-	4.71E-04 (3.71E-04,5.92E-04)	
Trunk	OU1	-0.0164 (-0.0496, 0.0122)		0.0275 (0.0182,0.0508)	3.35E-04 (2.64E-04,4.99E-04)	

presented almost twice the time spent in the phylogeny than the climbing state (Supplementary Table S4.9).

Examination of evolutionary models of body shape evolution revealed different evolutionary regimes for different morphological traits (Supplementary Table S4.10). For mouth length and hindlimb length, the best-supported model was a single-rate Brownian motion. For forelimb length and trunk length, the best-fit model was a single-optimum Ornstein– Uhlenbeck (OU1). For head height and head width the best-fit model was a multiple optima Ornstein–Uhlenbeck. Finally, head length followed a multiple-rate and multiple-optima Ornstein–Uhlenbeck model (OUMV). Examination of model estimates revealed that ground-dwelling species are evolving towards larger values of head length, head height, and head width as compared to climbers (Table 4.2). In addition, ground-dwellers exhibited higher evolutionary rates than climbers for head length (Table 4.2).

Finally, when testing for convergence, according to Ct1-4 results, we found no significant signs of convergence or divergence neither in climbing nor in ground-dwelling species considering head morphology. Similarly, we did not find significant levels of convergence

or divergence in ground-dwelling or climbing limb proportions (Supplementary Table S4.11).

4.4. Discussion

How habitat use influences morphological evolution through demands on functional performance has been a major theme in evolutionary biology (Garland & Losos, 1994). In this study, we explored morphological responses to the requirements imposed by different habitats depending on the structural axis along which species move. We investigated the distinction between lacertid lizards that predominantly use vertical vs. horizontal habitat axes considering two morpho-functional trait blocks: the head and the locomotor apparatus. Although macroevolutionary inferences have been made using about half of the species in the Lacertidae family, our results suggest mixed effects of habitat use on body shape macroevolutionary patterns. We did not find support for the broad hypotheses of limb dissimilarities based on biomechanical expectations regarding the locomotor apparatus (Kaliontzopoulou et al. 2010). Instead, we only uncovered differences in the length of the forelimbs between climbers and ground-dwellers, in a direction opposite to our expectations. By contrast, habitat use had a major effect on the evolution of head shape in lacertids, where we found morphological adaptations to climbing, in accordance with those previously reported from other groups (Openshaw & Keogh, 2014; Revell et al. 2007), as well as adaptations to navigate in the horizontal axis of the habitat. Indeed, we showed that the morphological features of the head follow different evolutionary trajectories for climbers and ground dwellers.

Lacertid ancestry

The preferred habitats of the assumed closest relatives of lacertids had led researchers to hypothesize that the common ancestor of this family was a ground-dweller (Arnold, 1998). Indeed, the families Teiidae and Gymnophtalmidae have been considered the sister clades of the Lacertidae, and both present the typical ground-dwelling lifestyle (Vitt & Pianka, 2004; Zweifel, 1998). Our results, nonetheless, based on an ML-based

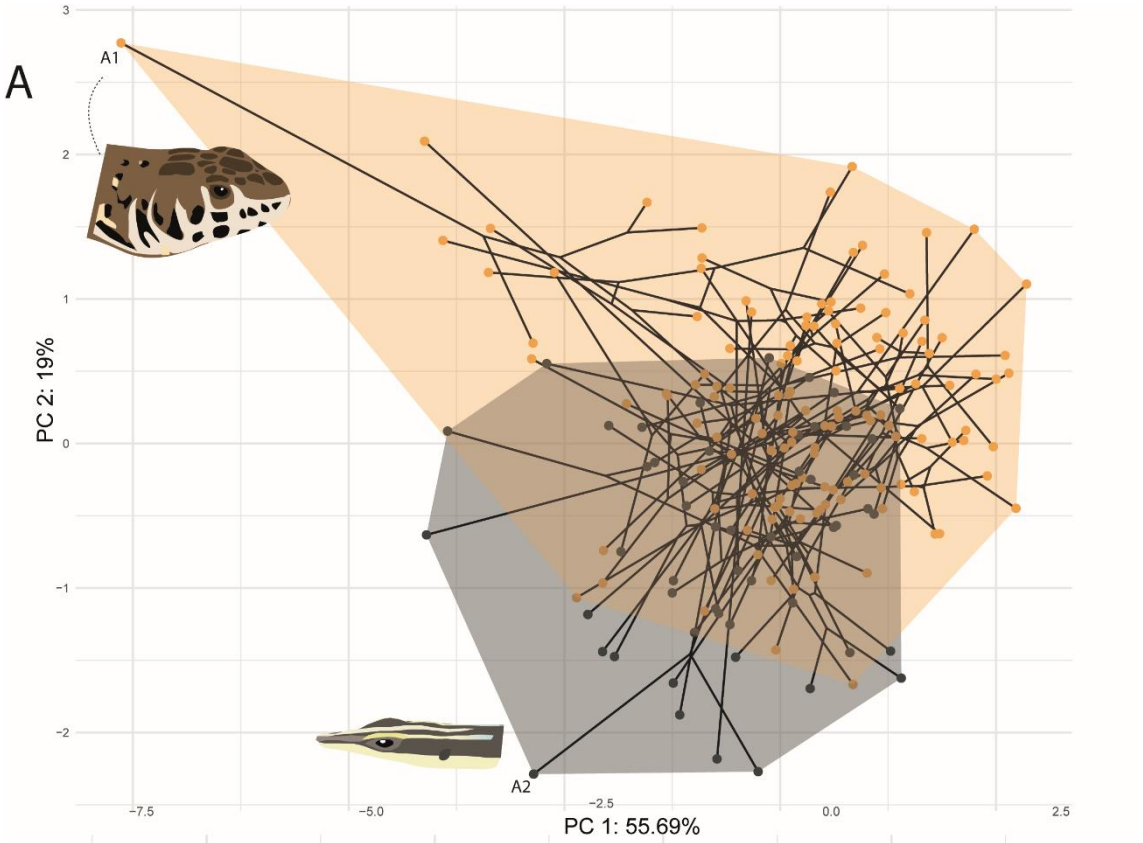
A
A1
A2
PC 2: 19%
PC 1: 55.69%
3
2
1
0
−1
−2
−7.5
−5.0
−2.5
0.0
2.5

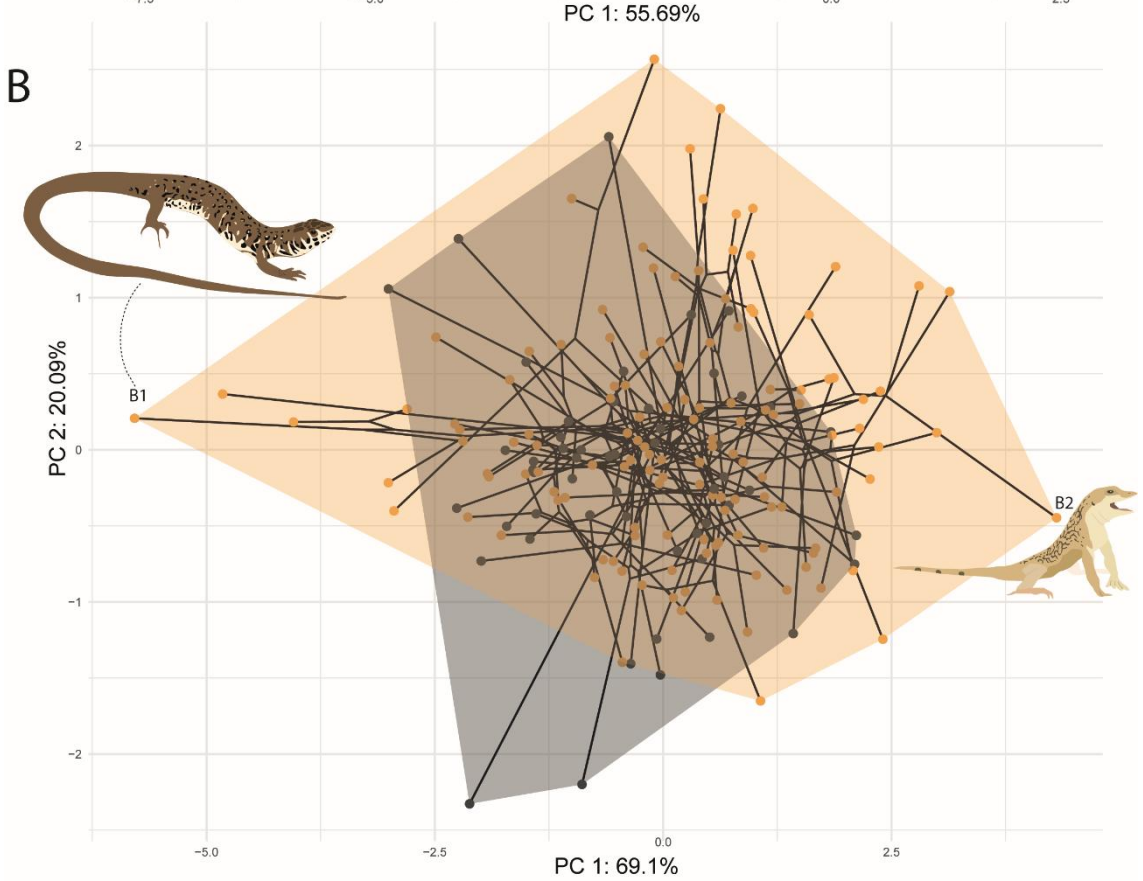
B
B1
B2
PC 2: 20.09%
PC 1: 69.1%
2
1
0
−1
−2
−5.0
−2.5
0.0
2.5

Figure 4.2. Phylomorphospace for the functional morphological trait blocks of head relative dimensions (A), and trunk and limb relative lengths (B). Each point represents a single species coloured by the correspondent habitat category. Illustrations represent the specific morphology in that part of the morphospace. A1: *Nucras lalandii*; A2: *Holaspis guentheri*; B1: *Nucras lalandii*; B2: *Meroles anchietae*.

reconstruction of habitat use, point in a different direction, and support the hypothesis that lacertids evolved from a climbing ancestor (Figure 4.3). This does not seem unreasonable, as species diversification of teiids and gymnophthalmids, on the one hand, and of lacertids, on the other, has occurred in very distant regions (New World vs Old World). Indeed, although these families share part of their evolutionary history (Vitt & Pianka, 2004) they diverged from each other 180 million years ago (Zheng & Wiens, 2016). Moreover, a recent phylogenomic inference of the deeper relationships of reptiles indicates that the sister clade of the Lacertidae is the Amphisbaenia, a group of limbless lizards (Zheng & Wiens, 2016) which presents mostly burrowing behaviours (Longrich et al. 2015). As such, the diversification of the Lacertoidea seems to have been dominated by frequent and radical ecological, morphological, and performance changes, making the estimation of the ancestral habitat use of lacertids from their relatives questionable. Nevertheless, a ground-dwelling common ancestor for amphisbaenians and lacertids, with an early adaptation to a climbing habitat for the Lacertidae ancestor, followed by a secondary occupation of the ground, also seems to be a plausible scenario.

Interestingly, the ancestral state reconstruction for lacertids suggests different dynamics of evolutionary transitions between habitat types than that observed in other lizards. A recurrent trend whereby species shift from a ground-dwelling to a climbing habitat has been implicitly observed in several groups (Collar et al. 2010, 2011; Melville & Swain, 2003; Revell et al. 2007). In these transitions, morphology undergoes specific modifications to cope with vertical requirements (Collar et al. 2010, 2010; Goodman et al. 2008; Revell et al. 2007). However, the directionality, frequency, and implications of these transitions have never been addressed in detail but have rather been a tacit product of morphological analyses. In these studies, most groups present a ground-dwelling ancestor and, therefore, adaptation typically occurs towards climbing. By contrast, our results highlight that, in lacertids, transitions from the vertical to the

horizontal axis have occurred at least six times more often than the reverse (Supplementary Table S4.9). Climbing habits are known to be biomechanically quite demanding and restrictive (Revell et al. 2007). As such, novel morphological adaptations to ground-dwelling could be acting as an evolutionary dead-end (Day et al. 2016). Such cases of the reverse transition—from climbing to the ground—have also been observed in particular species in other lizard groups (Collar et al. 2010), but they otherwise seem to be quite rare, making lacertids a unique example of this kind of evolutionary shift in habitat use.

Effects of habitat on phenotypic evolution

Demands of the climbing habitat type include elements such as the effect of gravity when climbing, vertical movements, jumping between adjacent rocks or branches, and hiding in small crevices when escaping from predators. These requirements are expected to affect performance and morphology (Arnold, 1983). Although previous studies found no morphological differences in limb proportions in lacertid lizards at different scales (Cordero et al. 2021; Gomes et al. 2016; Vanhooydonck & Van Damme, 1999), we identified significant variation in forelimb length but not in hindlimbs, the hindlimb to forelimb ratio, or trunk length, between climbers and ground-dwellers (Table 4.1). Although this result does not follow biomechanical expectations (Kaliontzopoulou et al. 2010), it is not striking for this group. Previous results illustrate a complex and not straightforward relationship in habitat–performance–morphology in lacertid lizards (Gomes et al. 2016). Accordingly, differences in limb length and body morphology associated with locomotor performance have not been observed (Aerts et al. 2000; Gomes et al. 2016; Vanhooydonck & Van Damme, 1999, 2001). In this study, we show that, when accounting for the phylogeny, climbing species present slightly longer forelimbs than ground-dwelling ones, which could be linked to locomotor mode. Nevertheless, the assessment of this relationship would require the analysis of quantitative performance data (e.g., speed, sprint speed, and climbing speed). In addition, other selective pressures could be acting on forelimb length evolution, such as the broadness of the surface (Revell et al. 2007) or the quantity of rocks in the habitat (Goodman et al. 2008).

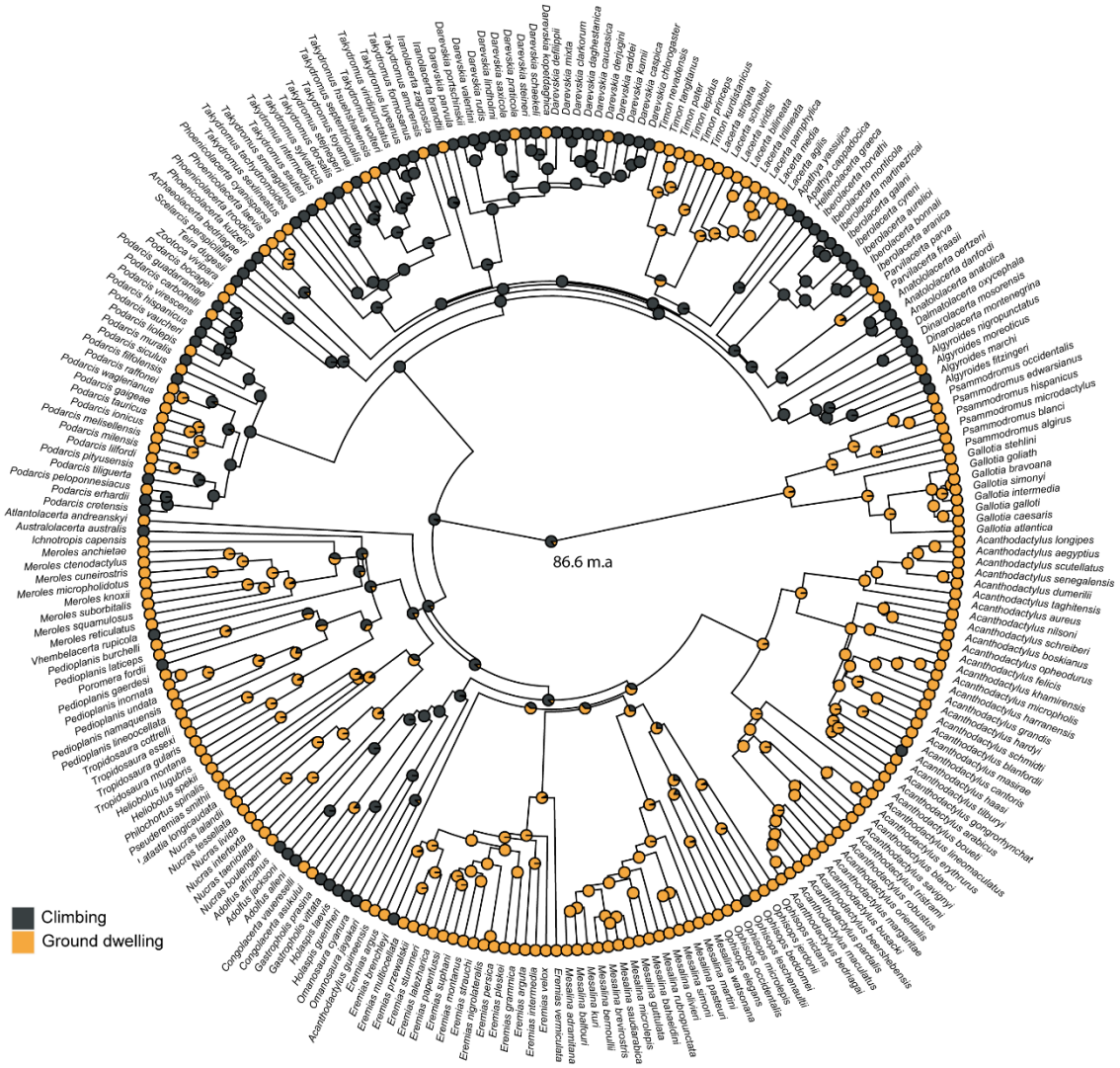

Figure 4.3. Evolution of habitat use in lacertid lizards reconstructed on the most recent phylogeny of the family with 246 species (obtained from Garcia-Porta et al. 2019) using the all-rates-different (ARD) transition matrix. The fraction of assignment to each state over the 100 simulations is represented by pie charts on the internal nodes. The circles at the tips represent the species' habitat use. The age of the node is presented. For further information, see Garcia-Porta et al. (2019).

In contrast with this limited differentiation of the locomotor apparatus, our results support the predictions made regarding the evolution of head shape in response to habitat use (Table 4.1). Climbing species present the typical flat head which helps them to, first, maintain the centre of mass of the body closer to the surface when climbing and, second, hide in small refugia when escaping from predators (Gomes et al. 2016; Goodman et al. 2008; Kaliontzopoulou et al. 2015; Kohlsdorf et al. 2008; Openshaw & Keogh, 2014; Revell et al. 2007). Since climbing species have the tendency to escape towards "known structures" such as holes and small crevices, and usually remain in the surroundings of the shelters (Diego- Rasilla, 2003; Vanhooydonck & Van Damme, 2003), escape behaviour is known to be a major determinant of morphological diversity in this group (Gomes et al. 2016; Husak & Fox, 2006). Therefore, natural selection would favour flatter heads for climbing lizards, which matches the observed patterns (Figure 4.1) and is also supported by evolution towards a lower evolutionary optimum for this morphological trait (Table 4.2). Ground-dwelling species, by contrast, present taller and more robust heads, which can be advantageous in horizontal habitats to have a broader vision to detect predators.

In addition to this apparently adaptive differentiation between climbers and ground-dwellers, where most head morphological traits follow a directional evolutionary model with two different adaptive optima (i.e., OUM, OUMV; Table 4.2, Supplementary Table S4.10), we also found evidence that habitat use has influenced the tempo of head shape evolution. Indeed, despite a lack of global differentiation in raw head shape disparity, when taking phylogeny into account we found that head length indeed evolved under different evolutionary rates (Table 4.2). Interestingly, the evolutionary optima estimated under this model for climbers and ground-dwellers are very similar, which translates into a lack of significant differences between present phenotypes (Figure 4.1). The apparent discrepancy between the evolutionary model in head length (OUMV) and the expected morphological output from it (i.e., no significant differences between groups in the phylogenetic ANOVA), may be a result of assuming a BM evolutionary model for ANOVAs, which is different from the best model. In terms of evolutionary rates, though, ground-dwelling species seem to have followed a faster pace of evolution for this morphological trait. This is expected as the ground-dwelling category encompasses species that explore a wide variety of structural habitats (deserts, forests floors,

grasslands, dunes, etc.), potentially affecting the diversification of this morphological trait (Collar et al. 2010). This pattern also matches the expectation that climbing species may present a narrower adaptive peak, and therefore a lower phenotypic rate, due to the restrictive nature of moving vertically (Collar et al. 2010; Kaliontzopoulou et al. 2015).

Convergence

Convergence can emerge due to constraints, random changes, or natural selection (Stayton, 2015). A typical convergent pattern of many lizard groups is observed in body shape among species adapted to climbing (Goodman & Isaac, 2008; Losos, 1992; Openshaw & Keogh, 2014; Revell et al. 2007), while a few cases of ground-dwelling convergence have also been reported (Gray et al. 2019; Huie et al. 2021). These convergence patterns can be performance-mediated, since the same ecological requirements in a specific habitat can lead to convergence in performance and also trigger convergence in morphology (Edwards, 2011). While this phenomenon was found in other lizard groups (Elstrott & Irschick, 2004; Losos, 1990), we did not identify indices of convergence in lacertid lizards.

Observing our results and contrary to expectations, we did not find any signs of convergence in the locomotor apparatus, neither in climbing nor in ground-dwelling lacertids (Supplementary Table S4.11). Nevertheless, taking into account the complex relationship between locomotor morphology and performance in this group (Gomes et al. 2016), the absence of limb convergence is far from surprising. It seems that locomotor performance and body shape are not responding in concert with similar selective pressures in lacertids. Rather, the selective pressures imposed by habitat may be acting on different performance and morphological aspects (Baeckens et al. 2020). For example, when examining the morphospace occupancy of the species (Figure 4.2B), we observe that, although both groups share the majority of the morphospace, some ground-dwelling species appear to be evolving towards different directions. One group, located in the left part of the morphospace, exhibits longer trunks and shorter limbs, while another group, in the right part, shows the opposite pattern with shorter trunks and longer limbs. This variation may be related to substrate type and escape strategies of ground-dwellers. Species on the right, such as those of the genera *Meroles*, *Eremias*, and *Acanthodactylus* are typically associated with sandy environments and are adapted to fast running (Edwards et al. 2016; MartÍn & López, 2003). In contrast, species like *Nucras*

and *Atlantolacerta*, found on the opposite extreme of the morphospace, are typically associated with rocky habitats and use short bursts of running to hide among rocks as their escape strategy (Huey et al. 1984, pers. observ). This suggests that, rather than climbing or ground-dwelling movement alone, other selective pressures may be influencing locomotor morphology in lacertid lizards.

In agreement with these results, our predictions regarding convergence in the shape of the head were neither confirmed by Ct measurements (Grossnickle et al. 2024). We expected both climbing and ground-dwelling heads to present significant levels of convergence, since the biomechanical constraints, stronger in climbing environments, would drive head morphology in the same direction for both groups. However, no signs of convergence were found in lacertid lizards (Table 4.2; Supplementary Table S4.11). This result is supported by the high levels of the phylogenetic signal of different morphological traits (Supplementary Table S4.5), which suggest that species resemble each other because of their shared evolutionary history rather than due to convergence processes. Moreover, disparity analyses showed no significant differences between the groups, further supporting the absence of convergence. Since neither group is converging towards a specific part of the morphospace, thereby reducing its disparity, no significant disparity differences were observed between both groups.

In contrast, we found that head-related traits follow a multi-optima Ornstein–Uhlenbeck model, which has been used as evidence of adaptation. In this case, ground-dwelling and climbing species evolve in different directions, each reaching an optimal head shape for their respective habitat use. However, the strength of selection exerted by each structural habitat does not seem sufficient to drive head shape evolution to be similar for all species occupying a specific habitat, as observed in other groups (Goodman & Isaac, 2008; Gray et al. 2019; Huie et al. 2021; Losos, 1992; Openshaw & Keogh, 2014; Revell et al. 2007). The level of specialization may be an important factor to consider, as in lacertid lizards, we observe highly specialized climbing and ground-dwelling species that may be driving morphological trends towards distinct optima. However, there is also a large group of species that fall between these two “putatively fully converged” morphologies (Figure 4.2A). Therefore, although the habitat imposes an adaptive regime on ground-dwelling and climbing heads, species may not have had enough time to converge. Alternatively, our classification of habitat use diversity in lacertids, which is

quite complex, into two distinct categories, may underlie these results. Although obtaining continuous habitat use data for such a wide number and diversity of species is at present not practically possible, the possibility remains that a future reanalysis of our data using continuous habitat-use data may further enhance evolutionary inferences. Nevertheless and more likely, according to our results, species are adapting to the same structural habitat (e.g., climbing or ground-dwelling) but are modifying different aspects of head shape, resulting in different morphologies that perform the same function (Thompson et al. 2017). Indeed, it has been demonstrated that head shape is involved in several ecological activities that can act on its evolution such as feeding, mating, or territory defense (Gomes et al. 2018; Herrel et al. 2001; Verwaijen et al. 2002). These ecological constraints could also affect head shape evolution. For example, while a climbing environment should drive heads to be narrower, sexual selection on males may act in the opposite direction to enhance bite force, thereby increasing mating success or success in male-male competition (Kaliontzopoulou et al. 2012). This highlights how different parts of morphology, although participating in the same functional task, can be selected differently to fulfil various ecological functions.

4.5. Conclusions

In conclusion, our findings highlight how lacertid lizards present specific but clear ecomorphological adaptations. They also show how similar selective pressures can act differently and produce different effects over different parts of an organism's body (Herrel et al. 2002). Indeed, the presence of different evolutionary rates and modes depending on the traits, highlights how different body regions can evolve differently even when they form part of the same functional block (Smith et al. 2016). Because of habitat-specific pressures, climbers and ground-dwelling species exhibit distinct head evolutionary trends, which become tangible when looking at head height differences. By contrast, the relationships between habitat, locomotor performance, and limb morphology remain complex for this lizard family. One element that appears to blur the relationship between form and function is the presence of a few highly specialized forms in response to habitat use among lacertids (Aerts et al. 2000). We find such species in both habitat categories. For example, *Dalmatolacerta oxycephala*, *Hellenolacerta graeca*, or species of the genus *Gastropholis* are extensively adapted to vertical locomotion. On the other hand,

species within genera such as *Acanthodactylus* or *Eremias* are found strictly in horizontal, open habitats. However, the bulk of lacertid lizards consists of species that, while displaying a clear preference for one habitat over another, may use other structures, such as the genus *Podarcis*. In this regard, the level of ecological specialization appears to be a determinant factor in morphological diversification and may also influence the detection of convergence in this study, since the broad habitat-use categories we have used may obscure real convergent patterns within the Lacertidae family. Lacertid lizards do not present a locomotor form clearly adapted to one habitat or another, instead, an all-purpose Bauplan appears to be selected for (Kaliontzopoulou et al. 2015). To meet particular locomotor requirements, some groups have developed specific structures, such as fringed toes in sand dwellers like some species within *Acanthodactylus*, prehensile tails in species of *Gastropholis*, rib expansion in species of *Holaspis* and longer tails in species of *Takydromus* (Hipsley et al. 2014). Thus, as is the case in geckos, these morphological structures may be blurring differentiation into distinct ecomorphs (Kulyomina et al. 2019; Zaaf & Van Damme, 2001). Ultimately, our study underscores that lacertid lizards embody an adaptable form, capable of both specialized and generalized responses to ecological pressures, contributing to a nuanced understanding of ecomorphological evolution in reptiles.

References

Adams, D. C., M. L. Collyer, and A. Kaliontzopoulou. 2022. Geomorph: Software for geometric morphometric analyses. R package version 4.0.4.

Aerts, P., R. Van Damme, B. Vanhooydonck, A. Zaaf, and A. Herrel. 2000. Lizard locomotion: how morphology meets ecology. Netherlands J. Zool. 50:261–277.

Aguilar-Puntriano, C., L. J. Avila, I. De la Riva, L. Johnson, M. Morando, J. Troncoso-Palacios, P. L. Wood Jr, and J. W. Sites Jr. 2018. The shadow of the past: Convergence of young and old South American desert lizards as measured by head shape traits. Ecol. Evol. 8:11399–11409.

Arnold, E. N. 1987. Resource partition among lacertid lizards in southern Europe. J. Zool. 211:739–782.

Arnold, E. N. 1998. Structural niche, limb morphology and locomotion in lacertid lizards (Squamata, Lacertidae); a preliminary survey. Bull. Nat. Hist. Mus., Zool 64:63–90.

Arnold, E. N. 1989. Towards a phylogeny and biogeography of the Lacertidae: relationships within an Old-World family of lizards derived from morphology. Bull. Nat. Hist. Mus., Zool. 55:209-257.

Arnold, S. 1983. Morphology, Performance and Fitness. Am. Zool. 23:347–361.

Baeckens, S., C. Goeyers, and R. Van Damme. 2020. Convergent Evolution of Claw Shape in a Transcontinental Lizard Radiation. Integr. Comp. Biol. 60:10–23.

Baken, E. K., and D. C. Adams. 2019. Macroevolution of arboreality in salamanders. Ecol. Evol. 9:7005–7016.

Baken, E. K., M. L. Collyer, A. Kaliontzopoulou, and D. C. Adams. 2021. geomorph v4.0 and gmShiny: Enhanced analytics and a new graphical interface for a comprehensive morphometric experience. Methods Ecol. Evol. 12:2355–2363.

Beaulieu, J. M., D.-C. Jhwueng, C. Boettiger, and B. C. O'Meara. 2012. Modelling Stabilizing Selection: Expanding the Ornstein–Uhlenbeck Model of Adaptive Evolution. Evolution. 66:2369–2383.

Bedford, G. S., and K. A. Christian. 1996. Tail morphology related to habitat of varanid lizards and some other reptiles. AMRE. 17:131–140.

Blackledge, T. A., and R. G. Gillespie. 2004. Convergent evolution of behavior in an adaptive radiation of Hawaiian web-building spiders. Proc. Natl. Acad. Sci. U S A. 101:16228–16233.

Collar, D. C., J. S. Reece, M. E. Alfaro, P. C. Wainwright, and R. S. Mehta. 2014. Imperfect Morphological Convergence: Variable Changes in Cranial Structures Underlie Transitions to Durophagy in Moray Eels. Am. Nat. 183:E168–E184.

Collar, D. C., J. A. Schulte II, and J. B. Losos. 2011. Evolution of extreme body size disparity in monitor lizards (*Varanus*). Evolution. 65:2664–2680. Blackwell Publishing Inc Malden, USA.

Collar, D. C., J. A. Schulte, B. C. O'Meara, and J. B. Losos. 2010. Habitat use affects morphological diversification in dragon lizards. J. Evol. Biol. 23:1033–1049.

Collyer, M. L., and D. C. Adams. 2018. RRPP: An r package for fitting linear models to high-dimensional data using residual randomization. Methods in Ecol. Evol. 9:1772–1779.

Collyer, M. L., and D. C. Adams. 2023. RRPP: Linear Model Evaluation with Randomized Residuals in a Permutation Procedure.

Cooper, N., G. H. Thomas, and R. G. FitzJohn. 2016. Shedding light on the 'dark side' of phylogenetic comparative methods. Methods in Ecol. Evol. 7:693–699.

Cordero, G. A., A. Maliuk, X. Schlindwein, I. Werneburg, and O. Yaryhin. 2021. Phylogenetic patterns and ontogenetic origins of limb length variation in ecologically diverse lacertine lizards. Biol. J. Linn. Soc.132:283–296.

Cressler, C. E., M. A. Butler, and A. A. King. 2015. Detecting adaptive evolution in Phylogenetic Comparative Analysis using the Ornstein–Uhlenbeck Model. Syst. Biol. 64:953–968.

Day, E. H., X. Hua, and L. Bromham. 2016. Is specialization an evolutionary dead end? Testing for differences in speciation, extinction and trait transition rates across diverse phylogenies of specialists and generalists. J. Evol. Biol. 29:1257–1267.

Diego-Rasilla, F. J. 2003. Influence of predation pressure on the escape behaviour of *Podarcis* muralis lizards. Behav. Process. 63:1–7.

Edwards, S. 2011. Convergence in Morphology is Preceded by Convergence in Performance in Lizards. P. in Lizards: Thermal ecology, genetic diversity and functional role in ecosystems. Nova Science Publishers.

Edwards, S., A. Herrel, B. Vanhooydonck, G. J. Measey, and K. A. Tolley. 2016. Diving in head first: trade-offs between phenotypic traits and sand-diving predator escape strategy in *Meroles* desert lizards. Biol. J. Linn. Soc.119:919–931.

Edwards, S., B. Vanhooydonck, A. Herrel, G. J. Measey, and K. A. Tolley. 2012. Convergent Evolution Associated with Habitat Decouples Phenotype from

Phylogeny in a Clade of Lizards. PLOS ONE 7:e51636. Public Library of Science.

Elstrott, J., and D. J. Irschick. 2004. Evolutionary correlations among morphology, habitat use and clinging performance in Caribbean *Anolis* lizards: COMPARATIVE CLINGING. Biol. J. Linn. Soc.83:389–398.

Foster, K. L., T. Garland Jr, L. Schmitz, and T. E. Higham. 2018. Skink ecomorphology: forelimb and hind limb lengths, but not static stability, correlate with habitat use and demonstrate multiple solutions. Biol. J. Linn. Soc.125:673–692.

Friedman, S. T., S. A. Price, K. A. Corn, O. Larouche, C. M. Martinez, and P. C. Wainwright. 2020. Body shape diversification along the benthic-pelagic axis in marine fishes. Proc. Biol. Sci. 287:20201053.

Friedman, S. T., S. A. Price, A. S. Hoey, and P. C. Wainwright. 2016. Ecomorphological convergence in planktivorous surgeonfishes. J. Evol. Biol. 29:965–978.

Friedman, S. T., S. A. Price, and P. C. Wainwright. 2021. The Effect of Locomotion Mode on Body Shape Evolution in Teleost Fishes. Integr. Org. Biol. 3:obab016.

Garcia-Porta, J., I. Irisarri, M. Kirchner, A. Rodríguez, S. Kirchhof, J. L. Brown, A. MacLeod, A. P. Turner, F. Ahmadzadeh, G. Albaladejo, J. Crnobrnja-Isailovic, I. De La Riva, A. Fawzi, P. Galán, B. Göçmen, D. J. Harris, O. Jiménez-Robles, U. Joger, O. Jovanović Glavaš, M. Karış, G. Koziel, S. Künzel, M. Lyra, D. Miles, M. Nogales, M. A. Oğuz, P. Pafilis, L. Rancilhac, N. Rodríguez, B. Rodríguez Concepción, E. Sanchez, D. Salvi, T. Slimani, A. S'khifa, A. T. Qashqaei, A. Žagar, A. Lemmon, E. Moriarty Lemmon, M. A. Carretero, S. Carranza, H. Philippe, B. Sinervo, J. Müller, M. Vences, and K. C. Wollenberg Valero. 2019. Environmental temperatures shape thermal physiology as well as diversification and genome-wide substitution rates in lizards. Nat. Commun. 10:4077.

Garland, T., and J. B. Losos. 1994. Ecological morphology of locomotor performance in squamate reptiles. P. in Ecological Morphology: IOB. University of Chicago Press, Chicago.

Gearty, W. 2023. deeptime: Plotting Tools for Anyone Working in Deep Time.

Gomes, V., M. A. Carretero, and A. Kaliontzopoulou. 2018. Run for your life, but bite for your rights? How interactions between natural and sexual selection shape functional morphology across habitats. Naturwissenschaften 105:9.

Gomes, V., M. A. Carretero, and A. Kaliontzopoulou. 2016. The relevance of morphology for habitat use and locomotion in two species of wall lizards. Acta Oecologica 70:87–95.

Goodman, B. A., and J. L. Isaac. 2008. Convergent body flattening in a clade of tropical rock-using lizards (Scincidae: Lygosominae). Biol. J. Linn. Soc.94:399–411.

Goodman, B. A., D. B. Miles, and L. Schwarzkopf. 2008. Life on the rocks: habitat use drives morphological and performance evolution in lizards. Ecology. 89:3462–3471.

Grabowski, M., J. Pienaar, K. L. Voje, S. Andersson, J. Fuentes-González, B. T. Kopperud, D. S. Moen, M. Tsuboi, J. Uyeda, and T. F. Hansen. 2023. A Cautionary Note on “A Cautionary Note on the Use of Ornstein Uhlenbeck Models in Macroevolutionary Studies.” Syst. Biol. 72:955–963.

Gray, J. A., E. Sherratt, M. N. Hutchinson, and M. E. H. Jones. 2019. Evolution of cranial shape in a continental-scale evolutionary radiation of Australian lizards. Evolution. 73:2216–2229.

Grossnickle, D. M., W. H. Brightly, L. N. Weaver, K. E. Stanchak, R. A. Roston, S. K. Pevsner, C. T. Stayton, P. D. Polly, and C. J. Law. 2024. Challenges and advances in measuring phenotypic convergence. Evolution. qpae081.

Harris, D. J., E. N. Arnold, and R. H. Thomas. 1998. Rapid speciation, morphological evolution, and adaptation to extreme environments in South African sand lizards (*Meroles*) as revealed by mitochondrial gene sequences. Mol. Phylogenet. Evol. 10:37–48.

Herrel, A., E. De Grauw, and J. A. Lemos-Espinal. 2001. Head shape and bite performance in xenosaurid lizards. J. Exp. Biol. 290:101–107.

Herrel, A., J. Meyers, and B. Vanhooydonck. 2002. Relations between microhabitat use and limb shape in phrynosomatid lizards. Biol. J. Linn. Soc. 77:149–163.

Hipsley, C. A., D. B. Miles, and J. Müller. 2014. Morphological disparity opposes latitudinal diversity gradient in lacertid lizards. Biol. Lett. 10:20140101. Royal Society.

Hipsley, C. A., and J. Müller. 2017. Developmental dynamics of ecomorphological convergence in a transcontinental lizard radiation. Evolution. 71:936–948.

Huey, R. B., A. F. Bennett, H. John-Alder, and K. A. Nagy. 1984. Locomotor capacity and foraging behaviour of kalahari lacertid lizards. Anim. Behav. 32:41–50.

Huie, J. M., I. Prates, R. C. Bell, and K. De Queiroz. 2021. Convergent patterns of adaptive radiation between island and mainland *Anolis* lizards. Biol. J. Linn. Soc.134:85–110.

Husak, J. F., and S. F. Fox. 2006. Field use of maximal sprint speed by collared lizards (*Crotaphytus collaris*): compensation and sexual selection. Evolution 60:1888–1895.

Irschick, D., and T. Garland. 2001. Integrating Function and Ecology in Studies of Adaptation: Investigations of Locomotor Capacity as a Model System. Annu. Rev. Ecol. Syst. 32:367–396. Annual Reviews.

IUCN. 2022. The IUCN Red List of Threatened Species.

Jaksić, F. M., H. Núnez, and F. P. Ojeda. 1980. Body proportions, microhabitat selection, and adaptive radiation of *Liolaemus* lizards in central Chile. Oecologia 45:178–181.

Kaliontzopoulou, A., and D. C. Adams. 2016. Phylogenies, the Comparative Method, and the Conflation of Tempo and Mode. Syst. Biol. 65:1–15.

Kaliontzopoulou, A., D. C. Adams, A. Van Der Meijden, A. Perera, and M. A. Carretero. 2012. Relationships between head morphology, bite performance and ecology in two species of *Podarcis* wall lizards. Evol. Ecol. 26:825–845.

Kaliontzopoulou, A., M. A. Carretero, and D. C. Adams. 2015. Ecomorphological variation in male and female wall lizards and the macroevolution of sexual dimorphism in relation to habitat use. J. Evol. Biol. 28:80–94.

Kaliontzopoulou, A., M. A. Carretero, and G. A. Llorente. 2010. Intraspecific ecomorphological variation: linear and geometric morphometrics reveal habitat-related patterns within *Podarcis bocagei* wall lizards. J. Evol. Biol. 23:1234–1244.

Kaliontzopoulou, A., M. A. Carretero, and G. A. Llorente. 2007. Multivariate and geometric morphometrics in the analysis of sexual dimorphism variation in *Podarcis* lizards. J. Morphol. 268:152–165.

Kohlsdorf, T., T. Garland Jr., and C. A. Navas. 2001. Limb and tail lengths in relation to substrate usage in *Tropidurus* lizards. J. Morphol. 248:151–164.

Kohlsdorf, T., M. B. Grizante, C. A. Navas, and A. Herrel. 2008. Head shape evolution in Tropidurinae lizards: does locomotion constrain diet? J. Evol. Biol. 21:781–790.

Kolmann, M. A., M. D. Burns, J. Y. K. Ng, N. R. Lovejoy, and D. D. Bloom. 2020. Habitat transitions alter the adaptive landscape and shape phenotypic evolution in needlefishes (Belonidae). Ecol. Evol. 10:3769–3783.

Kulyomina, Y., D. S. Moen, and D. J. Irschick. 2019. The relationship between habitat use and body shape in geckos. J. Morphol. 280:722–730.

Larouche, O., B. Benton, K. A. Corn, S. T. Friedman, D. Gross, M. Iwan, B. Kessler, C. M. Martinez, S. Rodriguez, H. Whelpley, P. C. Wainwright, and S. A. Price. 2020. Reef-associated fishes have more maneuverable body shapes at a macroevolutionary scale. Coral Reefs 39:1427–1439.

Longrich, N. R., J. Vinther, R. A. Pyron, D. Pisani, and J. A. Gauthier. 2015. Biogeography of worm lizards (Amphisbaenia) driven by end-Cretaceous mass extinction. Proc. R. Soc. B. 282:20143034. Royal Society.

Losos, J. B. 1992. The Evolution of Convergent Structure in Caribbean *Anolis* Communities. Syst. Biol. 41:403–420.

Losos, J. B. 1990. The evolution of form and function: morphology and locomotor performance in West Indian *Anolis* lizards. Evolution. 44:1189–1203.

MartÍn, J., and P. López. 2003. Changes in the Escape Responses of the Lizard *Acanthodactylus erythrurus* under Persistent Predatory Attacks. cope 2003:408–413. ASIH. .

Martinez, C. M., S. T. Friedman, K. A. Corn, O. Larouche, S. A. Price, and P. C. Wainwright. 2021. The deep sea is a hot spot of fish body shape evolution. Ecol. Lett. 24:1788–1799.

Melville, J., and R. Swain. 2003. Evolutionary correlations between escape behaviour and performance ability in eight species of snow skinks (*Niveoscincus*: Lygosominae) from Tasmania. J. Zool. 261:79–89.

Miles, D. B. 2014. Covariation between morphology and locomotor performance in sceloporine lizards. Pp. 207–236 in L. J. Vitt and E. R. Pianka, eds. Lizard ecology: historical and experimental perspectives. Princeton University Press.

Moen, D. S., H. Morlon, and J. J. Wiens. 2016. Testing Convergence Versus History: Convergence Dominates Phenotypic Evolution for over 150 Million Years in Frogs. Syst. Biol. 65:146–160.

Münkemüller, T., S. Lavergne, B. Bzeznik, S. Dray, T. Jombart, K. Schiffers, and W. Thuiller. 2012. How to measure and test phylogenetic signal. Methods in Ecol. Evol. 3:743–756.

Muschick, M., A. Indermaur, and W. Salzburger. 2012. Convergent evolution within an adaptive radiation of cichlid fishes. Curr. Biol. 22:2362–2368.

Openshaw, G. H., and J. S. Keogh. 2014. Head shape evolution in monitor lizards (*Varanus*): interactions between extreme size disparity, phylogeny and ecology. J. Evol. Biol. 27:363–373.

Outomuro, D., K.-D. B. Dijkstra, and F. Johansson. 2013. Habitat variation and wing coloration affect wing shape evolution in dragonflies. J. Evol. Biol. 26:1866–1874.

Pagel, M. 1999. Inferring the historical patterns of biological evolution. Nature. 401:877–884. Nature Publishing Group.

Paluh, D. J., and A. M. Bauer. 2017. Comparative skull anatomy of terrestrial and crevice-dwelling *Trachylepis* skinks (Squamata: Scincidae) with a survey of resources in scincid cranial osteology. PLoS One. 12:e0184414.

Price, S. A., and S. S. B. Hopkins. 2015. The macroevolutionary relationship between diet and body mass across mammals. Biol. J. Linn. Soc. doi: 10.1111/bij.12495.

Revell, L. J. 2010. Phylogenetic signal and linear regression on species data. Methods in Ecol. Evol. 1:319–329.

Revell, L. J. 2012. phytools: an R package for phylogenetic comparative biology (and other things). Methods Ecol. Evol. 3:217–223.

Revell, L. J. 2009. Size-Correction and Principal Components for Interspecific Comparative Studies. Evolution. 63:3258–3268.

Revell, L. J., M. A. Johnson, J. A. Schulte, J. J. Kolbe, and J. B. Losos. 2007. A Phylogenetic Test for Adaptive Convergence in Rock-Dwelling Lizards. Evolution 61:2898–2912. [Society for the Study of Evolution, Wiley].

Sidlauskas, B. 2008. Continuous and Arrested Morphological Diversification in Sister Clades of Characiform Fishes: A Phylomorphospace Approach. Evolution. 62:3135–3156.

Smith, K. R., V. Cadena, J. A. Endler, W. P. Porter, M. R. Kearney, and D. Stuart-Fox. 2016. Colour change on different body regions provides thermal and signalling advantages in bearded dragon lizards. Proc. R. Soc. B. 283:20160626. Royal Society.

Stayton, C. T. 2006. Testing Hypotheses of Convergence with Multivariate Data: Morphological and Functional Convergence Among Herbivorous Lizards. Evolution. 60:824–841.

Stayton, C. T. 2015. The definition, recognition, and interpretation of convergent evolution, and two new measures for quantifying and assessing the significance of convergence. Evolution. 69:2140–2153.

Stepanova, N., and M. C. Womack. 2020. Anuran limbs reflect microhabitat and distal, later-developing bones are more evolutionarily labile*. Evolution. 74:2005–2019.

Thompson, C., N. Ahmed, T. Veen, C. Peichel, A. Hendry, D. Bolnick, and Y. Stuart. 2017. Many-to-one form-to-function mapping weakens parallel morphological evolution. Evolution. 71:2738–2749.

Thompson, G., and P. Withers. 2005. The relationship between size-free body shape and choice of retreat for Western Australian *Ctenophorus* (Agamidae) dragon lizards. AMRE. 26:65–72.

Tulli, M. J., V. Abdala, and F. B. Cruz. 2011. Relationships among morphology, clinging performance and habitat use in Liolaemini lizards. J. Evol. Biol. 24:843–855.

Uetz. 2023. The Reptile Database.

Urošević, A., K. Ljubisavljević, and A. Ivanović. 2013. Patterns of cranial ontogeny in lacertid lizards: morphological and allometric disparity. J. Evol. Biol. 26:399–415.

Van Damme, R., P. Aerts, and B. Vanhooydonck. 1998. Variation in morphology, gait characteristics and speed of locomotion in two populations of lizards. Biol. J. Linn. Soc.63:409–427.

Van Damme, R., and B. Vanhooydonck. 2002. Speed versus manoeuvrability: association between vertebral number and habitat structure in lacertid lizards. J. Zool. 258:327–334.

Vanhooydonck, B., and R. Van Damme. 1999. Evolutionary relationships between body shape and habitat use in lacertid lizards. Evol. Ecol. Res. 1:785–803.

Vanhooydonck, B., and R. Van Damme. 2001. Evolutionary trade-offs in locomotor capacities in lacertid lizards: are splendid sprinters clumsy climbers? J. Evol. Biol. 14:46–54.

Vanhooydonck, B., and R. Van Damme. 2003. Relationships between locomotor performance, microhabitat use and antipredator behaviour in lacertid lizards. Funct. Ecol.17:160–169.

Vanhooydonck, B., R. Van Damme, and P. Aerts. 2000. Ecomorphological correlates of habitat partitioning in Corsican lacertid lizards. Funct. Ecol.

Vanhooydonck, B., R. Van Damme, and P. Aerts. 2002. Variation in speed, gait characteristics and microhabitat use in lacertid lizards. J. Exp. Biol. 205:1037–1046.

Verwaijen, D., R. Van Damme, and A. Herrel. 2002. Relationships between head size, bite force, prey handling efficiency and diet in two sympatric lacertid lizards. Funct. Ecol.16:842–850.

Vitt, L. J., and E. R. Pianka. 2004. Historical patterns in lizard ecology: what teiids can tell us about lacertids. Pp. 139–157 in V. Pérez-Mellado and A. Perera, eds. The Biology of Lacertid lizards. Evolutionary and Ecological Perspectives. Institut Menorquí d'Estudis. Recerca.

Zaaf, A., and R. Van Damme. 2001. Limb proportions in climbing and ground-dwelling geckos (Lepidosauria, Gekkonidae): a phylogenetically informed analysis. Zoomorphology. 121:45–53.

Zheng, Y., and J. J. Wiens. 2016. Combining phylogenomic and supermatrix approaches, and a time-calibrated phylogeny for squamate reptiles (lizards and snakes) based on 52 genes and 4162 species. Mol. Phylogenet. Evol. 94:537–547.

Zweifel, R. G. 1998. Encyclopedia of Reptiles & Amphibians. Academic Press.

Chapter 5:

Variable yet ubiquitous: Hierarchical scaling of head functional morphology in lizards

5.1. Introduction

Understanding the organization of phenotypic variation across hierarchical levels of biological complexity is crucial for comprehending the evolutionary mechanisms that shape patterns of biodiversity (Hansen and Martins 1996; Hallgrimsson and Hall 2005; Kaliontzopoulou et al. 2018; Simon et al. 2025a). Ecological pressures experienced by individuals at the population level can be strong enough to drive phenotypic divergence, leading to the emergence of macroevolutionary patterns that persist across higher biological levels, from individuals to populations, up to species, indicating that the mechanisms driving diversification may be uniform across these levels (Hansen and Martins 1996; Kaliontzopoulou et al. 2018; Taverne et al. 2021; Woodgate et al. 2025). Individuals harbor genetic and phenotypic variation that is selected through survival and reproduction (Lande 1976). Selective pressures and other evolutionary processes such as drift cause variation among individuals and give rise to variation in populations, which, if reinforced through divergence mechanisms (e.g., reproductive isolation), may gradually translate into phenotypic variation among different species (Turelli et al. 2001). This process often follows genetic and phenotypic lines of least resistance (Schluter 1996; McGlothlin et al. 2018; Rhoda et al. 2023; Tejero-Cicuéndez et al. 2023), where selection acts preferentially on traits that exhibit the greatest variation within populations, shaping long-term evolutionary trajectories. However, the selective landscape is rarely uniform, and organisms are exposed to a wide range of ecological pressures that vary across spatial and temporal scales (Arnold et al. 2001). These pressures interact with intrinsic constraints—such as developmental limitations or biomechanical trade-offs—which can restrict the range of possible phenotypic outcomes (Vermeij 1973; Collar et al. 2009). As a result, variation may be highly specific to each biological level, with microevolutionary trends at the population level not always translating predictably into macroevolutionary patterns (Simon et al. 2025b).

Across biological levels, the study of the interplay between organismal structure and function is fundamental to understanding evolutionary processes that drive phenotypic variation (Arnold 1992; Herrel et al. 2001b; Wainwright 2007; Kaliontzopoulou et al. 2012, 2018; Taverne et al. 2021). Performance, often recognized as a primary target of natural selection, plays a crucial role in shaping fitness outcomes (Huey and Stevenson 1979; Arnold 1983; Thompson et al. 2017). Because selection acts directly on performance-

related traits, a strong relationship between size, form, and function is expected, particularly for morphological traits that contribute to variation in performance (Arnold 1983; Wainwright 2007; Irschick et al. 2008; Taylor and Thomas 2014; Cruz et al. 2021). However, while this relationship is often expected to follow a one-to-one correspondence based on biomechanical principles – such as for the vertebrate lower jaw (Wainwright and Shaw 1999) –, it also exhibits high levels of variability, not only within species but also across hierarchical levels of organization. Additionally, body size has a direct impact on performance and shape (Gould 1966; Herrel et al. 2008; Tseng 2013), thus it is also expected to constitute a critical factor influencing the form-function relationship. Size, although an integral part of the phenotype and can influence the form-function relationship in non-proportional ways (Mitchell et al. 2024, 2025). Therefore, accounting for size effects may be necessary to disentangle other form-specific functional adaptations from allometric constraints. Different and sometimes conflicting selective pressures act on these phenotypic systems, leading to redundancy, where different morphological trait combinations can result in similar functional outcomes (Mitchell et al. 2024). This phenomenon, known as many-to-one mapping (Wainwright et al. 2005), occurs when function depends on nonlinear form-function relationships or arises as a response to multivariate morphological systems (Wainwright et al. 2005; Thompson et al. 2017).

For example, biologists have widely used the relationship between head shape and biting performance in lizards to address numerous ecomorphological questions. (Herrel et al. 2001b; Verwaijen et al. 2002; Kaliontzopoulou et al. 2012; De Meyer et al. 2019; Cruz et al. 2021). Bite force plays a critical role in a wide range of biological and ecological functions, including mating, territory defense, male-male interactions (Huyghe et al. 2005) and feeding (Taverne et al. 2021), often reflecting the combined influence of natural and sexual selection (Kaliontzopoulou et al. 2012). As such, several selective pressures have been shown to influence the evolution of bite force through morphological adaptations of the head (Kaliontzopoulou et al. 2012) (e.g., habitat occupation, refuge use). Additionally, selective pressures may operate differently across hierarchical biological levels. For example, sexual selection typically acts at the individual level within species through processes such as male–male competition and mating success (Huyghe et al. 2005; Lappin and Husak 2005; Lappin et al. 2006; Husak 2008;

Gomes et al. 2018), whereas ecological pressures related to habitat occupation and refuge use tend to structure phenotypic variation at broader population or species levels, reflecting differences among habitats and ecological niches (Kaliontzopoulou et al. 2012; Vicent-Castelló et al. 2025).

The biomechanical relationship between head dimensions and bite force has been repeatedly investigated, showing that a simple linear relation is not the rule for this form-function system (Herrel et al. 2001b; Verwaijen et al. 2002; De Meyer et al. 2019; Cruz et al. 2021). Indeed, head height and width have been shown to be strong, but not unique or universal, predictors of bite force, due to their influence on jaw adductor muscle size and orientation (Herrel et al. 2001b; Kaliontzopoulou et al. 2012). Moreover, it has been demonstrated that body size also plays a fundamental role in mediating these relationships, as both head shape and bite force scale with size (Kaliontzopoulou et al. 2008; Isip et al. 2022). Thus, despite the fact different morphological features of the head may be influenced by different selective pressures, both overall head size and specific shape components (e.g., head height, head width, jaw length) have been shown to directly affect biting performance (Kaliontzopoulou et al. 2008; Wittorski et al. 2016; Villalobos-Chaves and Santana 2022). Indeed, other anatomical elements can be also modified to produce similar bite force outcomes, for instance, musculature orientation and size, fiber diameter, etc. (Herrel et al. 2007a, 2008; Wittorski et al. 2016). This suggests that this complex head shape-bite force system is influenced by multiple selective pressures, leading to evolutionary modifications that enhance fitness by improving the functional outcome thought many-to-one morphological combinations.

In this study, we use lizards from the Old-World family Lacertidae to examine how form–function relationships emerge at the macroscale based on patterns observed at lower biological levels. We investigate how the relationship between head shape and bite force scales from individuals to species within the genus *Podarcis*, and ultimately to broader family-level patterns across the Lacertidae. We focus on *Podarcis* as a well-studied, ecologically diverse but also relatively cohesive group of lizards of moderate size variation and with generally similar life-histories and biological traits. Moreover, this group has been widely used to address ecomorphological and evolutionary questions (Herrel et al. 2001a; Verwaijen et al. 2002; McBrayer 2004; Kaliontzopoulou et al. 2012; Edwards et al. 2013; Gomes et al. 2018), revealing complex interactions among selective

pressures (e.g., sexual dimorphism, foraging mode, diet, male-male competition) that influence head morphology and whole-organism performance (Verwaijen et al. 2002; Gomes et al. 2018) at the intra- and interspecific levels (Verwaijen et al. 2002). To explore whether these form-function relationships are consistent across biological scales, we analyze individuals from species in the genus *Podarcis* to characterize intraspecific patterns; then we assess whether these patterns scale up across species within the genus; and finally, we integrate data from 71 lacertid species. We hypothesize that (1) body size significantly influences the relationship between head shape and bite force, but that aspects of this relationship persist even after accounting for allometric effects, (2) the covariation between head shape and bite force is detectable both at microevolutionary (within-species) and macroevolutionary (among-species) scales, and (3) this shape–function relationship is consistently maintained across hierarchical levels of biological organization. To address these hypotheses, we employed geometric morphometrics to describe considering the dorsal and lateral view, which were accompanied by bite force measurements. Different parts of head shape (dorsal and lateral) may be influenced by distinct selective pressures (e.g., sexual selection, habitat occupation, refuge use, size), potentially leading to different evolutionary patterns. However, we also expect the head to evolve as a single functional unit, accommodating diverse morphological configurations while producing similar functional outputs—consistent with the many-to-one mapping paradigm (Wainwright et al. 2005). Given the strong relationship between head shape and bite force, we expect this pattern to be mirrored across biological levels (Emerson and Arnold 1989). Moreover, when the effect of the size is not removed from the data, we expect the form-function pattern to be more straightforward, since the allometric effect should make this relationship to be less variable.

5.2. Material and methods

5.2.1. Data collection

Morphological and performance data from lacertid lizard individuals were obtained from different field campaigns and museum collections by the authors (Table S5.1). Morphological data included records for 875 individuals for dorsal and 883 for lateral shape; and performance data for 1151 individuals. Individuals obtained from fieldwork

were captured by noose and then released at the site of collection. From those individuals, morphological measurements, dorsal and lateral high-resolution pictures were taken and bite force was measured. From museum collections, only morphological measurements and high-resolution pictures were taken. Only adult males were utilized to remove any variation due to ontogeny and sexual dimorphism.

As linear morphological measurements, snout-vent length (SVL), pileus length and mouth length were measured to the closest 0.01 mm from each individual using electronic calipers (Table S5.1). Snout-vent length serves as the standard measure of body size for reptiles. Pileus length, defined as the distance from the tip of the snout to the posterior border of the parietal scales, and mouth length, measured from the tip of the snout to the posterior border of the last supralabial scale, were used to calibrate images for downstream geometric morphometric analysis.

To quantify head shape, we employed geometric morphometric (James Rohlf and Marcus 1993; Adams et al. 2004, 2013) based on high-resolution photographs of the dorsal and the right lateral side of the head. Pictures were taken for all individuals (both field-caught and from museum collections) using an Olympus Tough TG-5 digital camera. The lens of the camera was always parallel to the head surface. Head shape was characterized using two-dimensional landmark-based geometric morphometrics (James Rohlf and Marcus 1993; Adams et al. 2004, 2013). We digitized nine landmarks and three semilandmarks for the lateral shape and 10 landmarks and four semilandmarks for the dorsal shape (Figure 5.1) using the function *digitizeImages* available in the package “StereoMorph” (Olsen and Westneat 2015) and the software TPSdig2-32 (Rohlf 2006) and TPSutil32 (Rohlf 2015). Semilandmarks were used to quantify the shape of curved regions of the head, including the posterior margin of the dorsal view and the jaw and supraocular curvature in the lateral view (Figure 5.1). Landmarks were placed to capture the overall geometry of both lateral and dorsal head shape, ensuring that both internal and external structures were represented, following the approach described in previous studies (Kaliontzopoulou et al. 2007, 2010).

For those specimens where one or two landmarks were missing due to bad resolution of sections of images or missing scales, we reconstructed the positions of the missing landmarks using the thin plate spline (TPS) method to estimate the missing landmark positions based on the corresponding location in complete specimens (Gunz et al. 2009).

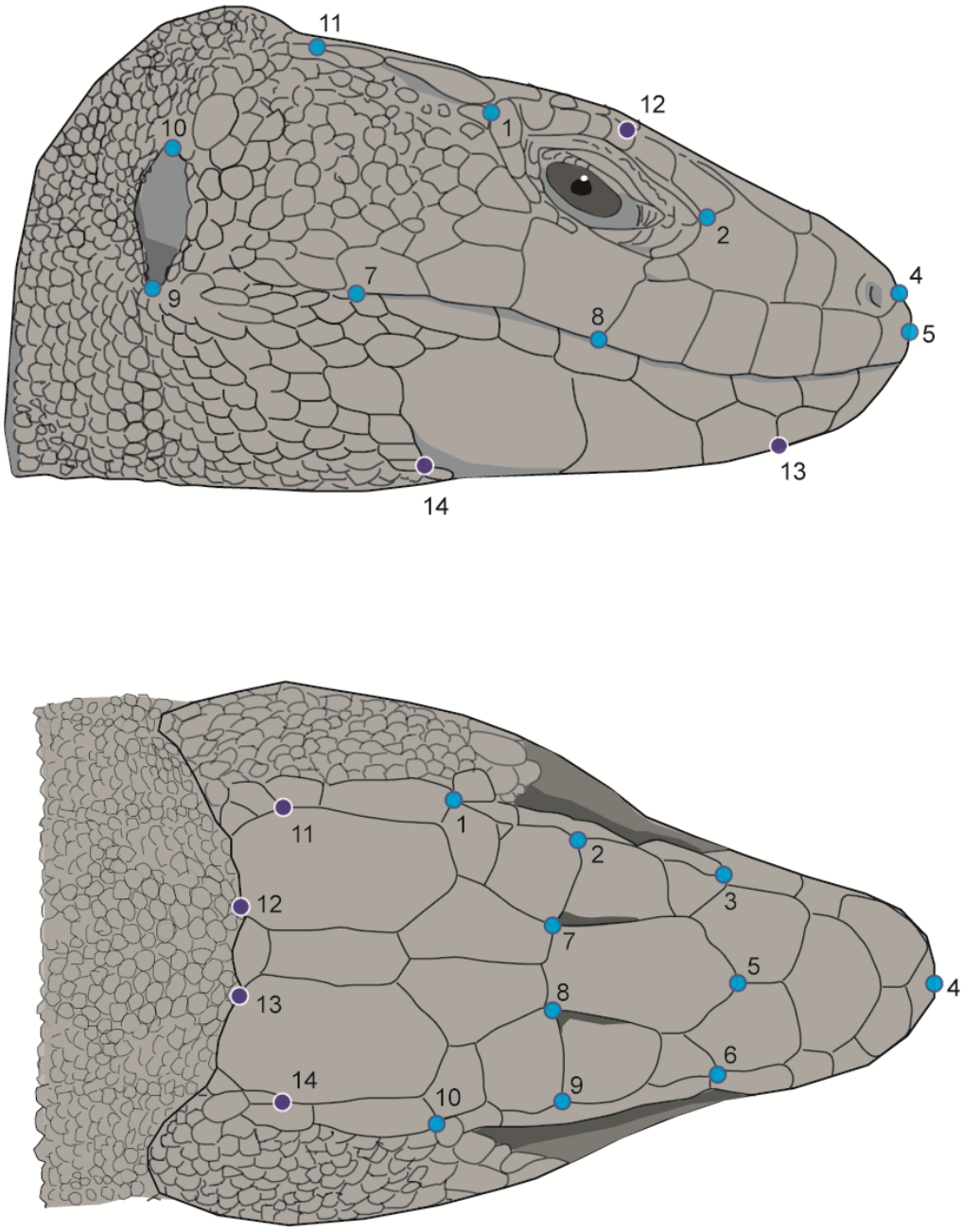

Figure 5.1. Landmarks (black outline) and semilandmarks (white outline) are used to quantify the shape of the dorsal (bottom) and lateral (top) view of the head.

We employed the function *estimate.missing* in the “geomorph” package (Baken et al. 2021; Adams et al. 2025). This procedure was implemented separately for individuals from each species so as not to confound variation across hierarchical levels. In addition, for lateral head shape, the position of missing landmarks was estimated separately for the skull and lower jaw, as the angle of opening of the jaws in each photograph would affect the missing landmark estimation in the complete landmark configuration. After estimation, both subsets were centered on the articulation point, combined back together, and reordered to match the original landmark order. We then used *fixed.angle* function in “geomorph” (Baken et al. 2021; Adams et al. 2025) to remove variation in the position of the lower jaw related to the skull by fixing the angle between them to a common angle see (Adams 1999). For dorsal head shape we removed the asymmetric component of shape variation and retained only the symmetric portion of head shape using the *bilat.symmetry* function in “geomorph” (Baken et al. 2021; Adams et al. 2025). Once all data were collected, corrected and estimated, a Generalized Procrustes Analysis (GPA) was performed to align all specimens to a common coordinate system and standardize components of non-shape variation (position, orientation and size) using the function *gpagen* in “geomorph” (Baken et al. 2021; Adams et al. 2025).

Bite force was measured employing an isometric Kistler force transducer (type 9203, Kistler Inc., Winterthur, Switzerland), mounted on a vertical holder made of stainless steel and connected to a Kistler charge amplifier (type 5995A, Kistler Inc., Winterthur, Switzerland). Bite force measurements were obtained by provoking lizards to bite on two parallel thin stainless-steel plates connected to the force transducer (see Herrel et al. 1999, 2001a for further information). The tip of the plates was delimited using a marker to ensure the bite was standardized at the point of force exertion for all specimens (Gomes et al. 2020). Each lizard was tested five times to ensure we obtained the maximal individual bite force, which was retained and log-transformed for further analyses.

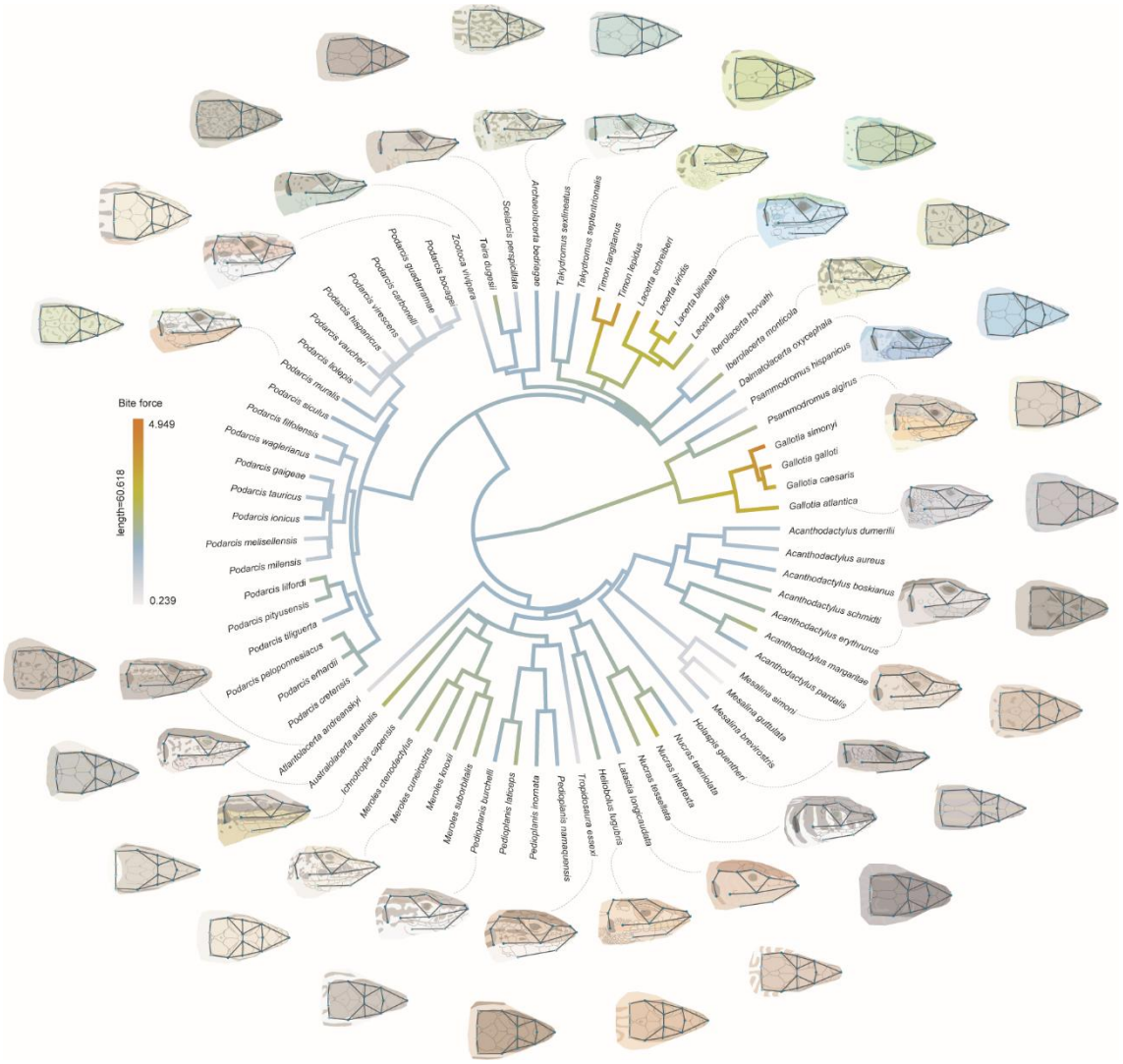

Figure 5.2. Phylogenetic tree showing raw bite force values across lacertid lizards. Branch colors represent relative bite force residuals after correcting for body size. At each tip, a representative species is shown for each genus, depicted with a stylized illustration of the dorsal and lateral head view and its corresponding mean shape outline derived from geometric morphometric data.

5.2.2. Comparative analyses

To examine the evolution of head shape and bite force, we applied phylogenetic comparative methods using the most comprehensive time-calibrated phylogeny available for Lacertidae (Garcia-Porta et al. 2019), which includes 246 species, pruned to match the species included at each biological level of analysis (intraspecific, genus, and family levels; Figure 5.2), using the function *drop.tip* implemented in "ape" package (Paradis et al. 2004).

Phylogenetic Signal of Form and Function

We applied two complementary approaches to evaluate phylogenetic signal in univariate traits (e.g., bite force and snout–vent length), using Blomberg's K statistic (Blomberg et al. 2003), and in high-dimensional morphological traits (dorsal and lateral head shape), using its multivariate extension, Kmult (Adams 2014). First, we assessed whether trait values were more similar among closely related species than expected by chance by testing against a random association of data to the tips of the phylogeny (K=0) (Blomberg et al. 2003; Adams 2014). This was accomplished using the *physignal* and *physignal.z* functions implemented in "geomorph". Second, we tested whether observed values deviated from expectations under Brownian Motion (BM) (K=1) model of evolution, by comparing empirical statistics to null distributions generated through phylogenetic simulations (Enríquez-Urzelai et al. 2022). To test if K was significantly different from 1, we employed the code available at http://blog.phytools.org/2011/12/testingfor-phylogenetic-signal-k.html for univariate data and an expansion of this method for multivariate data (Bellvert et al. 2023). Finally, for the multivariate datasets (dorsal and lateral shape) we evaluated whether the phylogenetic signal was distributed equally across shape dimensions or was concentrated in specific directions in shape space. To accomplish this, we employed the approach of Mitteroecker et al. 2025, which decomposes the phylogenetic signal into its constituent dimensions. We implemented the procedure using the function *physignal.eigen* in "geomorph" (Baken et al. 2021; Adams et al. 2024, 2025; Mitteroecker et al. 2025).

Phylogenetic Regression of Form and Function

To characterize the relationship between form and function across hierarchical levels of biological organization and the effect of size on this relationship, we conducted phylogenetic regressions at three hierarchical levels: (1) individuals within species, (2)

species means within the genus *Podarcis*, and (3) species means across the family Lacertidae. These analyses were performed using both the raw shape data and the residuals from a multivariate regression of shape on size. we conducted phylogenetic regressions at three hierarchical levels: (1) individuals within species, (2) species means within the genus *Podarcis*, and (3) species means across the family Lacertidae. These analyses were performed using both the raw shape data and the residuals from a multivariate regression of shape on size.

Removing the effects of allometric scaling was achieved by extracting residuals from regressions of bite force and shape against snout–vent length (SVL). To ensure continuity across the combined datasets used in our multi-scale analyses, we standardized all size corrections using snout–vent length (SVL), as this was the only size metric shared by all individuals across bite force and shape datasets, whereas centroid size (cs) was not always available. This approach allowed us to remove the effect of size, effectively eliminating the allometric component from the shape data (Klingenberg 2016). We consider this distinction important in the context of geometric morphometrics. While Procrustes analysis standardizes for size and scale by superimposing landmarks (i.e., performing a size correction), residuals from the shape-size regression enable us to further isolate specific form–function patterns by removing the influence of allometry, which is a procedure commonly applied in geometric morphometric studies (Klingenberg et al. 2003; Ivanović and Kalezić 2010; Klingenberg and Marugán-Lobón 2013; Klingenberg 2016).

At each level, we analyzed both dorsal and lateral head shape in relation to bite force. First, at the intraspecific level, we used extended phylogenetic generalized least squares (E-PGLS) (Adams and Collyer 2024) to regress bite force on dorsal and lateral head shape in individuals from 21 *Podarcis* species, including species as an interaction term. We employed this method because it allows us to investigate intraspecific variability while also accounting for the evolutionary relationships between species (i.e., phylogenetic nonindependence). We used the function lm.rrpp.ws implemented in the "RRPP" package (Collyer and Adams 2018, 2024). Then, at the genus level we calculated species means for bite force and both head shape views and performed phylogenetic regressions using a tree pruned to include only *Podarcis* species. Finally, at the family level, we repeated the regressions with species means for all lacertid

species and the full phylogeny. For genus and family level analyses we employed the function *lm.rrpp* implemented in the "RRPP" package (Collyer and Adams 2018, 2024).

In order to visualize the data, first, to biologically interpret shape variation we generated thin-plate spline (TPS) deformation grids using the function *plotRefToTarget* from the "geomorph" package (Baken et al. 2021; Adams et al. 2025). Predicted shapes for the minimum and maximum bite forces were obtained using the *shape.predictor* function implemented in "geomorph" (Baken et al. 2021; Adams et al. 2025). The mean shape of all species was used as a reference, and the grids were magnified threefold (3×) to enhance the visualization of landmark displacements (Figures 5.3-5.4). To describe the association between head shape and bite force and visualize its variation across species and hierarchical levels, we utilized scatter plots where the multivariate shape data were reduced into a univariate vector employing the regression score method (reg.type = "PredLine") (Adams and Nistri 2010).

Slope comparisons across biological levels

To determine whether from-function trends were consistent across biological levels of organization (individual, genus, and family), we compared the angular differences between the individual-level *Podarcis* species regressions and the macroevolutionary trends observed at the *Podarcis* genus and Lacertidae family levels, based on a modification of the procedure from Tejero-Cicuéndez et al. 2023. First, using the regressions described above, we obtained residuals from the genus- and family-level models. We then applied a permutation procedure, in which these residuals were randomly permuted (999 iterations), and model statistics were recalculated to generate an empirical null distribution for evaluating the observed test statistics (Freedman and and Lane 1983; Collyer and Adams 2007; Collyer et al. 2015). We then compared the individual regressions for each *Podarcis* species to the vector representing the genus slope and family slope, by calculating pairwise differences in their angular direction in morphospace and evaluating these relative to empirical sampling distributions obtained through "RRPP" (Adams and Collyer 2009; Collyer and Adams 2013). We also calculated the mean angle observed from the pairwise comparison among *Podarcis* species using shape residuals and raw shape data, in order to observe the difference in mean angles between raw and size-corrected data.

5.3. Results

Phylogenetic signal

Phylogenetic signal was significantly greater than expected by chance for all traits, as indicated by large effect sizes ($K \approx 0.5$ for dorsal and lateral head shape, $Z \approx 12–31$; $K \approx 0.3$ for bite force, $Z \approx 3$; Table S5.2). Moreover, comparisons against the expected value under Brownian motion revealed that K values for shape and bite force were significantly lower than 1, indicating less phylogenetic signal than predicted by a pure BM model. The exploratory analysis of the phylogenetic signal across multivariate dimensions revealed that, in both dorsal and lateral head shape, the signal was not evenly distributed but appears to be concentrated in the first K-components. (Table S5.2; Figure S5.1). This implied that the degree of phylogenetic signal was not 'weak' but rather was restricted to certain directions of shape space (see Mitteroecker et al. 2025 and Adams and Collyer 2019 for discussion). Finally, snout–vent length exhibited a K value not significantly different from 1, suggesting that its distribution across the phylogeny closely follows Brownian expectations.

Allometric patterns

Across all hierarchical levels, head shape showed significant associations with body size (SVL) in both dorsal and lateral configurations, except for the genus-level lateral analysis. At the individual level, SVL explained 9.9% of dorsal shape variation and 4.8% of lateral shape variation. This size–shape relationship persisted at broader evolutionary scales. At the genus level, SVL accounted for 24.7% of dorsal shape variation across species, whereas the association between SVL and lateral shape was not statistically significant, despite explaining 9.9% of the variation. At the family level, SVL explained 13.4% of dorsal shape variation and 6.0% of lateral shape variation (Table S5.3–S5.4). Bite force showed a strong allometric relationship with body size, with SVL explaining 75.9% of the variation in bite force (Table S5.5). Overall, allometric effects were detected across traits, head orientations, and hierarchical levels, although their statistical support and deformation magnitude varied among analyses.

Allometric deformation grids indicated that size-related shape variation was spatially structured and differed in magnitude between hierarchical levels (Figure S5.2-S5.3). In the dorsal view, increasing size was associated with lateral displacement of posterior

cranial landmarks, resulting in broader posterior head outlines, whereas smaller sizes exhibited narrower posterior configurations. These deformation patterns were observed at both genus and family levels, with greater landmark displacement and grid warping at the family level (Figure S5.2). In the lateral view, allometric variation was expressed as changes in head depth and anteroposterior proportions, with larger sizes showing increased mid-cranial depth and reduced snout elongation, and smaller sizes displaying shallower and more elongate head profiles. Consistent with the statistical results, lateral allometric deformation at the genus level was comparatively limited, whereas family-level lateral deformation was more pronounced (Figure S5.3).

Form-function associations

Focusing on the relationships between form and function when using raw data, we found a significant association between shape and bite force at the *Podarcis* individual level in both dorsal and lateral views, with this relationship differing across species, as indicated by a significant bite force ~ species interaction (Tables 5.1, S5.6-S5.7). At the genus and family level, contrasting patterns were found between dorsal and lateral shape. Dorsal shape exhibited a significant relationship with bite force at the genus, but not the family level. Instead, for lateral shape this pattern was reversed: there was no significant relationship between shape and bite force at the genus level, but there was at the family level (Tables 5.1, S5.6-S5.7).

When removing the allometric effect through regression of shape and bite force data against SVL we observed that form-function relationships were largely retained across the different biological levels. We found that, at the individual level, shape and bite force remained significantly associated considering both the dorsal and lateral head views, with species-specific differences maintained (Tables 5.2, S5.8-S5.9). Across *Podarcis* species, we found that in dorsal shape, the relationship between form and function was marginally significant (Tables 5.2, S5.8-S5.9), while in lateral shape this relationship was not significant (Tables 5.2, S5.8-S5.9). Finally, at the family level, both dorsal and lateral shape exhibited a positive association with bite force (Tables 5.2, S5.8-S5.9).

With respect to shape changes associated with maximum and minimum bite force, analyses using both raw and allometric-corrected data revealed relatively subtle variation at the genus level (*Podarcis*) in both dorsal and lateral views (Figures 5.3-5.4). In contrast, at the family level, shape variation was more pronounced, with specific cranial

regions showing stronger and more spatially differentiated responses to bite force variation. At the family level, when using raw data, in the dorsal view, bite-force variation was primarily expressed through changes in the mid-cranial region, where strong-biting individuals exhibited medial displacement of landmarks toward the midline, whereas weaker-biting individuals showed comparatively broader configurations (Figure 5.3). Across both views, posterior head landmarks remained comparatively stable, indicating that most bite-force–related variation was concentrated in the anterior and mid-cranial regions. In the lateral view, maximum bite force was associated with deformation patterns characterized by expansion of the anteroposterior region of the head, along with shortening and deepening of the snout (Figure 5.3). Individuals with lower bite force showed the opposite pattern, displaying a more elongate and slenderer configuration of the snout and jaw region.

After removal of the allometric component, bite force–related shape variation was still detected in both head views at the family level (Figure 5.3). In the dorsal view, size-corrected shape variation associated with bite force was mainly expressed in the posterior cranial region. Individuals with lower bite force showed greater displacement of posterior landmarks, resulting in relatively expanded posterior head configurations, whereas individuals with higher bite force displayed more constrained posterior regions (Figure 5.3). Displacement of mid-cranial landmarks was comparatively limited, indicating that bite force–related shape variation when the allometric effect is removed is concentrated toward the posterior portion of the cranial vault. In the lateral view, higher bite force was associated with localized deformation patterns involving subtle expansion of the mid-cranial region and moderate changes in snout depth. Individuals with lower bite force exhibited a more elongate and slender snout configuration, with shape differences primarily restricted to the anterior portion of the head (Figure 5.4).

Table 5.1. Results of phylogenetic regressions conducted to test for differences in raw dorsal and lateral shape and bite force relationship at different biological levels: using *Podarcis* individuals, *Podarcis* species and all Lacertidae species in this study. d.f.: degrees of freedom; Z: Z-score. P-values are based on 1000 residual permutations and significant p-values (at α = 0.05) are highlighted in bold.

Dorsal shape				***Lateral shape***			
Podarcis individuals				*Podarcis* individuals			
*Dorsal shape ~ Bite force * species I Podarcis phylogeny*				Lateral shape ~ Bite force * species I *Podarcis* phylogeny			
	d.f.	Z	p-val		d.f.	Z	p-val
bite	1	5.752	**0.001**	bite	1	6.569	**0.001**
Sp	21	20.513	**0.001**	sp	21	22.298	**0.001**
bite:sp	21	6.260	**0.001**	bite:sp	21	4.278	**0.001**
Residuals	626			Residuals	619		
Total	669			Total	662		
Podarcis species				*Podarcis* species			
Dorsal shape ~ Bite force I Podarcis phylogeny				Lateral shape ~ Bite force I *Podarcis* phylogeny			
bite	1	1.946	**0.026**	bite	1	-0.372	0.628
Residuals	20			Residuals	20		
Total	21			Total	21		
Lacertidae species				Lacertidae species			
Dorsal shape ~ Bite force I Lacertidae phylogeny				Lateral shape ~ Bite force I Lacertidae phylogeny			
bite	1	0.624	0.281	bite	1	2.422	**0.009**
Residuals	69			Residuals	69		
Total	70			Total	70		

Table 5.2. Results of phylogenetic regressions conducted to test for differences in allometric-corrected dorsal and lateral shape and bite force relationship at different biological levels: using *Podarcis* individuals, *Podarcis* species and all Lacertidae species in this study. d.f.: degrees of freedom; Z: Z-score. P-values are based on 1000 residual permutations and significant p-values (at α = 0.05) are highlighted in bold.

Dorsal shape				*Lateral shape*			
Podarcis individuals				*Podarcis* individuals			
*Dorsal shape ~ Bite force * species I Podarcis phylogeny*				Dorsal shape ~ Bite force * species I *Podarcis* phylogeny			
	d.f.	Z	p-val		d.f.	Z	p-val
bite	1	2.704	**0.005**	bite	1	3.857	**0.001**
Sp	21	17.473	**0.001**	Sp	21	21.347	**0.001**
bite:sp	21	8.193	**0.001**	bite:sp	21	5.475	**0.001**
Residuals	626			Residuals	619		
Total	669			Total	662		
Podarcis species				*Podarcis* species			
Dorsal shape ~ Bite force I Podarcis phylogeny				Dorsal shape ~ Bite force I *Podarcis* phylogeny			
bite	1	1.647	0.055	bite	1	0.505	0.316
Residuals	20			Residuals	20		
Total	21			Total	21		
Lacertidae species				Lacertidae species			
Dorsal shape ~ Bite force I Lacertidae phylogeny				Dorsal shape ~ Bite force I Lacertidae phylogeny			
bite	1	2.729	**0.003**	bite	1	2.925	**0.001**
Residuals	69			Residuals	69		
Total	70			Total	70		

Slope variation across levels

Slope comparisons across all phylogenetic levels (individual, genus, and family) revealed that patterns were not significantly more similar or more different than expected. This suggests that vector angles describing differences in the form-function relationship across biological levels are not different from what is expected for a random collection of vectors (Tables S5.10-S5.11, Figure S5.2). Importantly, this pattern was maintained regardless of whether the effect of body size was included or not (Table S5.10-S5.13, Figure S5.2). The only exception was *Podarcis melisellensis*, which was more different than expected from the family trend of association between raw lateral shape and bite force (Table S5.11, Figure S5.2), and *Podarcis milensis* which did not follow the genus-level trend in size-corrected lateral shape (Table S5.13, Figure S5.2).

5.4. Discussion

Understanding how form–function relationships scale across levels of biological organization is essential for uncovering the mechanisms driving morphological and performance diversity (Hansen and Martins 1996; Calsbeek et al. 2006; Kaliontzopoulou et al. 2018; Taverne et al. 2021; Woodgate et al. 2025). Our evidence from lacertid lizards suggests that the association between bite force and head shape is mostly evident at each evolutionary scale, however, the relationship between these traits is not consistent across levels of biological organization.

We found that body size is one of the elements driving the relationship between form and function within species and across the entire lacertid family, as it was expected due to the strong allometric effects on both morphology and performance (Gould 1966; Kaliontzopoulou et al. 2008, 2012). However, this phenotypic association remained significant even after removing the allometric effect, suggesting that, in lacertids, head shape itself carries functionally relevant variation beyond allometric-related scaling, pointing to an intrinsic link between form and function (Figures 5.3-5.4). At the intraspecific level, clear and significant relationships between morphology and performance were identified, with variation among *Podarcis* species suggesting that species-specific selective pressures influence this association. Interestingly, while this relationship was also evident at the macroscale, it was less present at the genus level.

Both head views (dorsal and lateral) seem to be contributing similarly to these trends, which implies that the head operates as a functional unit responding to external pressures, despite previous suggestions that its components may evolve under different regimes (Herrel et al. 2001b; Lappin et al. 2006). However, while the form–function association was consistently present, its direction was not conserved across the within-species, genus, and family levels. Instead, form–function vectors were no more similar or different than expected by chance. This may suggest that different evolutionary pressures operate at each level, or that the selective pressures that act on each level are the same, but organisms respond differently, due to developmental constraints or phylogenetic history, thus producing variable form-function outcomes.

Despite this variability, the presence of a significant relationship across levels supports the idea that performance outcomes constrain head morphology, even when evolutionary pathways differ. Therefore, we interpret that in lacertid lizards, the head shape-bite force relationship is a general functional relationship that persists even after removing the allometric effect and remains present across multiple evolutionary scales. However, this relationship does not follow a common evolutionary trajectory across levels, which is congruent with many-to-one mapping scenario (Wainwright et al. 2005; Thompson et al. 2017), where different phenotypic configurations can result in similar functional outcomes. Nevertheless, other scenarios are possible, such as the absence of multi-level selection or the influence of non-selective and potentially random processes, which could account for the absence of congruence across levels.

The role of size and head shape in bite force variation

Body size plays a central role in influencing several biological traits (Bergmann 1847; Christiansen and Adolfssen 2005; Lindstedt and Hoppeler 2023), where allometry frequently dominates the evolution of morphology and performance (Gould 1966; Arnold 1983; Wainwright 1994; Tejero-Cicuéndez et al. 2023; Mitchell et al. 2024). As predicted, we found that both shape and performance present aa strong allometric trend, which is partially mediating the form-function relationship in lacertid species (Kaliontzopoulou et al. 2012; Taverne et al. 2023). Increasing in size, implies an increase in the space available for accommodating musculature (Deeming 2022), which therefore produces an increase in bite force, that is presented in our results with the highest variation of bite force explained by size (Aguirre et al. 2002; Verwaijen et al. 2002; Isip et al. 2022).

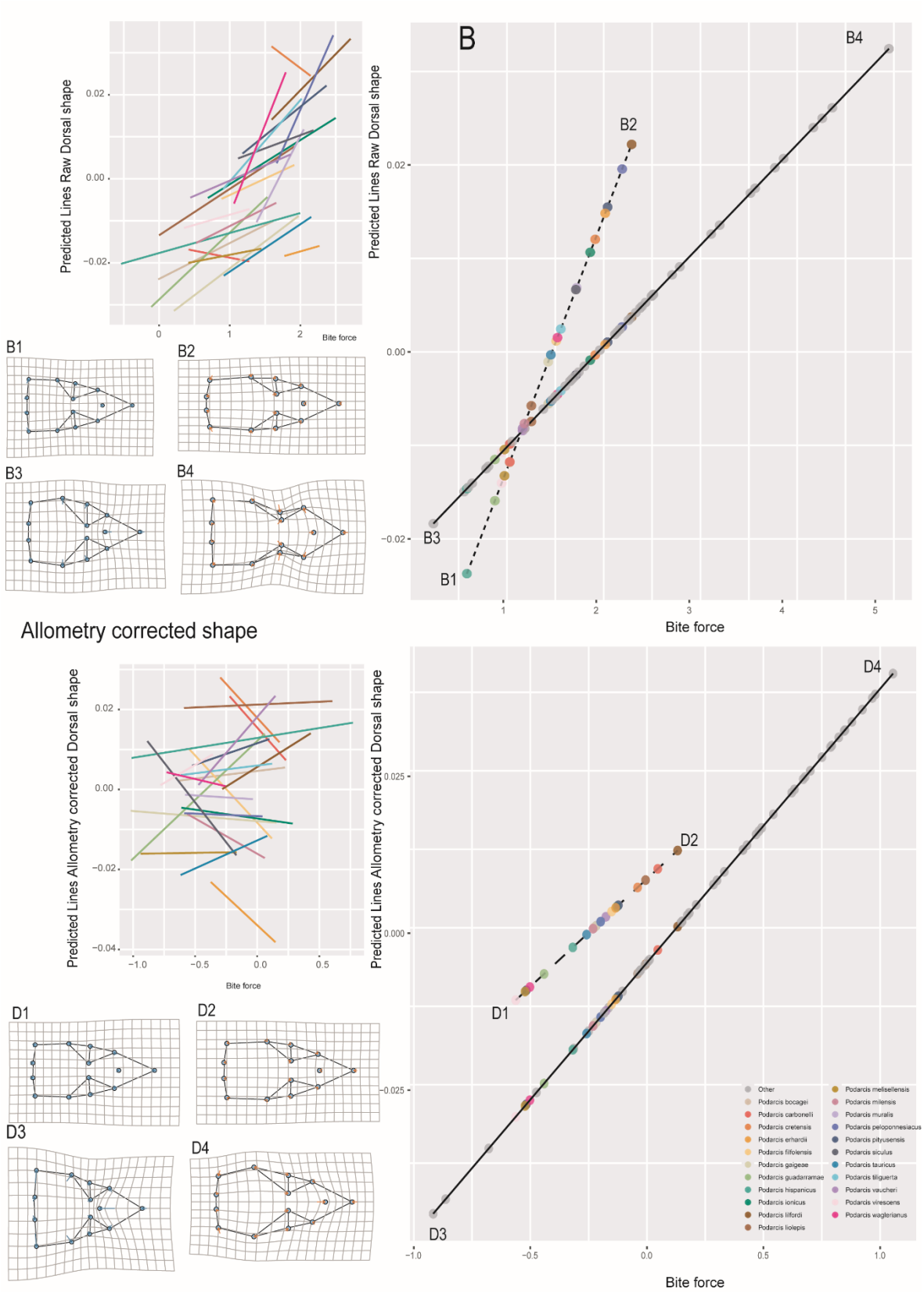
Predicted Lines Raw Dorsal shape
Bite force
B1
B2
B3
B4
B
Allometry corrected shape
Predicted Lines Allometry corrected Dorsal shape
D1
D2
D3
D4
Other
Podarcis bocagei
Podarcis carbonelli
Podarcis cretensis
Podarcis erhardii
Podarcis filfolensis
Podarcis gaigeae
Podarcis guadarramae
Podarcis hispanicus
Podarcis ionicus
Podarcis lilfordi
Podarcis liolepis
Podarcis melisellensis
Podarcis milensis
Podarcis muralis
Podarcis peloponnesiacus
Podarcis pityusensis
Podarcis siculus
Podarcis tauricus
Podarcis tiliguerta
Podarcis vaucheri
Podarcis virescens
Podarcis wagleriana

Figure 5.3. Visualization of the relationship between dorsal head shape and bite force using regression scores. Multivariate dorsal head shape was reduced to a univariate regression score by projecting individual shapes onto the shape–bite force regression vector (regression score method). Panels A and B show analyses using raw data for Podarcis individuals (A) and Lacertidae species (B). Panels C and D show the corresponding analyses after removal of the allometric component. In all panels, points represent individual specimens or species means, and lines depict species-specific regression trends in regression score space, illustrating the direction and relative strength of multivariate shape–bite force associations. Regression lines do not represent direct fits to raw multivariate shape data but are graphical summaries of multivariate relationships. In panel A, dots which correspond to individuals are not shown to avoid noise in the interpretation. Deformation grids (3× magnification) illustrate head shape associated with maximum (right) and minimum bite force (left) at the genus and family levels and correspond to the predicted shapes along each fitted regression.

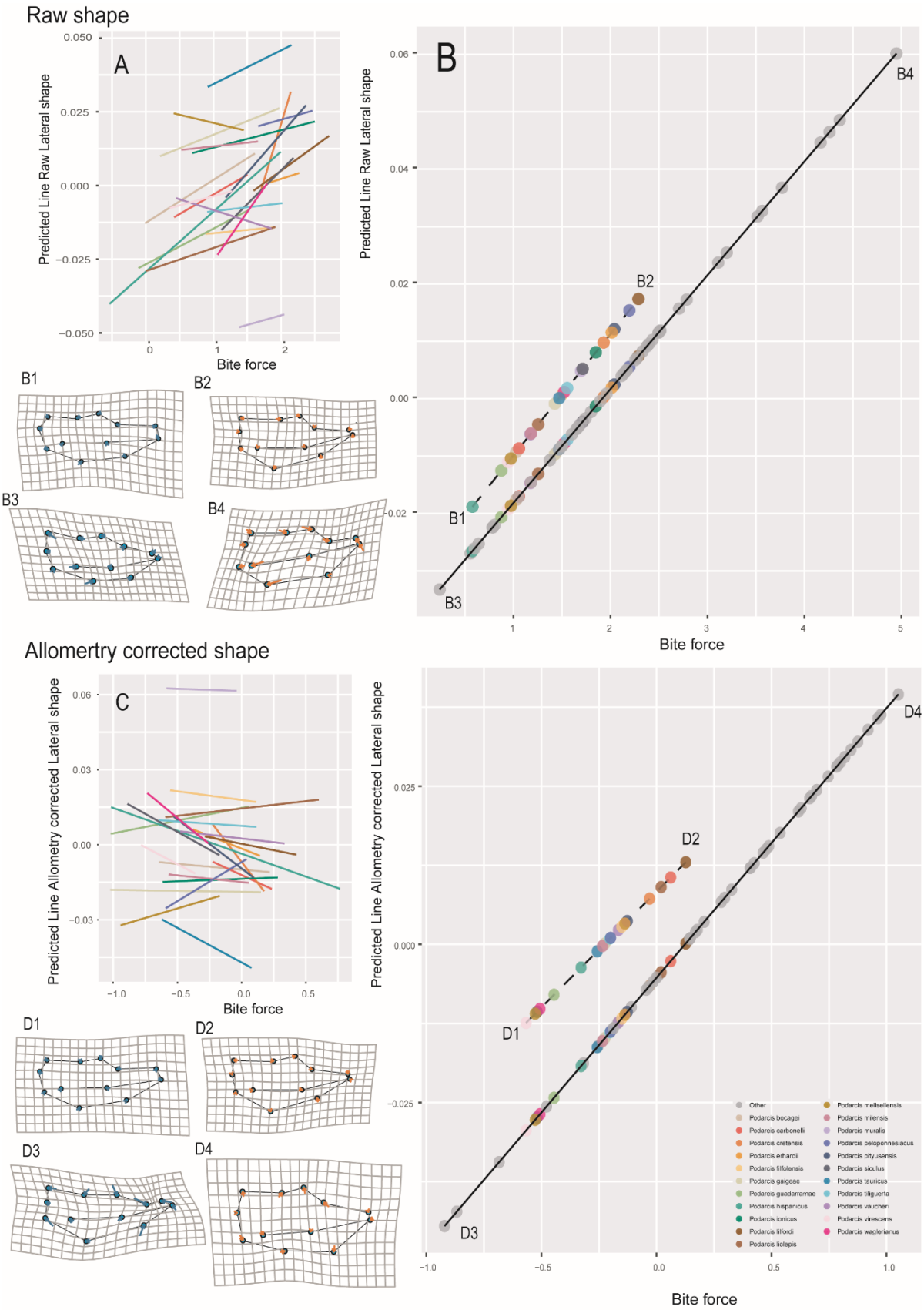
Raw shape
A
Predicted Line Raw Lateral shape
Bite force
B1
B2
B3
B4
B
Allomertry corrected shape
C
Predicted Line Allometry corrected Lateral shape
D1
D2
D3
D4
Other
Podarcis bocagei
Podarcis carbonelli
Podarcis cretensis
Podarcis erhardii
Podarcis filfolensis
Podarcis gaigeae
Podarcis guadarramae
Podarcis hispanicus
Podarcis ionicus
Podarcis lilfordi
Podarcis liolepis
Podarcis melisellensis
Podarcis milensis
Podarcis muralis
Podarcis peloponnesiacus
Podarcis pityusensis
Podarcis siculus
Podarcis tauricus
Podarcis tiliguerta
Podarcis vaucheri
Podarcis virescens
Podarcis waglerianus

Figure 5.4. Visualization of the relationship between latera head shape and bite force using regression scores. Multivariate lateral head shape was reduced to a univariate regression score by projecting individual shapes onto the shape–bite force regression vector (regression score method). Panels A and B show analyses using raw data for *Podarcis* individuals (A) and Lacertidae species (B). Panels D and E show the corresponding analyses after removal of the allometric component. In all panels, points represent individual specimens or species means, and lines depict species-specific regression trends in regression score space, illustrating the direction and relative strength of multivariate shape–bite force associations. Regression lines do not represent direct fits to raw multivariate shape data but are graphical summaries of multivariate relationships. In panel A, dots which correspond to individuals are not shown to avoid noise in the interpretation. Deformation grids (3× magnification) illustrate head shape associated with maximum and minimum bite force at the genus and family levels and correspond to the predicted shapes along each fitted regression.

Moreover, the unit under selection is expected to involve size-related elements, as there is no strict division between size and shape in nature. However, to address the questions in this study, we consider it crucial to examine performance and shape both before and after removing the effect of allometry, as size may obscure latent patterns in the form–function relationship.

Accordingly, our results indicate that size is not the sole driver of the form–function relationship. After accounting for allometric variation in both bite force and morphology, bite force–shape associations were maintained at both the intraspecific and family levels, and additional patterns emerged, such as a clear relationship between bite force and dorsal head shape at the family level that was not detected in the raw data (Tables S5.10–S5.13). This suggests that, although size plays a major role, form–function relationships are also shaped by intrinsic, size-independent factors beyond allometry alone (Figures 5.3–5.4), although the variation explained by the form-function models is limited (Tables 5.1-5.2, S6-S9). For example, elements such as the internal architecture of the jaw musculature (e.g. muscle fiber orientation, insertion sites, physiology) and the proportions between jaw in-levers and out-levers, play a critical role in determining bite force (Herrel et al. 1997, 1998; Kaliontzopoulou et al. 2012). These biomechanical and anatomical features can influence performance independently of overall body size and may help explain the persistence of form–function relationships beyond allometric scaling.

Once the allometric effect has been removed, a clear relationship between bite force and head shape is maintained at both the intraspecific and family levels (Figures 5.3-5.4). At the intraspecific level, however, this relationship varies among *Podarcis* species, as reflected by differences in the strength and direction of species-specific associations. This variation suggests that distinct selective pressures modulate how head shape translates into bite performance across species and how not a single morphological solution underline bite force responses across *Podarcis* species, suggesting a many-to-one mapping scenario (Mitchell et al. 2024). Previous work has shown that dietary specialization, sexual selection, and habitat use can each shape the form–function relationship in *Podarcis*, often in different and sometimes opposing ways (Kaliontzopoulou et al. 2012; Gomes et al. 2018; Taverne et al. 2023; Woodgate et al. 2025).

For example, species consuming harder prey may evolve broader, more robust heads associated with increased bite force, yet the specific morphological traits underlying performance differ among species such as *P. siculus* and *P. melisellensis*, indicating that no single form–function solution is shared across the genus (Taverne et al. 2020). In contrast, in *P. erhardii*, bite force variation is linked primarily to male–male competition rather than diet, highlighting the role of sexual selection in shaping performance (Donihue et al. 2016; Gomes et al. 2018; Woodgate et al. 2025). Habitat structure can further modify this relationship by imposing spatial constraints on head shape, particularly in climbing species, although such morphological changes do not always translate into performance differences (Kaliontzopoulou et al. 2012; Vicent-Castelló et al. 2025). Together, these findings indicate that allometry-independent form–function relationships provide a flexible framework upon which multiple ecological and social pressures act, producing divergent evolutionary trajectories despite shared functional demands.

In agreement with our expectations, both the dorsal and lateral view of the head present a clear link with bite force at intraspecific and family level. This suggests that although different head dimensions are probably under the effect of different selective pressures (Herrel et al. 2001b; Cruz et al. 2021; Vicent-Castelló et al. 2025; Woodgate et al. 2025), it seems that the entire structure acts as a single evolutionary unit in lacertid lizards. Therefore, the head may be navigating along the adaptive landscape to accommodate

variation, which is always responding to performance requirements, which goes accordingly with the many-to-one mapping scenario (Wainwright et al. 2005; Simon et al. 2025b). Nevertheless, we observed that each part of the head accommodates different morphological adaptations to explain bite force variation at different levels. For example, comparing how head varies at genus level versus family level, we observed that the head shape of *Podarcis* is much more conserved that at family level, probably due to phylogenetic relatedness and ecological similarities (Figures 5.3-5.4).

At the family level, however, we observe much more variation, since very different species in terms of ecology and phylogenetically distance are included in the analysis. In the dorsal view, bite force variation is primarily expressed through changes in the mid-cranial region involving the frontal and parietal bones (Figure 5.3-S5.2). In raw data, strong-biting taxa shows medial compression with landmarks displaced toward the midline, a pattern partially overlapping with size-related dorsal shape change. After accounting for allometry, this medial compression persists but becomes spatially restricted, indicating a size-independent association between dorsal cranial alignment and bite force. This mid-cranial compression may allow for an expansion of the jaw adductors thus producing stronger bites through cranial rigidity (Herrel et al. 2007c,b; Reilly et al. 2007; Dutel et al. 2021). By contrast, we observe that the posterior part of the cranial region remains relatively stable across analyses, with more variation in species with lower bite force. Although this may seem incongruent at first, the shortening of the head observed in the lower bite-force deformation grids (Figure 5.3) could produce a subtle expansion of the posterior cranium to compensate for bite-force output. At the family level, however, we observe much more variation, since very different species in terms of ecology and phylogenetically distant are included in the analysis.

In the lateral view, deformation grids show that maximum bite force is associated with expansion of the posterior region of the head and increased dorsoventral depth, patterns that closely resemble the size-related shape change (Figures 5.4, S5.3). These changes suggest an enlargement of the jaw adductor region, increasing the space available for muscle mass and thereby enhancing force production (Gröning et al. 2013; Taverne et al. 2021). In addition, strong bite force is associated with shortening and deepening of the snout, a configuration that may improve mechanical advantage by optimizing jaw levers and resistance to reaction forces during biting lever (Herrel et al. 2007a). This

could be associated to diet changes, such as herbivory, which make animals bigger and therefore strong biters like the big *Gallotia* species that are positioned to the right part of the scatter plot (Figure 5.3) (Barahona et al. 2000; Lopez-Darias et al. 2015). Conversely, weaker bite force corresponds to a more elongate and slender lateral profile, particularly in the snout and jaw region. This morphology is consistent with flatter head configurations observed in taxa facing spatial constraints, such as climbing species (Vicent-Castelló et al. 2025). Species that we found that present similar morphologies associated with weak bite force are for example *Iberolacerta* and *Holaspis* which happen to be both small animals adapted to climbing.

Importantly, comparisons between raw and allometry-adjusted deformation grids indicate that much of the lateral shape variation associated with bite force is mediated by allometry (Figure S5.3). Once size effects are removed, although bite force–related shape differences persist, it is reduced in magnitude and becomes more localized, primarily involving subtle increases in head depth and curvature in the mid-to-posterior cranial region. This suggests that, aside from overall scaling, bite force can be modulated through finer scale adjustments of cranial geometry rather than wholesale reorganization of the head.

Lack of coherence of the form–function relationship across hierarchical levels

We originally hypothesized that the link between head shape and bite force would be maintained across hierarchical levels of biological organization. This expectation was based on the assumption that similar biomechanical principles should govern the mapping of form to function across scales (Emerson and Arnold 1989). Therefore, if the form-function association were shaped by consistent selective pressures and constraints, we would expect that the direction of the multivariate regression vector to remain more similar than expected across levels, from individuals to genus up to family.

However, our results do not support this prediction. While the form-function relationship was present at some levels, the directions of the regression vectors were neither significantly more similar nor more divergent than expected by chance when compared across levels (Table S5.9-5.10, Figure S5.4). In other words, the scaling of the form-function relationship in lacertid lizards seems to follow a random pattern in multivariate space. One interpretation of these patterns is that changes in form-function dynamics at lower levels may lead to shifts in performance and potentially alter the adaptive

landscape over evolutionary time (Martin and Wainwright 2013; Simon et al. 2025b). One possible explanation, is that selective pressures shaping head shape-bite force relationship differ between species, producing species-specific responses that do not translate into consistent macroevolutionary trends, a pattern also observed in other taxa (Simon et al. 2025b). Alternatively, the same or similar selective pressures may act across species, but individual species might respond differently, yielding different form-function outcomes, due to genetic constraints or phylogenetic limitations (Simon and Moen 2023). For example, in this specific case, we observed that there are specific shape dimensions that are more phylogenetically constrained than others (Figure S5.1), therefore, the response to species-specific selective pressures would be mirrored in certain axis of the multivariate space (Mitteroecker et al. 2025).

Both head shape and bite force are known to be influenced by a variety of selective pressures. Whether trends are conserved across levels may therefore depend on how much each of these pressures contributes to fitness within and between species (Simon et al. 2025b; Woodgate et al. 2025) These divergent selective contexts can shape head morphology in different ways, ultimately modifying the head shape–performance relationship. In addition to ecological and behavioral factors, variation in form–function trajectories may also reflect functional constraints, such as the degree to which traits are integrated and must coordinate to perform biomechanical tasks (Ghalambor et al. 2003; Wainwright 2007; Walker 2007). Likewise, trade-offs between competing performance demands may constrain the directions in which morphology can evolve (Le Guilloux et al. 2020). For example, trade-offs between bite magnitude and endurance have been found in lacertid lizards (Gomes et al. 2020). Other trade-offs between bite force features, such as strength and velocity has been found in other groups (Herrel et al. 2009; Sansalone et al. 2024), as well as specific trade-offs between different performance categories, such as locomotion and bite force (Cameron et al. 2013), which may be present also in lacertid lizards. Depending on which functions are most critical in each context, selection may favor different morphological solutions, thereby altering the shape–performance link across species (Garland et al. 2022). As a result, even though form–function integration remains present, the evolutionary pathways it follows may vary substantially depending on the ecological and behavioral pressures acting on each species. In *Podarcis*, it is likely that all these factors are at play, but their relative influence

or the species' responses to them, may differ, leading to randomly-divergent form–function patterns that fail to align with those observed at higher levels of organization, as it was shown for specific *Podarcis* species (Woodgate et al. 2025).

5.5. Conclusions

Taken together, the results of this study highlight a central paradox: the form–function relationship between head shape and bite force is present and statistically strong across multiple levels of organization, yet the evolutionary trajectories that it follows differ across these scales. Despite the apparent randomness in vector orientation, the functional link is robust. This suggests a flexible system in which both selective pressures and other potential evolutionary constraints may shift or produce different responses, but performance remains consistently influenced by morphology (Ghalambor et al. 2003). This underscores a key evolutionary insight: strong form–function integration can persist even in the absence of a single, conserved evolutionary path which reflects the combination between constraints and evolvability in this comprehensive phenotypic evolution.

References

Adams, D. 1999. Methods for shape analysis of landmark data from articulated structures. Evol. Ecol. Res. 959–970.

Adams, D. C. 2014. A Generalized K Statistic for Estimating Phylogenetic Signal from Shape and Other High-Dimensional Multivariate Data. Syst. Biol. 63:685–697.

Adams, D. C., M. Collyer, A. Kaliontzopoulou, and E. Baken. 2024. geomorph: Geometric Morphometric Analyses of 2D and 3D Landmark Data.

Adams, D. C., and M. L. Collyer. 2009. A general framework for the analysis of phenotypic trajectories in evolutionary studies. Evolution. 63:1143–1154.

Adams, D. C., and M. L. Collyer. 2019. Comparing the strength of modular signal, and evaluating alternative modular hypotheses, using covariance ratio effect sizes with morphometric data. Evolution. 73:2352–2367.

Adams, D. C., and M. L. Collyer. 2024. Extending phylogenetic regression models for comparing within-species patterns across the tree of life. Methods in Ecol. Evol. 15:2234–2246.

Adams, D. C., and A. Nistri. 2010. Ontogenetic convergence and evolution of foot morphology in European cave salamanders (Family: Plethodontidae). BMC Evol Biol 10:216.

Adams, D. C., F. J. Rohlf, and D. E. Slice. 2013. A field comes of age: geometric morphometrics in the 21st century. Hystrix It. J. Mamm. 24:7–14. Associazione Teriologica Italiana.

Adams, D. C., F. J. Rohlf, and D. E. Slice. 2004. Geometric morphometrics: Ten years of progress following the 'revolution.' Italian J. Zool. 71:5–16. Taylor & Francis.

Adams, D., M. Collyer, A. Kaliontzopoulou, and E. Baken. 2025. Geomorph: Software for geometric morphometric analyses.

Aguirre, L. F., A. Herrel, R. van Damme, and E. Matthysen. 2002. Ecomorphological analysis of trophic niche partitioning in a tropical savannah bat community. Proc. Biol. Sci. 269:1271–1278.

Arnold, S. 1983. Morphology, Performance and Fitness. Am. Zool. 23:347–361.

Arnold, S. J. 1992. Constraints on Phenotypic Evolution. Am. Nat. 140:S85–S107. The University of Chicago Press.

Arnold, S. J., M. E. Pfrender, and A. G. Jones. 2001. The adaptive landscape as a conceptual bridge between micro- and macroevolution. Pp. 9–32 in A. P. Hendry and M. T. Kinnison, eds. Microevolution Rate, Pattern, Process. Springer Netherlands, Dordrecht.

Baken, E. K., M. L. Collyer, A. Kaliontzopoulou, and D. C. Adams. 2021. geomorph v4.0 and gmShiny: Enhanced analytics and a new graphical interface for a comprehensive morphometric experience. Methods Ecol. Evol. 12:2355–2363.

Barahona, F., S. E. Evans, J. A. Mateo, M. García-Márquez, and L. F. López-Jurado. 2000. Endemism, gigantism and extinction in island lizards: the genus *Gallotia* on the Canary Islands. J. Zool. 250:373–388.

Bellvert, A., S. Adrián-Serrano, N. Macías-Hernández, S. Toft, A. Kaliontzopoulou, and M. A. Arnedo. 2023. The Non-Dereliction in Evolution: Trophic Specialisation Drives Convergence in the Radiation of Red Devil Spiders (Araneae: Dysderidae) in the Canary Islands. Syst. Biol. 72:998–1012.

Bergmann, K. G. 1847. On the relations of the heat economy of animals to their size. Göttinger Studien. 3:595–708.

Blomberg, S. P., T. Garland, and A. R. Ives. 2003. Testing for phylogenetic signal in comparative data: behavioral traits are more labile. Evolution. 57:717–745.

Calsbeek, R., J. H. Knouft, and T. B. Smith. 2006. Variation in scale numbers is consistent with ecologically based natural selection acting within and between lizard species. Evol. Ecol. 20:377–394.

Cameron, S. F., M. L. Wynn, and R. S. Wilson. 2013. Sex-specific trade-offs and compensatory mechanisms: bite force and sprint speed pose conflicting demands on the design of geckos (*Hemidactylus frenatus*). J. Exp. Biol. 216:3781–3789.

Christiansen, P., and J. S. Adolfssen. 2005. Bite forces, canine strength and skull allometry in carnivores (Mammalia, Carnivora). J. Zool. 266:133–151.

Collar, D. C., B. C. O'Meara, P. C. Wainwright, and T. J. Near. 2009. Piscivory limits diversification of feeding morphology in Centrarchid fishes. Evolution. 63:1557–1573.

Collyer, M., and D. C. Adams. 2024. RRPP: Linear Model Evaluation with Randomized Residuals in a Permutation Procedure.

Collyer, M. L., and D. C. Adams. 2007. Analysis of Two-State Multivariate Phenotypic Change in Ecological Studies. Ecology. 88:683–692.

Collyer, M. L., and D. C. Adams. 2013. Phenotypic trajectory analysis: comparison of shape change patterns in evolution and ecology. Hystrix It. J. Mamm. 24:75–83. Associazione Teriologica Italiana.

Collyer, M. L., and D. C. Adams. 2018. RRPP: An r package for fitting linear models to high-dimensional data using residual randomization. Methods in Ecol. Evol. 9:1772–1779.

Collyer, M. L., D. J. Sekora, and D. C. Adams. 2015. A method for analysis of phenotypic change for phenotypes described by high-dimensional data. Heredity 115:357–365. Nature Publishing Group.

Cruz, F. B., D. L. Moreno Azocar, B. Vanhooydonck, J. A. Schulte, C. S. Abdala, and A. Herrel. 2021. Drivers and patterns of bite force evolution in liolaemid lizards. Biol. J. Linn. Soc.134:126–140.

De Meyer, J., D. J. Irschick, B. Vanhooydonck, J. B. Losos, D. Adriaens, and A. Herrel. 2019. The role of bite force in the evolution of head shape and head shape dimorphism in *Anolis* lizards. Funct. Ecol. 33:2191–2202.

Deeming, D. C. 2022. Inter-relationships among body mass, body dimensions, jaw musculature and bite force in reptiles. J. Zool. 318:23–33.

Donihue, C. M., K. M. Brock, J. Foufopoulos, and A. Herrel. 2016. Feed or fight: testing the impact of food availability and intraspecific aggression on the functional ecology of an island lizard. Funct. Ecol. 30:566–575.

Dutel, H., F. Gröning, A. C. Sharp, P. J. Watson, A. Herrel, C. F. Ross, M. E. H. Jones, S. E. Evans, and M. J. Fagan. 2021. Comparative cranial biomechanics in two lizard species: impact of variation in cranial design. J. Exp. Biol. 224:jeb234831.

Edwards, S., K. A. Tolley, B. Vanhooydonck, G. J. Measey, and A. Herrel. 2013. Is dietary niche breadth linked to morphology and performance in Sandveld lizards *Nucras* (Sauria: Lacertidae)?: Niche Breadth and Phenotype in *Nucras*. Biol. J. Linn. Soc. Lond. 110:674–688.

Emerson, S. B., and S. J. Arnold. 1989. Intra- and interspecific relation- ships between morphology, performance, and fitness. P. 451 in D. B. Wake and G. Roth, eds. Complex Organismal Functions. Integration and Evolution in Vertebrates. Wiley-Interscience, New York.

Enríquez-Urzelai, U., F. Martínez-Freiría, I. Freitas, A. Perera, Í. Martínez-Solano, D. Salvi, G. Velo-Antón, and A. Kaliontzopoulou. 2022. Allopatric speciation, niche conservatism and gradual phenotypic change in the evolution of European green lizards. J. Biogeogr. doi: 10.1111/jbi.14497. John Wiley & Sons.

Freedman, D., and D. and Lane. 1983. A Nonstochastic Interpretation of Reported Significance Levels. JBES. 1:292–298. ASA Website.

Garcia-Porta, J., I. Irisarri, M. Kirchner, A. Rodríguez, S. Kirchhof, J. L. Brown, A. MacLeod, A. P. Turner, F. Ahmadzadeh, G. Albaladejo, J. Crnobrnja-Isailovic, I. De La Riva, A. Fawzi, P. Galán, B. Göçmen, D. J. Harris, O. Jiménez-Robles, U. Joger, O. Jovanović Glavaš, M. Karış, G. Koziel, S. Künzel, M. Lyra, D. Miles, M. Nogales, M. A. Oğuz, P. Pafilis, L. Rancilhac, N. Rodríguez, B. Rodríguez Concepción, E. Sanchez, D. Salvi, T. Slimani, A. S'khifa, A. T. Qashqaei, A. Žagar, A. Lemmon, E. Moriarty Lemmon, M. A. Carretero, S. Carranza, H. Philippe, B. Sinervo, J. Müller, M. Vences, and K. C. Wollenberg Valero. 2019. Environmental temperatures shape thermal physiology as well as diversification and genome-wide substitution rates in lizards. Nat. Commun. 10:4077.

Garland, T., C. J. Downs, and A. R. Ives. 2022. Trade-Offs (and Constraints) in Organismal Biology. Physiol. Biochem. Zool. 95:82–112.

Ghalambor, C. K., J. A. Walker, and D. N. Reznick. 2003. Multi-trait Selection, Adaptation, and Constraints on the Evolution of Burst Swimming Performance1. Integr. Comp. Biol. 43:431–438.

Gomes, V., M. A. Carretero, and A. Kaliontzopoulou. 2018. Run for your life, but bite for your rights? How interactions between natural and sexual selection shape functional morphology across habitats. Naturwissenschaften 105:9.

Gomes, V., A. Herrel, M. A. Carretero, and A. Kaliontzopoulou. 2020. New Insights into Bite Performance: Morphological Trade-Offs Underlying the Duration and Magnitude of Bite Force. Physiol. Biochem. Zool. 93:175–184.

Gould, S. J. 1966. Allometry and Size in Ontogeny and Phylogeny. Biol. Rev. 41:587–638.

Gröning, F., M. E. H. Jones, N. Curtis, A. Herrel, P. O'Higgins, S. E. Evans, and M. J. Fagan. 2013. The importance of accurate muscle modelling for biomechanical analyses: a case study with a lizard skull. J. R. Soc. Interface. 10:20130216. Royal Society.

Gunz, P., P. Mitteroecker, S. Neubauer, G. W. Weber, and F. L. Bookstein. 2009. Principles for the virtual reconstruction of hominin crania. J. Hum. Evol. 57:48–62.

Hallgrimsson, B., and B. Hall. 2005. Variation and variability: Central concepts in biology. Variation: A central concept in biology 1–7.

Hansen, T., and E. Martins. 1996. Translating between microevolutionary process and macroevolutionary patterns: The correlation structure of interspecific data. Evolution. 50:1404–1417.

Herrel, A., P. Aerts, and D. De Vree. 1998. Static biting in lizards: functional morphology of the temporal ligaments. J. Zool. 244:135–143.

Herrel, A., P. Aerts, and F. D. Vree. 1997. Ecomorphology of the Lizard Feeding Apparatus: a Modelling Approach. Neth. J. Zool. 48:1-25.

Herrel, A., R. V. Damme, B. Vanhooydonck, and F. D. Vree. 2001a. The implications of bite performance for diet in two species of lacertid lizards. Canadian J. Zool. 79:662–670.

Herrel, A., E. De Grauw, and J. A. Lemos-Espinal. 2001b. Head shape and bite performance in xenosaurid lizards. J. Exp. Biol. 290:101–107.

Herrel, A., A. De Smet, L. F. Aguirre, and P. Aerts. 2008. Morphological and mechanical determinants of bite force in bats: do muscles matter? J. Exp. Biol. 211:86–91.

Herrel, A., R. S. James, and R. Van Damme. 2007a. Fight versus flight: physiological basis for temperature-dependent behavioral shifts in lizards. J. Exp. Biol. 210:1762–1767.

Herrel, A., L. D. Mcbrayer, and P. M. Larson. 2007b. Functional basis for sexual differences in bite force in the lizard *Anolis carolinensis*. Biol. J. Linn. Soc. 91:111–119.

Herrel, A., J. Podos, B. Vanhooydonck, and A. P. Hendry. 2009. Force–velocity trade-off in Darwin's finch jaw function: a biomechanical basis for ecological speciation? Funct. Ecol. 23:119–125.

Herrel, A., V. Schaerlaeken, J. J. Meyers, K. A. Metzger, and C. F. Ross. 2007c. The evolution of cranial design and performance in squamates: Consequences of skull-bone reduction on feeding behavior. Integr. Comp. Biol. 47:107–117.

Herrel, A., L. Spithoven, R. Van Damme, and F. DE Vree. 1999. Sexual dimorphism of head size in *Gallotia galloti*: testing the niche divergence hypothesis by functional analyses. Funct. Ecol. 13:289–297.

Huey, R., and R. D. Stevenson. 1979. Integrating Thermal Physiology and Ecology of Ectotherms: A Discussion of Approaches. Am. Zool. 19:357–366.

Husak, J. 2008. Sexual selection on locomotor performance. Evol. Ecol. Res. 10.

Huyghe, K., B. Vanhooydonck, H. Scheers, M. Molina-Borja, and R. Van Damme. 2005. Morphology, performance and fighting capacity in male lizards, *Gallotia galloti*. Funct. Ecol. 19:800–807.

Irschick, D., J. Meyers, J. Husak, and J. Le Galliard. 2008. How does selection operate on whole-organism functional performance capacities? A review and synthesis. , doi: 10.7275/R58G8HX6. University of Massachusetts Amherst Libraries.

Isip, J. E., M. E. H. Jones, and N. Cooper. 2022. Clade-wide variation in bite-force performance is determined primarily by size, not ecology. Proc. R. Soc. B. 289:20212493. Royal Society.

Ivanović, A., and M. L. Kalezić. 2010. Testing the hypothesis of morphological integration on a skull of a vertebrate with a biphasic life cycle: a case study of the alpine newt. J. Exp. Zool. B. Mol. Dev. Evol. 314:527–538.

James Rohlf, F., and L. F. Marcus. 1993. A revolution in morphometrics. Trends Ecol. Evol. 8:129–132.

Kaliontzopoulou, A., D. C. Adams, A. van der Meijden, A. Perera, and M. A. Carretero. 2012. Relationships between head morphology, bite performance and ecology in two species of *Podarcis* wall lizards. Evol. Ecol. 26:825–845.

Kaliontzopoulou, A., M. A. Carretero, and G. A. Llorente. 2008. Head shape allometry and proximate causes of head sexual dimorphism in *Podarcis* lizards: joining linear and geometric morphometrics. Biol. J. Linn. Soc.93:111–124.

Kaliontzopoulou, A., M. A. Carretero, and G. A. Llorente. 2010. Intraspecific ecomorphological variation: linear and geometric morphometrics reveal habitat-related patterns within *Podarcis bocagei* wall lizards. J. Evol. Biol. 23:1234–1244.

Kaliontzopoulou, A., M. A. Carretero, and G. A. Llorente. 2007. Multivariate and geometric morphometrics in the analysis of sexual dimorphism variation in *Podarcis* lizards. J. Morphol. 268:152–165.

Kaliontzopoulou, A., C. Pinho, and F. Martínez-Freiría. 2018. Where does diversity come from? Linking geographical patterns of morphological, genetic, and environmental variation in wall lizards. BMC Evo. Bio. 18:124.

Klingenberg, C. P. 2016. Size, shape, and form: concepts of allometry in geometric morphometrics. Dev. Genes. Evol. 226:113–137.

Klingenberg, C. P., and J. Marugán-Lobón. 2013. Evolutionary covariation in geometric morphometric data: analyzing integration, modularity, and allometry in a phylogenetic context. Syst. Biol. 62:591–610.

Klingenberg, C. P., K. Mebus, and J.-C. Auffray. 2003. Developmental integration in a complex morphological structure: how distinct are the modules in the mouse mandible? Evol. Dev. 5:522–531.

Lande, R. 1976. Natural Selection and Random Genetic Drift in Phenotypic Evolution. Evolution. doi: 10.2307/2407703. JSTOR.

Lappin, A. K., P. S. Hamilton, and B. Sullivan. 2006. Bite-force performance and head shape in a sexually dimorphic crevice-dwelling lizard, the common chuckwalla [*Sauromalus ater* (= obesus)]. Biol. J. Linn. Soc.88:215–222.

Lappin, A. K., and J. F. Husak. 2005. Weapon performance, not size, determines mating success and potential reproductive output in the collared lizard (*Crotaphytus collaris*). Am. Nat. 166:426–436.

Le Guilloux, M., A. Miralles, J. Measey, B. Vanhooydonck, J. C. O'Reilly, A. Lowie, and A. Herrel. 2020. Trade-offs between burrowing and biting force in fossorial scincid lizards? Biol. J. Linn. Soc. 130:310–319.

Lindstedt, S. L., and H. Hoppeler. 2023. Allometry: revealing evolution's engineering principles. J. Exp. Biol. 226:jeb245766.

Lopez-Darias, M., B. Vanhooydonck, R. Cornette, and A. Herrel. 2015. Sex-specific differences in ecomorphological relationships in lizards of the genus *Gallotia*. Funct. Ecol. 29:506–514.

Martin, C. H., and P. C. Wainwright. 2013. Multiple Fitness Peaks on the Adaptive Landscape Drive Adaptive Radiation in the Wild. Science 339:208–211. AAAS.

McBrayer, L. D. 2004. The relationship between skull morphology, biting performance and foraging mode in Kalahari lacertid lizards. Zool. J. Linn. Soc. 140:403–416.

McGlothlin, J. W., M. E. Kobiela, H. V. Wright, D. L. Mahler, J. J. Kolbe, J. B. Losos, and E. D. Brodie. 2018. Adaptive radiation along a deeply conserved genetic line of least resistance in *Anolis* lizards. Evol. Lett. 2:310–322.

Mitchell, D. R., E. Sherratt, and V. Weisbecker. 2024. Facing the facts: adaptive trade-offs along body size ranges determine mammalian craniofacial scaling. Biol. Rev. 99:496–524.

Mitchell, D. R., S. Wroe, M. Martin, and V. Weisbecker. 2025. Testing hypotheses of skull function with comparative finite element analysis: three methods reveal contrasting results. J. Exp. Biol. 228:JEB249747.

Mitteroecker, P., M. L. Collyer, and D. C. Adams. 2025. Exploring Phylogenetic Signal in Multivariate Phenotypes by Maximizing Blomberg's K. Syst. Biol. 74:215–229.

Olsen, A., and M. W. Westneat. 2015. StereoMorph: an R package for the collection of 3D landmarks and curves using a stereo camera set-up. Methods in Ecol. Evol. 6:351–356.

Paradis, E., J. Claude, and K. Strimmer. 2004. APE: Analyses of Phylogenetics and Evolution in R language. Bioinformatics. 20:289–290.

Reilly, S. M., L. D. McBrayer, and D. B. Miles. 2007. Lizard Ecology. Cambridge University Press.

Rhoda, D. P., A. Haber, and K. D. Angielczyk. 2023. Diversification of the ruminant skull along an evolutionary line of least resistance. Science Advances 9:eade8929. American Association for the Advancement of Science.

Rohlf, F. J. 2006. tpsDig, Digitize Landmarks and Outlines. Stony Brook, NY: Department of Ecology and Evolution, State University of New York.

Rohlf, F. J. 2015. tpsUtil, file utility program. Department of Ecology and Evolution, State University of New York at Stony Brook.

Sansalone, G., S. Wroe, G. Coates, M. R. G. Attard, and C. Fruciano. 2024. Unexpectedly uneven distribution of functional trade-offs explains cranial morphological diversity in carnivores. Nat. Commun. 15:3275. Nature Publishing Group.

Schluter, D. 1996. Adaptive Radiation Along Genetic Lines of Least Resistance. Evolution 50:1766–1774. Oxford University Press.

Simon, M. N., E. A. Courtois, A. Herrel, and D. S. Moen. 2025a. Macroevolutionary divergence along Allometric Lines of Least Resistance in frog hindlimb traits and its effect on locomotor evolution. Am. Nat. 205:637–655. The University of Chicago Press.

Simon, M. N., and D. S. Moen. 2023. Bridging Performance and Adaptive Landscapes to Understand Long-Term Functional Evolution. Physiol. Biochem. Zool. 96:304–320.

Simon, M., M. Wildman, and D. S. Moen. 2025b. Form–function relationships within species are uncoupled from those across species in swimming and jumping performance in arboreal frogs. Evolution. qpaf058.

Taverne, M., H. Dutel, M. Fagan, A. Štambuk, D. Lisičić, Z. Tadić, A.-C. Fabre, and A. Herrel. 2021. From micro to macroevolution: drivers of shape variation in an island radiation of *Podarcis* lizards. Evolution. 75:2685–2707.

Taverne, M., N. King-Gillies, M. Krajnović, D. Lisičić, Ó. Mira, D. Petricioli, I. Sabolić, A. Štambuk, Z. Tadić, C. Vigliotti, B. Wehrle, and A. Herrel. 2020. Proximate and ultimate drivers of variation in bite force in the insular lizards *Podarcis melisellensis* and *Podarcis sicula*. Biol. J. Linn. Soc.131:88–108.

Taverne, M., P. J. Watson, H. Dutel, R. Boistel, D. Lisicic, Z. Tadic, A.-C. Fabre, M. J. Fagan, and A. Herrel. 2023. Form–function relationships underlie rapid dietary changes in a lizard. Proc. R. Soc. B. 290:20230582. Royal Society.

Taylor, G. K., and A. L. R. Thomas. 2014. Evolutionary Biomechanics: Selection, Phylogeny, and Constraint. Oxford University Press.

Tejero-Cicuéndez, H., I. Menéndez, A. Talavera, G. Mochales-Riaño, B. Burriel-Carranza, M. Simó-Riudalbas, S. Carranza, and D. C. Adams. 2023. Evolution along allometric lines of least resistance: morphological differentiation in Pristurus geckos. Evolution. 77:2547–2560.

Thompson, C., N. Ahmed, T. Veen, C. Peichel, A. Hendry, D. Bolnick, and Y. Stuart. 2017. Many-to-one form-to-function mapping weakens parallel morphological evolution. Evolution. 71:2738–2749.

Tseng, Z. J. 2013. Testing Adaptive Hypotheses of Convergence with Functional Landscapes: A Case Study of Bone-Cracking Hypercarnivores. PLOS ONE. 8:e65305. Public Library of Science.

Turelli, M., N. H. Barton, and J. A. Coyne. 2001. Theory and speciation. Trends in Ecol. Evol. 16:330–343.

Vermeij, G. J. 1973. Adaptation, Versatility, and Evolution. Systematic Zoology 22:466–477. [Oxford University Press, Society of Systematic Biologists, Taylor & Francis, Ltd.].

Verwaijen, D., R. Van Damme, and A. Herrel. 2002. Relationships between head size, bite force, prey handling efficiency and diet in two sympatric lacertid lizards. Funct. Ecol.16:842–850.

Vicent-Castelló, P., A. Herrel, D. J. Harris, and A. Kaliontzopoulou. 2025. Walking or hanging: the role of habitat use for body shape evolution in lacertid lizards. J. Evol. Biol. voaf003.

Villalobos-Chaves, D., and S. E. Santana. 2022. Craniodental traits predict feeding performance and dietary hardness in a community of Neotropical free-tailed bats (Chiroptera: Molossidae). Funct. Ecol. 36:1690–1699.

Wainwright, P. C. 1994. Functional morphology as a tool in ecological research. Pp. 42–59 in P. C. Wainwright and S. M. Reilly, eds. Ecological Morphology: IOB. . Chicago University Press, Chicago.

Wainwright, P. C. 2007. Functional Versus Morphological Diversity in Macroevolution. Annual review of ecology, evolution, and systematics 38:381–401. Annual Reviews, Palo Alto, CA.

Wainwright, P. C., M. E. Alfaro, D. I. Bolnick, and C. D. Hulsey. 2005. Many-to-One Mapping of Form to Function: A General Principle in Organismal Design?. Integr. Comp. Biol. 45:256–262.

Wainwright, P. C., and S. S. Shaw. 1999. Morphological basis of kinematic diversity in feeding sunfishes. J. Exp. Biol. 202:3101–3110.

Walker, J. A. 2007. A General Model of Functional Constraints on Phenotypic Evolution. Am. Nat. 170:681–689. The University of Chicago Press.

Wittorski, A., J. B. Losos, and A. Herrel. 2016. Proximate determinants of bite force in *Anolis* lizards. J. Anat. 228:85–95.

Woodgate, S. C., A. Pérez-Cembranos, V. Pérez-Mellado, and J. Müller. 2025. Microgeographic diversity does not drive macroevolutionary divergence in bite force of the Ibiza wall lizard, *Podarcis pityusensis*. Evolution. qpaf140.

Chapter 6:

General discussion and conclusions

6.1. Key findings

Phenotypic traits have long been recognized as central components of evolutionary processes, providing the primary interface through which organisms interact with their environment and on which selection acts. Within this framework, the ecomorphological paradigm has provided an important lens for investigating how morphology, performance, and ecology are linked, and how functional demands shape phenotypic evolution across ecological contexts (Arnold 1983; Kaliontzopoulou et al. 2015). More recently, increasing attention has been paid to the complexity of these relationships, particularly the role of allometry (Klingenberg 2016; Baken and Adams 2019; Tejero-Cicuéndez et al. 2023) and the scale-dependence of evolutionary processes (Kaliontzopoulou et al. 2018; Li et al. 2018; Taverne et al. 2020, 2021). Growing evidence suggests that phenotypic traits may respond differently to similar selective pressures across biological levels, and that strong functional integration can coexist with evolutionary decoupling among traits, challenging simple and linear interpretations of adaptive evolution (Simon et al. 2025). Understanding how ecological factors such as structural habitat and climate interact with morphology and performance across scales is therefore essential for explaining patterns of phenotypic diversity and macroevolutionary change (Arnold 1998; Olalla-Tárraga et al. 2006; Slavenko et al. 2019; Vicent-Castelló et al. 2025a).

The general aims of this thesis were to investigate how shape, performance, and body size evolve in response to ecological constraints, and to assess how these relationships are structured across different biological levels. Using lacertid lizards as a model system, the studies presented here explored how adaptation to structural habitat and climatic conditions shape phenotypic evolution, and how integrated trait systems can exhibit trait-specific and scale-dependent evolutionary responses. To achieve a comprehensive view of these processes, this work brought together morphological data (linear and geometric descriptors of body size and body shape), performance data (bite force), ecological information (structural habitat use and macroclimatic variables), and phylogenetic comparative methods within a multilevel analytical framework. In this last chapter, I synthesize and discuss the key findings of the thesis in relation to phenotypic integration, evolutionary decoupling, and the ecomorphological paradigm. Finally, I outline broader

implications for understanding the evolution of complex phenotypes and directions for future research endeavours.

Phenotypic evolution as a multilevel process

One of the major challenges in evolutionary biology is to explain how microevolutionary processes give rise to macroevolutionary patterns (Hansen and Martins 1996; Taverne et al. 2021; Tsuboi et al. 2024). In Chapters 3 and 5, I employed a multilevel approach focusing on body size, on one hand, and form–function relationships, on the other, to evaluate how the biological scale of analysis influences the evolutionary patterns we describe and corresponding evolutionary interpretations we derive, and to address how specific phenotypic relationships scale across levels of biological organization.

Our findings highlight that the biological scale on which evolutionary patterns are analyzed must be explicitly considered to properly understand how phenotypic diversity emerges and is structured from individuals and populations up to species, genera, and families. A direct and linear transition from microevolutionary processes to macroevolutionary patterns is not necessarily the appropriate framework for interpreting evolution (Hansen and Martins 1996; Taverne et al. 2021). Micro- and macroevolutionary dynamics may be present a direct correlation (Taverne et al. 2021) or instead be disconnected (Simon et al. 2025; Chapter 3). Although such interactions have been extensively discussed in genetics, I argue that this perspective is equally applicable to phenotypic evolution (Hogeweg 2002).

One of the central insights derived from this thesis is that different biological levels exhibit distinct phenotypic evolutionary responses. Phenotypes are expressed, selected, and filtered at the individual level, where variation arises and is acted upon by selection (Lande 1976; Li et al. 2018). When variation is shared among individuals, it may accumulate within populations and eventually become fixed at the species level (Turelli et al. 2001). However, this scaling process is shaped by the interaction of multiple selective pressures, such as habitat occupation, sexual selection competition and other behaviours. These selective pressures may act differently, and often in opposing directions, on specific traits across biological levels (Kaliontzopoulou et al. 2018; Taverne et al. 2021). Alternatively, the selective pressures may be similar, but the response of the individuals may be different due to developmental or phylogenetic constraints

(Figures 5.3-5.4). The coexistence of these pressures modulates the final phenotype and can lead to divergent evolutionary outcomes across scales.

Consistent with this view, in the study presented in Chapter 5 we observed that the relationship between head shape and bite force, a key component of the lizard phenotype, is not mirrored across biological levels of organization. Indeed, not only do we not observe the same pattern across hierarchical levels, but this pattern is in fact not more different or more similar than expected. This suggests that distinct combinations of selective pressures shape the form–function relationship at each scale, rather than a single, conserved process operating uniformly from individuals to populations, up to higher taxonomic levels such as genera and the entire Lacertidae family (Taverne et al. 2021). In addition, we observed that body size represents a cornerstone element in the interplay between head shape and bite force (Figures 5.3–5.4), which is not unexpected given the well-established influence of body size on multiple biological aspects, including morphology and performance (LaBarbera 1989; Blackburn et al. 1999; Collar et al. 2011). Indeed, the lower total angles observed between *Podarcis* species when the allometric effect is not removed from the data suggest a strong structuring role of size in this form–function relationship. However, the contribution of body size to form–function dynamics is not straightforward, as we also observed that body size itself evolves in a context-dependent manner. Consequently, the influence of body size on other phenotypic characters depends not only on macroclimatic and structural habitat conditions but is also shaped by phylogenetic and geographic context (Figure 3.2). This scale dependence may further complicate interactions among phenotypic traits and underscores the need to explicitly account for biological level when interpreting evolutionary patterns, highlighting the importance of addressing multilevel scenarios in macroevolutionary studies (Li et al. 2018).

Integration, trait-specific selection and ecological decoupling

A central theme emerging from this thesis is the apparent paradox between phenotypic integration and evolutionary decoupling. Phenotypic integration is understood as the existence of complex patterns of covariation among traits within an organism (Pigliucci 2003), while evolutionary decoupling is considered as the process where different structures of a whole functional block experience a certain grade of evolutionary independence allowing for the emergence of novel functional features (Ronco and

Salzburger 2021). Importantly, these two concepts are not mutually exclusive, as strong phenotypic integration can coexist with evolutionary decoupling when different components of an integrated system respond unevenly to selection.

In accordance with this view, the findings of this thesis lead to the conclusion that across lacertid lizards, morphology, performance and size are clearly correlated: head shape covaries with bite force, both scale with body size and together they form an integrated functional system (Figure 5.3-5.4). This integration is primarily functional and biomechanical in nature, as performance emerges from the coordinated interaction of head shape and size-related traits (Simon et al. 2025). However, evolutionary responses to specific selective pressures, such as environmental features, are far from uniform (Klingenberg 2016). Instead, different components of the phenotype respond to selection in partially independent ways. In the case of head morphology, individual traits such as head height, head width, head length, and mouth length (Figure 4.1) exhibit contrasting evolutionary responses to structural habitat, with some traits showing clear adaptive trends while others appear largely unaffected by this environmental axis. In contrast, body size shows a different pattern, tending to diversify across structural habitats rather than converge toward a single optimum (Figure 3.2). Together, these trait-specific responses generate diverse evolutionary trajectories that nevertheless converge on similar functional outcomes.

Head shape, bite force, and body size are tightly linked through biomechanics, development, and allometric scaling, forming an integrated system in which changes in one component inevitably influence the others (Verwaijen et al. 2002; Christiansen and Adolfssen 2005; Lappin et al. 2006; Anderson et al. 2008; De Meyer et al. 2019). This integration is evident in the stable association between head morphology and biting performance across biological levels that we observe in Chapter 3, even after accounting for the dominant effects of body size. Head shape therefore carries functional signal beyond simple scaling (Figure 5.3-5.4), indicating that selection can act on shape itself to modulate performance. However, this strong form–function association does not translate into a single, conserved evolutionary pathway. Instead, the direction and magnitude of morphological responses associated with performance vary among species, across clades, and between evolutionary scales, highlighting a fundamental decoupling between phenotypic integration and evolutionary predictability. Such

decoupling is expressed not as a breakdown of form–function relationships, but as divergence in the direction, magnitude, or trait combinations through which integrated systems evolve. In this context, integration should not be interpreted as evolutionary constraint in a strict sense, but rather as a framework within which multiple solutions can be explored.

A key mechanism underlying this pattern is the many-to-one mapping between form and function (Wainwright et al. 2005; Thompson et al. 2017). Similar levels of bite force can be achieved through different combinations of head dimensions, cranial proportions, and internal anatomical features, such as muscle architecture or lever mechanics (Collar and Wainwright 2006; Taverne et al. 2020; Cruz et al. 2021). This redundancy allows lineages to maintain functional performance while diverging morphologically, weakening the expectation of morphological convergence under similar ecological pressures (Alfaro et al. 2005). As a result, selection may consistently favor certain performance outcomes, such as high bite force or efficient feeding, without necessarily favoring the same morphological traits in all contexts. This helps explain why form–function relationships remain statistically robust while their evolutionary trajectories appear random when compared across hierarchical levels (Figure S5.4). In this way, many-to-one-mapping provides a functional explanation for how integrated systems retain performance while permitting evolutionary decoupling among morphological components.

The contrasting evolutionary patterns observed for shape and size have important implications for understanding the evolution of whole-organism performance. Because size strongly influences bite force and other functional traits, diversification in size can generate substantial variation in performance even among morphologically similar species. Conversely, species of similar sizes may achieve comparable performance through different cranial configurations. This highlights that ecological selection often targets functional outcomes, not specific trait values, allowing different components of an integrated phenotype to evolve semi-independently.

Body size as the backbone of phenotypic evolution

Body size is one of the most conspicuous morphological traits of species and a fundamental component of phenotypic evolution (LaBarbera 1989; Gaston and Blackburn 1996; Blackburn et al. 1999; Slavenko et al. 2019). It plays a central role because it is directly linked to multiple biological aspects and it mediates the scaling

relationships of many other phenotypic features, including shape, performance, and physiology (Brown et al. 1993; Verwaijen et al. 2002; Collar et al. 2011; Mitchell et al. 2024). Numerous studies have demonstrated the importance of body size in determining how organisms interact with their environment and how this, in turn, influences survival and fitness (LaBarbera 1989; Brown et al. 1993). Consequently, body size is expected to be both a direct target of natural selection and a key factor structuring the evolution of other traits through allometric relationships (Gould 1966).

In Chapter 5 of this thesis, we observed that body size lies at the core of the relationship between head shape and bite force (Figure 5.3-5.4). Bite force performance scales positively with body size, and cranial shape also shows a strong association with size, reflecting well-established allometric relationships described across reptiles and other vertebrates (Tables S5.3-5.5). Importantly, these form–function allometries are maintained across different biological levels, indicating a striking stability in how size structures integrated phenotypic systems. However, in Chapter 3 we also found that the evolutionary trajectories of body size itself are highly dependent on geographic and phylogenetic context (Figure 3.3-3.4). Macroclimatic and structural habitat variables affect body size evolution differently across phylogenetic scales, with patterns observed at the tribe level diverging from those detected at broader or finer scales. This indicates that while allometric relationships may be conserved, the position of species along those relationships can shift depending on evolutionary context.

Indeed, rather than evolving toward common optima within similar habitats (as observed for some aspects of head shape) body size exhibits substantial diversification, often varying widely among species occupying comparable structural environments. This decoupling suggests that body size is influenced by a broader suite of selective pressures, including thermoregulation, life-history strategies, energetic demands, and ecological interactions, which can blur or interact with habitat-related constraints (Olalla-Tárraga et al. 2006; Terribile et al. 2009; Collar et al. 2011; Klingenberg 2016; Benítez-López et al. 2021; Mitchell et al. 2024). As a result, context-dependent evolution of body size may indirectly shape the evolution of morphology and performance by altering how traits are expressed along conserved allometric axes. This scale dependence further complicates interactions among phenotypic traits and underscores the need to explicitly account for biological level when interpreting evolutionary patterns, highlighting the

importance of addressing multilevel scenarios in macroevolutionary studies (Li et al. 2018; Tejero-Cicuéndez et al. 2023).

Summarizing structural habitat to a vertical-horizontal axis

Structural habitat acts as a key ecological dimension influencing phenotypic evolution, although its effects are strongly trait-dependent (Saulnier Masson et al. 2023). A central conceptual contribution of this thesis lies in framing habitat use along a vertical-horizontal axis rather than relying on traditional, substrate-based habitat categories (Goodman et al. 2008; Collar et al. 2010). By focusing on the structural dimensions of the environment, specifically whether species predominantly exploit vertical or horizontal surfaces, this approach captures the functional and biomechanical challenges organisms face more directly than classifications based on habitat type alone. Vertical and horizontal habitat use impose fundamentally different demands on locomotion, posture, spatial navigation and refuge use, which in turn shape morphological and performance traits, as demonstrated in this thesis (Goodman and Isaac 2008; Goodman et al. 2008; Collar et al. 2010; Kaliontzopoulou et al. 2015; Gomes et al. 2018; Vicent-Castelló et al. 2025a). This framework allows very different habitats, such as rock faces and tree trunks, to be unified under a common functional context, emphasizing shared biomechanical constraints rather than ecological differences. Importantly, this perspective reveals patterns that may be obscured when habitats are treated as discrete categories, particularly in groups where species frequently exploit multiple substrates or exhibit intermediate levels of specialization. For example, some *Podarcis* species adapted to climb use tree branches and rock surfaces indiscriminately. By transforming habitat use into a continuous structural axis, the vertical–horizontal framework provides a more generalizable and mechanistic basis for interpreting ecomorphological evolution, highlighting how organisms respond to the geometry of their environment rather than to habitat labels per se.

In Chapter 4 of this thesis, we discovered that, for example, head height presented a clear adaptive pattern with significant differences between structural habitat categories, while other morphological features remain statistically the same. The use of vertical versus horizontal habitat axes imposes clear functional demands, particularly related to spatial constraints, locomotion, and refuge use (Goodman and Isaac 2008; Goodman et al. 2008; Collar et al. 2010; Kaliontzopoulou et al. 2015). These demands are most

consistently reflected in head shape, where certain configurations are repeatedly associated with navigating structurally more complex environments (Goodman et al. 2008). This suggests that head morphology is subject to relatively strong functional canalization imposed by habitat structure (Goodman et al. 2008; Openshaw and Keogh 2014). However, in the case of lacertid lizards, convergence is incomplete, as species often modify different aspects of cranial shape to meet similar functional challenges. An explanation for the disparity in evolutionary responses, could be the interaction of multiple selective pressures acting on the same traits. Head shape, for example, is involved not only in feeding but also in mating (Lappin and Husak 2005), territorial defense (Calsbeek and Marnocha 2006), and refuge use (Kaliontzopoulou et al. 2015). These functions may impose conflicting demands, particularly when sexual selection favors increased bite force or head robustness while ecological constraints favor flatter or narrower heads (Lappin et al. 2006; Kaliontzopoulou et al. 2015). The resulting evolutionary outputs represent alternative solutions rather than simple optimization toward a single adaptive peak. Importantly, the relative importance of these pressures can vary among species and across evolutionary timescales, further contributing to the observed lack of continuity in form–function trends. We also observed that structural habitat critically affects body size evolution, but showing a completely different pattern that the one shape experiences. When talking about size adaptation, we observe a diversification pattern rather than evolution towards specific peaks, suggesting a complex interplay between phenotype and structural habitat.

Implementing this kind of dichotomous classification also presents challenges, as the vertical–horizontal axis represents a continuum, and species may exploit both structural dimensions depending on ecological context. Recent studies have shown that lacertid lizards present differences in claw morphology associated with substrate type (Baeckens et al. 2020); therefore, overlooking substrate properties within a vertical–horizontal locomotion framework may limit the detection of additional, finer-scale patterns of morphological and functional differentiation. Nonetheless, at broader evolutionary scales the vertical–horizontal approach remains a useful and biologically meaningful abstraction, and future studies integrating information on both the geometry and natural properties of the environment would provide a more comprehensive perspective and further enrich ecomorphological analyses.

6.2. Future perspectives

The results of this thesis provide answers to long-standing questions on how phenotypes evolve, while also generating new questions for future research. Building on these findings, an important avenue for future research lies in extending the analysis of form–function relationships beyond bite force performance to include other key performance traits, such as those related to locomotion. As exemplified in this thesis, performance represents the functional interface between morphology and ecology, examining multiple performance systems is essential for understanding how integrated phenotypes respond to ecological constraints. Structural habitat is expected to impose strong and contrasting demands on traits such as climbing ability, sprint speed, maneuverability, stability, and previous work in lizards (Garland and Losos 1994; Arnold 1998; Van Damme et al. 1998; Vanhooydonck and Van Damme 2001; Zaaf and Van Damme 2001; Gomes et al. 2018) - specifically in this thesis - it has been shown that limb proportions and limb segment relationships can differ between species that predominantly use vertical versus horizontal substrates (Vicent-Castelló et al. 2025b). Implementing a more comprehensive approach to locomotor performance, using video-recorded trials to quantify traits such as maximum speed, maneuverability, and acceleration, together with high-quality morphological descriptors such as the lengths of specific limb segments, would allow a more direct assessment of how habitat structure shapes functional trade-offs across the body, and whether patterns of performance convergence or divergence mirror those observed for biting performance.

In addition, head morphology itself may play a crucial role in habitat use: habitat-driven changes in head shape, such as flattening or narrowing in climbers, could influence access to refuges, use of crevices, and movement within structurally complex environments (Saulnier Masson et al. 2023). This raises the possibility that head morphology acts not only as a response to habitat structure, but also as a trait that feeds back into ecological specialization and habitat exploitation. Because bite force is tightly linked to head shape, it would therefore be expected that structural habitat may also constrain bite force, either directly through functional demands or indirectly via its influence on cranial morphology. For instance, in the lateral head structure associated with minimum bite force in chapter 3 we can observe the typical head structure of species adapted to climbing, such as *Holaspis* or *Dalmatolacerta oxycephala*. Exploring this link

would help clarify whether habitat-driven constraints act primarily on morphology, performance, or both. In a many-to-one mapping scenario, morphological adaptations to structural habitat may not directly translate into bite force variation, because other internal modifications may produce similar performance outputs. This could be explicitly investigated using a multibody dynamics modeling approach (Moazen et al. 2008; Gröning et al. 2013; Watson et al. 2014), which allows the integration of external morphology with internal anatomical parameters to simulate bite force production and cranial mechanics. By combining empirical morphological data with biomechanical models, it would be possible to test whether alternative morphological configurations associated with different habitats converge on similar performance through distinct mechanical pathways (Saulnier Masson et al. 2023).

Finally, future studies could explore how allometric relationships differ among habitats, as traits often scale with body size in non-uniform ways. Allometry provides a powerful framework to investigate whether ecological constraints act by modifying trait values, scaling relationships, or both (Klingenberg 2016). Habitat-specific allometric slopes may reveal whether certain traits are disproportionately emphasized or constrained in structural contexts, potentially uncovering hidden axes of adaptation that are obscured when allometric patterns are assumed to be universal (Tejero-Cicuéndez et al. 2023). Comparing allometric trajectories across habitats would therefore allow testing whether integration and decoupling emerge through changes in scaling, rather than through shifts in mean trait values alone. Together, these approaches would provide a more integrative understanding of how morphology, performance, and ecology interact across multiple functional systems, and how structural habitat shapes not only trait values, but also the scaling relationships that govern phenotypic evolution.

6.3. Concluding remarks

This thesis set out to understand how morphology, performance, and ecology interact to shape phenotypic evolution across biological and phylogenetic scales. Using lacertid lizards as a model system, it combined phylogenetic comparative methods with multilevel analyses to evaluate how body size, body shape, and bite performance evolve in response to structural habitat and climatic variation. The results consistently show that

phenotypic evolution is neither uniform across lineages nor consistent across scales. Instead, it is strongly context-dependent and structured by both ecological and historical factors.

Body size evolution within Lacertidae does not follow a single macroevolutionary trajectory. Although structural habitat and climate influence size variation, their effects differ among major phylogenetic groups. Patterns detected within tribes or subfamilies are not necessarily maintained at the family level, highlighting that evolutionary inferences depend critically on the phylogenetic scale of analysis. These findings indicate that ecogeographic trends cannot be generalized without accounting for lineage-specific histories. Body size evolves under multiple interacting selective pressures, and their relative contribution varies across clades and environments.

Structural habitat use also influences morphological evolution, but its effects are not evenly distributed across the body. The comparison between vertical and horizontal habitat use reveals that head morphology shows clearer evolutionary responses than trunk and limb traits. This suggests that different morphological modules respond differently to similar ecological gradients. Habitat-driven divergence is therefore trait-specific rather than a uniform whole-body shift. Some morphological components appear tightly associated with functional demands imposed by habitat use, whereas others show weaker or more variable responses.

The analyses of head shape and bite force clarify how form–function relationships scale across hierarchical levels. Associations between morphology and performance are present at the individual, species, and family levels, indicating that functional relationships are maintained across scales. However, the direction and strength of these associations differ among levels of organization. This pattern supports a many-to-one mapping scenario, in which multiple morphological configurations can produce comparable performance outcomes. Such mapping allows performance to remain functionally relevant while morphological evolution proceeds along different paths.

An important implication of these findings is that phenotypic integration and evolutionary decoupling are not contradictory. Traits can be functionally integrated in producing performance while exhibiting distinct evolutionary dynamics. Integration does not necessarily impose rigid constraints; instead, it can allow alternative morphological

solutions to similar functional challenges. This distinction is central for interpreting macroevolutionary patterns in complex trait systems, where apparent stability in performance may coexist with substantial morphological diversification.

Across all chapters, body size and allometry emerge as key structuring factors. Size mediates the relationship between morphology and performance, and separating size-dependent from size-independent components of variation is essential for detecting meaningful functional patterns. Even after accounting for allometry, shape retains functional relevance, indicating that performance is influenced by more than simple scaling effects. At the same time, size itself evolves in response to ecological context, reinforcing its dual role as both a driver and an outcome of evolutionary processes.

Taken together, these results demonstrate that ecological drivers such as structural habitat and climate shape phenotypic evolution in a scale-dependent and lineage-specific manner. Their effects are filtered through phylogenetic history and mediated by functional relationships among traits. Patterns observed at one scale may weaken or disappear at another, and performance may remain relatively stable despite morphological change. Understanding phenotypic diversification therefore requires integrating ecological context, functional structure, and evolutionary history within the same analytical framework.

In summary, phenotypic evolution in lacertid lizards reflects the interaction between ecological pressures, functional organization, and historical contingency. By explicitly combining macroevolutionary and multilevel perspectives, this thesis provides a coherent account of how complex phenotypes diversify under interacting constraints. Such integrative approaches are essential for advancing our understanding of adaptive evolution and for linking mechanistic form–function relationships to large-scale patterns of diversification.

References

Alfaro, M. E., D. I. Bolnick, and P. C. Wainwright. 2005. Evolutionary Consequences of Many-to-One Mapping of Jaw Morphology to Mechanics in Labrid Fishes. Am. Nat. 165:E140–E154. The University of Chicago Press.

Anderson, R. A., L. D. McBrayer, and A. Herrel. 2008. Bite force in vertebrates: opportunities and caveats for use of a nonpareil whole-animal performance measure. Biol. J. Linn. Soc. 93:709–720.

Arnold, E. N. 1998. Structural niche, limb morphology and locomotion in lacertid lizards (Squamata, Lacertidae); a preliminary survey. Bull. Nat. Hist. Mus., Zool. 64:63–90.

Arnold, S. 1983. Morphology, Performance and Fitness. Am. Zool. 23:347–361.

Baeckens, S., C. Goeyers, and R. Van Damme. 2020. Convergent Evolution of Claw Shape in a Transcontinental Lizard Radiation. Integr. Comp. Biol. 60:10–23.

Baken, E. K., and D. C. Adams. 2019. Macroevolution of arboreality in salamanders. Ecol. Evol. 9:7005–7016.

Benítez-López, A., L. Santini, J. Gallego-Zamorano, B. Milá, P. Walkden, M. A. J. Huijbregts, and J. A. Tobias. 2021. The island rule explains consistent patterns of body size evolution in terrestrial vertebrates. Nat Ecol. Evol. 5:768–786.

Blackburn, T. M., K. J. Gaston, and N. Loder. 1999. Geographic gradients in body size: a clarification of Bergmann's rule. Divers. Distrib. 5:165–174.

Brown, J. H., P. A. Marquet, and M. L. Taper. 1993. Evolution of body size: consequences of an energetic definition of fitness. Am. Nat. 142:573–584.

Calsbeek, R., and E. Marnocha. 2006. Context Dependent Territory Defense: The Importance of Habitat Structure in *Anolis sagrei*. Ethology. 112:537–543.

Christiansen, P., and J. S. Adolfssen. 2005. Bite forces, canine strength and skull allometry in carnivores (Mammalia, Carnivora). J. Zool. 266:133–151.

Collar, D. C., J. A. Schulte II, and J. B. Losos. 2011. Evolution of Extreme Body Size Disparity in Monitor Lizards (*Varanus*). Evolution. 65:2664–2680.

Collar, D. C., J. A. Schulte, B. C. O'Meara, and J. B. Losos. 2010. Habitat use affects morphological diversification in dragon lizards. J. Evol. Biol. 23:1033–1049.

Collar, D. C., and P. C. Wainwright. 2006. Discordance Between Morphological and Mechanical Diversity in the Feeding Mechanism of Centrarchid Fishes. Evolution. 60:2575–2584.

Cruz, F. B., D. L. Moreno Azocar, B. Vanhooydonck, J. A. Schulte, C. S. Abdala, and A. Herrel. 2021. Drivers and patterns of bite force evolution in liolaemid lizards. Biol. J. Linn. Soc.134:126–140.

De Meyer, J., D. J. Irschick, B. Vanhooydonck, J. B. Losos, D. Adriaens, and A. Herrel. 2019. The role of bite force in the evolution of head shape and head shape dimorphism in *Anolis* lizards. Funct. Ecol. 33:2191–2202.

Garland, T., and J. B. Losos. 1994. Ecological morphology of locomotor performance in squamate reptiles. P. in Ecological Morphology: IOB. University of Chicago Press, Chicago.

Gaston, K. J., and T. M. Blackburn. 1996. Range Size-Body Size Relationships: Evidence of Scale Dependence. Oikos. 75:479–485. [Nordic Society Oikos, Wiley].

Gomes, V., M. A. Carretero, and A. Kaliontzopoulou. 2018. Run for your life, but bite for your rights? How interactions between natural and sexual selection shape functional morphology across habitats. Naturwissenschaften. 105:9.

Goodman, B. A., and J. L. Isaac. 2008. Convergent body flattening in a clade of tropical rock-using lizards (Scincidae: Lygosominae). Biol. J. Linn. Soc.94:399–411.

Goodman, B. A., D. B. Miles, and L. Schwarzkopf. 2008. Life on the rocks: habitat use drives morphological and performance evolution in lizards. Ecology. 89:3462–3471.

Gould, S. J. 1966. Allometry and Size in Ontogeny and Phylogeny. Biol. Rev. 41:587–638.

Gröning, F., M. E. H. Jones, N. Curtis, A. Herrel, P. O'Higgins, S. E. Evans, and M. J. Fagan. 2013. The importance of accurate muscle modelling for biomechanical

analyses: a case study with a lizard skull. J. R. Soc. Interface. 10:20130216. Royal Society.

Hansen, T., and E. Martins. 1996. Translating between microevolutionary process and macroevolutionary patterns: The correlation structure of interspecific data. Evolution. 50:1404–1417.

Hogeweg, P. 2002. Multilevel processes in evolution and development: Computational models and biological insights. Pp. 217–239 in M. Lässig and A. Valleriani, eds. Biological Evolution and Statistical Physics. Springer, Berlin, Heidelberg.

Kaliontzopoulou, A., M. A. Carretero, and D. C. Adams. 2015. Ecomorphological variation in male and female wall lizards and the macroevolution of sexual dimorphism in relation to habitat use. J. Evol. Biol. 28:80–94.

Kaliontzopoulou, A., C. Pinho, and F. Martínez-Freiría. 2018. Where does diversity come from? Linking geographical patterns of morphological, genetic, and environmental variation in wall lizards. BMC Evol. Biol. 18:124.

Klingenberg, C. P. 2016. Size, shape, and form: concepts of allometry in geometric morphometrics. Dev. Genes. Evol. 226:113–137.

LaBarbera, M. 1989. Analyzing Body Size as a Factor in Ecology and Evolution. Annual Review of Ecology, Evolution, and Systematics 20:97–117. Annual Reviews.

Lande, R. 1976. Natural Selection and Random Genetic Drift in Phenotypic Evolution. Evolution. doi: 10.2307/2407703. JSTOR.

Lappin, A. K., P. S. Hamilton, and B. Sullivan. 2006. Bite-force performance and head shape in a sexually dimorphic crevice-dwelling lizard, the common chuckwalla [*Sauromalus ater* (= obesus)]. Biol. J. Linn. Soc. 88:215–222.

Lappin, A. K., and J. F. Husak. 2005. Weapon performance, not size, determines mating success and potential reproductive output in the collared lizard (*Crotaphytus collaris*). Am. Nat. 166:426–436.

Li, J., J.-P. Huang, J. Sukumaran, and L. L. Knowles. 2018. Microevolutionary processes impact macroevolutionary patterns. BMC Evol. Biol. 18:123.

Mitchell, D. R., E. Sherratt, and V. Weisbecker. 2024. Facing the facts: adaptive trade-offs along body size ranges determine mammalian craniofacial scaling. Biol. Rev. 99:496–524.

Moazen, M., N. Curtis, S. E. Evans, P. O'Higgins, and M. J. Fagan. 2008. Rigid-body analysis of a lizard skull: Modelling the skull of *Uromastyx hardwickii*. J. Biomech. 41:1274–1280.

Olalla-Tárraga, M. Á., M. Á. Rodríguez, and B. A. Hawkins. 2006. Broad-scale patterns of body size in squamate reptiles of Europe and North America. J. Biogeogr. 33:781–793.

Openshaw, G. H., and J. S. Keogh. 2014. Head shape evolution in monitor lizards (*Varanus*): interactions between extreme size disparity, phylogeny and ecology. J. Evol. Biol. 27:363–373.

Pigliucci, M. 2003. Phenotypic integration: studying the Ecol. Evol. of complex phenotypes. Ecol. Lett. 6:265–272.

Ronco, F., and W. Salzburger. 2021. Tracing evolutionary decoupling of oral and pharyngeal jaws in cichlid fishes. Evol. Lett. 5:625–635.

Saulnier Masson, R., K. Daoues, J. Measey, and A. Herrel. 2023. The evolution of bite force and head morphology in scincid lizards: diet and habitat use as possible drivers. Biol. J. Linn. Soc. 140:58–73.

Simon, M., M. Wildman, and D. S. Moen. 2025. Form–function relationships within species are uncoupled from those across species in swimming and jumping performance in arboreal frogs. Evolution. qpaf058.

Slavenko, A., A. Feldman, A. Allison, A. Bauer, M. Böhm, L. Chirio, G. Colli, I. Das, T. Doan, M. LeBreton, M. Martins, D. Meirte, Z. Nagy, C. Nogueira, O. Pauwels, D. Pincheira-Donoso, U. Roll, P. Wagner, Y. Wang, and S. Meiri. 2019. Global patterns of body size evolution in squamate reptiles are not driven by climate. Glob. Ecol. Biogeogr. doi: 10.1111/geb.12868.

Taverne, M., H. Dutel, M. Fagan, A. Štambuk, D. Lisičić, Z. Tadić, A.-C. Fabre, and A. Herrel. 2021. From micro to macroevolution: drivers of shape variation in an island radiation of *Podarcis* lizards. Evolution. 75:2685–2707.

Taverne, M., N. King-Gillies, M. Krajnović, D. Lisičić, Ó. Mira, D. Petricioli, I. Sabolić, A. Štambuk, Z. Tadić, C. Vigliotti, B. Wehrle, and A. Herrel. 2020. Proximate and ultimate drivers of variation in bite force in the insular lizards *Podarcis melisellensis* and *Podarcis sicula*. Biol. J. Linn. Soc.131:88–108.

Tejero-Cicuéndez, H., I. Menéndez, A. Talavera, G. Mochales-Riaño, B. Burriel-Carranza, M. Simó-Riudalbas, S. Carranza, and D. C. Adams. 2023. Evolution along allometric lines of least resistance: morphological differentiation in Pristurus geckos. Evolution. 77:2547–2560.

Terribile, L. C., M. Á. Olalla-Tárraga, J. A. F. Diniz-Filho, and M. Á. Rodríguez. 2009. Ecological and evolutionary components of body size: geographic variation of venomous snakes at the global scale: snake body size variation. Biol. J. Linn. Soc.98:94–109.

Thompson, C., N. Ahmed, T. Veen, C. Peichel, A. Hendry, D. Bolnick, and Y. Stuart. 2017. Many-to-one form-to-function mapping weakens parallel morphological evolution. Evolution. 71:2738–2749.

Tsuboi, M., T. Gaboriau, and T. Latrille. 2024. An introduction to the special issue: inferring macroevolutionary patterns and processes from microevolutionary mechanisms. J. Evol. Biol. 37:1395–1401.

Turelli, M., N. H. Barton, and J. A. Coyne. 2001. Theory and speciation. Trends in Ecol. Evol. 16:330–343.

Van Damme, R., P. Aerts, and B. Vanhooydonck. 1998. Variation in morphology, gait characteristics and speed of locomotion in two populations of lizards. Biol. J. Linn. Soc.63:409–427.

Vanhooydonck, B., and R. Van Damme. 2001. Evolutionary trade-offs in locomotor capacities in lacertid lizards: are splendid sprinters clumsy climbers? J. Evol. Biol. 14:46–54.

Verwaijen, D., R. Van Damme, and A. Herrel. 2002. Relationships between head size, bite force, prey handling efficiency and diet in two sympatric lacertid lizards. Funct. Ecol. 16:842–850.

Vicent-Castelló, P., U. Enriquez-Urzelai, F. Martínez-Freíria, J. Garcia-Porta, and A. Kaliontzopoulou. 2025a. Context-dependent body size evolution in lacertid lizards: differential role of structural habitat and climate across radiations. Evolution. qpaf130.

Vicent-Castelló, P., A. Herrel, D. J. Harris, and A. Kaliontzopoulou. 2025b. Walking or hanging: the role of habitat use for body shape evolution in lacertid lizards. J. Evol. Biol. voaf003.

Wainwright, P. C., M. E. Alfaro, D. I. Bolnick, and C. D. Hulsey. 2005. Many-to-One Mapping of Form to Function: A General Principle in Organismal Design?. Integr. Comp. Biol. 45:256–262.

Watson, P. J., F. Gröning, N. Curtis, L. C. Fitton, A. Herrel, S. W. McCormack, and M. J. Fagan. 2014. Masticatory biomechanics in the rabbit: a multi-body dynamics analysis. J. R. Soc. Interface. 11:20140564.

Zaaf, A., and R. Van Damme. 2001. Limb proportions in climbing and ground-dwelling geckos (Lepidosauria, Gekkonidae): a phylogenetically informed analysis. Zoomorphology. 121:45–53.

Appendix:

Supplementary information

Supplementary information for chapter 3

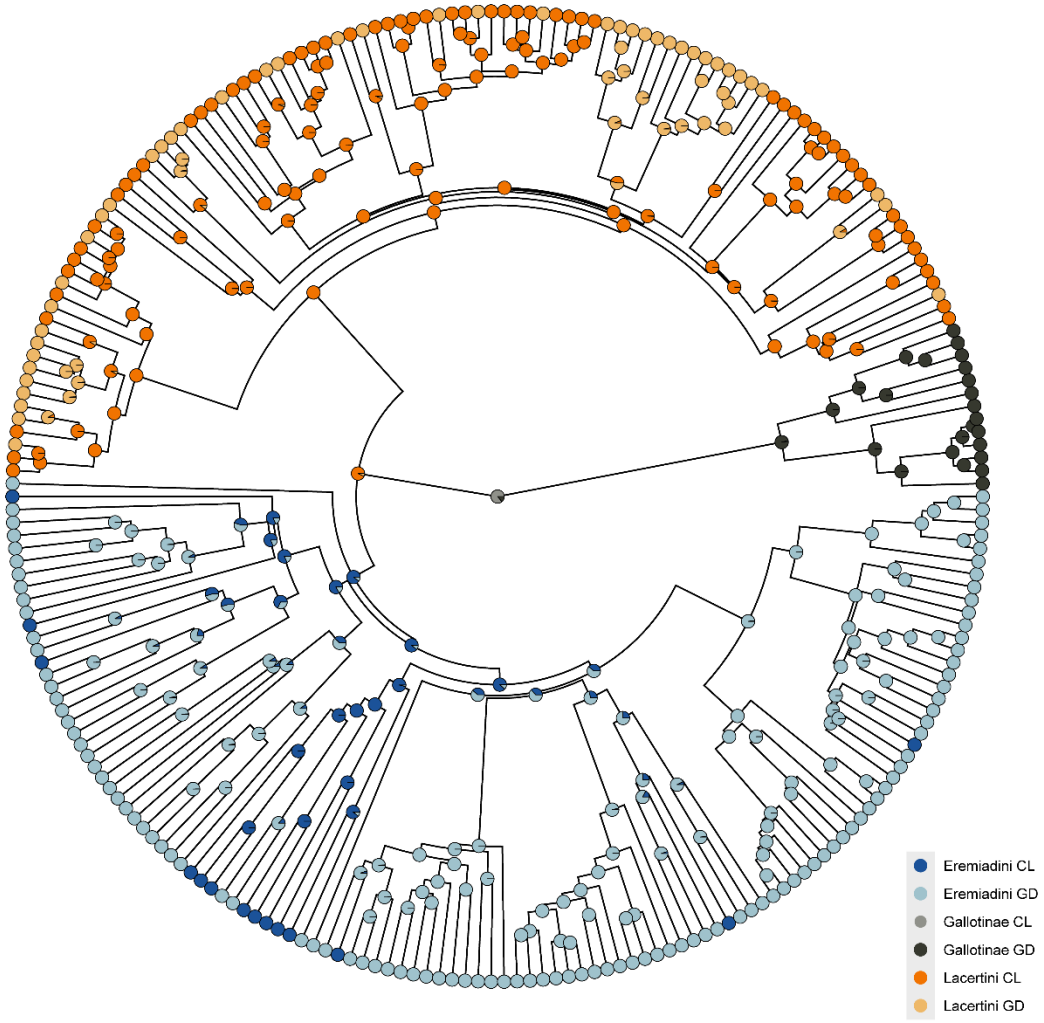

Figure S3.1. Summary of 100 evolutionary reconstructions of habitat use in lacertid lizards. The reconstruction is made from the most recent phylogeny of the family with 246 species (obtained from García-Porta et al 2019) using the all-rates-different (ARD) transition matrix. The reconstruction has been manually reclassified to assign species of each structural habitat category to different groups depending on their phylogenetic group (Gallotinae, Lacertini,

Eremiadini). Nodes in between tribes were randomly assigned to one tribe or another in 50:50 proportion. The fraction of assignment to each state over the 100 simulations is represented by pie charts on the internal nodes. The circles at the tips represent the species habitat use plus tribe.

Table S3.1. Mean SVL sample size (N) and standard deviation (SD; when possible) per species included in this study.

Species	***N***	***SVL***	***SD***	***Reference***
Acanthodactylus aegyptius	33	44.90	4.10	Baha el din, 2013
Acanthodactylus arabicus	7	54.00	4.20	this study
Acanthodactylus aureus	20	49.60	3.11	this study
Acanthodactylus bedriagai		64.62		Baeckens et al 2015
Acanthodactylus beershebensis		66.26		Baeckens et al 2015
Acanthodactylus blanci	4	74.08	4.35	this study
Acanthodactylus blanfordii	4	66.92	6.62	this study
Acanthodactylus boskianus	19	62.77	6.68	this study
Acanthodactylus busacki	7	61.90	8.60	Tamar et al 2017
Acanthodactylus cantoris	5	68.70	9.68	this study
Acanthodactylus dumerilii	11	52.83	2.67	this study
Acanthodactylus erythrurus	14	71.06	4.42	this study
Acanthodactylus felicis	1	52.98		this study
Acanthodactylus gongrorhynchatus	3	50.76	1.09	this study
Acanthodactylus grandis	6	73.77	17.90	this study
Acanthodactylus guineensis	4	48.69	6.13	this study
Acanthodactylus haasi	4	48.15	4.14	this study

Acanthodactylus hardyi	6	55.96	2.98	this study
Acanthodactylus harranensis	9	81.66	1.66	Beser et al 2019
Acanthodactylus khamirensis	9	47.10	0.90	Heidari et al 2013
Acanthodactylus lineomaculatus	4	68.40	2.11	this study
Acanthodactylus longipes	5	58.02	2.72	this study
Acanthodactylus maculatus	5	60.36	5.17	this study
Acanthodactylus margaritae	5	74.03	5.43	this study
Acanthodactylus masirae	5	53.34	3.56	this study
Acanthodactylus micropholis	3	56.20	2.19	this study
Acanthodactylus nilsoni	7	71.10	2.30	Heidari et al 2013
Acanthodactylus opheodurus	3	53.77	2.81	this study
Acanthodactylus orientalis	2	59.00	2.79	this study
Acanthodactylus pardalis	14	59.93	4.92	this study
Acanthodactylus robustus	1	66.03		this study
Acanthodactylus savignyi	2	45.65	0.43	this study
Acanthodactylus schmidti	10	61.68	7.98	this study
Acanthodactylus schreiberi	4	69.16	4.45	this study
Acanthodactylus scutellatus	5	58.55	8.47	this study
Acanthodactylus senegalensis	6	41.58		Ineich et al 2014
Acanthodactylus tilburyi	3	46.53	2.42	this study
Acanthodactylus tristrami	4	79.25	5.22	this study
Adolfus africanus	6	60.71	4.05	this study
Adolfus alleni	4	58.03	2.75	this study

Adolfus jacksoni		75.25		Baeckens et al 2015
Algyroides fitzingeri	3	36.03	1.38	this study
Algyroides marchi	6	44.28	2.42	this study
Algyroides moreoticus	5	45.45	3.45	this study
Algyroides nigropunctatus	7	62.88	3.88	this study
Anatololacerta anatolica	3	71.52	6.46	this study
Anatololacerta danfordi		67.50		Baeckens et al 2015
Anatololacerta oertzeni		43.40		Baeckens et al 2015
Apathya cappadocica	3	67.74	6.13	this study
Apathya yassujica	23	59.23	2.97	Karamiani et al 2015
Archaeolacerta bedriagae	20	71.28	9.51	this study
Atlantolacerta andreanskyi	15	45.40	1.53	this study
Australolacerta australis	6	68.61	3.56	this study
Congolacerta asukului		55.40		Baeckens et al 2015
Congolacerta vauereselli	3	53.85	2.87	this study
Dalmatolacerta oxycephala	21	60.41	3.21	this study
Darevskia armeniaca		61.50		Baeckens et al 2015
Darevskia brauneri		59.52		Baeckens et al 2015
Darevskia caspica	19	59.00	3.60	Ahmadzadeh et al 2013
Darevskia caucasica	4	53.82	4.18	this study
Darevskia chlorogaster	5	58.40	3.21	this study
Darevskia clarkorum		59.33		Baeckens et al 2015
Darevskia daghestanica		51.83		Baeckens et al 2015

Darevskia defilippii	15	51.20	1.80	Ahmadzadeh et al 2013
Darevskia derjugini	5	54.63	4.73	this study
Darevskia kamii	11	61.90	3.30	Ahmadzadeh et al 2013
Darevskia kopetdaghica	2	54.80	2.80	Ahmadzadeh et al 2013
Darevskia parvula	1	46.82		this study
Darevskia portschinskii		53.00		Baeckens et al 2015
Darevskia praticola	4	48.04	2.98	this study
Darevskia raddei	16	62.82	0.15	Dehghami et al 2014
Darevskia rudis	5	64.96	2.41	this study
Darevskia saxicola	1	66.05		this study
Darevskia schaekeli	2	52.10	0.40	Ahmadzadeh et al 2013
Darevskia steineri	3	53.50	2.70	Ahmadzadeh et al 2013
Darevskia valentini	1	70.54		this study
Dinarolacerta montenegrina		51.50		Baeckens et al 2015
Dinarolacerta mosorensis	6	62.95	2.40	this study
Eremias argus	6	53.48	2.11	this study
Eremias arguta	5	61.26	5.85	this study
Eremias brenchleyi	3	47.24	2.07	this study
Eremias grammica	3	62.52	6.03	this study
Eremias intermedia	6	55.36	2.97	this study
Eremias montanus		59.50		Bahmani et al 2011
Eremias multiocellata	3	62.85	2.72	this study
Eremias papenfussi	2	58.00		Mozaffari et al 2011

Eremias persica	6	77.68	6.91	this study
Eremias pleskei	2	52.95	4.14	this study
Eremias przewalskii	3	72.65	3.61	this study
Eremias scripta		44.00		Baeckens et al 2015
Eremias strauchi	2	64.17	2.60	this study
Eremias stummeri	50	51.48	0.62	Dujsebayeva et al 2009
Eremias suphani	20	63.89	5.16	Dusen et al 2013
Eremias velox	5	61.96	3.80	this study
Gallotia atlantica	18	88.86	7.96	this study
Gallotia bravoana	13	184.62	7.47	this study
Gallotia caesaris	18	91.10	8.21	this study
Gallotia galloti	17	111.82	5.78	this study
Gallotia intermedia	1	154.76		this study
Gallotia simonyi	12	235.31	11.48	this study
Gallotia stehlini	15	190.30	22.79	this study
Gastropholis prasina		109.00		Hipsley and Müller
Gastropholis vittata	2	78.46	0.59	this study
Heliobolus lugubris	21	55.88	2.90	this study
Heliobolus spekii	6	43.99	2.87	this study
Hellenolacerta graeca	2	65.28	12.99	this study
Holaspis guentheri	10	48.40	1.46	this study
Holaspis laevis	3	43.97	3.84	this study
Iberolacerta aranica		53.32		Baeckens et al 2015

Iberolacerta aurelioi	123	52.41	2.66	Arribas and Galan, 2005
Iberolacerta bonnali	1	51.57		this study
Iberolacerta cyreni	5	66.63	5.79	this study
Iberolacerta galani		60.87		Baeckens et al 2015
Iberolacerta horvathi	18	56.53	2.83	this study
Iberolacerta martinezricai		59.89		Baeckens et al 2015
Iberolacerta monticola	9	71.21	4.04	this study
Ichnotropis bivittata		67.69		Baeckens et al 2015
Ichnotropis capensis	8	56.58	10.62	this study
Ichnotropis squamulosa	8	56.47	2.72	this study
Iranolacerta brandtii	2	66.19	1.34	this study
Iranolacerta zagrosica		67.80		Baeckens et al 2015
Lacerta agilis	2	68.44	2.98	this study
Lacerta bilineata	3	98.34	13.83	this study
Lacerta media		98.50		Baeckens et al 2015
Lacerta pamphylica		94.40		Baeckens et al 2015
Lacerta schreiberi	6	96.68	8.19	this study
Lacerta strigata		97.14		Baeckens et al 2015
Lacerta trilineata		131.59		Baeckens et al 2015
Lacerta viridis	3	105.53	23.14	this study
Latastia longicaudata	11	90.95	10.92	this study
Meroles anchietae	16	50.53	5.30	this study
Meroles ctenodactylus	11	68.77	8.92	this study

Meroles cuneirostris	12	56.43	4.61	this study
Meroles knoxii	22	52.68	4.40	this study
Meroles micropholidotus		55.13		Baeckens et al 2015
Meroles reticulatus	2	54.00	1.97	this study
Meroles squamulosus	1	59.37		this study
Meroles suborbitalis	13	61.24	3.55	this study
Mesalina adramitana	5	42.09	2.61	this study
Mesalina bahaeldini		41.70		Baeckens et al 2015
Mesalina balfouri	4	50.59	3.28	this study
Mesalina bernoullii	26	46.30	4.65	Smid et al 2016
Mesalina brevirostris	5	46.37	5.00	this study
Mesalina guttulata	18	42.85	2.49	this study
Mesalina kuri		54.20		Baeckens et al 2015
Mesalina martini	5	39.75	1.79	this study
Mesalina microlepis	8	51.90	1.81	Smid et al 2016
Mesalina olivieri	5	42.28	1.98	this study
Mesalina pasteuri	3	46.41	6.61	this study
Mesalina rubropunctata	6	48.99	3.49	this study
Mesalina simoni	5	44.69	2.87	this study
Mesalina watsonana	5	45.19	3.02	this study
Nucras boulengeri	5	59.26	3.23	this study
Nucras holubi	2	48.74	0.75	this study
Nucras intertexta	17	66.42	12.05	this study

Nucras lalandii		85.37		Baeckens et al 2015
Nucras livida		72.00		Baeckens et al 2015
Nucras ornata		63.64		Baeckens et al 2015
Nucras taeniolata	9	62.28	17.34	this study
Nucras tessellata	6	65.28	7.20	this study
Omanosaura cyanura	3	46.35	6.67	this study
Omanosaura jayakari	4	152.05	14.53	this study
Ophisops beddomei	2	36.50		Vyas, 2003
Ophisops elegans	5	47.74	2.43	this study
Ophisops jerdonii	5	40.72	3.76	this study
Ophisops leschenaultii	4	50.43	3.38	this study
Ophisops microlepis	3	60.54	4.64	this study
Ophisops nictans	2	47.49	5.43	this study
Ophisops occidentalis	8	40.58	1.50	this study
Parvilacerta fraasii	4	58.07	2.21	this study
Parvilacerta parva	6	48.89	2.79	this study
Pedioplanis benguellensis		39.29		Baeckens et al 2015
Pedioplanis breviceps		48.82		Baeckens et al 2015
Pedioplanis burchelli	11	53.18	5.72	this study
Pedioplanis haackei		47.30		Baeckens et al 2015
Pedioplanis huntleyi		55.30		Baeckens et al,. 2015
Pedioplanis husabensis		47.70		Baeckens et al 2015
Pedioplanis inornata	10	50.03	5.19	this study

Pedioplanis laticeps	11	60.94	6.60	this study
Pedioplanis lineoocellata	15	56.10	4.68	this study
Pedioplanis namaquensis	13	51.30	2.35	this study
Pedioplanis spinalis	3	50.53	3.65	this study
Pedioplanis undata	6	50.25	2.61	this study
Philochortus spinalis		51.50		Baeckens et al 2015
Phoenicolacerta cyanisparsa		65.00		Baeckens et al 2015
Phoenicolacerta kulzeri	1	58.16		this study
Phoenicolacerta laevis	6	66.08	17.04	this study
Phoenicolacerta troodica	55	53.50	4.55	Rizk and Nassar, 2015
Podarcis bocagei	15	55.94	4.85	this study
Podarcis carbonelli	15	49.13	1.40	this study
Podarcis cretensis	15	67.25	1.92	this study
Podarcis erhardii	15	73.27	3.33	this study
Podarcis filfolensis	15	62.10	2.15	this study
Podarcis gaigeae	15	62.82	4.25	this study
Podarcis guadarramae	15	59.68	4.13	this study
Podarcis hispanicus	15	52.27	3.58	this study
Podarcis ionicus	15	74.29	1.93	this study
Podarcis levendis	14	75.88	4.94	this study
Podarcis lilfordi	15	72.51	2.21	this study
Podarcis liolepis	9	60.60	2.21	this study
Podarcis melisellensis	15	58.60	3.37	this study

Podarcis milensis	15	60.23	3.88	this study
Podarcis muralis	16	67.60	3.18	this study
Podarcis peloponnesiacus	15	80.71	3.09	this study
Podarcis pityusensis	15	73.15	4.74	this study
Podarcis siculus	15	76.37	2.90	this study
Podarcis tauricus	15	65.20	3.74	this study
Podarcis tiliguerta	15	57.09	3.86	this study
Podarcis vaucheri	15	58.41	3.39	this study
Podarcis virescens	10	57.70	5.13	this study
Podarcis waglerianus	15	70.35	2.12	this study
Poromera fordii	5	59.61	2.53	this study
Psammodromus algirus	17	72.97	4.59	this study
Psammodromus blanci	3	39.39	4.34	this study
Psammodromus edwarsianus	4	44.71	4.57	this study
Psammodromus hispanicus	11	41.75	4.13	this study
Psammodromus microdactylus	6	43.43	2.38	this study
Psammodromus occidentalis		44.30		Baeckens et al 2015
Pseuderemias smithii	6	42.76	1.11	this study
Scelarcis perspicillata	4	52.73	4.00	this study
Takydromus amurensis		54.00		Baeckens et al 2015
Takydromus dorsalis	1	55.93		this study
Takydromus formosanus	5	45.81	2.31	this study
Takydromus hsuehshanensis	78	60.50	0.40	Huang, 1998

Takydromus intermedius	1	43.60		Wang et al 2017
Takydromus luyeanus	1	52.62		this study
Takydromus sauteri	2	52.17	1.79	this study
Takydromus septentrionalis	6	64.96	2.64	this study
Takydromus sexlineatus	10	53.99	3.12	this study
Takydromus smaragdinus	4	46.47	4.78	this study
Takydromus sylvaticus	5	53.00	3.00	Tang et al 2007
Takydromus tachydromoides	2	54.75	0.91	this study
Takydromus toyamai	2	52.15	3.85	this study
Takydromus viridipunctatus	1	53.47		this study
Takydromus wolteri	2	45.22	0.81	this study
Teira dugesii	6	61.11	4.94	this study
Timon kurdistanicus	1	102.32		this study
Timon lepidus	15	133.53	21.23	this study
Timon nevadensis	19	197.38	16.00	Font et al 2009
Timon pater	4	149.98	7.66	this study
Timon princeps		125.88		Baeckens et al 2015
Timon tangitanus	1	155.92		this study
Tropidosaura cottrelli	1	60.65		this study
Tropidosaura essexi	8	42.76	4.15	this study
Tropidosaura gularis	10	56.60	4.74	this study
Tropidosaura montana	1	55.54		this study
Vhembelacerta rupicola	6	43.54	2.47	this study

Zootoca vivipara	21	49.85	3.45	this study

Table S3.3. Climatic variables and structural habitat

SP	Structural habitat	Pavg	Pmax	Pmin	Tavg	Tmax	Tmin	TmaxMax	TminMax	TmaxMin	TminMin	NDVIavg	NDVImax	NDVImin	TseasonAvrg	Tseasonmax	Tseasonmin	PseaonAvg	PseasonMax	PseasonMin
Acanthodactylus aegyptius	GD	-1.067	-1.045	-0.686	0.698	0.633	0.496	0.759	0.675	0.427	0.333	-0.589	0.633	-0.585	-0.166	-0.265	0.072	0.759	0.826	0.313
Acanthodactylus arabicus	GD	-0.958	-0.933	-0.656	1.373	1.022	1.338	0.941	1.288	1.039	1.393	-0.980	-1.344	-0.617	-1.157	-1.211	-0.978	0.403	0.882	0.392
Acanthodactylus aureus	GD	-1.076	-1.013	-0.680	1.030	0.642	1.109	0.683	1.184	0.531	1.046	-1.123	-1.068	-0.633	-0.940	-0.433	-1.240	0.801	1.815	0.711
Acanthodactylus bedriagai	GD	-0.484	-0.621	-0.353	-0.209	0.231	-0.247	0.178	-0.236	0.272	-0.393	-0.646	-0.532	-0.410	0.332	0.211	0.587	-1.130	-0.954	-0.644
Acanthodactylus beershebensis	GD	-0.417	-0.437	-0.621	0.325	0.195	0.208	0.233	0.327	0.120	0.116	-0.852	-1.114	-0.521	-0.202	-0.472	0.226	1.489	0.543	2.265
Acanthodactylus blanci	GD	-0.257	-0.428	-0.345	0.024	0.389	-0.006	0.262	-0.008	0.517	-0.117	-0.010	1.200	-0.362	0.285	0.044	0.429	-0.845	-0.813	-0.564
Acanthodactylus blanfordii	GD	-0.904	-0.819	-0.576	1.045	1.587	0.384	1.816	0.523	1.215	0.267	-1.187	-1.451	-0.729	0.582	0.703	-0.009	1.130	0.939	1.070
Acanthodactylus boskianus	GD	-0.950	-0.990	-0.515	1.317	1.412	0.842	1.585	1.033	1.089	0.666	-1.077	-1.068	-0.649	-0.010	0.614	-0.880	1.153	2.719	-1.042
Acanthodactylus busacki	GD	-1.024	-0.986	-0.682	0.678	0.431	0.718	0.480	0.803	0.327	0.656	-1.083	-1.007	-0.617	-0.640	0.072	-1.053	0.659	0.374	0.791
Acanthodactylus cantoris	GD	-0.415	0.174	-0.553	1.411	1.784	0.760	1.751	0.823	1.679	0.653	0.076	0.940	-0.585	0.277	0.498	-0.275	2.130	1.956	0.512
Acanthodactylus dumerilii	GD	-1.019	-1.031	-0.640	0.904	1.418	0.497	1.423	0.649	1.294	0.316	-1.125	-1.574	-0.633	0.338	0.580	-0.878	-0.049	1.645	-0.644
Acanthodactylus erythrurus	GD	-0.302	-0.442	-0.357	-0.219	-0.015	-0.135	-0.050	-0.134	0.020	-0.207	0.091	0.648	-0.426	0.135	0.116	-0.177	-0.673	-0.389	-0.803
Acanthodactylus felicis	GD	-0.919	-0.912	-0.574	1.250	0.834	1.195	0.693	1.098	0.936	1.268	-0.922	-1.037	-0.490	-0.946	-0.936	-0.989	0.459	0.232	0.512
Acanthodactylus gongrorhynchat	GD	-1.008	-0.911	-0.682	1.848	2.548	1.018	2.493	1.257	2.421	0.795	-1.207	-1.788	-0.633	0.092	0.089	0.287	1.577	1.448	1.827
Acanthodactylus grandis	GD	-0.956	-0.919	-0.686	0.843	1.657	0.116	1.732	0.414	1.423	-0.151	-0.971	-0.792	-0.585	1.012	0.750	0.941	0.623	0.232	0.990
Acanthodactylus guineensis	GD	0.761	1.720	-0.502	1.682	1.163	1.935	0.963	1.820	1.317	1.725	-0.228	0.143	-0.186	-1.534	-1.252	-1.637	1.448	1.504	0.711
Acanthodactylus haasi	CL	-0.978	-0.927	-0.638	1.561	1.854	0.975	1.975	1.197	1.693	0.762	-1.142	-1.650	-0.649	0.011	0.489	-0.661	1.094	1.419	1.110
Acanthodactylus hardyi	GD	-0.904	-0.915	-0.682	1.114	1.896	0.318	1.940	0.615	1.681	0.048	-1.051	-1.390	-0.585	0.918	0.619	1.160	0.580	0.148	0.910
Acanthodactylus harranensis	GD	-0.404	-0.348	-0.649	0.256	1.134	-0.238	1.192	-0.001	0.965	-0.460	-0.428	-1.221	0.197	1.131	0.602	1.784	0.485	-0.276	1.309
Acanthodactylus khamirensis	GD	-0.789	-0.610	-0.628	1.635	1.869	1.114	1.640	1.007	2.015	1.226	0.323	1.200	-0.649	-0.097	-0.347	0.296	1.999	1.080	2.703
Acanthodactylus lineomaculatus	GD	-0.405	-0.260	-0.686	0.247	-0.048	0.451	-0.039	0.352	-0.071	0.573	0.458	0.342	-0.106	-0.603	-0.597	-0.903	0.330	-0.191	0.791
Acanthodactylus longipes	GD	-1.095	-1.096	-0.643	1.270	1.783	0.627	1.883	0.841	1.508	0.435	-1.150	-1.773	-0.633	0.492	0.585	-0.193	0.285	2.267	-1.042

Acanthodactylus maculatus	GD	-0.799	-0.854	-0.577	0.335	0.898	0.057	0.848	0.140	0.884	-0.082	-0.957	-0.608	-0.601	0.510	0.526	0.295	-0.622	-0.191	-0.683
Acanthodactylus margaritae	GD	-0.762	-0.552	-0.686	0.419	-0.123	0.659	-0.044	0.546	-0.223	0.795	0.351	1.200	-0.298	-0.956	-0.935	-0.862	0.604	-0.107	1.309
Acanthodactylus masirae	GD	-0.989	-0.970	-0.665	1.711	1.574	1.442	1.596	1.503	1.430	1.374	-0.562	1.200	-0.649	-0.887	-0.756	-0.782	0.852	0.430	1.189
Acanthodactylus micropholis	GD	-0.861	-0.806	-0.560	1.184	1.545	0.561	1.718	0.651	1.351	0.490	-1.162	-1.313	-0.745	0.389	0.513	-0.042	1.039	0.967	0.950
Acanthodactylus nilsoni	GD	0.035	-0.130	-0.426	0.947	2.155	0.144	2.127	0.431	2.015	-0.131	-0.911	-1.650	-0.330	1.234	0.703	1.880	0.940	0.063	1.787
Acanthodactylus opheodurus	GD	-0.943	-0.885	-0.629	1.423	1.846	0.785	1.891	1.001	1.635	0.585	-1.113	-1.528	-0.665	0.148	0.591	-0.707	0.864	0.798	0.950
Acanthodactylus orientalis	GD	-0.783	-0.709	-0.686	0.720	1.725	-0.024	1.767	0.253	1.532	-0.269	-0.769	-0.210	-0.569	1.150	0.836	1.097	0.702	0.148	1.110
Acanthodactylus pardalis	GD	-0.940	-0.830	-0.686	0.463	0.253	0.445	0.273	0.539	0.196	0.372	-1.044	-1.267	-0.505	-0.370	-0.543	-0.064	1.299	0.798	1.468
Acanthodactylus robustus	GD	-0.917	-0.905	-0.686	0.345	0.938	-0.172	1.077	0.097	0.679	-0.405	-0.945	-1.221	-0.553	0.818	0.625	0.870	0.434	0.204	0.990
Acanthodactylus savignyi	GD	-0.107	-0.152	-0.543	0.011	0.321	0.038	0.207	0.015	0.432	0.004	0.121	0.756	-0.346	0.146	0.099	0.111	-0.275	-0.587	-0.205
Acanthodactylus schmidti	GD	-0.959	-0.859	-0.652	1.587	2.190	0.826	2.200	1.080	1.999	0.587	-1.135	-1.451	-0.665	0.333	0.591	-0.213	1.294	1.504	1.110
Acanthodactylus schreiberi	GD	-0.256	0.177	-0.639	0.359	0.517	0.291	0.436	0.265	0.571	0.341	0.469	0.173	0.740	0.002	0.097	0.011	1.038	0.713	1.070
Acanthodactylus scutellatus	GD	-1.086	-1.081	-0.639	1.179	1.389	0.637	1.599	0.837	1.057	0.459	-1.147	-1.696	-0.633	0.226	0.378	0.151	0.419	2.352	-1.042
Acanthodactylus senegalensis	GD	-0.968	-0.737	-0.678	1.874	1.773	1.437	1.840	1.552	1.542	1.327	-1.056	-1.374	-0.617	-0.594	-0.258	-1.102	2.700	2.409	0.871
Acanthodactylus tilburyi	GD	-1.024	-0.983	-0.686	0.917	1.540	0.228	1.637	0.525	1.296	-0.041	-1.075	-1.742	-0.553	0.821	0.505	0.844	0.580	0.459	1.030
Acanthodactylus tristrami	GD	-0.697	-0.633	-0.665	0.104	0.322	-0.174	0.464	0.053	0.107	-0.364	-0.850	-0.869	-0.521	0.381	0.378	0.517	0.915	0.515	1.110
Adolfus africanus	CL	1.431	0.900	1.365	1.000	-0.179	1.551	-0.150	1.476	-0.208	1.622	1.081	1.031	0.389	-1.992	-1.685	-1.913	-0.488	0.035	-0.723
Adolfus alleni	CL	1.465	1.120	1.046	-0.707	-2.306	0.309	-2.009	0.236	-2.518	0.410	0.924	0.618	0.612	-1.999	-1.998	-1.729	-0.682	-0.813	-0.245
Adolfus jacksoni	CL	1.656	1.040	2.331	0.716	-0.613	1.397	-0.542	1.291	-0.667	1.507	1.420	1.001	0.580	-2.105	-1.993	-1.923	-1.116	0.006	-0.962
Algyroides fitzingeri	CL	0.083	-0.015	-0.287	-0.257	-0.181	-0.043	-0.426	-0.190	0.134	0.059	1.342	1.169	1.522	-0.168	-0.353	0.171	-0.573	-0.813	-0.325
Algyroides marchi	CL	-0.219	-0.389	-0.360	-0.707	-0.203	-0.571	-0.213	-0.563	-0.188	-0.686	0.761	0.066	1.043	0.323	-0.052	0.826	-1.150	-1.378	-0.524
Algyroides moreoticus	GD	0.257	0.416	-0.204	-0.290	-0.202	-0.151	-0.392	-0.212	0.042	-0.078	1.040	0.710	1.299	0.029	-0.195	0.272	0.089	-0.333	0.512
Algyroides nigropunctatus	CL	0.938	0.629	1.135	-0.608	-0.511	-0.486	-0.665	-0.549	-0.288	-0.382	0.700	0.526	0.596	0.234	0.166	0.485	-1.125	-0.644	-1.162
Anatololacerta anatolica	CL	0.085	0.282	-0.277	-0.533	-0.323	-0.525	-0.342	-0.423	-0.286	-0.601	0.469	0.556	0.229	0.373	0.089	0.654	-0.198	-0.107	-0.285
Anatololacerta danfordi	CL	0.004	0.109	-0.343	-0.806	-0.633	-0.758	-0.633	-0.728	-0.594	-0.742	-0.069	0.388	-0.330	0.551	0.230	0.710	-0.106	0.006	-0.126

Anatololacerta oertzeni	CL	0.160	0.442	-0.333	-0.327	-0.085	-0.302	-0.153	-0.251	-0.007	-0.320	0.440	0.327	-0.090	0.424	0.153	0.500	0.429	0.289	0.193
Apathya cappadocica	CL	-0.070	-0.107	-0.568	-0.538	0.190	-0.884	0.180	-0.728	0.176	-0.993	-0.453	0.219	-0.969	1.190	0.977	0.967	0.084	0.006	-0.006
Apathya yassujica	CL	-0.910	-0.757	-0.686	-0.078	0.586	-0.469	0.912	-0.236	0.113	-0.659	-1.220	-1.987	-0.601	0.957	0.455	1.590	1.243	0.289	2.106
Archaeolacerta bedriagae	CL	0.162	0.043	-0.113	-0.554	-0.526	-0.254	-0.791	-0.438	-0.167	-0.097	1.200	0.587	1.522	-0.181	-0.386	0.188	-0.789	-1.011	-0.444
Atlantolacerta andreanskyi	GD	-0.400	-0.511	-0.503	-0.848	-0.634	-0.690	-0.678	-0.743	-0.539	-0.625	-0.759	-0.853	-0.505	0.340	0.104	0.613	-0.588	-0.813	-0.325
Australolacerta australis	CL	-0.433	-0.448	-0.082	-0.237	-0.747	0.114	-0.585	0.138	-0.883	-0.011	-0.143	-0.532	0.021	-0.642	-0.800	-0.315	-0.331	-0.644	-0.365
Congolacerta asukului	GD	2.273	1.902	-0.018	-0.467	-2.120	0.532	-1.975	0.320	-2.091	0.719	1.408	0.664	1.937	-2.140	-2.153	-1.860	-0.399	-0.898	0.313
Congolacerta vauereselli	GD	1.431	0.952	1.136	0.517	-0.924	1.280	-0.769	1.159	-0.977	1.358	1.454	1.047	1.554	-2.155	-2.095	-1.931	-0.958	-0.728	-0.962
Dalmatolacerta oxycephala	CL	0.865	0.497	1.264	-0.786	-0.686	-0.643	-0.778	-0.699	-0.526	-0.543	0.282	0.005	0.596	0.264	0.003	0.614	-1.360	-1.350	-1.281
Darevskia caspica	CL	-0.267	-0.412	-0.205	-0.582	-0.342	-0.651	-0.437	-0.835	-0.203	-0.427	-0.016	0.005	-0.617	0.812	0.889	0.775	-0.458	-0.361	-0.126
Darevskia caucasica	CL	0.495	0.289	0.884	-2.081	-2.203	-1.696	-2.169	-1.826	-2.085	-1.503	-0.734	-0.562	-0.984	0.539	0.252	0.801	-0.703	-0.926	-0.644
Darevskia chlorogaster	CL	-0.046	-0.217	-0.094	-0.470	-0.215	-0.543	-0.313	-0.669	-0.082	-0.381	0.086	0.005	-0.841	0.635	0.814	0.775	-0.636	-0.474	-0.405
Darevskia clarkorum	CL	1.505	0.826	2.458	-0.961	-1.092	-0.710	-1.338	-0.933	-0.703	-0.445	0.791	-0.041	1.426	0.309	0.028	0.745	-1.694	-1.802	-1.201
Darevskia daghestanica	CL	0.127	0.125	0.135	-1.949	-2.016	-1.605	-1.969	-1.717	-1.933	-1.432	-0.745	-0.915	-0.984	0.673	0.487	1.095	-0.471	-0.898	0.074
Darevskia defilippii	CL	-0.379	-0.447	-0.286	-0.588	-0.229	-0.710	-0.276	-0.790	-0.160	-0.596	-0.395	0.005	-0.969	0.865	0.868	0.788	-0.295	-0.304	-0.126
Darevskia derjugini	GD	1.402	0.612	2.694	-1.294	-1.323	-1.068	-1.412	-1.154	-1.119	-0.933	0.196	0.357	-0.969	0.427	0.297	0.713	-1.794	-1.435	-1.361
Darevskia kamii	CL	-0.566	-0.524	-0.445	-0.306	0.224	-0.525	0.169	-0.567	0.268	-0.448	-0.398	-0.547	-0.442	0.927	0.769	1.159	-0.117	-0.474	-0.006
Darevskia kopetdaghica	GD	-0.475	-0.501	-0.266	-0.766	0.015	-1.033	0.004	-0.975	0.019	-1.040	-0.909	-1.390	-0.761	1.440	0.889	2.090	0.182	-0.446	0.950
Darevskia parvula	CL	0.289	-0.045	1.221	-1.691	-1.618	-1.526	-1.596	-1.540	-1.534	-1.451	-0.674	0.587	-1.000	0.802	0.751	0.712	-1.337	-1.237	-1.162
Darevskia portschinskii	CL	-0.109	-0.080	0.142	-0.909	-0.522	-0.922	-0.620	-0.930	-0.366	-0.866	-0.310	-0.654	-0.250	0.835	0.493	1.288	-0.851	-1.096	-0.524
Darevskia praticola	GD	0.143	-0.110	0.964	-0.996	-0.644	-1.078	-0.751	-1.084	-0.468	-1.022	0.198	0.480	-0.202	0.833	0.930	0.787	-1.377	-1.067	-1.241
Darevskia raddei	CL	-0.366	-0.394	-0.057	-1.309	-0.791	-1.488	-0.738	-1.385	-0.809	-1.529	-1.037	-0.087	-1.016	1.140	0.958	1.357	-0.649	-0.531	-0.564
Darevskia rudis	CL	0.362	-0.097	1.333	-1.301	-1.377	-1.083	-1.416	-1.154	-1.232	-0.967	0.135	0.587	-1.016	0.427	0.573	0.521	-1.343	-1.067	-1.162
Darevskia saxicola	CL	0.547	0.330	0.818	-1.988	-2.159	-1.580	-2.084	-1.730	-2.099	-1.370	-0.204	-0.164	-0.601	0.409	0.206	0.829	-0.826	-0.870	-0.763
Darevskia schaekeli	CL	-0.735	-0.676	-0.499	-1.045	-0.709	-1.143	-0.709	-1.243	-0.663	-0.992	-0.690	-0.501	-0.617	1.269	0.903	1.487	-0.090	-0.389	0.074

Darevskia steineri	CL	-0.481	-0.450	-0.525	-0.032	0.487	-0.255	0.399	-0.339	0.553	-0.136	-0.033	-0.838	0.596	0.749	0.429	1.233	0.030	-0.559	0.751
Darevskia valentini	CL	-0.133	-0.248	0.072	-1.550	-1.314	-1.548	-1.215	-1.464	-1.354	-1.571	-0.781	0.066	-1.016	0.942	0.968	0.835	-0.819	-0.700	-0.803
Dinarolacerta montenegrina	CL	0.951	0.306	1.950	-1.779	-2.020	-1.325	-1.938	-1.370	-1.979	-1.224	-0.824	-1.604	-0.202	0.205	-0.179	0.754	-1.827	-2.000	-1.122
Dinarolacerta mosorensis	CL	0.916	0.544	1.460	-1.048	-1.034	-0.835	-1.069	-0.875	-0.923	-0.749	0.216	-0.118	0.532	0.230	-0.077	0.647	-1.488	-1.407	-1.281
Eremias argus	GD	-0.382	0.001	-0.510	-1.753	-0.540	-2.463	-0.322	-2.385	-0.789	-2.463	-0.885	-0.041	-0.953	2.612	3.143	1.551	1.288	0.911	0.472
Eremias arguta	GD	-0.650	-0.796	-0.099	-1.567	-0.188	-2.185	-0.242	-2.052	-0.033	-2.246	-1.252	1.154	-1.096	2.619	2.521	1.672	-1.305	-0.587	-1.201
Eremias brenchleyi	CL	0.076	0.653	-0.277	-0.775	0.024	-1.303	0.077	-1.319	-0.054	-1.231	-0.350	0.143	-0.346	1.647	1.624	1.471	0.956	1.222	0.153
Eremias grammica	GD	-0.773	-0.808	-0.482	-0.673	0.738	-1.386	0.730	-1.202	0.676	-1.509	-1.111	0.173	-1.032	1.990	2.373	1.618	-0.307	0.063	-0.923
Eremias intermedia	GD	-0.836	-0.850	-0.531	-0.693	0.810	-1.437	0.749	-1.259	0.812	-1.557	-1.108	-0.624	-1.000	2.113	2.393	1.675	-0.478	0.063	-0.962
Eremias montanus	GD	0.014	-0.074	-0.605	-0.744	0.116	-1.109	0.337	-0.719	-0.187	-1.443	-1.267	-1.558	-0.921	1.132	0.666	1.621	0.568	-0.191	1.349
Eremias multiocellata	GD	-0.875	-0.701	-0.629	-2.415	-1.121	-3.082	-0.832	-2.997	-1.415	-3.077	-1.328	-1.451	-1.048	3.066	3.539	2.967	1.229	0.826	0.472
Eremias papenfussi	GD	-0.683	-0.586	-0.612	-0.739	-0.065	-1.066	-0.097	-1.032	-0.033	-1.054	-1.257	-1.436	-1.048	1.384	0.877	1.952	0.208	-0.276	0.831
Eremias persica	GD	-0.832	-0.744	-0.599	0.286	1.067	-0.321	1.297	-0.140	0.680	-0.464	-1.197	-1.482	-0.969	1.031	0.916	0.529	0.875	0.798	0.631
Eremias pleskei	GD	-0.606	-0.563	-0.323	-0.804	-0.004	-1.300	0.000	-1.196	-0.019	-1.352	-0.968	-1.359	-0.569	1.451	1.000	1.947	-0.638	-0.813	-0.245
Eremias przewalskii	GD	-0.831	-0.720	-0.627	-1.990	-1.174	-2.428	-0.753	-2.310	-1.646	-2.468	-1.205	-0.685	-1.032	2.099	2.669	1.239	0.934	0.882	-0.325
Eremias strauchi	GD	-0.518	-0.525	-0.361	-0.804	-0.186	-1.086	-0.143	-0.989	-0.236	-1.131	-0.999	0.020	-0.953	1.196	0.979	1.337	-0.162	-0.220	-0.405
Eremias stummeri	GD	-0.534	-0.510	-0.354	-2.204	-1.911	-2.207	-1.595	-2.231	-2.179	-2.112	-1.528	-1.681	-1.096	2.019	1.875	2.522	-0.116	-0.248	-0.763
Eremias suphani	GD	-0.142	-0.192	-0.332	-1.626	-1.070	-1.715	-1.038	-1.583	-1.038	-1.784	-1.243	-1.252	-1.000	1.222	0.762	1.736	-0.587	-0.926	-0.006
Eremias velox	GD	-0.861	-0.934	-0.392	-1.203	0.076	-1.896	0.167	-1.733	-0.057	-1.993	-1.219	0.725	-1.064	2.281	2.470	1.832	-0.283	0.798	-1.162
Gallotia atlantica	GD	-0.891	-0.783	-0.686	0.566	-0.159	0.962	-0.346	0.747	0.082	1.188	2.073	1.200	2.720	-1.287	-1.398	-0.949	0.954	0.176	1.548
Gallotia bravoana	GD	-0.581	-0.424	-0.686	0.164	-0.594	0.704	-0.879	0.428	-0.192	0.994	2.073	1.200	2.720	-1.117	-1.295	-0.716	0.712	-0.107	1.548
Gallotia caesaris	GD	-0.533	-0.386	-0.686	0.233	-0.526	0.761	-0.827	0.496	-0.110	1.040	2.073	1.200	2.720	-1.149	-1.295	-0.787	0.769	-0.022	1.548
Gallotia galloti	GD	-0.381	-0.291	-0.644	-0.141	-0.777	0.406	-0.980	0.194	-0.467	0.640	1.095	1.200	1.011	-1.001	-0.878	-0.782	0.653	-0.050	1.349
Gallotia intermedia	GD	-0.571	-0.405	-0.686	0.200	-0.507	0.703	-0.734	0.467	-0.186	0.954	1.649	1.200	1.011	-1.139	-1.111	-0.878	0.681	-0.022	1.468
Gallotia simonyi	GD	-0.544	-0.386	-0.686	0.268	-0.484	0.786	-0.804	0.538	-0.046	1.049	2.073	1.200	2.720	-1.169	-1.329	-0.787	0.845	0.006	1.667

Gallotia stehlini	GD	-0.682	-0.621	-0.649	0.317	-0.304	0.737	-0.515	0.541	-0.021	0.948	1.403	1.200	0.692	-1.251	-1.276	-0.988	0.700	-0.022	1.428
Gastropholis prasina	CL	0.580	0.948	0.706	1.210	0.261	1.574	0.074	1.414	0.465	1.735	1.157	1.200	1.411	-1.682	-1.720	-1.491	-0.171	-0.502	0.313
Gastropholis vittata	CL	0.754	1.094	0.436	1.250	0.304	1.610	0.185	1.485	0.414	1.732	1.164	0.940	1.011	-1.670	-1.680	-1.408	-0.026	0.289	0.113
Heliobolus lugubris	GD	-0.414	-0.102	-0.646	0.802	0.136	0.809	0.769	1.004	-0.408	0.498	0.100	0.449	-0.490	-0.757	-0.408	-1.182	1.165	0.826	1.149
Heliobolus spekii	GD	-0.314	-0.072	-0.027	1.356	0.282	1.854	0.279	1.817	0.258	1.833	-0.412	0.618	-0.458	-1.788	-1.286	-1.731	1.137	1.278	0.153
Hellenolacerta graeca	CL	0.239	0.381	-0.197	-0.309	-0.217	-0.172	-0.395	-0.226	0.015	-0.107	1.040	0.710	1.299	0.028	-0.192	0.266	0.063	-0.333	0.472
Holaspis guentheri	CL	2.174	1.813	1.553	1.331	0.248	1.799	0.102	1.687	0.410	1.903	1.322	1.016	0.804	-1.997	-1.841	-1.842	-0.589	-0.163	-0.843
Holaspis laevis	CL	0.874	1.563	-0.303	1.280	0.419	1.512	0.513	1.522	0.254	1.501	1.391	1.047	1.235	-1.517	-1.354	-1.512	1.113	0.713	1.189
Iberolacerta aranica	CL	1.349	0.600	2.545	-1.698	-2.039	-0.875	-2.221	-1.157	-1.658	-0.619	0.247	0.066	-0.266	-0.136	-0.448	0.351	-2.035	-2.141	-1.361
Iberolacerta aurelioi	CL	1.473	0.690	2.470	-2.019	-2.435	-1.138	-2.633	-1.386	-2.003	-0.862	-0.887	-1.666	-0.266	-0.160	-0.487	0.348	-2.054	-2.170	-1.361
Iberolacerta bonnali	CL	1.300	0.587	1.923	-1.754	-2.103	-0.921	-2.297	-1.195	-1.703	-0.628	-0.919	-1.221	-0.793	-0.175	-0.454	0.288	-2.042	-2.141	-1.361
Iberolacerta cyreni	CL	0.068	-0.173	-0.002	-1.063	-0.983	-0.706	-1.050	-0.806	-0.831	-0.678	0.716	0.342	0.979	0.196	-0.119	0.710	-1.298	-1.463	-0.763
Iberolacerta galani	CL	1.077	0.792	0.651	-1.347	-1.627	-0.776	-1.749	-0.999	-1.354	-0.613	0.844	0.311	0.995	-0.074	-0.400	0.407	-1.056	-1.378	-0.365
Iberolacerta horvathi	CL	1.626	0.727	2.439	-1.592	-1.782	-1.213	-1.797	-1.351	-1.638	-1.080	0.134	0.143	-0.681	0.347	0.245	0.759	-1.617	-1.689	-1.122
Iberolacerta martinezricai	CL	0.620	0.579	-0.154	-0.695	-0.743	-0.356	-0.908	-0.500	-0.485	-0.298	1.265	0.480	1.826	0.187	-0.177	0.711	-0.898	-1.265	-0.205
Iberolacerta monticola	CL	1.068	0.652	0.977	-1.034	-1.511	-0.445	-1.637	-0.645	-1.246	-0.256	1.177	0.848	1.299	-0.427	-0.446	-0.521	-1.283	-1.265	-0.923
Ichnotropis capensis	GD	0.189	0.745	-0.596	0.812	-0.014	0.942	0.546	1.039	-0.373	0.614	0.886	0.848	0.405	-1.084	-0.765	-1.712	1.209	0.769	1.030
Iranolacerta brandtii	GD	-0.554	-0.511	-0.369	-1.161	-0.637	-1.355	-0.541	-1.234	-0.722	-1.420	-1.118	-1.344	-1.032	1.034	0.721	1.373	-0.617	-0.672	-0.564
Iranolacerta zagrosica	CL	-0.668	-0.604	-0.649	-1.214	-0.669	-1.425	-0.549	-1.186	-0.781	-1.604	-1.695	-2.447	-1.080	1.059	0.542	1.704	0.750	-0.078	1.588
Lacerta agilis	GD	-0.182	-0.310	0.284	-1.936	-1.117	-2.178	-1.160	-2.148	-0.866	-2.136	-0.726	0.602	-1.064	2.083	2.540	0.549	-1.186	-0.191	-1.241
Lacerta bilineata	GD	0.419	-0.061	1.265	-0.810	-0.957	-0.500	-1.091	-0.658	-0.722	-0.376	0.870	1.016	-0.617	-0.009	0.179	-0.128	-1.726	-0.954	-1.480
Lacerta media	GD	-0.222	-0.348	-0.270	-0.840	-0.309	-1.062	-0.265	-0.914	-0.351	-1.160	-0.645	0.327	-1.016	1.036	0.954	0.704	-0.159	0.091	-0.803
Lacerta pamphylica	GD	0.289	0.678	-0.422	-0.267	-0.129	-0.239	-0.273	-0.313	0.054	-0.134	0.473	0.388	-0.026	0.324	0.123	0.539	0.655	0.119	0.950
Lacerta schreiberi	GD	0.773	0.421	0.486	-0.696	-1.008	-0.287	-1.106	-0.426	-0.814	-0.198	1.103	0.940	0.708	-0.284	-0.004	-0.488	-1.046	-0.954	-1.002
Lacerta strigata	GD	-0.328	-0.481	0.295	-0.826	-0.261	-1.009	-0.389	-1.011	-0.087	-0.960	-0.286	0.143	-0.889	1.078	1.077	0.855	-0.921	-0.587	-0.843

Lacerta trilineata	GD	0.074	-0.091	0.336	-0.658	-0.474	-0.631	-0.573	-0.609	-0.326	-0.616	0.447	0.848	-0.042	0.422	0.343	0.419	-0.897	-0.078	-1.122
Lacerta viridis	GD	0.091	-0.244	0.965	-1.004	-0.809	-1.017	-0.933	-1.060	-0.592	-0.961	0.499	1.185	0.277	0.701	0.898	0.671	-1.428	-0.954	-1.201
Latastia longicaudata	GD	-0.350	-0.108	-0.378	1.649	1.109	1.642	1.200	1.715	0.896	1.493	-0.657	0.051	-0.601	-1.195	-0.302	-1.660	2.201	2.832	-0.086
Meroles anchietae	GD	-1.070	-0.996	-0.682	0.461	-0.467	0.922	-0.031	1.159	-1.002	0.679	-1.193	-1.650	-0.729	-1.443	-1.275	-1.287	1.033	1.391	-0.126
Meroles ctenodactylus	GD	-1.041	-1.039	-0.611	0.176	-0.666	0.626	-0.259	0.826	-1.140	0.437	-1.127	-1.528	-0.745	-1.309	-1.042	-1.310	-0.499	0.063	-0.405
Meroles cuneirostris	GD	-1.068	-1.023	-0.658	0.279	-0.591	0.725	-0.121	0.980	-1.162	0.456	-1.143	-1.650	-0.729	-1.344	-1.042	-1.302	0.092	0.826	-0.365
Meroles knoxii	GD	-0.816	-0.848	-0.432	0.210	-0.379	0.509	-0.113	0.646	-0.693	0.351	-0.844	-0.608	-0.713	-0.910	-0.559	-1.293	-0.503	-0.531	-1.082
Meroles micropholidotus	GD	-1.119	-1.080	-0.686	0.421	-0.554	0.929	-0.176	1.166	-1.004	0.703	-1.198	-1.880	-0.697	-1.556	-1.560	-1.301	-0.003	0.232	-0.126
Meroles reticulatus	GD	-0.993	-0.898	-0.686	0.760	-0.215	1.149	0.042	1.267	-0.539	1.040	-1.196	-1.482	-0.713	-1.504	-1.475	-1.236	1.941	1.561	0.990
Meroles squamulosus	GD	0.139	0.653	-0.523	0.905	0.132	1.001	0.556	1.093	-0.217	0.791	0.873	0.940	0.117	-1.030	-0.513	-1.419	1.177	0.854	0.871
Meroles suborbitalis	GD	-0.832	-0.736	-0.525	0.359	-0.037	0.438	0.430	0.722	-0.648	0.156	-0.921	-1.145	-0.665	-0.521	-0.347	-1.201	0.384	1.024	-0.803
Mesalina adramitana	GD	-0.986	-0.908	-0.639	1.709	2.074	1.071	2.130	1.318	1.854	0.834	-1.120	-1.604	-0.681	-0.206	0.488	-0.613	1.104	1.448	0.990
Mesalina bahaeldini	GD	-1.088	-1.082	-0.686	0.284	0.202	0.137	0.367	0.298	0.082	0.003	-1.134	-1.758	-0.633	-0.107	-0.398	0.347	0.224	-0.191	0.512
Mesalina balfouri	GD	-0.925	-0.817	-0.564	1.305	0.586	1.691	0.149	1.361	1.096	1.921	1.632	1.200	0.053	-1.523	-1.622	-1.194	-0.182	-0.531	0.273
Mesalina bernoullii	GD	-0.490	-0.499	-0.594	0.305	0.336	0.088	0.435	0.273	0.183	-0.062	-0.637	-0.807	-0.521	0.136	-0.133	0.527	1.432	0.572	1.986
Mesalina brevirostris	GD	-0.907	-0.895	-0.535	1.188	1.615	0.547	1.698	0.754	1.371	0.354	-1.016	0.204	-0.681	0.447	0.634	-0.037	1.086	1.787	1.030
Mesalina guttulata	GD	-1.028	-1.037	-0.585	1.319	1.516	0.789	1.662	0.980	1.209	0.615	-1.117	-1.482	-0.633	0.123	0.559	-0.644	0.962	2.578	-1.042
Mesalina kuri	GD	-1.042	-0.881	-0.686	1.405	0.668	1.832	0.184	1.474	1.228	2.098	2.073	1.200	2.720	-1.668	-1.734	-1.359	1.508	0.713	1.867
Mesalina martini	GD	-0.894	-0.905	-0.591	1.944	1.788	1.823	1.490	1.739	2.039	1.901	-1.051	-0.976	-0.729	-0.963	-0.845	-0.914	0.124	1.900	-0.325
Mesalina microlepis	GD	-0.809	-0.758	-0.685	0.277	0.896	-0.221	1.004	0.015	0.679	-0.421	-0.780	0.005	-0.505	0.792	0.676	0.551	0.553	0.176	1.030
Mesalina olivieri	GD	-0.934	-0.979	-0.516	0.762	1.030	0.432	1.075	0.611	0.885	0.268	-1.020	-0.593	-0.617	0.174	0.568	-0.961	0.338	1.674	-0.683
Mesalina pasteuri	GD	-1.092	-1.082	-0.652	1.384	1.781	0.741	1.909	0.944	1.472	0.557	-1.151	-1.773	-0.633	0.362	0.579	-0.077	0.695	2.295	-1.042
Mesalina rubropunctata	GD	-1.091	-1.091	-0.641	1.221	1.564	0.655	1.703	0.869	1.258	0.462	-1.151	-1.758	-0.649	0.307	0.569	0.043	0.431	2.352	-1.042
Mesalina simoni	GD	-0.544	-0.506	-0.681	0.294	0.270	0.372	0.364	0.432	0.118	0.335	-0.166	0.342	-0.490	-0.308	-0.283	-0.732	0.083	-0.361	0.552
Mesalina watsonana	GD	-0.783	-0.733	-0.509	0.548	1.225	-0.086	1.446	0.088	0.831	-0.228	-0.979	0.020	-0.953	0.905	0.912	0.210	0.954	1.561	0.592

Nucras boulengeri	GD	0.439	0.613	-0.094	0.962	-0.181	1.392	-0.093	1.333	-0.287	1.453	0.805	1.093	0.117	-1.764	-1.668	-1.774	0.525	0.600	-0.245
Nucras intertexta	GD	-0.434	-0.224	-0.588	0.622	0.117	0.603	0.756	0.815	-0.527	0.297	0.051	0.281	-0.314	-0.559	-0.358	-0.928	0.740	0.798	0.512
Nucras lalandii	GD	0.186	0.109	-0.043	-0.052	-0.812	0.283	-0.356	0.321	-1.326	0.188	0.897	0.894	0.325	-0.915	-0.613	-1.027	-0.408	-0.333	-1.281
Nucras livida	GD	-0.582	-0.632	-0.147	-0.020	-0.444	0.151	-0.060	0.360	-0.913	-0.032	-0.557	-0.225	-0.442	-0.537	-0.394	-0.535	-1.094	-0.728	-1.281
Nucras taeniolata	GD	-0.075	-0.348	0.413	0.240	-0.502	0.672	-0.198	0.644	-0.865	0.651	0.822	0.480	0.692	-1.123	-1.111	-1.058	-1.640	-1.576	-1.162
Nucras tessellata	GD	-0.794	-0.735	-0.458	0.370	0.039	0.402	0.485	0.684	-0.551	0.121	-0.903	-1.083	-0.617	-0.410	-0.344	-0.770	0.248	0.798	-1.082
Omanosaura cyanura	CL	-0.728	-0.595	-0.571	1.476	1.544	1.075	1.434	1.057	1.555	1.101	-1.091	-1.650	-0.633	-0.265	-0.423	0.015	0.940	0.741	0.990
Omanosaura jayakari	GD	-0.777	-0.621	-0.595	1.573	1.729	1.102	1.644	1.152	1.705	1.057	-1.107	-1.742	-0.633	-0.318	-0.459	-0.001	1.393	1.532	0.990
Ophisops beddomei	GD	2.411	5.525	-0.648	1.428	0.994	1.639	0.669	1.430	1.324	1.607	0.673	0.894	0.500	-1.420	-0.979	-1.509	2.327	1.815	1.149
Ophisops elegans	GD	-0.400	-0.498	-0.347	-0.325	0.245	-0.643	0.296	-0.476	0.150	-0.767	-0.609	0.510	-0.984	0.913	0.921	0.588	0.143	0.487	-0.564
Ophisops jerdonii	GD	0.209	1.080	-0.338	1.461	1.548	1.156	1.411	1.123	1.586	1.054	0.321	0.802	-0.505	-0.347	0.478	-1.228	1.966	1.900	0.392
Ophisops leschenaultii	CL	0.801	1.812	-0.402	1.569	1.492	1.531	1.253	1.475	1.673	1.521	0.547	0.740	0.405	-1.004	-0.686	-1.464	1.607	1.561	1.070
Ophisops microlepis	GD	0.921	3.201	-0.470	1.468	1.917	1.202	1.726	1.161	2.006	1.034	0.831	0.924	0.500	-0.425	-0.490	-0.194	2.690	1.674	3.062
Ophisops occidentalis	GD	-0.592	-0.711	-0.497	0.072	0.485	-0.035	0.420	0.003	0.523	-0.160	-0.748	-0.378	-0.505	0.297	0.260	-0.017	-0.731	0.459	-0.723
Parvilacerta fraasii	GD	0.113	0.544	-0.686	-0.915	-0.929	-0.816	-0.843	-0.734	-0.976	-0.852	-0.407	-0.578	-0.346	0.297	-0.060	0.749	0.889	0.176	1.508
Parvilacerta parva	GD	-0.249	-0.404	-0.166	-1.186	-0.991	-1.201	-0.865	-1.090	-1.090	-1.258	-0.552	0.158	-0.921	0.722	0.768	1.030	-0.818	-0.813	-0.444
Pedioplanis burchelli	GD	-0.258	-0.363	0.043	-0.171	-0.724	0.071	-0.302	0.230	-1.220	-0.056	0.083	0.418	-0.410	-0.618	-0.500	-0.831	-0.763	-0.559	-1.281
Pedioplanis inornata	GD	-0.906	-0.792	-0.615	0.435	0.052	0.494	0.505	0.779	-0.543	0.196	-1.030	-1.466	-0.697	-0.554	-0.362	-1.135	0.494	0.939	-0.365
Pedioplanis laticeps	GD	-0.774	-0.797	-0.346	0.135	-0.134	0.194	0.280	0.454	-0.667	-0.080	-0.890	-1.129	-0.633	-0.314	-0.372	-0.223	-0.651	-0.333	-0.883
Pedioplanis lineoocellata	GD	-0.526	-0.434	-0.431	0.432	-0.026	0.461	0.540	0.688	-0.758	0.243	-0.178	0.250	-0.569	-0.510	-0.365	-0.885	0.326	0.628	-0.962
Pedioplanis namaquensis	GD	-0.653	-0.545	-0.502	0.484	0.032	0.511	0.586	0.785	-0.696	0.259	-0.493	-0.194	-0.617	-0.526	-0.355	-1.115	0.537	0.882	-0.763
Pedioplanis undata	GD	-0.597	-0.269	-0.686	0.734	-0.115	0.895	0.468	1.157	-0.829	0.646	-0.510	-0.256	-0.665	-1.092	-0.983	-1.129	1.724	1.052	2.185
Philochortus spinalis	GD	-0.161	0.054	-0.234	1.150	0.393	1.468	0.560	1.538	0.141	1.350	-0.575	-0.302	-0.633	-1.535	-1.079	-1.694	0.481	1.137	0.113
Phoenicolacerta cyanisparsa	GD	-0.038	0.221	-0.642	0.074	0.678	-0.329	0.687	-0.224	0.601	-0.397	0.075	-0.256	0.309	0.877	0.590	1.215	0.558	0.006	1.189
Phoenicolacerta kulzeri	CL	-0.223	0.119	-0.686	-0.347	-0.355	-0.399	-0.294	-0.300	-0.416	-0.451	-0.688	-0.578	-0.585	0.178	-0.003	0.469	1.100	0.430	1.508

Phoenicolacerta laevis	GD	0.128	0.350	-0.468	-0.146	-0.011	-0.258	-0.023	-0.257	-0.004	-0.226	0.259	0.250	-0.186	0.344	0.396	0.172	0.500	0.600	0.034
Phoenicolacerta troodica	GD	-0.260	0.171	-0.620	0.305	0.500	0.241	0.409	0.227	0.567	0.278	1.047	1.200	0.660	0.072	-0.143	0.370	0.972	0.261	1.508
Podarcis bocagei	GD	1.288	0.896	0.725	-0.780	-1.229	-0.284	-1.338	-0.458	-1.005	-0.150	1.239	0.940	1.283	-0.444	-0.372	-0.521	-1.003	-1.067	-0.843
Podarcis carbonelli	GD	1.105	1.024	-0.072	-0.477	-0.838	-0.083	-0.985	-0.263	-0.593	0.002	1.193	1.200	0.628	-0.321	-0.270	-0.382	-0.463	-0.898	0.233
Podarcis cretensis	CL	0.141	0.510	-0.594	-0.029	-0.089	0.114	-0.430	-0.080	0.344	0.335	0.922	0.204	1.458	-0.180	-0.453	0.284	0.671	-0.078	1.349
Podarcis erhardii	CL	0.118	-0.147	0.450	-0.657	-0.491	-0.622	-0.639	-0.632	-0.282	-0.608	0.581	0.572	0.580	0.410	0.242	0.603	-1.152	-0.559	-1.082
Podarcis filfolensis	CL	-0.175	-0.015	-0.649	0.363	0.359	0.505	-0.046	0.313	0.840	0.716	2.073	1.200	2.720	-0.297	-0.602	0.196	0.523	-0.248	1.349
Podarcis gaigeae	GD	-0.352	-0.268	-0.371	0.016	0.114	0.099	-0.404	-0.146	0.759	0.370	2.073	1.200	2.720	-0.073	-0.259	0.377	0.005	-0.502	0.392
Podarcis guadarramae	CL	0.472	0.203	0.152	-0.590	-0.705	-0.290	-0.801	-0.399	-0.540	-0.268	0.982	0.940	0.421	-0.052	0.005	-0.477	-0.944	-0.954	-0.843
Podarcis hispanicus	CL	0.078	-0.223	0.194	-0.514	-0.494	-0.289	-0.549	-0.348	-0.397	-0.309	0.671	0.786	0.053	0.005	0.016	-0.341	-1.113	-0.757	-1.201
Podarcis ionicus	GD	-0.096	-0.361	0.113	-0.420	-0.294	-0.247	-0.348	-0.289	-0.212	-0.261	0.462	0.848	0.101	0.011	-0.079	0.167	-1.213	-0.672	-1.201
Podarcis lilfordi	GD	-0.148	-0.132	-0.460	0.067	0.019	0.294	-0.242	0.161	0.340	0.445	2.004	1.200	1.746	-0.275	-0.551	0.190	-0.599	-1.011	-0.006
Podarcis liolepis	GD	0.088	-0.265	0.630	-0.694	-0.720	-0.426	-0.752	-0.489	-0.635	-0.409	0.582	0.848	0.053	0.002	-0.091	-0.126	-1.573	-1.378	-1.321
Podarcis melisellensis	GD	1.008	0.580	1.332	-0.595	-0.450	-0.478	-0.645	-0.589	-0.179	-0.327	0.466	0.081	0.676	0.250	0.009	0.624	-1.332	-1.294	-1.122
Podarcis milensis	GD	-0.345	-0.179	-0.625	0.233	0.156	0.360	-0.350	0.060	0.780	0.671	2.073	1.200	2.720	-0.184	-0.395	0.237	0.622	-0.107	1.309
Podarcis muralis	CL	0.363	-0.175	1.495	-0.950	-0.993	-0.745	-1.106	-0.854	-0.782	-0.657	0.707	1.185	-0.505	0.256	0.353	0.003	-1.596	-0.898	-1.440
Podarcis peloponnesiacus	GD	0.239	0.381	-0.197	-0.309	-0.217	-0.172	-0.395	-0.226	0.015	-0.107	1.040	0.710	1.299	0.028	-0.192	0.266	0.063	-0.333	0.472
Podarcis pityusensis	GD	0.042	-0.082	0.307	-0.011	-0.118	0.248	-0.280	0.126	0.089	0.395	2.073	1.200	2.720	-0.365	-0.561	-0.259	-0.823	-1.096	-0.723
Podarcis siculus	GD	0.275	-0.042	0.722	-0.454	-0.330	-0.330	-0.545	-0.470	-0.042	-0.213	0.818	1.169	0.788	0.159	0.244	0.217	-1.226	-0.757	-1.201
Podarcis tauricus	GD	0.001	-0.375	0.773	-0.744	-0.480	-0.786	-0.630	-0.799	-0.264	-0.739	0.483	0.924	0.373	0.596	0.553	0.515	-1.365	-0.559	-1.201
Podarcis tiliguerta	CL	0.083	-0.015	-0.287	-0.257	-0.181	-0.043	-0.426	-0.190	0.134	0.059	1.342	1.169	1.522	-0.168	-0.353	0.171	-0.573	-0.813	-0.325
Podarcis vaucheri	CL	-0.238	-0.336	-0.496	-0.125	0.104	-0.076	0.028	-0.084	0.183	-0.133	-0.082	0.664	-0.458	0.161	0.137	0.051	-0.468	-0.333	-0.604
Podarcis virescens	CL	-0.099	-0.178	-0.365	-0.235	-0.020	-0.135	-0.092	-0.174	0.066	-0.219	0.732	0.786	0.117	0.172	0.036	-0.371	-0.750	-0.841	-0.763
Podarcis waglerianus	GD	-0.201	-0.186	-0.518	-0.041	-0.008	0.120	-0.222	0.023	0.254	0.244	1.067	0.664	1.331	-0.116	-0.261	0.158	-0.220	-0.389	0.193
Poromera fordii	CL	2.015	1.701	1.825	1.301	0.236	1.761	0.069	1.646	0.420	1.865	1.256	0.863	0.979	-1.966	-1.740	-1.808	-0.380	-0.304	-0.564

Psammodromus algirus	GD	-0.473	-0.578	-0.536	-0.029	0.277	-0.057	0.241	-0.024	0.293	-0.142	-0.452	0.480	-0.553	0.227	0.347	-0.251	-0.578	-0.333	-0.644
Psammodromus blanci	GD	-0.238	-0.361	-0.474	-0.081	0.214	-0.051	0.146	-0.051	0.276	-0.135	-0.161	0.756	-0.394	0.188	0.115	0.065	-0.530	-0.615	-0.524
Psammodromus edwarsianus	GD	0.039	0.060	-0.389	-0.151	-0.114	0.006	-0.225	-0.053	0.027	-0.022	0.955	0.802	0.660	-0.016	0.027	-0.409	-0.440	-0.531	-0.484
Psammodromus hispanicus	GD	-0.085	-0.284	-0.078	-0.369	-0.232	-0.215	-0.291	-0.255	-0.148	-0.269	0.599	0.679	0.069	0.083	0.020	-0.103	-0.931	-0.644	-0.962
Psammodromus microdactylus	GD	-0.118	-0.163	-0.586	-0.132	-0.086	-0.026	-0.149	-0.023	-0.008	-0.024	-0.010	0.051	-0.298	-0.003	-0.103	-0.110	-0.149	-0.220	0.153
Psammodromus occidentalis	GD	0.052	0.064	-0.365	-0.169	-0.135	-0.007	-0.246	-0.068	0.007	-0.033	0.967	0.802	0.676	-0.017	0.027	-0.409	-0.468	-0.531	-0.524
Pseuderemias smithii	GD	-0.468	0.076	-0.529	1.617	0.744	1.972	0.704	1.962	0.729	1.978	-0.692	-1.022	-0.426	-1.823	-1.485	-1.653	1.665	1.589	0.950
Scelarcis perspicillata	CL	-0.450	-0.528	-0.547	-0.306	-0.093	-0.244	-0.102	-0.231	-0.084	-0.278	-0.474	0.189	-0.553	0.211	0.161	0.130	-0.455	-0.446	-0.405
Takydromus amurensis	GD	0.267	0.945	-0.242	-1.675	-0.534	-2.417	-0.388	-2.452	-0.692	-2.306	-0.679	0.756	-0.969	2.562	2.684	1.864	0.979	0.741	0.871
Takydromus dorsalis	CL	2.794	1.599	4.179	1.140	0.834	1.136	0.188	0.700	1.589	1.576	1.907	1.200	2.385	-0.765	-0.998	-0.325	-1.675	-1.887	-0.962
Takydromus formosanus	CL	2.799	4.085	0.100	0.883	0.450	0.888	0.158	0.606	0.775	1.180	0.640	0.725	0.277	-0.825	-0.815	-0.743	0.971	0.459	1.389
Takydromus hsuehshanensis	GD	4.526	3.931	2.279	-0.715	-1.550	-0.287	-1.468	-0.545	-1.545	0.004	1.825	1.001	2.416	-0.969	-1.109	-0.616	-0.657	-0.785	-0.405
Takydromus intermedius	GD	0.723	1.061	-0.183	-0.692	-0.925	-0.603	-0.851	-0.796	-0.958	-0.369	0.545	0.802	-0.138	0.055	0.276	-0.445	0.571	0.374	0.432
Takydromus luyeanus	CL	3.044	3.420	1.639	0.875	0.368	0.957	-0.055	0.628	0.871	1.296	1.577	0.924	2.081	-1.059	-1.078	-0.752	-0.069	-0.361	0.074
Takydromus sauteri	CL	2.784	3.155	1.611	0.932	0.660	0.872	0.291	0.572	1.072	1.184	0.542	1.077	0.277	-0.623	-0.665	-0.497	0.254	0.459	-0.962
Takydromus septentrionalis	GD	0.675	0.690	0.100	-0.616	-0.371	-0.800	-0.350	-0.945	-0.380	-0.610	0.239	0.802	-0.697	0.698	1.501	-0.318	0.261	0.374	-0.006
Takydromus sexlineatus	GD	2.687	1.696	3.253	1.313	0.409	1.535	0.187	1.324	0.668	1.734	1.324	1.185	0.580	-1.523	-0.383	-1.935	-0.088	0.430	-1.241
Takydromus smaragdinus	CL	3.116	2.326	3.926	0.857	0.707	0.820	0.144	0.425	1.365	1.226	2.013	1.200	2.480	-0.437	-0.635	-0.069	-1.353	-1.548	-0.763
Takydromus sylvaticus	CL	1.936	2.241	0.910	0.252	0.528	-0.082	0.382	-0.343	0.665	0.209	1.014	0.664	0.740	0.497	0.426	0.529	-0.340	-0.672	-0.086
Takydromus tachydromoides	CL	1.825	1.430	2.363	-0.908	-0.283	-1.049	-0.394	-1.253	-0.129	-0.797	0.103	1.093	-0.889	1.067	1.174	1.075	-1.058	-0.841	-0.962
Takydromus toyamai	CL	2.951	1.676	4.922	1.152	0.874	1.136	0.237	0.721	1.612	1.556	2.073	1.200	2.720	-0.762	-0.995	-0.321	-1.713	-1.915	-1.002
Takydromus viridipunctatus	CL	4.118	2.911	4.950	0.682	0.511	0.639	0.033	0.315	1.074	0.982	1.791	1.200	1.890	-0.504	-0.642	-0.375	-1.189	-1.011	-1.082
Takydromus wolteri	CL	0.451	0.983	-0.133	-1.194	-0.480	-1.638	-0.392	-1.733	-0.565	-1.482	-0.229	0.556	-0.937	1.613	2.641	0.253	0.694	0.741	0.153
Teira dugesii	CL	0.967	0.616	0.976	0.053	-0.604	0.583	-0.992	0.235	-0.081	0.948	1.360	0.510	2.001	-1.144	-1.244	-0.937	-0.801	-0.531	-0.524
Timon kurdistanicus	GD	0.232	0.477	-0.684	-0.158	0.926	-0.716	0.838	-0.515	0.957	-0.870	-0.341	-0.516	-0.346	1.438	0.959	1.944	0.735	0.204	1.149

Timon lepidus	GD	0.066	-0.199	0.118	-0.444	-0.412	-0.236	-0.475	-0.295	-0.310	-0.254	0.693	0.832	0.117	-0.003	0.014	-0.348	-1.036	-0.672	-1.162
Timon nevadensis	GD	-0.389	-0.474	-0.328	-0.155	0.003	-0.024	-0.058	-0.042	0.070	-0.071	0.228	0.510	0.053	-0.064	-0.131	0.086	-0.841	-0.587	-0.723
Timon pater	GD	-0.284	-0.426	-0.448	-0.013	0.356	-0.048	0.255	-0.051	0.450	-0.145	-0.207	0.756	-0.458	0.257	0.199	0.252	-0.705	-0.615	-0.683
Timon princeps	GD	-0.254	-0.103	-0.640	-0.061	0.840	-0.552	0.895	-0.283	0.695	-0.777	-0.756	-0.700	-1.000	1.211	0.959	1.357	0.802	0.543	0.671
Timon tangitanus	GD	-0.418	-0.508	-0.572	-0.243	-0.098	-0.159	-0.122	-0.148	-0.070	-0.179	-0.376	0.342	-0.521	0.107	0.257	-0.167	-0.369	-0.220	-0.365
Tropidosaura cottrelli	GD	0.507	0.559	-0.226	-1.236	-2.250	-0.593	-1.785	-0.675	-2.643	-0.572	0.640	0.127	1.027	-0.811	-0.915	-0.476	-0.051	-0.531	0.353
Tropidosaura essexi	GD	0.415	0.496	-0.216	-0.884	-1.768	-0.368	-1.326	-0.408	-2.208	-0.371	0.729	0.127	1.027	-0.792	-0.900	-0.476	-0.051	-0.446	0.353
Tropidosaura gularis	GD	-0.336	-0.612	0.443	-0.064	-0.668	0.294	-0.455	0.351	-0.896	0.261	-0.237	0.265	-0.234	-0.887	-0.788	-0.882	-1.670	-0.813	-1.401
Tropidosaura montana	GD	-0.058	-0.318	0.551	-0.065	-0.760	0.314	-0.463	0.364	-1.086	0.291	0.503	0.924	-0.138	-0.922	-0.823	-1.000	-0.928	-0.446	-1.361
Vhembelacerta rupicola	CL	0.485	0.975	-0.213	0.450	-0.340	0.673	0.020	0.634	-0.511	0.587	1.039	0.694	0.804	-1.043	-1.133	-0.734	0.561	-0.191	1.349
Zootoca vivipara	GD	-0.110	-0.175	0.241	-2.578	-1.578	-2.815	-1.571	-2.791	-1.472	-2.755	-0.892	1.185	-1.176	2.482	3.846	0.140	-0.772	0.515	-1.201

Table S3.3

SP	***Reference***
Acanthodactylus aegyptius	Baha El Din 2007
Acanthodactylus arabicus	IUCN red list
Acanthodactylus aureus	IUCN red list
Acanthodactylus bedriagai	IUCN red list
Acanthodactylus beershebensis	IUCN red list
Acanthodactylus blanci	IUCN red list
Acanthodactylus blanfordii	IUCN red list
Acanthodactylus boskianus	IUCN red list
Acanthodactylus busacki	IUCN red list
Acanthodactylus cantoris	IUCN red list
Acanthodactylus dumerilii	IUCN red list
Acanthodactylus erythrurus	IUCN red list
Acanthodactylus felicis	IUCN red list
Acanthodactylus gongrorhynchat	IUCN red list
Acanthodactylus grandis	IUCN red list
Acanthodactylus guineensis	IUCN red list
Acanthodactylus haasi	IUCN red list
Acanthodactylus hardyi	GBIF
Acanthodactylus harranensis	IUCN red list
Acanthodactylus khamirensis	Smid et al 2014
Acanthodactylus lineomaculatus	Bons and Geniez1995
Acanthodactylus longipes	IUCN red list
Acanthodactylus maculatus	IUCN red list
Acanthodactylus margaritae	Tamar et al 2017
Acanthodactylus masirae	IUCN red list
Acanthodactylus micropholis	IUCN red list
Acanthodactylus nilsoni	IUCN red list
Acanthodactylus opheodurus	IUCN red list
Acanthodactylus orientalis	IUCN red list
Acanthodactylus pardalis	IUCN red list
Acanthodactylus robustus	IUCN red list
Acanthodactylus savignyi	IUCN red list
Acanthodactylus schmidti	IUCN red list
Acanthodactylus schreiberi	IUCN red list
Acanthodactylus scutellatus	IUCN red list
Acanthodactylus senegalensis	IUCN red list
Acanthodactylus tilburyi	IUCN red list
Acanthodactylus tristrami	IUCN red list
Adolfus africanus	IUCN red list
Adolfus alleni	IUCN red list

Adolfus jacksoni	IUCN red list
Algyroides fitzingeri	IUCN red list
Algyroides marchi	IUCN red list
Algyroides moreoticus	IUCN red list
Algyroides nigropunctatus	IUCN red list
Anatololacerta anatolica	IUCN red list
Anatololacerta danfordi	IUCN red list
Anatololacerta oertzeni	IUCN red list
Apathya cappadocica	IUCN red list
Apathya yassujica	IUCN red list
Archaeolacerta bedriagae	IUCN red list
Atlantolacerta andreanskyi	IUCN red list
Australolacerta australis	IUCN red list
Congolacerta asukului	IUCN red list
Congolacerta vaueresselli	IUCN red list
Dalmatolacerta oxycephala	IUCN red list
Darevskia caspica	Smid et al 2014
Darevskia caucasica	IUCN red list
Darevskia chlorogaster	IUCN red list
Darevskia clarkorum	IUCN red list
Darevskia daghestanica	IUCN red list
Darevskia defilippii	IUCN red list
Darevskia derjugini	IUCN red list
Darevskia kamii	iNaturalist
Darevskia kopetdaghica	IUCN red list
Darevskia parvula	IUCN red list
Darevskia portschinskii	IUCN red list
Darevskia praticola	IUCN red list
Darevskia raddei	IUCN red list
Darevskia rudis	IUCN red list
Darevskia saxicola	IUCN red list
Darevskia schaekeli	iNaturalist
Darevskia steineri	IUCN red list
Darevskia valentini	IUCN red list
Dinarolacerta montenegrina	IUCN red list
Dinarolacerta mosorensis	IUCN red list
Eremias argus	IUCN red list
Eremias arguta	IUCN red list
Eremias brenchleyi	GBIF
Eremias grammica	IUCN red list
Eremias intermedia	IUCN red list
Eremias montanus	IUCN red list
Eremias multiocellata	IUCN red list

Eremias papenfussi	Mozaddari et al 2011
Eremias persica	IUCN red list and iNaturalist
Eremias pleskei	IUCN red list
Eremias przewalskii	IUCN red list
Eremias strauchi	IUCN red list
Eremias stummeri	IUCN red list
Eremias suphani	IUCN red list
Eremias velox	IUCN red list
Gallotia atlantica	IUCN red list
Gallotia bravoana	IUCN red list
Gallotia caesaris	IUCN red list
Gallotia galloti	IUCN red list
Gallotia intermedia	IUCN red list
Gallotia simonyi	IUCN red list
Gallotia stehlini	IUCN red list
Gastropholis prasina	IUCN red list
Gastropholis vittata	IUCN red list
Heliobolus lugubris	IUCN red list
Heliobolus spekii	IUCN red list
Hellenolacerta graeca	IUCN red list
Holaspis guentheri	IUCN red list
Holaspis laevis	IUCN red list
Iberolacerta aranica	IUCN red list
Iberolacerta aurelioi	IUCN red list
Iberolacerta bonnali	IUCN red list
Iberolacerta cyreni	IUCN red list
Iberolacerta galani	IUCN red list
Iberolacerta horvathi	IUCN red list
Iberolacerta martinezricai	IUCN red list
Iberolacerta monticola	IUCN red list
Ichnotropis capensis	IUCN red list
Iranolacerta brandtii	IUCN red list
Iranolacerta zagrosica	IUCN red list
Lacerta agilis	IUCN red list
Lacerta bilineata	IUCN red list
Lacerta media	IUCN red list
Lacerta pamphylica	IUCN red list
Lacerta schreiberi	IUCN red list
Lacerta strigata	IUCN red list
Lacerta trilineata	IUCN red list
Lacerta viridis	IUCN red list
Latastia longicaudata	IUCN red list
Meroles anchietae	IUCN red list

Meroles ctenodactylus	IUCN red list
Meroles cuneirostris	IUCN red list
Meroles knoxii	IUCN red list
Meroles micropholidotus	IUCN red list
Meroles reticulatus	IUCN red list
Meroles squamulosus	IUCN red list
Meroles suborbitalis	IUCN red list
Mesalina adramitana	IUCN red list
Mesalina bahaeldini	IUCN red list
Mesalina balfouri	IUCN red list
Mesalina bernoullii	Smid et al 2017
Mesalina brevirostris	IUCN red list
Mesalina guttulata	IUCN red list
Mesalina kuri	IUCN red list
Mesalina martini	IUCN red list
Mesalina microlepis	GBIF
Mesalina olivieri	IUCN red list
Mesalina pasteuri	IUCN red list
Mesalina rubropunctata	IUCN red list
Mesalina simoni	IUCN red list
Mesalina watsonana	IUCN red list
Nucras boulengeri	IUCN red list
Nucras intertexta	IUCN red list
Nucras lalandii	IUCN red list
Nucras livida	IUCN red list
Nucras taeniolata	IUCN red list
Nucras tessellata	IUCN red list
Omanosaura cyanura	IUCN red list
Omanosaura jayakari	IUCN red list
Ophisops beddomei	IUCN red list
Ophisops elegans	IUCN red list
Ophisops jerdonii	IUCN red list
Ophisops leschenaultii	IUCN red list
Ophisops microlepis	IUCN red list
Ophisops occidentalis	IUCN red list
Parvilacerta fraasii	IUCN red list
Parvilacerta parva	IUCN red list
Pedioplanis burchelli	IUCN red list
Pedioplanis inornata	IUCN red list
Pedioplanis laticeps	IUCN red list
Pedioplanis lineoocellata	IUCN red list
Pedioplanis namaquensis	IUCN red list
Pedioplanis undata	IUCN red list

Philochortus spinalis	IUCN red list
Phoenicolacerta cyanisparsa	IUCN red list
Phoenicolacerta kulzeri	IUCN red list
Phoenicolacerta laevis	IUCN red list
Phoenicolacerta troodica	IUCN red list
Podarcis bocagei	IUCN red list
Podarcis carbonelli	IUCN red list
Podarcis cretensis	IUCN red list
Podarcis erhardii	IUCN red list
Podarcis filfolensis	IUCN red list
Podarcis gaigeae	IUCN red list
Podarcis guadarramae	GBIF
Podarcis hispanicus	IUCN red list
Podarcis ionicus	GBIF
Podarcis lilfordi	IUCN red list
Podarcis liolepis	GBIF
Podarcis melisellensis	IUCN red list
Podarcis milensis	IUCN red list
Podarcis muralis	IUCN red list
Podarcis peloponnesiacus	IUCN red list
Podarcis pityusensis	IUCN red list
Podarcis siculus	IUCN red list
Podarcis tauricus	IUCN red list
Podarcis tiliguerta	IUCN red list
Podarcis vaucheri	IUCN red list
Podarcis virescens	Ceiro-Dias et al 2018
Podarcis waglerianus	IUCN red list
Poromera fordii	IUCN red list
Psammodromus algirus	IUCN red list
Psammodromus blanci	IUCN red list
Psammodromus edwarsianus	GBIF
Psammodromus hispanicus	IUCN red list
Psammodromus microdactylus	IUCN red list
Psammodromus occidentalis	GBIF
Pseuderemias smithii	IUCN red list
Scelarcis perspicillata	IUCN red list
Takydromus amurensis	IUCN red list
Takydromus dorsalis	IUCN red list
Takydromus formosanus	IUCN red list
Takydromus hsuehshanensis	IUCN red list
Takydromus intermedius	IUCN red list
Takydromus luyeanus	IUCN red list
Takydromus sauteri	IUCN red list

Takydromus septentrionalis	IUCN red list
Takydromus sexlineatus	IUCN red list
Takydromus smaragdinus	IUCN red list
Takydromus sylvaticus	IUCN red list
Takydromus tachydromoides	IUCN red list
Takydromus toyamai	IUCN red list
Takydromus viridipunctatus	IUCN red list
Takydromus wolteri	IUCN red list
Teira dugesii	IUCN red list
Timon kurdistanicus	GBIF
Timon lepidus	IUCN red list
Timon nevadensis	GBIF
Timon pater	IUCN red list
Timon princeps	IUCN red list
Timon tangitanus	IUCN red list
Tropidosaura cottrelli	IUCN red list
Tropidosaura essexi	IUCN red list
Tropidosaura gularis	IUCN red list
Tropidosaura montana	IUCN red list
Vhembelacerta rupicola	IUCN red list
Zootoca vivipara	IUCN red list

Table S3.4. Results of the phylogenetic signal analysis of body size (SVL) per groups: the entire family, subfamily Gallotinae, tribe Eremiadini and tribe Lacertini. Significant p-values (at α = 0.05) are highlighted in bold.

	K	K≠0 (p-val)	K≠1 (p - val)
Lacertidae	0.720	**0.001**	0.166
Gallotinae	1.236	**0.001**	0.707
Eremiadini	0.614	**0.001**	**0.047**
Lacertini	1.220	**0.001**	0.493

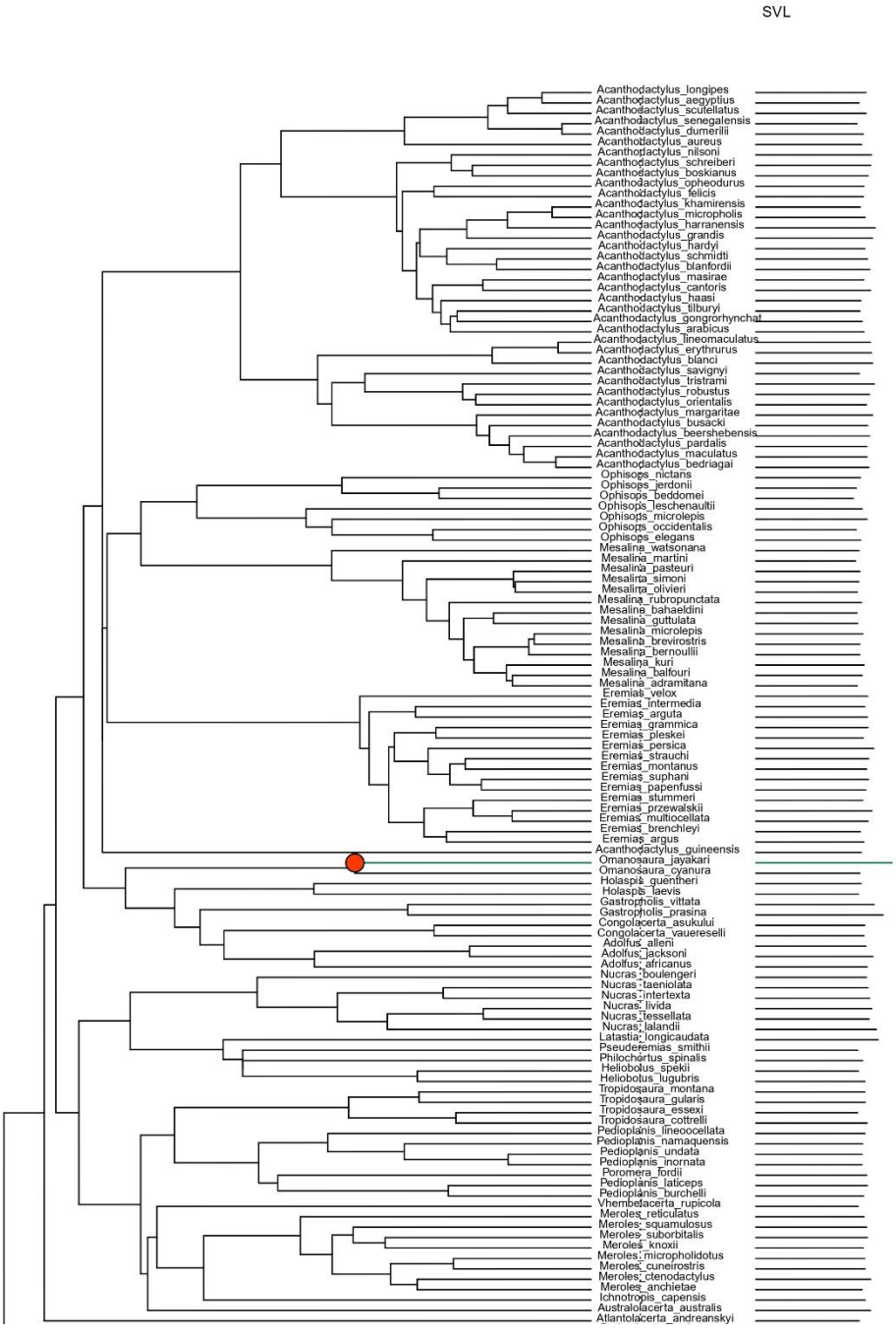
SVL
Acanthodactylus_longipes
Acanthodactylus_aegyptius
Acanthodactylus_scutellatus
Acanthodactylus_senegalensis
Acanthodactylus_dumerilii
Acanthodactylus_aureus
Acanthodactylus_nilsoni
Acanthodactylus_schreiberi
Acanthodactylus_boskianus
Acanthodactylus_opheodurus
Acanthodactylus_felicis
Acanthodactylus_khamirensis
Acanthodactylus_micropholis
Acanthodactylus_harranensis
Acanthodactylus_grandis
Acanthodactylus_hardyi
Acanthodactylus_schmidti
Acanthodactylus_blanfordii
Acanthodactylus_masirae
Acanthodactylus_cantoris
Acanthodactylus_haasi
Acanthodactylus_tilburyi
Acanthodactylus_gongrorhynchus
Acanthodactylus_arabicus
Acanthodactylus_lineomaculatus
Acanthodactylus_erythrurus
Acanthodactylus_blanci
Acanthodactylus_savigryi
Acanthodactylus_tristrami
Acanthodactylus_robustus
Acanthodactylus_orientalis
Acanthodactylus_margaritae
Acanthodactylus_busacki
Acanthodactylus_beershebensis
Acanthodactylus_pardalis
Acanthodactylus_maculatus
Acanthodactylus_bedriagai
Ophisops_nictans
Ophisops_jerdonii
Ophisops_beddomei
Ophisops_leschenaultii
Ophisops_microlepis
Ophisops_occidentalis
Ophisops_elegans
Mesalina_watsonana
Mesalina_martini
Mesalina_pasteuri
Mesalina_simoni
Mesalina_olivieri
Mesalina_rubropunctata
Mesalina_bahaeldini
Mesalina_guttulata
Mesalina_microlepis
Mesalina_brevirostris
Mesalina_bernoullii
Mesalina_kuri
Mesalina_balfouri
Mesalina_adramitana
Eremias_velox
Eremias_intermedia
Eremias_arguta
Eremias_grammica
Eremias_pleskei
Eremias_persica
Eremias_strauchi
Eremias_montanus
Eremias_suphani
Eremias_papenfussi
Eremias_stummeri
Eremias_przewalskii
Eremias_multiocellata
Eremias_brenchleyi
Eremias_argus
Acanthodactylus_guineensis
Omanosaura_jayakari
Omanosaura_cyanura
Holaspis_guentheri
Holaspis_laevis
Gastropholis_vittata
Gastropholis_prasina
Congolacerta_asukului
Congolacerta_vauereselli
Adolfus_alleni
Adolfus_jacksoni
Adolfus_africanus
Nucras_boulengeri
Nucras_taeniolata
Nucras_intertexta
Nucras_livida
Nucras_tessellata
Nucras_lalandii
Latastia_longicaudata
Pseuderemias_smithii
Philochortus_spinalis
Heliobolus_spekii
Heliobolus_lugubris
Tropidosaura_montana
Tropidosaura_gularis
Tropidosaura_essexi
Tropidosaura_cottrelli
Pedioplanis_lineoocellata
Pedioplanis_namaquensis
Pedioplanis_undata
Pedioplanis_inornata
Poromera_fordii
Pedioplanis_laticeps
Pedioplanis_burchelli
Vhembelacerta_rupicola
Meroles_reticulatus
Meroles_squamulosus
Meroles_suborbitalis
Meroles_knoxii
Meroles_micropholidotus
Meroles_cuneirostris
Meroles_ctenodactylus
Meroles_anchietae
Ichnotropis_capensis
Australolacerta_australis
Atlantolacerta_andreanskyi

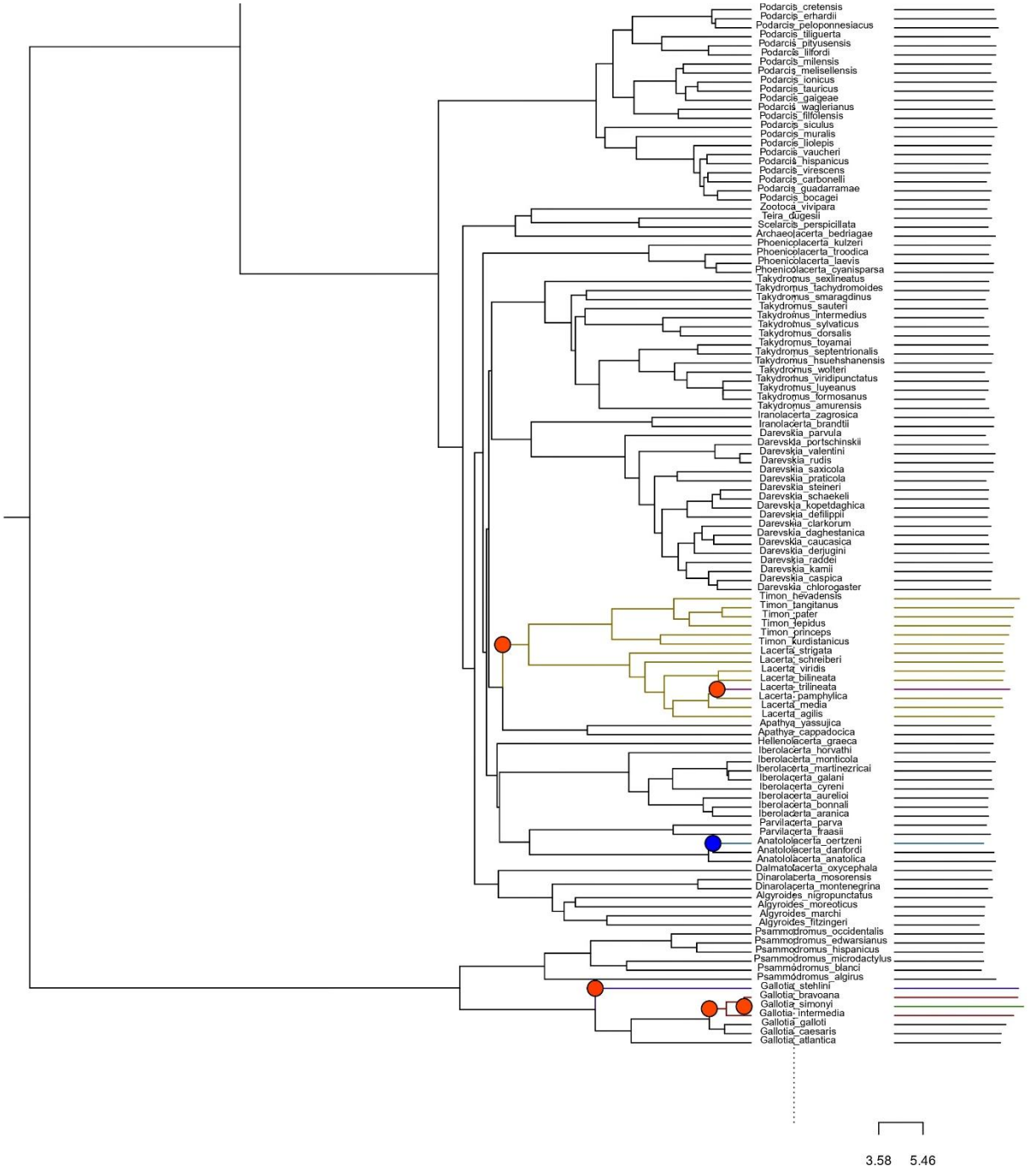

Figure S3.2. Detected shifts along the phylogeny employing the function *PhyloEM*. Red indicates changes towards bigger sizes and blue towards smaller sizes.

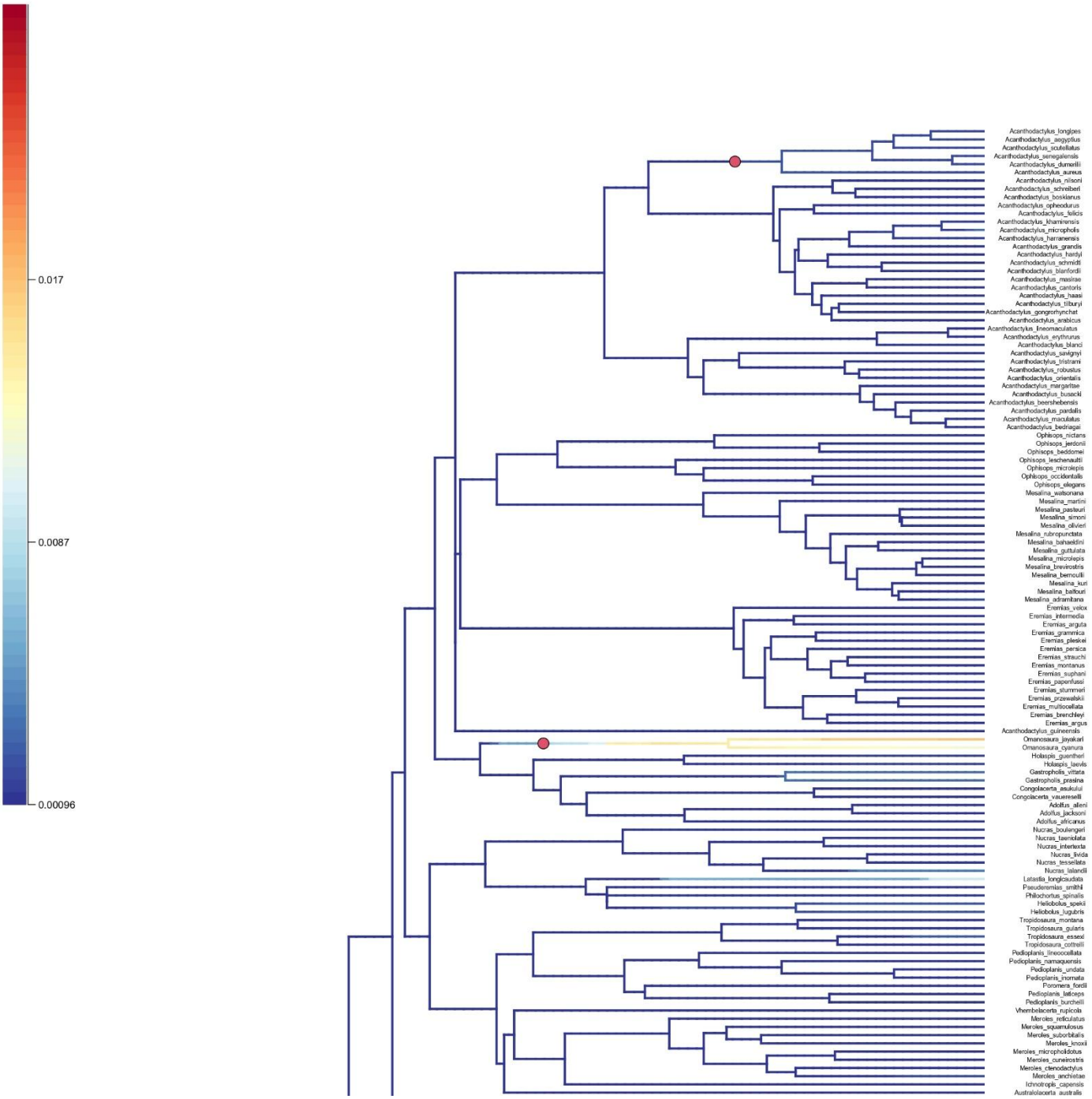
0.017
0.0087
0.00096
Acanthodactylus_longipes
Acanthodactylus_aegyptius
Acanthodactylus_scutellatus
Acanthodactylus_senegalensis
Acanthodactylus_dumerilii
Acanthodactylus_aureus
Acanthodactylus_nilsoni
Acanthodactylus_schreiberi
Acanthodactylus_boskianus
Acanthodactylus_opheodurus
Acanthodactylus_felicis
Acanthodactylus_khamiensis
Acanthodactylus_micropholis
Acanthodactylus_harranensis
Acanthodactylus_grandis
Acanthodactylus_hardyi
Acanthodactylus_schmidti
Acanthodactylus_blanfordii
Acanthodactylus_masirae
Acanthodactylus_cantoris
Acanthodactylus_haasi
Acanthodactylus_tilburyi
Acanthodactylus_gongrorhynchat
Acanthodactylus_arabicus
Acanthodactylus_lineomaculatus
Acanthodactylus_erythrurus
Acanthodactylus_blanci
Acanthodactylus_savignyi
Acanthodactylus_tristrami
Acanthodactylus_robustus
Acanthodactylus_orientalis
Acanthodactylus_margaritae
Acanthodactylus_busacki
Acanthodactylus_beershebensis
Acanthodactylus_pardalis
Acanthodactylus_maculatus
Acanthodactylus_bedriagai
Ophisops_nictans
Ophisops_jerdonii
Ophisops_beddomei
Ophisops_leschenaultii
Ophisops_microlepis
Ophisops_occidentalis
Ophisops_elegans
Mesalina_watsonana
Mesalina_martini
Mesalina_pasteuri
Mesalina_simoni
Mesalina_olivieri
Mesalina_rubropunctata
Mesalina_bahaeldini
Mesalina_guttulata
Mesalina_microlepis
Mesalina_brevirostris
Mesalina_bemoulli
Mesalina_kuri
Mesalina_balfouri
Mesalina_adramitana
Eremias_velox
Eremias_intermedia
Eremias_arguta
Eremias_grammica
Eremias_pleskei
Eremias_persica
Eremias_strauchi
Eremias_montanus
Eremias_suphani
Eremias_papenfussi
Eremias_stummeri
Eremias_przewalskii
Eremias_multiocellata
Eremias_brenchleyi
Eremias_argus
Acanthodactylus_guineensis
Omanosaura_jayakari
Omanosaura_cyanura
Holaspis_guentheri
Holaspis_laevis
Gastropholis_vittata
Gastropholis_prasina
Congolacerta_asuluiui
Congolacerta_vauereselli
Adolfus_alleni
Adolfus_jacksoni
Adolfus_africanus
Nucras_boulengeri
Nucras_taeniolata
Nucras_intertexta
Nucras_livida
Nucras_tessellata
Nucras_lalandii
Latastia_longicaudata
Pseuderemias_smithi
Philochortus_spinalis
Heliobolus_spekii
Heliobolus_lugubris
Tropidosaura_montana
Tropidosaura_gularis
Tropidosaura_essexi
Tropidosaura_cottrelli
Pedioplanis_lineocellata
Pedioplanis_namaquensis
Pedioplanis_undata
Pedioplanis_inornata
Poromera_fordii
Pedioplanis_laticeps
Pedioplanis_burchelli
Vhembelacerta_rupicola
Meroles_reticulatus
Meroles_squamulosus
Meroles_suborbitalis
Meroles_knoxii
Meroles_micropholidotus
Meroles_cuneirostris
Meroles_ctenodactylus
Meroles_anchietae
Ichnotropis_capensis
Australolacerta_australis

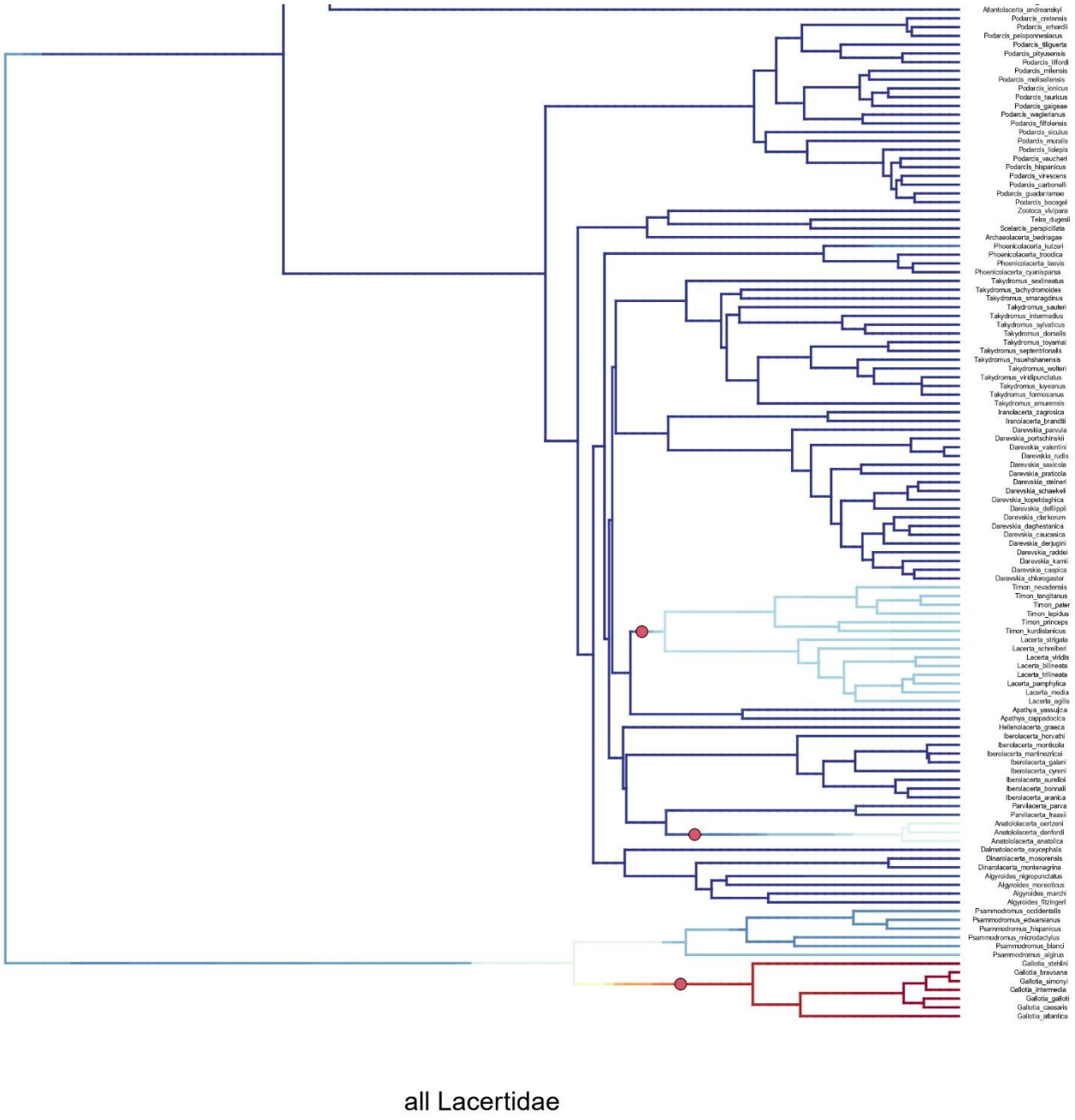

Figure S3.3. Detected shifts along the phylogeny employing Bayesian Analysis of Macroevolutionary Mixtures (BAMM).

Table S3.5. Results of phylogenetic ANOVAs conducted to test for differences in log-snout-vent-length across structural habitat categories. d.f.: degrees of freedom; R^2: R squared; F: F-value; Z: Z-score. P-values are based on 1000 residual permutations and significant p-values (at α = 0.05) are highlighted in bold.

		Df	**SS**	**MS**	**R^2**	**F**	**Z**	**Pr(>F)**
Lacertidae	Structural habitat	1	0.004	0.004	0.008	1.843	1.010	0.170
	Residuals	232	0.535	0.002	0.992			
	Total	233	0.539					
Lacertini	Structural habitat	1	0.002	0.002	0.009	0.919	0.480	0.326
	Residuals	100	0.210	0.002	0.991			
	Total	101	0.212					
Eremiadini	Structural habitat	1	0.004	0.004	0.024	2.936	1.340	0.086
	Residuals	117	0.164	0.001	0.976			
	Total	118	0.169					

Table S3.6. Phylogenetic generalized least squares (PGLS) regression models of SVL on each of the climatic variables in the family Lacertidae, subfamily Gallotinae and tribes Lacertini and Eremiadini.

	AICc OU	AICc BM	ΔAIC	Best model	R^2_{pred1}	Regression coefficient	p-val
Lacertidae					y ~ 1 I Phylo		
Pmax	-58.713	-51.683	-7.031	OU	-2.15E-03	-0.033	0.117
Pmin	-56.410	-50.432	-5.978	OU	1.41E-03	0.005	0.705
TmaxMax	-56.278	-50.088	-6.190	OU	-6.69E-04	-0.002	0.914
TminMin	-56.748	-50.883	-5.865	OU	1.75E-03	-0.014	0.489
NDVImax	-56.379	-50.188	-6.190	OU	-7.19E-04	0.006	0.738
NDVImin	-56.926	-50.479	-6.446	OU	-1.93E-03	0.014	0.418
PseasonMin	-58.812	-54.277	-4.535	OU	8.68E-03	-0.024	0.107
Gallotinae							
Pmax	21.046	19.712	1.333	BM	-4.15E-03	-0.044	0.949
Pmin	20.074	19.273	0.802	BM	-4.39E-02	-0.633	0.549
TmaxMax	20.541	19.628	0.913	BM	8.83E-03	-0.167	0.788
TminMin	14.711	18.339	-3.628	BM	-2.25E-01	0.475	0.291
NDVImax	20.338	19.142	1.196	BM	-9.03E-02	0.185	0.495
NDVImin	20.106	19.193	0.913	BM	-1.64E-01	0.115	0.515
PseasonMin	13.867	16.718	-2.851	BM	-2.57E-01	0.452	0.119
Lacertini							
Pmax	-60.958	-62.942	1.984	BM	-2.36E-02	-0.039	0.157
Pmin	-59.163	-61.163	2.000	BM	3.10E-03	0.007	0.604
TmaxMax	-58.891	-60.888	1.997	BM	2.16E-04	-0.001	0.982
TminMin	-58.918	-60.916	1.998	BM	-2.12E-03	-0.004	0.868
NDVImax	-59.716	-61.707	1.991	BM	-1.12E-03	-0.025	0.371
NDVImin	-58.891	-60.888	1.997	BM	-3.02E-04	-0.001	0.976
PseasonMin	-64.366	-66.366	2.000	BM	3.04E-02	-0.043	**0.021**
Eremiadini							
Pmax	-50.818	-49.176	-1.642	BM	1.18E-03	-0.011	0.652
Pmin	-51.538	-49.970	-1.569	BM	6.01E-03	0.051	0.322
TmaxMax	-50.282	-48.969	-1.313	BM	-5.66E-04	-0.001	0.971
TminMin	-53.436	-53.572	0.136	BM	1.55E-02	-0.053	**0.034**
NDVImax	-50.906	-49.895	-1.011	BM	-3.99E-04	0.019	0.341
NDVImin	-50.632	-49.381	-1.251	BM	8.91E-04	0.018	0.525
PseasonMin	-52.287	-51.825	-0.461	BM	3.45E-03	-0.027	0.094

Table S3.7. Comparison of the fit of different evolutionary models for SVL across 100 randomly chosen simmaps. The best-fit model is highlighted in bold letter. See Material and Methods for further information about the evolutionary models.

Models	Likelihood	AICc	ΔAICc	AICc weight
White Noise	-51.790	107.632	206.194	1.682E-45
BM1	28.335	-52.618	45.944	1.056E-10
OU1	32.549	-56.923	41.639	9.092E-10
BMS habitat	30.452	-54.800	43.822	3.145E-10
OUM habitat	33.320	-58.464	40.146	1.965E-09
BMS habitat+tribe	**56.423**	**-98.350**	**0.212**	**9.003E-01**
OUM habitat+tribe	37.878	-59.116	39.689	2.721E-09
BMS tribe	51.062	-93.950	4.612	9.974E-02
OUM tribe	33.520	-56.776	41.786	8.447E-10
EnvExp1	35.670	-65.235	33.327	5.801E-08
EnvExp2	35.169	-64.234	34.328	3.517E-08
EnvExp3	35.699	-65.294	33.268	5.975E-08
EnvLin4	-48.354	102.812	201.374	1.873E-44
EnvLin5	33.385	-60.665	37.897	5.904E-09
EnvLin6	33.230	-60.356	38.205	5.060E-09
EnvOU	32.549	-56.923	41.639	9.092E-10

Table S3.8. Estimates of evolutionary rates (σ^2) with standard deviation (sd) obtained from the best-fit multi-rate Brownian Motion model, with different rates for structural habitats (ground-dwelling: GD, and climbing: CL) and for phylogenetic groups, that is, the subfamily Gallotinae and the tribes Lacertini and Eremiadini.

	Gallotinae		Lacertini		Eremiadini
	GD	CL	GD	CL	GD
σ^2	0.01229 (1.82E-04)	0.00161 (1.03E-04)	0.00323 (2.47E-04)	0.00289 (8.02E-04)	0.00121 (7.83E-05)

Supplementary information for chapter 4

Table S4.1. Mean values (in mm) of the eight morphological traits and number of individuals measured for each species (N) with standard deviation (sd) in brackets under the mean value. SVL: Snout-vent length, HL: Head length, HW: Head width, HH: Head height, ML: Mouth length; FLL: Fore limb length, HLL: Hind limb length, Trk: Trunk.

Species	N	SVL	HL	HW	HH	ML	FLL	HLL	Trk
Acanthodactylus arabicus	7	54.003 (4.199)	20.366 (1.72)	9.184 (0.717)	7.071 (0.755)	10.839 (0.825)	19.19 (0.633)	38.837 (1.769)	22.833 (1.855)
Acanthodactylus aureus	5	50.674 (3.732)	18.852 (0.882)	8.756 (0.826)	6.684 (0.426)	10.59 (0.439)	17.926 (1.373)	33.88 (2.542)	22.174 (2.074)
Acanthodactylus blanci	4	74.075 (4.354)	25.685 (1.213)	11.815 (0.585)	9.72 (0.617)	13.332 (0.691)	24.098 (1.342)	45.422 (2.269)	33.06 (3.921)
Acanthodactylus blanfordii	4	66.92 (6.618)	25.332 (3.31)	10.725 (0.853)	8.008 (0.713)	13.025 (1.057)	21.51 (1.673)	41.465 (4.37)	28.43 (4.475)
Acanthodactylus boskianus	5	68.462 (7.912)	25.842 (3.496)	11.03 (1.437)	8.42 (1.354)	13.852 (1.271)	24.744 (3.554)	43.326 (4.724)	29.424 (4.539)
Acanthodactylus cantoris	5	68.704 (9.678)	25.744 (3.881)	10.324 (1.723)	8.112 (1.181)	13.338 (1.92)	25.524 (2.934)	44.922 (5.252)	29.542 (4.491)
Acanthodactylus erythrurus	5	67.824 (3.817)	22.836 (1.486)	10.938 (0.549)	8.802 (0.492)	12.692 (0.587)	22.266 (1.609)	41.326 (3.319)	29.324 (3.267)
Acanthodactylus felicis	1	52.98 ( )	23.4 ( )	8.84 ( )	6.64 ( )	10.71 ( )	20.73 ( )	40.94 ( )	21.7 ( )
Acanthodactylus gongrorhynchat	3	50.757 (1.087)	18.433 (0.198)	7.497 (0.179)	5.643 (0.333)	9.883 (0.396)	16.653 (0.425)	37.627 (1.008)	23.15 (0.252)
Acanthodactylus grandis	6	73.77 (17.904)	27.163 (5.979)	12.885 (2.832)	10.213 (2.589)	13.985 (2.707)	24.307 (3.68)	42.967 (8.032)	31.322 (10.532)
Acanthodactylus guineensis	4	48.685 (6.135)	17.72 (2.166)	7.528 (0.265)	5.902 (0.498)	9.867 (0.73)	16.488 (1.694)	27.808 (2.246)	21.782 (5.033)
Acanthodactylus haasi	4	48.153 (4.139)	18.27 (1.558)	7.113 (1.08)	5.455 (0.612)	9.44 (0.616)	18.578 (1.306)	34.015 (3.092)	22.71 (2.728)
Acanthodactylus hardyi	6	55.958 (2.981)	20.602 (2.056)	9.947 (0.648)	6.955 (0.659)	10.602 (0.692)	20.883 (0.991)	36.107 (2.789)	25.148 (2.276)
Acanthodactylus lineomaculatus	4	68.395 (2.106)	24.523 (2.272)	10.942 (1.018)	8.685 (0.796)	13.342 (0.704)	22.183 (1.321)	41.82 (2.011)	28.183 (2.995)
Acanthodactylus longipes	5	58.02 (2.719)	21.182 (0.679)	9.198 (0.842)	6.682 (0.215)	12.026 (0.534)	20.302 (1.478)	42.654 (2.263)	24.806 (1.066)
Acanthodactylus maculatus	5	60.364 (5.165)	22.698 (2.362)	10.438 (1.127)	7.738 (1.05)	11.38 (1.128)	20.75 (2.471)	36.296 (3.803)	25.424 (1.646)
Acanthodactylus masirae	5	53.338 (3.556)	18.362 (5.596)	9.05 (0.709)	6.698 (0.715)	11.058 (0.585)	19.954 (1.351)	40.506 (0.73)	22.732 (1.926)

Acanthodactylus micropholis	3	56.203 (2.19)	19.683 (0.773)	8.777 (0.627)	6.913 (0.038)	9.547 (0.31)	22.73 (0.863)	42.683 (0.08)	25.72 (2.877)
Acanthodactylus opheodurus	3	53.773 (2.811)	20.87 (1.259)	8.917 (0.299)	6.72 (0.193)	10.913 (0.526)	20.68 (1.07)	40.513 (0.49)	24.32 (2.168)
Acanthodactylus orientalis	2	58.995 (2.793)	23.36 (0.75)	10.11 (0.184)	7.245 (0.078)	11.62 (0.042)	19.045 (0.247)	31.675 (2.51)	23.165 (3.217)
Acanthodactylus pardalis	6	62.558 (6.044)	22.772 (2.668)	10.483 (1.146)	7.858 (0.743)	11.328 (1.05)	19.687 (1.509)	33.458 (2.223)	27.305 (4.727)
Acanthodactylus robustus	1	66.03 ( )	25.19 ( )	12.3 ( )	9.81 ( )	13.29 ( )	20.8 ( )	35.6 ( )	26.88 ( )
Acanthodactylus savignyi	2	45.645 (0.431)	16.42 (0.113)	7.245 (0.049)	5.75 (0.127)	9.24 (0.354)	16.415 (0.021)	29.315 (1.054)	21.065 (2.524)
Acanthodactylus schmidti	4	63.972 (9.85)	23.668 (3.442)	9.7 (0.927)	7.665 (0.929)	12.557 (2.007)	22.335 (4.128)	42.22 (5.187)	30.308 (7.586)
Acanthodactylus schreiberi	4	69.155 (4.446)	25.77 (2.376)	10.515 (1.013)	8.428 (0.513)	13.552 (0.764)	23.182 (2.528)	43.36 (3.316)	29.675 (3.039)
Acanthodactylus scutellatus	5	58.55 (8.472)	21.644 (3.12)	9.398 (1.051)	7.086 (0.764)	11.494 (1.292)	20.264 (2.388)	38.554 (3.756)	25.612 (4.111)
Acanthodactylus tilburyi	3	46.53 (2.419)	17.613 (0.441)	7.107 (0.369)	5.367 (0.188)	9.347 (0.208)	17.127 (0.783)	35.637 (0.66)	21.513 (1.282)
Acanthodactylus tristrami	4	79.248 (5.218)	28.558 (2.786)	12.078 (1.996)	9.693 (0.883)	14.66 (1.193)	27.05 (3.172)	44.142 (3.614)	37.807 (4.583)
Adolfus africanus	6	60.71 (4.052)	21.003 (1.592)	9.228 (0.666)	6.415 (0.437)	14.377 (0.906)	23.888 (1.157)	35.613 (3.002)	25.432 (2.824)
Adolfus alleni	4	58.032 (2.747)	19.622 (0.643)	9.09 (0.565)	7.075 (0.473)	12.16 (0.14)	16.175 (0.836)	24.482 (1.574)	28.407 (2.055)
Algyroides fitzingeri	3	36.027 (1.378)	12.87 (0.702)	5.02 (0.195)	3.073 (0.19)	7.503 (0.655)	10.62 (0.857)	16.343 (1.197)	16.423 (1.686)
Algyroides marchi	6	44.277 (2.422)	15.812 (0.544)	6.603 (0.621)	4.445 (0.494)	10.585 (0.506)	15.01 (1.431)	23.215 (1.329)	20.258 (2.658)
Algyroides moreoticus	6	45.45 (3.084)	15.355 (1.547)	6.687 (0.772)	4.775 (0.471)	9.18 (0.917)	14.125 (1.021)	23.236 (0.973)	23 (2.954)
Algyroides nigropunctatus	7	62.884 (3.883)	22.726 (1.878)	9.764 (0.846)	7.011 (0.712)	15.193 (1.565)	20.933 (1.673)	35.38 (3.114)	27.264 (1.288)
Anatololacerta anatolica	3	71.517 (6.46)	25.657 (1.782)	11.57 (0.672)	8.807 (0.107)	13.843 (0.345)	25 (1.954)	43.78 (3.537)	33.85 (1.65)
Apathya cappadocica	3	67.74 (6.132)	22.303 (2.507)	10.08 (1.021)	6.53 (0.879)	13.957 (2.825)	23.697 (1.378)	40.253 (4.944)	32.94 (5.375)
Archaeolacerta bedriagae	6	79.275 (3.143)	29.013 (3.771)	13.795 (1.08)	8.662 (0.885)	16.048 (1.365)	28.198 (2.895)	44.305 (2.914)	35.833 (1.633)
Atlantolacerta andreanskyi	3	41.47 (3.185)	8.853 (0.592)	5.257 (0.308)	3.683 (0.35)	5.737 (0.401)	11.263 (0.665)	14.937 (1.39)	22.283 (2.505)
Australolacerta australis	2	69.9 (5.515)	23.62 (3.564)	9.845 (0.785)	6.305 (0.12)	14.625 (0.46)	20.97 (0.877)	34.29 (2.899)	29.325 (1.633)
Congolacerta vauereselli	3	53.85 (2.868)	19.683 (0.963)	7.847 (0.664)	5.553 (0.638)	12.357 (1.014)	21.843 (1.546)	31.653 (2.375)	24.363 (2.499)
Dalmatolacerta oxycephala	6	62.112 (2.423)	22.79 (1.558)	9.385 (0.282)	5.323 (0.255)	11.005 (0.613)	22.575 (1.11)	34.528 (2.042)	26.932 (2.967)

Darevskia caucasica	4	53.82 (4.179)	17.255 (1.455)	7.61 (0.647)	5.048 (0.253)	8.985 (0.353)	17.458 (0.52)	27.715 (1.237)	27.168 (4.507)
Darevskia chlorogaster	5	58.404 (3.21)	20.104 (1.688)	9.126 (0.623)	6.792 (0.275)	10.58 (1.089)	21.852 (1.775)	35.748 (2.323)	28.448 (0.777)
Darevskia derjugini	5	54.626 (4.732)	16.434 (1.01)	7.556 (0.413)	5.678 (0.378)	9.462 (0.698)	17.666 (0.459)	26.584 (1.29)	28.25 (5.582)
Darevskia parvula	1	46.82 ( )	16.1 ( )	6.21 ( )	3.55 ( )	7.76 ( )	17.15 ( )	28.83 ( )	21.29 ( )
Darevskia praticola	4	48.042 (2.983)	16.093 (0.632)	6.982 (0.339)	5.418 (0.413)	8.968 (0.936)	14.86 (1.141)	25.25 (1.795)	23.685 (0.681)
Darevskia rudis	5	64.956 (2.413)	22.468 (0.671)	10.228 (0.44)	6.578 (0.339)	12.628 (1.063)	21.894 (1.687)	36.636 (1.996)	30.274 (1.518)
Darevskia saxicola	1	66.05 ( )	22.18 ( )	9.91 ( )	6.91 ( )	11.55 ( )	24.3 ( )	37.93 ( )	28.41 ( )
Darevskia valentini	1	70.54 ( )	23.56 ( )	10.55 ( )	6.49 ( )	13.21 ( )	25.5 ( )	38.6 ( )	36.05 ( )
Dinarolacerta mosorensis	6	62.953 (2.395)	22.837 (1.427)	9.735 (0.549)	5.562 (0.582)	12.145 (1.003)	22.902 (0.859)	36.065 (2.68)	28.485 (1.636)
Eremias argus	6	53.48 (2.113)	18.403 (1.007)	8.393 (0.303)	7.023 (0.411)	10.152 (1.204)	17.818 (1.245)	28.907 (3.011)	23.825 (0.534)
Eremias arguta	5	61.26 (5.855)	21.758 (2.994)	10.254 (1.565)	8.104 (1.143)	10.44 (1.393)	22.29 (1.76)	32.686 (3.738)	28.872 (3.057)
Eremias brenchleyi	3	47.237 (2.068)	17.457 (1.131)	7.367 (0.448)	5.597 (0.225)	8.927 (0.368)	18.887 (1.012)	32.563 (1.19)	20.557 (1.898)
Eremias grammica	3	62.52 (6.027)	20.207 (2.226)	9.133 (1.167)	6.79 (0.317)	10.6 (1.127)	23.097 (2.027)	38.107 (4.137)	30.017 (2.739)
Eremias intermedia	6	55.355 (2.972)	19.158 (1.822)	8.803 (0.897)	6.732 (0.888)	9.6 (0.67)	19.545 (0.384)	32.783 (2.264)	24.967 (1.952)
Eremias multiocellata	3	62.853 (2.718)	21.783 (3.043)	10.6 (1.735)	8.333 (1.165)	10.09 (0.39)	21.003 (2.792)	31.85 (2.923)	28.767 (1.559)
Eremias persica	6	77.677 (6.905)	27.795 (2.01)	12.468 (0.897)	9.742 (0.621)	13.738 (2.077)	29.018 (2.672)	48.958 (4.335)	37.85 (4.754)
Eremias pleskei	2	52.945 (4.137)	18.625 (2.171)	7.365 (1.28)	5.365 (1.252)	9.185 (0.049)	18.805 (1.025)	33.27 (0.156)	25.025 (2.015)
Eremias przewalskii	3	72.653 (3.61)	24.463 (0.406)	10.683 (0.541)	8.473 (0.418)	12.563 (0.575)	24.8 (0.347)	40.48 (0.786)	36.42 (4.016)
Eremias strauchi	2	64.17 (2.602)	23.315 (2.638)	10.94 (0.325)	8.22 (0.014)	10.585 (0.884)	24.49 (0.792)	42.95 (0.608)	29.015 (0.87)
Eremias velox	5	61.96 (3.797)	21.28 (2.656)	9.006 (0.892)	7.276 (0.63)	10.172 (0.533)	22.234 (1.636)	35.62 (2.851)	29.92 (1.798)
Gallotia atlantica	3	88.657 (6.887)	30.447 (1.299)	14.987 (0.761)	10.837 (1.606)	16.51 (0.962)	28.27 (4.489)	48.03 (3.65)	43.74 (4.568)
Gallotia bravoana	10	187.3 (6.897)	46.41 (2.404)	31.751 (1.618)	23.379 (1.678)	31.693 (1.507)	64.621 (3.599)	91.577 (4.335)	95.347 (5.745)
Gallotia caesaris	3	82.433 (4.975)	29.347 (1.28)	14.943 (0.469)	11.64 (1.29)	15.867 (1.308)	29.087 (2.312)	51.053 (2.024)	33.297 (3.138)
Gallotia galloti	2	112.765 (0.474)	40.24 (1.23)	20.945 (0.389)	17.79 (0.141)	19.09 (0.537)	37.11 (2.475)	65.045 (4.815)	52.2 (1.089)

Gallotia intermedia	5	128.722 (21.447)	31.106 (6.997)	20.034 (4.923)	14.77 (3.447)	22.386 (5.038)	50.536 (5.98)	71.422 (8.742)	63.524 (9.192)
Gallotia simonyi	1	222.67 ( )	80.16 ( )	43.1 ( )	31.58 ( )	41.21 ( )	77.78 ( )	111.15 ( )	113.04 ( )
Gallotia stehlini	10	204.149 (16.758)	51.098 (10.163)	34.006 (7.459)	26.197 (6.093)	34.344 (6.397)	70.272 (11.088)	95.198 (13.712)	102.391 (16.233)
Gastropholis prasina	2	97.885 (8.86)	25.595 (1.775)	12.51 (0.283)	10.08 (0.467)	16.69 (1.527)	33.04 (0.806)	43.495 (2.751)	47.36 (0)
Gastropholis vittata	2	78.46 (0.594)	26.205 (4.787)	10.9 (0.382)	8.665 (0.615)	13.645 (0.841)	24.325 (0.064)	35.835 (1.492)	37.31 (1.075)
Heliobolus lugubris	6	53.012 (2.48)	18.825 (1.531)	8.675 (0.752)	6.707 (0.635)	9.98 (0.785)	19.877 (1.11)	40.598 (2.047)	22.993 (1.544)
Heliobolus spekii	6	43.993 (2.868)	16.113 (0.763)	7.56 (0.404)	5.538 (0.327)	8.948 (0.612)	15.9 (0.489)	35.137 (1.928)	18.833 (1.569)
Hellenolacerta graeca	2	65.275 (12.99)	24.355 (5.183)	9.815 (1.789)	6.47 (1.047)	11.335 (3.132)	22.435 (2.85)	35.945 (4.151)	27.44 (3.493)
Holaspis guentheri	5	47.9 (1.734)	16.266 (1.412)	6.092 (0.723)	3.232 (0.664)	8.184 (1.045)	15.832 (1.909)	21.786 (3.319)	23.136 (0.761)
Holaspis laevis	3	43.967 (3.837)	16.023 (0.945)	6.913 (0.309)	3.09 (0.262)	8.743 (0.379)	15.995 (1.145)	22.27 (1.593)	20.713 (3.905)
Iberolacerta bonnali	1	51.57 ( )	16.89 ( )	7.37 ( )	4.5 ( )	7.6 ( )	15.71 ( )	25.84 ( )	26.86 ( )
Iberolacerta cyreni	5	66.626 (5.794)	23.724 (0.811)	10.43 (0.196)	6.316 (0.504)	12.292 (0.524)	21.936 (0.63)	36.002 (1.78)	31.998 (5.471)
Iberolacerta horvathi	3	57.493 (4.834)	19.607 (0.919)	8.253 (0.39)	5.097 (0.307)	10.177 (0.225)	18.697 (0.875)	30.277 (1.127)	27.907 (4.625)
Iberolacerta monticola	3	67.07 (0.835)	24.32 (0.763)	11.403 (0.333)	7.293 (0.229)	11.993 (0.895)	23.327 (1.786)	34.987 (0.618)	30.567 (0.137)
Ichnotropis capensis	2	73.15 (4.54)	26.745 (1.11)	9.82 (1.117)	8.92 (0.41)	14.485 (1.365)	23.63 (1.131)	40.88 (3.366)	32.89 (1.881)
Iranolacerta brandtii	2	66.185 (1.336)	23.66 (1.301)	9.995 (0.516)	7.745 (0.332)	13.36 (0.198)	21.725 (0.544)	38.035 (6.611)	31.245 (0.955)
Lacerta agilis	10	93.164 (4.69)	30.798 (2.295)	15.212 (1.199)	13.563 (1.251)	19.138 (1.455)	27.946 (1.968)	40.901 (2.542)	47.386 (2.963)
Lacerta bilineata	10	122.367 (3.619)	41.003 (2.188)	19.757 (1.053)	17.514 (1.142)	26.366 (1.504)	39.617 (3.187)	66.502 (5.357)	58.989 (2.177)
Lacerta media	10	130.674 (7.049)	45.177 (3.661)	21.097 (1.702)	19.739 (1.001)	28.722 (1.573)	41.4 (2.222)	70.324 (3.158)	62.659 (3.78)
Lacerta pamphylica	4	96.425 (4.55)	32.555 (1.655)	14.56 (1.032)	12.635 (0.767)	20.683 (1.51)	32.735 (1.403)	62.51 (3.19)	47.075 (2.27)
Lacerta schreiberi	10	109.578 (2.31)	38.451 (2.37)	19.648 (0.963)	16.763 (1.66)	24.482 (1.224)	35.506 (1.059)	53.3 (2.007)	51.682 (3.204)
Lacerta strigata	10	97.836 (3.434)	32.749 (1.364)	15.247 (0.674)	13.094 (0.638)	21.334 (1.352)	31.551 (2.008)	52.827 (3.46)	46.837 (2.298)
Lacerta trilineata	10	156.6 (6.332)	54.464 (3.59)	28.036 (2.237)	24.251 (2.015)	34.642 (2.482)	46.437 (2.788)	82.722 (4.127)	74.872 (4.955)
Lacerta viridis	10	123.067 (5.965)	42.186 (3.866)	21.161 (0.839)	17.967 (0.786)	26.55 (1.613)	38.978 (2.407)	63.245 (5.112)	58.23 (4.816)

Latastia longicaudata	5	98.804 (8.137)	34.21 (1.651)	13.118 (1.54)	11.064 (0.786)	17.468 (2.226)	28.506 (2.853)	57.934 (5.636)	46.952 (6.502)
Meroles anchietae	1	57.01 ( )	18.12 ( )	10.28 ( )	7.52 ( )	11.21 ( )	25.75 ( )	44.39 ( )	22.46 ( )
Meroles ctenodactylus	5	77.856 (2.963)	29.498 (1.273)	14.06 (0.363)	10.828 (0.537)	17.654 (0.605)	28.37 (1.586)	55.568 (2.093)	30.844 (2.999)
Meroles cuneirostris	5	57.476 (4.894)	21.134 (1.661)	10.384 (0.404)	7.42 (0.63)	12.096 (1.119)	19.554 (2.063)	40.768 (3.992)	24.326 (4.021)
Meroles knoxii	7	53.817 (6.673)	20.217 (2.406)	8.187 (1.204)	6.161 (0.828)	9.556 (1.748)	18.73 (2.061)	38.241 (6.124)	24.532 (2.897)
Meroles reticulatus	6	49.902 (3.859)	14.648 (1.212)	8.937 (0.699)	6.835 (0.839)	11.088 (1.042)	19.387 (1.202)	32.512 (2.191)	20.493 (2.83)
Meroles squamulosus	1	59.37 ( )	20.13 ( )	9.06 ( )	7.06 ( )	11.64 ( )	19.9 ( )	34.76 ( )	28.09 ( )
Meroles suborbitalis	3	60.41 (1.946)	22.18 (0.806)	10.25 (0.814)	7.053 (0.325)	11.643 (0.284)	22.443 (1.441)	43.63 (1.343)	25.177 (2.664)
Mesalina adramitana	5	42.094 (2.611)	15.512 (1.217)	6.29 (0.569)	4.132 (0.34)	6.674 (0.496)	14.796 (1.18)	28.902 (1.495)	18.47 (2.422)
Mesalina bahaeldini	1	44.64 ( )	11.82 ( )	6.61 ( )	4.66 ( )	7.92 ( )	16.75 ( )	25.98 ( )	21.42 ( )
Mesalina balfouri	4	50.585 (3.278)	17.505 (1.698)	6.735 (0.681)	5.29 (0.883)	8.678 (1.758)	16.75 (1.738)	29.742 (3.104)	24.065 (1.082)
Mesalina brevirostris	4	46.373 (5.777)	16.42 (1.122)	7.082 (0.99)	4.798 (0.588)	7.658 (0.802)	16.625 (1.013)	29.108 (2.45)	22.615 (4.309)
Mesalina guttulata	6	41.013 (2.463)	16.222 (1.155)	6.432 (0.505)	4.38 (0.35)	8.23 (1.002)	15.898 (0.925)	28.708 (1.699)	18.342 (1.413)
Mesalina martini	5	39.75 (1.791)	14.488 (0.481)	5.554 (0.45)	3.214 (0.537)	6.698 (0.649)	13 (1.092)	22.31 (2.057)	17.03 (2.131)
Mesalina olivieri	5	42.28 (1.985)	15.144 (0.372)	5.99 (0.299)	4.102 (0.239)	7.49 (0.789)	14.66 (0.381)	25.2 (0.956)	19.63 (1.495)
Mesalina pasteuri	3	46.413 (6.61)	17.053 (1.747)	7.167 (0.81)	5.217 (0.869)	8.48 (1.225)	16.14 (1.41)	29.093 (2.379)	20.583 (4.305)
Mesalina rubropunctata	6	48.987 (3.488)	18.408 (1.196)	8.097 (0.348)	5.217 (0.426)	8.578 (0.399)	18.802 (1.276)	30.202 (1.493)	22.255 (2.393)
Mesalina simoni	1	41.58 ( )	14.42 ( )	5.9 ( )	4.02 ( )	6.35 ( )	13.92 ( )	24.17 ( )	17.41 ( )
Mesalina watsonana	5	45.19 (3.019)	16.862 (1.47)	6.706 (0.609)	4.654 (0.53)	7.46 (0.843)	16.4 (1.045)	30.054 (2.988)	20.96 (1.974)
Nucras boulengeri	5	59.256 (3.226)	18.568 (1.514)	8.31 (0.731)	7.024 (0.99)	9.948 (1.064)	17.298 (0.994)	26.874 (3.129)	31.562 (2.678)
Nucras intertexta	6	56.15 (11.404)	17.232 (3.639)	9.863 (7.251)	6.315 (1.882)	8.568 (1.329)	14.642 (3.39)	25.51 (4.919)	31.002 (6.715)
Nucras lalandii	7	87.72 (8.557)	15.089 (1.208)	9.96 (0.806)	8.369 (0.761)	10.677 (0.803)	21.357 (1.753)	29.703 (2.904)	51.853 (7.925)
Nucras taeniolata	3	83.3 (10.067)	27.087 (5.256)	12.093 (1.709)	10.975 (1.795)	12.427 (3.537)	23.177 (1.891)	38.297 (5.331)	43.52 (4.808)
Nucras tessellata	5	66.074 (7.743)	19.326 (1.763)	8.604 (1.09)	6.772 (0.591)	9.838 (0.419)	18.838 (1.626)	34.904 (3.888)	34.378 (5.1)

Omanosaura cyanura	3	46.35 (6.666)	17.293 (2.761)	6.277 (0.775)	3.71 (0.563)	8.95 (0.636)	15.927 (1.864)	28.09 (2.252)	20.357 (4.04)
Omanosaura jayakari	4	152.053 (14.53)	56.132 (4.879)	27.837 (2.482)	21.22 (2.173)	25.345 (1.624)	52.592 (3.491)	91.662 (5.162)	67.692 (6.447)
Ophisops elegans	5	47.74 (2.429)	16.63 (1.293)	7.12 (0.483)	5.594 (0.463)	7.96 (0.646)	16.732 (1.016)	32.186 (1.131)	22.802 (0.548)
Ophisops jerdonii	5	40.716 (3.759)	13.526 (1.226)	5.124 (0.231)	4.294 (0.498)	6.976 (0.572)	13.46 (0.814)	22.18 (1.181)	19.97 (3.27)
Ophisops leschenaultii	4	50.43 (3.376)	16.225 (0.924)	6.995 (0.44)	4.732 (0.292)	7.995 (0.617)	18.048 (1.497)	31.148 (2.241)	25.355 (2.878)
Ophisops microlepis	3	60.543 (4.64)	20.433 (1.339)	8.72 (0.658)	7.01 (0.815)	11.193 (0.745)	21.72 (1.003)	40.947 (0.483)	27.683 (1.625)
Ophisops nictans	2	47.49 (5.431)	15.675 (0.771)	6.815 (0.46)	4.96 (0.156)	8.365 (0.474)	17.165 (2.765)	32.56 (3.705)	21.495 (2.001)
Ophisops occidentalis	8	40.578 (1.504)	14.256 (1.018)	6.254 (0.405)	4.96 (0.17)	6.99 (0.634)	14.815 (0.888)	26.163 (1.467)	18.881 (1.404)
Parvilacerta fraasii	4	58.07 (2.215)	19.2 (1.17)	8.738 (0.599)	6.88 (0.943)	10.51 (1.06)	18.178 (0.171)	29.382 (0.449)	28.452 (2.326)
Parvilacerta parva	6	48.887 (2.795)	16.317 (0.627)	7.07 (0.483)	5.662 (0.278)	8.602 (0.596)	15.645 (0.906)	24.988 (1.434)	23.828 (2.812)
Pedioplanis burchelli	5	56.396 (6.101)	19.416 (1.617)	8.512 (0.938)	5.482 (0.715)	8.928 (0.663)	19.724 (1.045)	36.1 (3.422)	26.096 (2.061)
Pedioplanis inornata	1	50.6 ( )	17.99 ( )	6.66 ( )	4.19 ( )	7.86 ( )	19.93 ( )	34.55 ( )	22.93 ( )
Pedioplanis laticeps	3	61.55 (3.569)	22.133 (1.542)	9.687 (1.85)	7.033 (1.666)	10.437 (0.795)	22.88 (1.044)	43.94 (3.987)	27.183 (1.217)
Pedioplanis lineoocellata	10	55.811 (1.218)	13.334 (0.748)	7.618 (0.923)	5.276 (1.079)	9.862 (0.87)	20.02 (1.001)	33.764 (2.106)	26.926 (7.937)
Pedioplanis namaquensis	3	50.23 (0.269)	17.76 (1.638)	6.773 (0.594)	5.14 (0.378)	7.523 (1.13)	16.947 (1.245)	34.01 (2.372)	23.637 (1.507)
Pedioplanis undata	6	50.248 (2.611)	19.338 (1.523)	7.275 (0.696)	4.978 (0.529)	7.682 (0.363)	19.268 (0.711)	37.09 (2.213)	19.812 (4.734)
Philochortus spinalis	3	50.533 (3.648)	17.73 (1.505)	7.173 (0.394)	6.31 (0.04)	8.607 (0.2)	16.543 (1.42)	32.58 (1.418)	23.023 (1.053)
Phoenicolacerta kulzeri	1	58.16 ( )	17.99 ( )	8 ( )	5.34 ( )	8.2 ( )	17.9 ( )	30.9 ( )	30.95 ( )
Phoenicolacerta laevis	6	66.078 (17.035)	24.103 (5.522)	11.233 (3.363)	8.522 (2.864)	12.7 (2.903)	24.653 (6.023)	41.332 (9.67)	31.158 (8.993)
Podarcis bocagei	10	64.076 (0.89)	21.852 (1.327)	9.52 (0.582)	7.251 (0.681)	12.98 (0.533)	19.282 (1.141)	31.926 (1.491)	31.18 (1.224)
Podarcis carbonelli	10	63.502 (1.443)	20.931 (1.333)	9.064 (0.392)	7.776 (0.497)	12.735 (0.346)	18.497 (0.932)	31.38 (1.642)	32.41 (1.217)
Podarcis cretensis	10	68.258 (1.416)	23.671 (1.088)	9.402 (0.643)	7.716 (0.73)	14.049 (0.257)	21.163 (0.966)	35.66 (1.304)	34.153 (2.103)
Podarcis erhardii	10	72.28 (1.427)	24.159 (0.886)	10.05 (0.464)	8.171 (0.52)	14.162 (0.504)	23.444 (0.928)	41.781 (1.824)	35.478 (1.402)
Podarcis filfolensis	10	66.505 (0.786)	23.649 (1.234)	10.253 (0.589)	8.261 (0.626)	13.741 (0.461)	21.65 (1.272)	38.581 (1.221)	30.984 (1.926)

Podarcis gaigeae	10	64.866 (3.492)	21.704 (1.281)	8.562 (0.56)	7.764 (0.737)	13.298 (0.715)	19.564 (1.233)	33.182 (2.244)	33.292 (2.189)
Podarcis guadarramae	10	63.018 (1.334)	21.783 (1.258)	8.29 (0.354)	5.953 (0.413)	12.536 (0.548)	20.017 (0.603)	32.822 (1.367)	30.551 (1.129)
Podarcis hispanicus	10	62.043 (2.064)	20.515 (1.368)	9.353 (0.283)	7.112 (0.405)	12.588 (0.361)	19.313 (0.908)	33.002 (1.364)	31.135 (2.508)
Podarcis ionicus	10	75.479 (1.467)	26.955 (1.155)	10.753 (0.666)	9.038 (0.649)	16.281 (0.645)	22.581 (1.493)	40.246 (1.91)	35.916 (1.789)
Podarcis lilfordi	10	74.294 (0.877)	26.232 (1.532)	10.494 (0.373)	8.664 (0.282)	15.584 (0.52)	24.889 (0.571)	41.252 (1.349)	35.037 (1.309)
Podarcis liolepis	10	67.849 (1.983)	22.419 (0.815)	10.574 (0.82)	8.099 (0.428)	13.97 (0.413)	22.074 (0.811)	34.763 (1.039)	33.716 (1.079)
Podarcis melisellensis	6	56.242 (1.647)	20.527 (0.661)	8.097 (0.225)	6.607 (0.25)	12.29 (0.3)	20.353 (0.312)	34.162 (0.767)	25.145 (0.95)
Podarcis milensis	10	63.006 (2.668)	21.348 (1.337)	8.891 (0.88)	7.42 (0.944)	12.755 (0.711)	19.653 (1.235)	33.605 (1.528)	31.497 (1.226)
Podarcis muralis	10	70.781 (1.135)	25.746 (1.35)	10.205 (1.043)	8.128 (1.264)	14.912 (0.736)	22.966 (2.526)	37.868 (3.961)	32.597 (1.668)
Podarcis peloponnesiacus	10	84.609 (1.155)	29.188 (1.217)	12.981 (0.68)	10.469 (0.746)	18.025 (0.904)	27.359 (1.287)	48.014 (1.167)	40.943 (2.326)
Podarcis pityusensis	10	79.953 (1.503)	28.867 (1.422)	12.831 (0.861)	11.182 (1.061)	16.54 (0.734)	26.818 (1.761)	43.747 (2.44)	36.752 (2.414)
Podarcis siculus	10	78.289 (1.628)	27.879 (0.842)	11.373 (0.564)	9.73 (1.027)	17.292 (0.492)	26.527 (1.13)	47.36 (1.799)	36.587 (1.421)
Podarcis tauricus	10	68.629 (2.329)	23.268 (1.126)	9.573 (0.535)	8.265 (0.488)	14.177 (0.693)	20.359 (1.413)	35.545 (2.017)	33.057 (2.276)
Podarcis tiliguerta	10	63.864 (1.646)	23.323 (0.649)	9.819 (0.717)	7.778 (0.694)	13.354 (0.596)	22.948 (0.722)	40.169 (1.503)	29.164 (1.983)
Podarcis vaucheri	10	65.214 (0.878)	22.849 (1.04)	9.886 (0.86)	7.717 (0.764)	13.874 (0.78)	21.415 (0.541)	35.531 (1.088)	31.239 (1.688)
Podarcis virescens	10	63.827 (2.155)	22.097 (1.136)	8.716 (0.562)	6.622 (0.507)	13.048 (0.704)	20.142 (1.005)	34.214 (1.186)	31.214 (1.304)
Podarcis waglerianus	10	71.871 (1.182)	25.915 (0.994)	10.065 (0.551)	7.983 (0.555)	15.588 (0.467)	23.954 (1.031)	43.46 (1.207)	33.046 (1.182)
Poromera fordii	5	59.614 (2.527)	21.088 (1.455)	8.89 (0.773)	6.848 (0.537)	11.572 (0.835)	24.45 (1.527)	38.12 (1.473)	26.148 (1.644)
Psammodromus algirus	2	73.515 (3.175)	25.225 (1.294)	12.29 (0.41)	9.955 (0.573)	13.885 (0.332)	24.49 (2.135)	43.295 (0.926)	36.47 (3.748)
Psammodromus blanci	3	39.393 (4.341)	12.693 (0.987)	5.563 (0.631)	4.32 (0.154)	6.893 (0.653)	12.1 (0.139)	20.77 (0.997)	20.517 (3.907)
Psammodromus edwarsianus	4	44.708 (4.573)	14.957 (1.111)	6.215 (0.268)	4.883 (0.367)	6.385 (0.294)	15 (0.981)	26.57 (1.107)	22.47 (2.185)
Psammodromus hispanicus	5	40.244 (5.457)	13.862 (1.294)	6.022 (0.57)	4.528 (0.5)	6.642 (0.839)	13.754 (1.494)	23.432 (2.711)	19.678 (1.192)
Psammodromus microdactylus	6	43.428 (2.378)	15.187 (1.027)	6.468 (0.088)	4.893 (0.195)	7.667 (0.389)	14.12 (0.839)	21.887 (0.468)	21.327 (2.465)
Pseuderemias smithii	6	42.763 (1.113)	14.85 (1.137)	6.74 (0.257)	4.917 (0.414)	7.847 (0.818)	13.698 (0.984)	33.137 (2.653)	19.958 (0.643)

Scelarcis perspicillata	3	54.097 (3.565)	17.56 (0.75)	8.113 (0.021)	4.987 (1.217)	9.24 (0.209)	17.44 (0.684)	27.017 (1.756)	26.717 (4.133)
Takydromus dorsalis	1	55.93 ( )	19.78 ( )	6.6 ( )	5.25 ( )	9.93 ( )	20.76 ( )	32.02 ( )	26.24 ( )
Takydromus formosanus	5	45.806 (2.315)	15.816 (1.8)	5.71 (0.37)	4.656 (0.308)	7.866 (0.671)	15.548 (1.178)	21.844 (1.444)	21.344 (2.719)
Takydromus luyeanus	1	52.62 ( )	17.81 ( )	7.31 ( )	6.37 ( )	9.16 ( )	17.62 ( )	26.55 ( )	24.9 ( )
Takydromus sauteri	2	52.165 (1.789)	17.96 (0.311)	6.125 (0.233)	4.75 (0.014)	8.76 (0.028)	20.48 (0.156)	25 (0.99)	27.505 (0.078)
Takydromus septentrionalis	6	64.955 (2.64)	21.875 (2.016)	9.145 (0.98)	7.657 (0.775)	10.9 (0.828)	24.023 (2.369)	33.837 (1.108)	32.942 (2.442)
Takydromus sexlineatus	4	56.775 (1.514)	19.052 (1.63)	6.422 (0.253)	5.58 (0.289)	9.867 (1.206)	20.405 (1.01)	28.733 (1.795)	27.532 (1.222)
Takydromus smaragdinus	4	46.468 (4.777)	16.907 (1.41)	5.625 (0.278)	4.692 (0.342)	8.642 (0.91)	18.262 (1.17)	24.39 (2.932)	22.69 (2.306)
Takydromus stejnegeri	4	46.312 (2.454)	11.317 (0.387)	5.678 (0.256)	4.855 (0.118)	7.73 (0.385)	16.24 (0.246)	21.058 (1.862)	22.055 (1.983)
Takydromus tachydromoides	2	54.745 (0.912)	18.995 (1.308)	7.81 (0.467)	6.455 (0.332)	10.265 (0.233)	20.25 (0.537)	30.65 (1.004)	25.39 (0.354)
Takydromus toyamai	2	52.15 (3.847)	17.97 (0.184)	6.06 (0.269)	5.275 (0.262)	8.79 (0.679)	18.5 (0.156)	24.95 (1.513)	24.975 (3.981)
Takydromus viridipunctatus	1	53.47 ( )	19.34 ( )	7.33 ( )	5.91 ( )	10.59 ( )	17.69 ( )	25.1 ( )	26.88 ( )
Takydromus wolteri	2	45.215 (0.813)	15.33 (1.428)	5.47 (0.269)	5.225 (0.601)	7.51 (0.311)	15.66 (0.269)	21.005 (0.417)	22.27 (1.004)
Teira dugesii	6	61.105 (4.937)	21.07 (1.5)	9.903 (0.982)	7.163 (0.772)	11.477 (0.975)	22.4 (1.948)	34.123 (1.548)	27.74 (1.977)
Timon kurdistanicus	8	116.988 (9.463)	39.579 (3.163)	18.589 (1.862)	15.169 (1.827)	24.432 (2.728)	37.725 (3.554)	67.448 (4.276)	56.57 (4.089)
Timon lepidus	10	214.5 (13.285)	82.118 (6.608)	43.356 (6.571)	35.29 (4.464)	55.197 (3.959)	66.454 (2.941)	104.854 (6.196)	92.271 (7.901)
Timon nevadensis	10	202.5 (3.536)	76.728 (4.039)	41.776 (3.461)	35.66 (3.868)	53.39 (3.503)	63.321 (3.257)	99.283 (5.937)	90.854 (5.36)
Timon pater	14	158.529 (10.225)	58.919 (4.41)	31.416 (3.527)	26.439 (3.598)	38.886 (5.623)	53.033 (4.547)	83.939 (4.681)	69.715 (4.767)
Timon princeps	8	118.951 (15.946)	41.36 (6.18)	19.226 (3.399)	16.386 (3.201)	25.444 (3.85)	40.216 (4.199)	70.391 (6.758)	57.02 (9.313)
Timon tangitanus	10	151.797 (5.714)	55.633 (3.934)	28.641 (2.331)	22.782 (1.986)	35.813 (2.172)	49.481 (4.061)	77.508 (6.258)	63.693 (5.072)
Tropidosaura cottrelli	1	60.65 ( )	21.74 ( )	10.08 ( )	6.3 ( )	11.48 ( )	18.54 ( )	30.22 ( )	23.97 ( )
Tropidosaura essexi	1	45 ( )	15.18 ( )	6.29 ( )	4.81 ( )	8.68 ( )	13.81 ( )	22.13 ( )	19.32 ( )
Tropidosaura montana	1	55.54 ( )	17.74 ( )	7.2 ( )	5.82 ( )	8.89 ( )	16.45 ( )	25.5 ( )	29.72 ( )
Vhembelacerta rupicola	10	45.204 (3.089)	10.762 (0.38)	5.089 (0.286)	3.509 (0.231)	7.967 (0.429)	15.559 (0.938)	23.673 (1.152)	26.099 (3.017)

Zootoca vivipara	6	49.292 (4.096)	15.317 (1.54)	7.252 (0.725)	5.54 (0.392)	8.365 (0.584)	14.592 (1.512)	21.878 (2.763)	23.852 (2.466)

Table S4.2. Habitat use category assigned to each species, and corresponding reference. Abbreviations refer to ground-dwelling (GD) and climbers (CL).

	Habitat	Reference
Acanthodactylus aegyptius	GD	Baha el din, 2007
Acanthodactylus arabicus	GD	Sindaco et al 2012
Acanthodactylus aureus	GD	Vanhooydonck and Van Damme, 1999
Acanthodactylus bedriagai	GD	Geniez and Miras 2006
Acanthodactylus beershebensis	GD	Werner et al. 2006
Acanthodactylus blanci	GD	Nouira and Joger, 2003
Acanthodactylus blanfordii	GD	Van Der Kooij, 2000
Acanthodactylus boskianus	GD	Van Der Kooij, 2000
Acanthodactylus boueti	GD	Branch et al 2013
Acanthodactylus busacki	GD	Geniez et al 2010
Acanthodactylus cantoris	GD	Van Damme and Vanhooydonk, 2002
Acanthodactylus dumerilii	GD	Sword et al. 2000
Acanthodactylus erythrurus	GD	Gil et al. 1993
Acanthodactylus felicis	GD	Van Der Kooij, 2000
Acanthodactylus gongrorhynchatus	GD	Salvador Milla, 2015
Acanthodactylus grandis	GD	Van Damme and Vanhooydonk, 2002
Acanthodactylus guineensis	GD	Chirio 2021
Acanthodactylus haasi	CL	Van Der Kooij, 2000
Acanthodactylus hardyi	GD	Crochet et al. 2003
Acanthodactylus harranensis	GD	Baran et al. 2005
Acanthodactylus khamirensis	GD	Heidari et al. 2013
Acanthodactylus lineomaculatus	GD	Martinez del Marmol, 2013
Acanthodactylus longipes	GD	Vanhooydonck and Van Damme, 1999
Acanthodactylus maculatus	GD	Van Damme and Vanhooydonk, 2002
Acanthodactylus margaritae	GD	Tamar et al. 2017

Acanthodactylus masirae	GD	Carranza et al 2023
Acanthodactylus micropholis	GD	Van Damme and Vanhooydonk, 2002
Acanthodactylus nilsoni	GD	Hatami, 2014
Acanthodactylus opheodurus	GD	Van Der Kooij, 2000
Acanthodactylus orientalis	GD	Al-Sadoon et al. 2016
Acanthodactylus pardalis	GD	Vanhooydonck and Van Damme, 1999
Acanthodactylus robustus	GD	Amr et al 2012
Acanthodactylus savignyi	GD	Van Damme and Vanhooydonk, 2002
Acanthodactylus schmidti	GD	Van Der Kooij, 2000
Acanthodactylus schreiberi	GD	Akman, 2019
Acanthodactylus scutellatus	GD	Vanhooydonck and Van Damme, 1999
Acanthodactylus senegalensis	GD	Crochet et al. 2003
Acanthodactylus taghitensis	GD	Geniez and Foucart, 1995
Acanthodactylus tilburyi	GD	Disi, 2013
Acanthodactylus tristrami	GD	Van Damme and Vanhooydonk, 2002
Adolfus africanus	CL	Vanhooydonck and Van Damme, 1999
Adolfus alleni	CL	Spawls et al. 2014
Adolfus jacksoni	CL	Vanhooydonck and Van Damme, 1999; Spawls et al. 2021
Algyroides fitzingeri	CL	Vanhooydonck and Van Damme, 1999
Algyroides marchi	CL	Vanhooydonck and Van Damme, 1999
Algyroides moreoticus	GD	Vanhooydonck and Van Damme, 1999; Böhme et al. 2009a
Algyroides nigropunctatus	CL	Vanhooydonck and Van Damme, 1999; Böhme et al. 2009b
Anatololacerta anatolica	CL	Tok et al. 2009a
Anatololacerta danfordi	CL	Tok et al. 2009b
Anatololacerta oertzeni	CL	Böhme et al 2009c
Apathya cappadocica	CL	Tok et al 2009c
Apathya yassujica	CL	Karamiani et al. 2015
Archaeolacerta bedriagae	CL	Vanhooydonck and Van Damme, 1999
Atlantolacerta andreanskyi	GD	S'khifa et al. 2020
Australolacerta australis	CL	Bates et al. 2014
Congolacerta asukului	GD	Greenbaum et al. 2011

Congolacerta vaueresselli	GD	Greenbaum et al. 2011
Dalmatolacerta oxycephala	CL	Vanhooydonck and Van Damme, 1999
Darevskia caspica	CL	Ahmadzadeh et al. 2013
Darevskia caucasica	CL	Tarkhnishvili et al. 2020
Darevskia chlorogaster	CL	Vanhooydonck and Van Damme, 1999
Darevskia clarkorum	CL	Tarkhnishvili et al. 2020
Darevskia daghestanica	CL	Tarkhnishvili et al. 2020
Darevskia defilippii	CL	Ahmadzadeh et al. 2013
Darevskia derjugini	GD	Tarkhnishvili et al. 2020
Darevskia kamii	CL	Ahmadzadeh et al. 2013; Yousefkhani et al. 2022
Darevskia kopetdaghica	GD	Ahmadzadeh et al. 2013
Darevskia lindholmi	CL	Uetz et al 2023
Darevskia mixta	CL	Tarkhnishvili et al. 2020
Darevskia parvula	CL	Tarkhnishvili et al. 2020
Darevskia portschinskii	CL	Tarkhnishvili et al. 2020
Darevskia praticola	GD	Tarkhnishvili et al. 2020
Darevskia raddei	CL	Tarkhnishvili et al. 2020
Darevskia rudis	CL	Tarkhnishvili et al. 2020
Darevskia saxicola	CL	Tuniyev et al. 2009
Darevskia schaekeli	CL	Ahmadzadeh et al. 2013; Yousefkhani et al. 2022
Darevskia steineri	CL	Ahmadzadeh et al. 2013; Yousefkhani et al. 2022
Darevskia valentini	CL	Sillero et al. 2016
Dinarolacerta montenegrina	CL	Ljubisavljevi et al. 2017
Dinarolacerta mosorensis	CL	Ljubisavljevi et al. 2017
Eremias argus	GD	Kim et al. 2012
Eremias arguta	GD	Ahmadzadeh et al. 2008
Eremias brenchleyi	CL	Wei guo et al. 2005
Eremias grammica	GD	Ananjeva et al 2019
Eremias intermedia	GD	Hosseinian-Yousefkhani and Rastegar-Pouyan, 2013
Eremias lalezharica	GD	Hosseinian-Yousefkhani and Rastegar-Pouyan, 2013
Eremias montanus	GD	Bahmani et al. 2011

Eremias multiocellata	GD	Bi et al. 2015
Eremias nigrolateralis	GD	Vanhooydonck and Van Damme, 1999
Eremias papenfussi	GD	Mozaffari et al. 2011
Eremias persica	GD	Vanhooydonck and Van Damme, 1999
Eremias pleskei	GD	Farashi and Alizadeh-Noughani, 2019
Eremias przewalskii	GD	Orlova et al. 2019
Eremias strauchi	GD	Ahmadzadeh et al. 2008
Eremias stummeri	GD	Dujsebayeva et al. 2019
Eremias suphani	GD	Rastegar-Pouyani et al. 2013
Eremias velox	GD	Vanhooydonck and Van Damme, 1999
Eremias vermiculata	GD	Terbish et al. 2019
Gallotia atlantica	GD	Pleguezuelos et al. 2002
Gallotia bravoana	GD	Pleguezuelos et al. 2002
Gallotia caesaris	GD	Pleguezuelos et al. 2002
Gallotia galloti	GD	Vanhooydonck and Van Damme, 1999
Gallotia goliath	GD	-
Gallotia intermedia	GD	Miras et al 2009a
Gallotia simonyi	GD	Miras et al 2009b
Gallotia stehlini	GD	Miras et al 2009c
Gastropholis prasina	CL	Spawls et al 2015
Gastropholis vittata	CL	Van Damme and Vanhooydonk, 2002
Heliobolus lugubris	GD	Bates et al. 2014
Heliobolus spekii	GD	Vanhooydonck and Van Damme, 1999
Hellenolacerta graeca	CL	Böhme and Lymberakis,2009
Holaspis guentheri	CL	Rödel et al, 2021
Holaspis laevis	CL	Wagner et al 2021
Iberolacerta aranica	CL	Speybroeck, 2016
Iberolacerta aurelioi	CL	Speybroeck, 2016
Iberolacerta bonnali	CL	Speybroeck, 2016
Iberolacerta cyreni	CL	Speybroeck, 2016
Iberolacerta galani	CL	Speybroeck, 2016

Iberolacerta horvathi	CL	Speybroeck, 2016
Iberolacerta martinezricai	CL	Speybroeck, 2016
Iberolacerta monticola	CL	Speybroeck, 2016
Ichnotropis capensis	GD	Vanhooydonck and Van Damme, 1999
Iranolacerta brandtii	GD	Rezazadeh et al. 2010
Iranolacerta zagrosica	CL	Rezazadeh et al. 2010
Lacerta agilis	GD	Speybroeck, 2016
Lacerta bilineata	GD	Vanhooydonck and Van Damme, 2003
Lacerta media	GD	Ahmadzadeh et al. 2008
Lacerta pamphylica	GD	Tok et al. 2009d
Lacerta schreiberi	GD	Speybroeck, 2016
Lacerta strigata	GD	Tuniyev et al. 2009b
Lacerta trilineata	GD	Mayer and Beyerlein, 1999
Lacerta viridis	GD	Crnobrnja Isailovic et al. 2009
Latastia longicaudata	GD	Howel et al. 2021
Meroles anchietae	GD	Eifler, 2020
Meroles ctenodactylus	GD	Bates et al. 2014
Meroles cuneirostris	GD	Bates et al. 2014
Meroles knoxii	GD	Bates et al. 2014
Meroles micropholidotus	GD	Arnold, 1995
Meroles reticulatus	GD	Edwards et al. 2016
Meroles squamulosus	GD	Bates et al. 2014
Meroles suborbitalis	GD	Bates et al. 2014
Mesalina adramitana	GD	Wilms et al. 2012
Mesalina bahaeldini	GD	Werner and El Din, 2006
Mesalina balfouri	GD	Sindaco et al. 2011
Mesalina bernoullii	GD	Sindaco and Jeremcenko, 2008
Mesalina brevirostris	GD	Vanhooydonck and Van Damme, 1999
Mesalina guttulata	GD	Vanhooydonck and Van Damme, 1999
Mesalina kuri	GD	Sindaco et al. 2011b
Mesalina martini	GD	Baha el Din et al.2021

Mesalina microlepis	GD	Hraoui-Bloquet et al. 2002
Mesalina olivieri	GD	Wilms et al. 2018
Mesalina pasteuri	GD	Pizzigalli et al. 2021
Mesalina rubropunctata	GD	Wilms et al.2021
Mesalina saudiarabica	GD	Šmíd et al. 2017
Mesalina simoni	GD	Slimani et al. 2006
Mesalina watsonana	GD	Ananjeva et al. 2021
Nucras boulengeri	GD	Van der Meer, 2010
Nucras intertexta	GD	Bates et al. 2014
Nucras lalandii	GD	Bates et al. 2014
Nucras livida	GD	Bates et al. 2014
Nucras taeniolata	GD	Bates et al. 2014
Nucras tessellata	GD	Bates et al. 2014
Omanosaura cyanura	CL	Van Der Kooij, 2000
Omanosaura jayakari	GD	Van Der Kooij, 2000
Ophisops beddomei	GD	Srinivasulu, 2014
Ophisops elegans	GD	Speybroeck, 2016
Ophisops jerdonii	GD	Srinivasulu, 2021
Ophisops leschenaultii	CL	Ukuwela, 2021
Ophisops microlepis	GD	Vyas, 2021
Ophisops nictans	GD	Agarwal and Ramakrishnan, 2017
Ophisops occidentalis	GD	Nouira et al. 2006
Parvilacerta fraasii	GD	Hraoui-Bloquet et al.2006
Parvilacerta parva	GD	Sahin and Kuyucu 2021
Pedioplanis burchelli	GD	Bates et al. 2014
Pedioplanis gaerdesi	GD	Becker and Bauer, 2020
Pedioplanis inornata	GD	Bates et al. 2014
Pedioplanis laticeps	GD	Bates et al. 2014
Pedioplanis lineoocellata	GD	Bates et al. 2014
Pedioplanis namaquensis	GD	Bates et al. 2014
Pedioplanis undata	GD	Orriols 2011

Philochortus spinalis	GD	Orriols 2011
Phoenicolacerta cyanisparsa	GD	Tok et al. 2009e
Phoenicolacerta kulzeri	CL	Disi, 2006
Phoenicolacerta laevis	GD	Orriols 2011
Phoenicolacerta troodica	GD	Crochet 2009
Podarcis bocagei	GD	Speybroeck, 2016
Podarcis carbonelli	GD	Speybroeck, 2016
Podarcis cretensis	CL	Speybroeck, 2016
Podarcis erhardii	CL	Vanhooydonck and Van Damme, 1999
Podarcis filfolensis	CL	Vanhooydonck and Van Damme, 1999
Podarcis gaigeae	GD	Speybroeck, 2016
Podarcis guadarramae	CL	Speybroeck, 2016
Podarcis hispanicus	CL	Diego-Rasilla, 2003
Podarcis ionicus	GD	Psonis et al. 2018
Podarcis lilfordi	GD	Speybroeck, 2016
Podarcis liolepis	GD	Speybroeck, 2016
Podarcis melisellensis	GD	Speybroeck, 2016
Podarcis milensis	GD	Speybroeck, 2016
Podarcis muralis	CL	Vanhooydonck and Van Damme, 1999
Podarcis peloponnesiacus	GD	Mayer and Beyerlein, 1999
Podarcis pityusensis	GD	Speybroeck, 2016
Podarcis raffonei	GD	Speybroeck, 2016
Podarcis siculus	GD	Mayer and Beyerlein, 1999
Podarcis tauricus	GD	Mayer and Beyerlein, 1999
Podarcis tiliguerta	CL	Vanhooydonck and Van Damme, 1999
Podarcis vaucheri	CL	Kaliontzopoulou et al. 2015
Podarcis virescens	CL	Caeiro-Dias, 2021
Podarcis waglerianus	GD	Speybroeck, 2016
Poromera fordii	CL	Orriols 2011
Psammodromus algirus	GD	Speybroeck, 2016
Psammodromus blanci	GD	Orriols 2011

Psammodromus edwarsianus	GD	Speybroeck, 2016
Psammodromus hispanicus	GD	Speybroeck, 2016
Psammodromus microdactylus	GD	Orriols 2011
Psammodromus occidentalis	GD	Speybroeck, 2016
Pseuderemias smithii	GD	Orriols 2011
Scelarcis perspicillata	CL	S'khifa et al. 2020
Takydromus amurensis	GD	Orlova et al.2021
Takydromus dorsalis	CL	Kidera and Ota, 2017a
Takydromus formosanus	CL	Norval., et al. 2016
Takydromus hsuehshanensis	GD	Huang et al.2014
Takydromus intermedius	GD	Cai and Wang 2019
Takydromus luyeanus	CL	Lue and Lin, 2008
Takydromus sauteri	CL	Huang, 2006
Takydromus septentrionalis	GD	Wang et al. 2019
Takydromus sexlineatus	GD	Vanhooydonck and Van Damme, 1999
Takydromus smaragdinus	CL	Kidera and Ota, 2017b
Takydromus stejnegeri	GD	Lue and Lin, 2008
Takydromus sylvaticus	CL	Sheng Tang, 2007
Takydromus tachydromoides	CL	Kidera and Ota, 2017c
Takydromus toyamai	CL	Kidera and Ota, 2017d
Takydromus viridipunctatus	CL	Lue and Lin, 2008
Takydromus wolteri	CL	Kyo-Sung and Hong-Shik, 2013
Teira dugesii	CL	Rocha et al. 2020
Timon kurdistanicus	GD	Ilgaz and Kumlutas, 2008
Timon lepidus	GD	Speybroeck, 2016
Timon nevadensis	GD	Speybroeck, 2016
Timon pater	GD	Vanhooydonck and Van Damme, 1999
Timon princeps	GD	Tok et al. 2009f
Timon tangitanus	GD	Mateo Miras et al. 2009
Tropidosaura cottrelli	GD	Bates et al. 2014
Tropidosaura essexi	GD	Bates et al. 2014

Tropidosaura gularis	GD	Bates et al. 2014
Tropidosaura montana	GD	Bates et al. 2014
Vhembelacerta rupicola	CL	Bates et al. 2014
Zootoca vivipara	GD	Vanhooydonck and Van Damme, 1999

References from habitat use categorization

Agarwal I, Ramakrishnan U. 2017 A phylogeny of open-habitat lizards (Squamata: Lacertidae: *Ophisops*) supports the antiquity of Indian grassy biomes. J. Biogeogr. 44, 2021-2032.

Ahmadzadeh F, Flecks M, Carretero MA, Mozaffari O, Böhme W, Harris, DJ, Freitas S, Rödder D. 2013 Cryptic Speciation Patterns in Iranian Rock Lizards Uncovered by Integrative Taxonomy. Plos One 8(12): e80563. https://doi.org/10.1371/journal.pone.0080563

Ahmadzadeh F, Kiabi BH, Kami HG, Hojjatt V. 2008 A preliminary study of the lizard fauna and their habitats in northwestern Iran. AHR. 11, 1-9.

Al-Sadoon MK, Paray BA, Al-Otaibi HS. 2016 Survey of the reptilian fauna of the Kingdom of Saudi Arabia. V. The lizard fauna of Turaif region. Saudi J. Biol. Sci. 23, 642-648.

Amr ZSS, Al Johany AMH, Disi AM. 2012 *Acanthodactylus robustus*. The IUCN Red List of Threatened Species 2012: e.T164724A1070603. http://dx.doi.org/10.2305/IUCN.UK.2012.RLTS.T164724A1070603.en

Ananjeva NB, Orlov NL, Papenfuss T, Shadei Bafti S, Chirikova M, Orlova V, Nazarov R, Rustamov A, Shi L, Guo X. 2019. *Eremias grammica*. The IUCN Red List of Threatened Species 2019: e.T164660A127944769. http://dx.doi.org/10.2305/IUCN.UK.2019-3.RLTS.T164660A127944769.en

Ananjeva NB, Orlov NL, Papenfuss T, Shafiei Bafti S, Nilson G, Nazarov R, Rustamov A. *Mesalina watsonana*. The IUCN Red List of Threatened Species

2021: e.T164677A1066663. https://dx.doi.org/10.2305/IUCN.UK.20213.RLTS.T164677A1066663.en

Baha El Din S, Sindaco R, Spawls S. 2021 *Mesalina martini*. The IUCN Red List of Threatened Species 2021: e.T198383A2522875. https://dx.doi.org/10.2305/IUCN.UK.2021-1.RLTS.T198383A2522875.en

Baha El Din SM. 2007 A new lizard of the *Acanthodactylus scutellatus* group (Squamata: Lacertidae) from Egypt. Zool. Middle East **40-1**, 21-32.

Bahmani Z, Rastegar-Pouyani N, Gharzi A. 2011 A new record of *Eremias montanus* Rastegar-Pouyani & Rastegar-Pouyani, 2001 (Sauria: Lacertidae) from Kurdistan Province, Western Iran. ARC. 5, 11-14.

Baptista N, Bauer AM, Becker F, Conradie W. 2020 *Meroles anchietae*. The IUCN Red List of Threatened Species 2020: e.T196981A110221608. https://dx.doi.org/10.2305/IUCN.UK.2020-3.RLTS.T196981A110221608.en

Howell K, Msuya CA, Ngalason W, Niagate B, Wagner P, Wilms T, Al Jumaily MM, Sindaco R, Baha El Din S. 2021 *Latastia longicaudata*. The IUCN Red List of Threatened Species 2021: e.T197494A2490375. https://dx.doi.org/10.2305/IUCN.UK.2021-1.RLTS.T197494A2490375.en

Baran I, Kumlutas Y, Lanza B, Sindaco R, Ilgaz C, Avci A, Crucitti P. 2005 *Acanthodactylus harranensis*, a new species of lizard from southeastern Turkey (Reptilia: Sauria: Lacertidae). Boll. Mus. reg. Sci. nat. Torino. 23, 323-341.

Bates MF, Branch WR, Bauer AM, Burger M, Marais J, Alexander GJ, De Villiers MS. (eds). 2014 Atlas and Red List of the Reptiles of South Africa, Lesotho and Swaziland. Suricata 1. South African National Biodiversity Institute, Pretoria.

Bauer AM, Becker F. 2020 *Meroles micropholidotus*. The IUCN Red List of Threatened Species 2020: e.T110221695A110221717. https://dx.doi.org/10.2305/IUCN.UK.2020-3.RLTS.T110221695A110221717.en

Becker F, Bauer AM. 2020 *Pedioplanis gaerdesi*. The IUCN Red List of Threatened Species 2020: e.T178213A120594881. https://dx.doi.org/10.2305/IUCN.UK.2020-3.RLTS.T178213A120594881.en

Bi J, Wang Y, Li S, Zeng Z. 2015 Is habitat preference associated with locomotor performance in Multiocellated Racerunners (*Eremias multiocellata*) from a desert steppe? AHR. 6, 143-149.

Böhme W, Lymberakis P, Ajtic R, Haxhiu I, Isailovic JC, Sindaco R. 2009a *Algyroides nigropunctatus*. The IUCN Red List of Threatened Species 2009: e.T61466A12490013.http://dx.doi.org/10.2305/IUCN.UK.2009.RLTS.T61466A12490013.en

Böhme W, Lymberakis P, Tok V, Ugurtas IH, Sevinç M, Chrochet PA, Kaska Y, Kumlutas Y, Ugur K, Avci A, Üzüm N, Yeniyurt C, Akarsu F, Lumberakis P. 2009c *Anatololacerta oertzeni*. The IUCN Red List of Threatened Species 2009: e.T61527A12504829. http://dx.doi.org/10.2305/IUCN.UK.2009.RLTS.T61527A12504829.en

Böhme W, Lymberakis P. 2009 *Hellenolacerta graeca*. The IUCN Red List of Threatened Species 2009: e.T61523A12502676. http://dx.doi.org/10.2305/IUCN.UK.2009.RLTS.T61523A12502676.en

Böhme W, Lymberakis P. 2009b *Algyroides moreoticus*. The IUCN Red List of Threatened Species 2009: e.T61465A12489765. http://dx.doi.org/10.2305/IUCN.UK.2009.RLTS.T61465A12489765.en

Branch WR, Rödel MO, Segniagbeto G, Penner J. 2013 *Acanthodactylus boueti*. The IUCN Red List of Threatened Species 2013: e.T13151858A13151861. http://dx.doi.org/10.2305/IUCN.UK.2013-1.RLTS.T13151858A13151861.en

Caeiro-Dias G. 2021 Arboreal behaviour in a population of Geniez's wall lizard *Podarcis virescens*. The Herpetological Bulletin. 158, 42-43.

Cai B, Wang Y. 2019 *Takydromus intermedius*. The IUCN Red List of Threatened Species 2019: e.T102342208A102342210. http://dx.doi.org/10.2305/IUCN.UK.2019-2.RLTS.T102342208A102342210.en

Carranza S, Els J, Burriel-Carranza B. 2023 *Acanthodactylus masirae*. The IUCN Red List of Threatened Species 2023: e.T199608A214909008. https://dx.doi.org/10.2305/IUCN.UK.2023-1.RLTS.T199608A214909008.en

Chirio L. 2021 *Acanthodactylus guineensis*. The IUCN Red List of Threatened Species 2021: e.T13151869A13151872. https://dx.doi.org/10.2305/IUCN.UK.2021 2.RLTS.T13151869A13151872.en

Crnobrnja Isailovic J, Vogrin M, Corti C, Pérez-Mellado V, Sá-Sousa P, Cheylan M, Pleguezuelos J, Nettmann HK, Sterijovski B, Lymberakis P, Podloucky R, Cogalniceanu D, Avci A. 2009 *Lacerta viridis*. The IUCN Red List of Threatened Species 2009:e.T61530A12507156. http://dx.doi.org/10.2305/IUCN.UK.2009.RLTS.T61530A12507156.en

Crochet PA, Geniez P, Ineich I. 2003 A multivariate analysis of the fringe-toed lizards of the *Acanthodactylus scutellatus* group (Squamata: Lacertidae): systematic and biogeographical implications. Zool. J. Linn. Soc. 137, 117-155.

Crochet P-A, Lymberakis P, Hraoui-Bloquet S, Sadek R, Werner YL, Tok V, Ugurtas IH, Sevinç M, Kaska Y, Kumlutas Y, Kaya U, Avci A, Üzüm N, Yeniyurt C, Akarsu F. 2009 *Phoenicolacerta laevis*. The IUCN Red List of Threatened Species 2009: e.T164570A86642956. http://dx.doi.org/10.2305/IUCN.UK.2009.RLTS.T164570A5908737.en

Diego-Rasilla FJ, Pérez-Mellado V. 2003 Home range and habitat selection by *Podarcis hispanica* (Squamata, Lacertidae) in Western Spain. Folia Zool. 52, 87-89.

Disi AM. 2011 Review of the lizard fauna of Jordan, Zool. Middle East. , 54, 89-102, DOI: 10.1080/09397140.2011.10648900

Disi M, Hraoui-Bloquet S, Sadek R, Werner Y. 2006 *Phoenicolacerta kulzeri*. The IUCN Red List of Threatened Species 2006: e.T61524A12503047. http://dx.doi.org/10.2305/IUCN.UK.2006.RLTS.T61524A12503047.en

Dujsebayeva T, Malakhov BV, Berezovikov NN, Guo X, Liu J, Cherednichenko AV. 2019 Comparative analysis of the distribution and habitats of two *Eremias* species (Reptilia, Lacertidae) using niche-based GIS modeling. Russ. J. Herpetol. 26, 281-304.

Edwards S, Herrel A, Vanhooydonck B, Measey GJ, Tolley K. 2016 Diving in head first: trade-offs between phenotypic traits and sand-diving predator escape strategy in *Meroles* desert lizards. Biol. J. Linn. Soc. 119, 919-931.

Farashi A, Alizadeh-Noughani M. 2019 Conservation of Pleske's racerunner (*Eremias pleskei*) in a changing climate. Ann. Zool. Fennici. 56, 93-106.

Geniez P, Foucart A. 1995 Un nouvel Acanthodactyle en Algérie: *Acanthodactylus taghitensis* n. sp. (Reptilia, Sauria, Lacertidae). Bull. Mus. natl. Hist, nat. 17, 3-9.

Geniez P, Miras JAM. 2006 *Acanthodactylus bedriagai*. The IUCN Red List of Threatened Species 2006: e.T61453A12488579. http://dx.doi.org/10.2305/IUCN.UK.2006.RLTS.T61453A12488579.en

Geniez P, Miras M, Joger JA, Pleguezuelos J, Slimani T, El Mouden EH. 2010 *Acanthodactylus busacki*. The IUCN Red List of Threatened Species 2010: e.T178569A7572735.http://dx.doi.org/10.2305/IUCN.UK.20104.RLTS.T178569A757735.en

Greenbaum E, Villanueva CO, Kusamba C, Aristote MM, Branch WR. 2011 A molecular phylogeny of Equatorial African Lacertidae, with the description of a new genus and species from eastern Democratic Republic of the Congo. 163, 913-942.

Hatami K, Sayyadi F, Parto P, Yousefand N, Rastegar-Pouyani N. 2014 Evaluating the Size of Erythrocytes in the Blood of *Acanthodactylus nilsoni* (Sauria: Lacertidae) from Iran. WJZ. 9, 80-85.

Heidari N, Pouyani N, Rastegar-Pouyani E, Rajabizadeh M. 2013 A new species of *Acanthodactylus* Fitzinger 1834 (Sauria: Lacertidae) from southern Iran. Zootaxa 3722, 333-346.

Hosseinian Yousefkhani SS, Rastergar Pouyani E. 2013 Severe conditions on *Eremias intermedia* (STRAUCH, 1876) and *Eremias lineolata* (NIKOLSKY, 1896) (Sauria: Lacertidae) in Sarakhs, Northeastern Iran - L@CERTIDAE (Eidechsen Online), 2013 [3]: 17-20.

Hraoui-Bloquet S, Sadek R, Werner Y, Lymberakis P, Tok V, Ugurtas IH, Sevinç M, Böhme W, Kaska Y, Kumlutas Y, Kaya U, Avci A, Üzüm N, Yeniyurt C, Akarsu F. 2009 *Acanthodactylus schreiberi*. The IUCN Red List of Threatened Species 2009: e.T61462A12489118.http://dx.doi.org/10.2305/IUCN.UK.2009.RLTS.T61462A12489118.en

Hraoui-Bloquet S, Sadek RA, Sindaco R, Venchi A. 2002 The herpetofauna of Lebanon: new data on distribution. Zool. Middle East. 27, 35-46

Hraoui-Bloquet S, Sadez R. 2006 Parvilacerta fraasii. The IUCN Red List of Threatened Species 2006: e.T61522A12502475. http://dx.doi.org/10.2305/IUCN.UK.2006.RLTS.T61522A12502475.en

Huang S-P, Porter WP, Tu M-C, Chiou C-R. 2014 Forest cover reduces thermally suitable habitats and affects responses to a warmer climate predicted in a high-elevation lizard. Oecologia. DOI 10.1007/s00442-014-2882-1

Huang W-S. 2006a Ecology and Reproductive Patterns of the Grass Lizard, *Takydromus sauteri*, in a Tropical Rain Forest of an East. J. Herpetol. 40, 267-273.

Ilgaz Ç, Kumlutas Y. 2008 The Morphology and Distribution of *Timon princeps* (Blanford 1874) (Sauria: Lacertidae) in Southeastern Anatolia, Turkey. The North-west. J. Zool. 4, 247-262.

Joger U, Slimani T, El Mouden H, Geniez P. 2006. *Mesalina simonii*. The IUCN Red List of Threatened Species 2006: e.T61535A12509619. http://dx.doi.org/10.2305/IUCN.UK.2006.RLTS.T61535A12509619.en

Karamiani R, Dabid S, Rastegar-Pouyani N. 2015 Sexual dimorphism of the Yassujian lizard, *Apathya yassujica* (Nilson et al. 2003) (Sauria: Lacertidae) from Iran. ARC. 9, 42-48.

Kidera N, Ota H. 2017a *Takydromus dorsalis*. The IUCN Red List of Threatened Species 2017: e.T96265980A96266039. http://dx.doi.org/10.2305/IUCN.UK.2017-3.RLTS.T96265980A96266039.en

Kidera N, Ota H. 2017b *Takydromus smaragdinus*. The IUCN Red List of Threatened Species 2017: e.T96266149A96266154. http://dx.doi.org/10.2305/IUCN.UK.2017-3.RLTS.T96266149A96266154.en

Kidera N, Ota H. 2017c *Takydromus tachydromoides*. The IUCN Red List of Threatened Species 2017: e.T96266178A96266321. http://dx.doi.org/10.2305/IUCN.UK.2017-3.RLTS.T96266178A96266321.en

Kidera N, Ota H. 2017d *Takydromus toyamai*. The IUCN Red List of Threatened Species 2017: e.T178488A96878070. http://dx.doi.org/10.2305/IUCN.UK.2017-3.RLTS.T178488A96878070.en

Kim IH, Ra NY, Park D. 2012 Habitat Use, Home Range, and Hibernaculum of the Mongolian Racerunner, *Eremias argus* (Lacertidae, Reptilia) in a Coastal Sand Dune in South Korea. AHR. 3, 133-140.

Kyo-Sung K, Hong-Shik O. 2013 Biological Characteristics of *Takydromus wolteri* (Squamata: Lacertidae) Living on Jeju Island. J. Educ. Res. 10.15564/JERI.2013.11.15.2.13

Ljubisavljevi K, Polovic L, Ikovic V, Vuksanovic S, Vukov TD. 2017 Habitat use of endemic Balkan rock lizards (*Dinarolacerta* spp.). Salamandra. 53, 279-284.

Lue K-L, Lin S-M. 2008 Two new cryptic species of *Takydromus* (Squamata: Lacertidae) from Taiwan. Herpetologica. 64, 379-395.

Mayer W, Beyerlein P. 1999 Ecological niche segregation of seven sympatric lacertid lizards in the Peloponnese highlands. Nat. Croat. 8, 339–344.

Miras JAM, El Mouden EH, Pleguezuelos J, Slimani T, Martínez-Solano I. 2009 *Timon tangitanus*. The IUCN Red List of Threatened Species 2009:e.T61585A12500163.
http://dx.doi.org/10.2305/IUCN.UK.2009.RLTS.T61585A12500163.en

Miras JAM, Pérez-Mellado V, Martínez-Solano I. 2009a *Gallotia intermedia*. The IUCN Red List of Threatened Species 2009: e.T61505A12494026.
http://dx.doi.org/10.2305/IUCN.UK.2009.RLTS.T61505A12494026.en

Miras JAM, Pérez-Mellado V, Martínez-Solano I. 2009b 2009. *Gallotia simonyi*. The IUCN Red List of Threatened Species 2009: e.T8881A12935900.
http://dx.doi.org/10.2305/IUCN.UK.2009.RLTS.T8881A12935900.en

Miras JAM, Pérez-Mellado V, Martínez-Solano I. 2009c *Gallotia stehlini*. The IUCN Red List of Threatened Species 2009: e.T61506A12494509.
http://dx.doi.org/10.2305/IUCN.UK.2009.RLTS.T61506A12494509.en

Mozaffari O, Ahmadzadeh D, Parham JF. 2011 *Eremias papenfussi* sp. nov., a new lacertid lizard (Sauria: Lacertidae) from Tehran Province, Iran. Zootaxa. 3114, 57-62.

Norval G, Mao J-J, Goldberg S, Huang S-C. 2016 Additional notes on the reproduction of the Formosan Grass Lizard, *Takydromus formasanus* (Boulenger

1894) (Squamata: Lacertidae), from Southwestern Taiwan. IRCF Reptiles and Amphibians. 23, 28-31.

Nouira MS, Joger U. 2006 *Acanthodactylus blanci*. The IUCN Red List of Threatened Species 2006: e.T61455A12488766. http://dx.doi.org/10.2305/IUCN.UK.2006.RLTS.T61455A12488766.en

Orlova V, Milto K, Borkin L, Zhao W, Shin Y. 2021 *Takydromus amurensis*. The IUCN Red List of Threatened Species 2021: e.T47755997A47756006. https://dx.doi.org/10.2305/IUCN.UK.2021-2.RLTS.T47755997A47756006.en

Orlova V, Terbish K, Wang Y, Guo X, Shi L, Bi J. 2019 *Eremias przewalskii*. The IUCN Red List of Threatened Species 2019: e.T47755920A47755929. http://dx.doi.org/10.2305/IUCN.UK.2019-2.RLTS.T47755920A47755929.en

Orriols FA. 2011 Preliminary analysis of correlated evolution of morphology and ecological diversification in lacertid lizards. Butll. Soc. Cat. Herp. 19. 29-48.

Pleguezuelos JM, Márquez R, Lizana M (eds.) 2002 Atlas y Libro Rojo de los Anfibios y Reptiles de España. Dirección General de Conservación de la Naturaleza-Asociación Herpetológica Española (2ª impresión), Madrid, 587 pp.

Psonis N, Antoniou A, Kukushkin O, Jabblonski D, Petrov B, Crnobrnja-Isailovic J, Sotiropoulos K, Gherghel I, Lymberakis P, Poulakakis N. 2018 Hidden diversity in the *Podarcis tauricus* (Sauria, Lacertidae) species subgroup in the light of multilocus phylogeny and species delimitation. Mol. Phylogenet. Evol. 106, 6-17

Rastegar-Pouyani E, Avci A, Kumlutas Y, Igaz Ç, Hosseinian-Yousefkhani SS. 2013 New country record and range extension of *Eremias suphani* Başoğlu & Hellmich, 1968 from Iran. Amphibian & Reptile Conservation. 6, 35-39.

Rezazadeh E, Hassanzadeh-Kiabi B, Ahmadzadeh F. 2010 Contribution to the knowledge of *Iranolacerta brandtii* de filippi 1863 (Sauria: Lacertidae) from the northwest of Iran. Russ. J. Herpetol. 17, 223-230.

Rocha R. Borgues P, Cardoso P, Kusrini MD, Martín-Esquivel JL, Menezes D, Mota-Ferreira M, Nunes S, Serra-Gonçalves C, Sim-Sim M, Sepúlveda P, Teixeira D, Traveset A. 2020 Stone-stacking as a looming threat to rock-dwelling biodiversity. HWC. 14, 129-134.

Rödel MO, Penner J, Wagner P. 2021 *Holaspis guentheri*. The IUCN Red List of Threatened Species 2021: e.T13151944A13151949. https://dx.doi.org/10.2305/IUCN.UK.2021-2.RLTS.T13151944A13151949.en

S'khifa A, Koziel G, Vences M, Carretero MA, Slimani T. 2020 Ecophysiology of a lacertid community in the high Moroccan mountains suggests conservation guidelines. J. Therm. Biol. 94, 102743.

Sahin MK, Kuyucu AC. 2021 Thermal biology of two sympatric Lacertids lizards (*Lacerta diplochondrodes* and *Parvilacerta parva*) from Western Anatolia. J. Therm. Biol. doi: 10.1016/j.jtherbio.2021.103094

Sillero N, Corti C, Carretero MA. 2016 Home ranges of parthenogenetic and bisexual species in a community of *Darevskia* lizards (Reptilia: Lacertidae). Zool Middle East. 62, 306-318.

Sindaco R, Anderson S, Busais SMS, Jumaily MM. 2012 *Acanthodactylus arabicus*. The IUCN Red List of Threatened Species 2012: e.T177908A1499691. http://dx.doi.org/10.2305/IUCN.UK.2012.RLTS.T177908A1499691.en

Sindaco R, Grieco C, Riservato E. 2011 *Mesalina balfouri*. The IUCN Red List of Threatened Species 2011: e.T199739A9124462. http://dx.doi.org/10.2305/IUCN.UK.2011-2.RLTS.T199739A9124462.en

Sindaco R, Grieco C, Riservato E. 2011b *Mesalina kuri*. The IUCN Red List of Threatened Species 2011: e.T199740A9124581. http://dx.doi.org/10.2305/IUCN.UK.2011-2.RLTS.T199740A9124581.en

Sindaco R, Jeremcenko VK. 2008 The reptiles of the Western Palearctic. Edizioni Belvedere, Latina (Italy), 579 pp

Šmíd J, Moravec J, Gvoždík V, Štundl J, Frynta D, Lymberakis P, Kaptli P, Wilms T, Schmitz A, Shobrak M, Yousefkhan SH, Rastegar-Pouyani E, Castilla A, Els J, Mayer W. 2016 Cutting the Gordian Knot: Phylogenetic and ecological diversification of the Mesalina brevirostris species complex (Squamata, Lacertidae). Zool. Scr. 10.1111/zsc.12254

Spawls S, Malonza P, Beraduccii J. 2021 *Adolfus jacksoni*. The IUCN Red List of Threatened Species 2021: e.T20878000A20878008. https://dx.doi.org/10.2305/IUCN.UK.2021- 2.RLTS.T20878000A20878008.en

Spawls S, Malonza P, Msuya CA, Beraduccii J. 2015 *Gastropholis prasina*. The IUCN Red List of Threatened Species 2015: e.T13151906A13151910. http://dx.doi.org/10.2305/IUCN.UK.2015-2.RLTS.T13151906A13151910.en

Spawls S, Malonza P, Wagner P, Branch WR. 2014 *Adolfus alleni*. The IUCN Red List of Threatened Species 2014: e.T60755628A45791802. http://dx.doi.org/10.2305/IUCN.UK.2014-3.RLTS.T60755628A45791802.en

Speybroeck J, Beukema W, Bok B, Van Der Voort J, Velikov I. 2016 Field Guide to the Amphibians and Reptiles of Britain and Europe. (British Wildlife Publishing Field Guides).

Srinivasulu B, Srinivasili C, Vijayakumar SP, Ganesan SR, Ramesh M. 2014 *Ophisops beddomei*. The IUCN Red List of Threatened Species 2014: e.T172618A1353104. http://dx.doi.org/10.2305/IUCN.UK.2014-1.RLTS.T172618A1353104.en

Srinivasulu B, Srinivasulu C, Vijayakumar SP, Ganesan SR, Ramsh M, Papenfuss R, Mohapatra P, Sreekar R, Madala M. 2021. *Ophisops jerdonii*. The IUCN Red List of Threatened Species 2021: e.T178461A1535145. https://dx.doi.org/10.2305/IUCN.UK.2021- 3.RLTS.T178461A1535145.en

Tamar K, Geniez P, Brito JC, Crochet PA. 2017 Systematic revision of *Acanthodactylus busacki* (Squamata: Lacertidae) with a description of a new species from Morocco. Zootaxa. 4276, 357- 386.

Tang X-S, Lu S-Q, Chou W-h. 2007 Description of Male *Takydromus sylvaticus* (Squamata: Lacertidae) from China, with notes on sexual dimorphism and a revision of the morphological diagnosis of the species. Zoological science. 24, 496-503.

Tarkhnishvili D, Gabelaia M, Adriaens D. 2020 Phenotypic divergence, convergence and evolution of Caucasian rock lizards (*Darevskia*). Biol. J. Linn. Soc. 130, 142-155.

Terbish K, Orlova V, Chirikova M, Munkhbaatar M, Guo X, Shi L, Bi J. 2019 *Eremias vermiculata*. The IUCN Red List of Threatened Species 2019: e.T47755971A47755978.http://dx.doi.org/10.2305/IUCN.UK.2019-2.RLTS.T47755971A47755978.en

Tok V, Ugurtas I, Sevinç M, Böhme W, Crochet PA. 2009d *Lacerta pamphylica*. The IUCN Red List of Threatened Species 2009: e.T164735A5921481. http://dx.doi.org/10.2305/IUCN.UK.2009.RLTS.T164735A5921481.en

Tok V, Ugurtas I, Sevinç M, Crochet P-A, Kaska Y, Kumlitas Y, Avci A. 2009f *Timon princeps*. The IUCN Red List of Threatened Species 2009:e.T164629A5913265. http://dx.doi.org/10.2305/IUCN.UK.2009.RLTS.T164629A5913265.en

Tok V, Ugurtas I, Sevinç M, Crochet P-A, Kaska Y, Kumlutas Y, Avci A, Sindaco R. 2009e *Phoenicolacerta cyanisparsa*. The IUCN Red List of Threatened Species 2009: e.T61520A12501576. http://dx.doi.org/10.2305/IUCN.UK.2009.RLTS.T61520A12501576.en

Tok V, Ugurtas IH, Sevinç M, Böhme W, Chrochet PA, Kaska Y, Kumlutas Y, Kaya U, Avci A, Üzüm N, Yeniyurt C, Akarsu F, Lymberakis P. 2009a *Anatololacerta anatolica*. The IUCN Red List of Threatened Species 2009: e.T61517A86150780.
http://dx.doi.org/10.2305/IUCN.UK.2009.RLTS.T61517A12499809.en

Tok V, Ugurtas IH, Sevinç M, Böhme W, Crochet PA, Kaska Y, Kumlutas Y, Kaya U, Avci A, Üzüm N, Yeniyurt C, Akarsu F. 2009b *Anatololacerta danfordi*. The IUCN Red List of Threatened Species 2009: e.T164744A86443842. http://dx.doi.org/10.2305/IUCN.UK.2009.RLTS.T164744A5922456.en

Tok V, Ugurtas IH, Sevinç M, Crochet PA, Disi AMM, Anderson S, Kaya U. 2009c *Apathya cappadocica*. The IUCN Red List of Threatened Species 2009: e.T164575A5909166.
http://dx.doi.org/10.2305/IUCN.UK.2009.RLTS.T164575A5909166.en

Tuniyeb B, Ananjeva NB, Agasyan A, Orlov NL, Tuniyeb S, Anderson S. 2009b *Lacerta strigata*. The IUCN Red List of Threatened Species 2009: e.T157287A114558813.http://dx.doi.org/10.2305/IUCN.UK.2009.RLTS.T157287A5070727.en

Tuniyev B, Ananjeva N, Agasyan A, Orlov N, Tuniyev S. 2009a *Darevskia saxicola*. The IUCN Red List of Threatened Species 2009: e.T164617A5912515. http://dx.doi.org/10.2305/IUCN.UK.2009.RLTS.T164617A5912515.en

Uetz P, Freed P, Aguilar R, Reyes F, Kudera J, Hošek J (eds.) (2023) The Reptile Database, http://www.reptile-database.org, accessed [15/02/2024]

Ukuwela K, Kannishka S, Wickramasinghe LJM. 2021. *Ophisops leschenaultii*. The IUCN Red List of Threatened Species 2021: e.T172684A1366580. https://dx.doi.org/10.2305/IUCN.UK.2021-3.RLTS.T172684A1366580.en

Van Damme R, Vanhooydonck B. 2002 Speed versus manoeuvrability: association between vertebral number and habitat structure in lacertid lizards. J. Zool. Lond. 258, 327-334.

Van der Kooij, J. 2000 The herpetofauna of the Sultanate of Oman. Part 2: the geckos. *Podarcis*. 1, 105–120.

Van Der Meer MH, Whiting MJ, Branch WR. 2010 Ecology of Southern African Sandveld Lizards (Lacertidae, Nucras). Copeia. 4, 568-577.

Vanhooydonck B, Van Damme R. 1999 Evolutionary relationships between body shape and habitat use in lacertid lizards. Evol. Ecol. Res. **1**, 785–805.

Vanhooydonck B, Van Damme R. 2003 Relationships between locomotor performance, microhabitat use and antipredator behaviour in lacertid lizards. Func. Ecol. 17, 160-169.

Vyas R, Mohapatra P, Srinivasulu C. 2021. *Ophisops microlepis*. The IUCN Red List of Threatened Species 2021: e.T149404654A123301791. https://dx.doi.org/10.2305/IUCN.UK.2021-3.RLTS.T149404654A123301791.en

Wagner P, Branch WR, Safari I, Chenga I, Malonza PK. 2021 *Holaspis laevis*. The IUCN Red List of Threatened Species 2021: e.T13151955A13151957 https://dx.doi.org/10.2305/IUCN.UK.20212.RLTS.T13151955A13151957.en

Wang T, Ji X, Bi J. 2019 Takydromus septentrionalis. The IUCN Red List of Threatened Species 2019: e.T102342469A102342471. http://dx.doi.org/10.2305/IUCN.UK.2019-2.RLTS.T102342469A102342471.en

Wei-Guo D, Chi-xian L, Lu S, Xiang J. 2005 Morphological correlates of locomotor performance in four species of lizards using different habitats. Zoological research. 26, 41-46.

Werner Y, Disi M, Mousa Disi AM. 2006 *Acanthodactylus beershebensis*. The IUCN Red List of Threatened Species 2006: e.T61454A12488658. http://dx.doi.org/10.2305/IUCN.UK.2006.RLTS.T61454A12488658.en

Werner Y, El Din SB. 2006 *Mesalina bahaeldini*. The IUCN Red List of Threatened Species 2006: e.T61534A12509520. http://dx.doi.org/10.2305/IUCN.UK.2006.RLTS.T61534A12509520.en

Wilms T, Aloufi AAH, Al Johany AMH, Els J. 2012 *Mesalina adramitana*. The IUCN Red List of Threatened Species 2012: e.T199611A2606621. http://dx.doi.org/10.2305/IUCN.UK.2012.RLTS.T199611A2606621.en

Wilms T, Wagner P, Niagate B, Al Johany AMH, Amr ZSS, Baha El Din S, Disi AM, Böhme W. 2018 *Mesalina olivieri*. The IUCN Red List of Threatened Species 2018: e.T164667A1065571.http://dx.doi.org/10.2305/IUCN.UK.20182.RLTS.T164667A1065571.en

Yousefkhani SSH, Nabizadeh H, Grismer LL. 2022 Ecomorphological differences among forest and rock dwelling species of *Darevskia* Arribas, 1999 (Squamata, Lacertide) in the Elburz Mountains, Iran. Herpetozoa. 35, 245–256.

Table S4.3. Transition matrices for the two fitted models: Equal Rates (ER) and All Rates Different (ARD), in the stochastic character mapping reconstruction. Values are shown in pairs. Mean root node prior probabilities also shown.

Equal Rates (ER)

	Climbers	Ground-dwellers
Climbers	- 0.009	0.009
Ground-dwellers	0.009	- 0.009
Root node prob	0.500	0.500

All Rates Different (ARD)

	Climbers	Ground-dwellers
Climbers	- 0.023	0.023
Ground-dwellers	0.002	- 0.002
Root node prob	0.500	0.500

Table S4.4. Model comparison results for the ancestral state reconstruction using Stochastic character maps, using two models of evolution: Equal rates (EQ) and All Rates Different (ARD). Loglikelihood, Akaike information criterion, and Akaike weights included.

Model:	Equal Rates (EQ)	All Rates Different (ARD)
LogL	-108.484	-95.739
AIC	218.968	203.479
Akaike weights	4.329E-04	9.995E-01

Table S4.5. Phylogenetic signal of morphological traits. **λ** corresponds to Pagel's λ. Significant p-values (at α = 0.05) are highlighted in bold.

	λ	p - val	λ ≠1 (p - val)
Head length	*0.705*	**0.000**	**0.000**
Head width	*0.850*	**0.000**	**0.000**
Head height	*0.870*	**0.000**	**0.000**
Mouth length	*0.953*	**0.000**	**0.000**
Fore-limb length	*0.899*	**0.000**	**0.000**
Hind-limb length	0.988	**0.000**	0.439
Trunk	*0.815*	**0.000**	**0.000**

Table S4.6. Percentage of variance explained by the principal components of the PCA performed with the morphological traits of the head (top) and the PCA performed with the limbs and trunk lengths (bottom), and their correlations with size-corrected morphological traits.

(a) Head PCA	PC1	PC2	PC3	PC4
% of variance explained	55.99	18.76	16.01	9.23
Head length	0.485	-0.472	-0.626	0.387
Head width	0.552	0.330	-0.265	-0.718
Head height	0.503	0.598	0.282	0.557
Mouth length	0.456	-0.557	0.677	-0.156

(b) Limbs and trunk PCA	PC1	PC2	PC3

% of variance explained	69.46	19.74	10.79
Forelimb length	0.828	-0.462	0.317
Hindlimb length	0.891	-0.099	-0.441
Trunk	-0.776	-0.607	-0.169

Table S4.7. Results for the comparison of morphological disparity between habitat types for the two functional blocks of traits. Variance for climbers and for ground-dweller species and the absolute difference between groups are shown.

Head (a)

	Procrustes variance	Absolute difference	p-val
Climbers	0.057	0.005	0. 708
Ground-dwellers	0.051		

Limbs and trunk (b)

	Procrustes variance	Absolute difference	p-val
Climbers	0.024	0.010	0.142
Ground-dwellers	0.035		

Table S4.8. Results of the phylogenetic MANOVAs using the morphological traits of each functional block. For head shape we used: head length, head width, head height and mouth length. For limbs and trunk: fore-limb length, hind-limb length and trunk. d.f: degrees of freedom; Z: Z-score. P-values are based on 1000 residual permutations and significant p-values (at $\alpha = 0.05$) are shown in bold.

		d.f	Pillai	Z	p-val
Head	Habitat	1	0.162	3.780	**0.001**
	Residuals	184			
Limbs and trunk	Habitat	1	0.0470	1.359	0.089
	Residuals	184			

Table S4.9. Transitions reconstructed between habitat use categories under the All Rates Different (ARD) evolutionary model. The direction of the transition is shown as: row -> column (e.g. climber -> ground dwelling in the first row). Mean total time spent in each state is also shown in total and in proportional time.

Transitions

	Ground-dwelling	climbing
Climbers	38.392	-
Ground-dwelling	-	6.288

Mean total time

	Total	Proportional
Climbers	1646.385	0.366
Ground-dwelling	2848.325	0.633

Table S4.10. Comparison of average model fits all morphological variables. The best model is highlighted in bold letters. See Material and Methods for further information about the evolutionary models.

Trait	Model	Likelihood	AICc	ΔAICc	AICc weight
Head length	BM1	97.454	-190.842	90.371	2.34E-20
	OU1	139.319	-272.506	8.707	1.26E-02
	BMS	122.176	-238.220	43.317	4.53E-10
	OUM	139.422	-270.622	10.599	4.93E-03
	OUMV	**145.773**	**-281.213**	**0.000**	**9.82E-01**
Head width	BM1	181.701	-359.336	19.080	4.03E-05
	OU1	191.116	-376.099	2.317	1.76E-01
	BMS	182.589	-359.047	19.373	3.49E-05
	OUM	**193.295**	**-378.369**	**0.015**	**5.47E-01**
	OUMV	193.671	-377.008	1.408	2.77E-01

Head height	BM1	134.046	-264.027	41.121	2.13E-09
	OU1	140.185	-274.239	30.910	3.51E-07
	BMS	136.429	-266.726	38.369	8.20E-09
	OUM	**155.629**	**-303.037**	**2.502**	**6.30E-01**
	OUMV	156.155	-301.977	3.172	3.70E-01
Mouth length	**BM1**	**190.787**	**-377.509**	**0.231**	**2.80E-01**
	OU1	191.932	-377.732	0.008	3.13E-01
	BMS	191.378	-376.624	1.116	1.80E-01
	OUM	192.082	-375.943	1.797	1.28E-01
	OUMV	192.894	-375.454	2.285	1.00E-01
Fore-limb length	BM1	209.286	-414.507	6.976	1.62E-02
	OU1	**213.718**	**-421.304**	**0.179**	**4.84E-01**
	BMS	209.458	-412.784	8.699	6.83E-03
	OUM	214.444	-420.666	0.817	3.52E-01
	OUMV	214.587	-418.841	2.642	1.41E-01
Hind-limb length	**BM1**	**156.850**	**-309.635**	**0.041**	**4.35E-01**
	OU1	156.852	-307.573	2.103	1.55E-01
	BMS	157.344	-308.555	1.114	2.53E-01
	OUM	157.426	-306.630	3.037	9.68E-02
	OUMV	158.000	-305.667	4.009	5.98E-02
Trunk	BM1	235.720	-467.374	16.810	1.43E-04
	OU1	**245.158**	**-484.184**	**0.000**	**6.38E-01**
	BMS	235.753	-465.374	18.810	5.25E-05
	OUM	245.320	-482.420	1.764	2.64E-01
	OUMV	245.387	-480.441	3.743	9.81E-02

Table S4.11. Convergence results (Ct1-4) from the convevol analyses for ground-dwelling (a) and climbing species (b). Significant values based on *50-* simulations are highlighted in bold letter (at α = 0.05).

Trait	Ct1	p-val	Ct2	p-val	Ct3	p-val	Ct4	p-val
Ground-dwelling (a)								
Head length	-0.072	0.64	-0.002	0.66	0.006	0.38	-0.001	0.48
Head width	-0.189	1.00	-0.009	1.00	-0.035	0.98	-0.002	0.94
Head height	-3.416e-03	0.28	7.463e-03	0.10	2.469e-02	0.08	1.611e-05	0.08
Mouth length	-0.071	0.58	-0.005	0.84	-0.013	0.72	-0.001	0.52
All head	-0.175	0.96	-0.036	1.00	-0.049	0.70	-0.002	0.14
Fore-limb length	-0.205	0.98	-0.008	1.00	-0.039	1.00	-0.003	0.98
Hind-limb length	-0.212	0.98	-0.011	-0.011	-0.040	1.00	1.00	0.94
Trunk	-0.094	0.78	-0.010	0.98	-0.023	0.94	-0.004	1.00
All locomotor	-0.221	1.00	-0.033	1.00	-0.064	1.00	-0.004	1.00
Climbing (b)								
Head length	-0.580	0.96	-0.023	0.82	-0.103	0.88	-0.003	0.68
Head width	-0.224	0.72	-0.001	0.36	-0.022	0.54	-0.001	0.38
Head height	-0.040	0.34	-0.008	0.54	-0.015	0.50	-0.001	0.44
Mouth length	-0.203	0.64	-0.012	0.68	-0.034	0.56	-0.002	0.58
All head	-0.268	0.68	-0.051	0.82	0.076	0.60	-0.003	0.34
Fore-limb length	-0.517	0.96	-0.035	1.00	-0.13	1.00	-0.007	1.00
Hind-limb length	-0.128	0.56	-0.015	0.70	-0.029	0.54	-0.003	0.64
Trunk	-0.639	0.96	-0.013	0.84	-0.085	0.90	-0.003	0.76

All locomotor	-0.270	0.68	-0.044	0.86	-0.083	0.80	-0.004	0.80

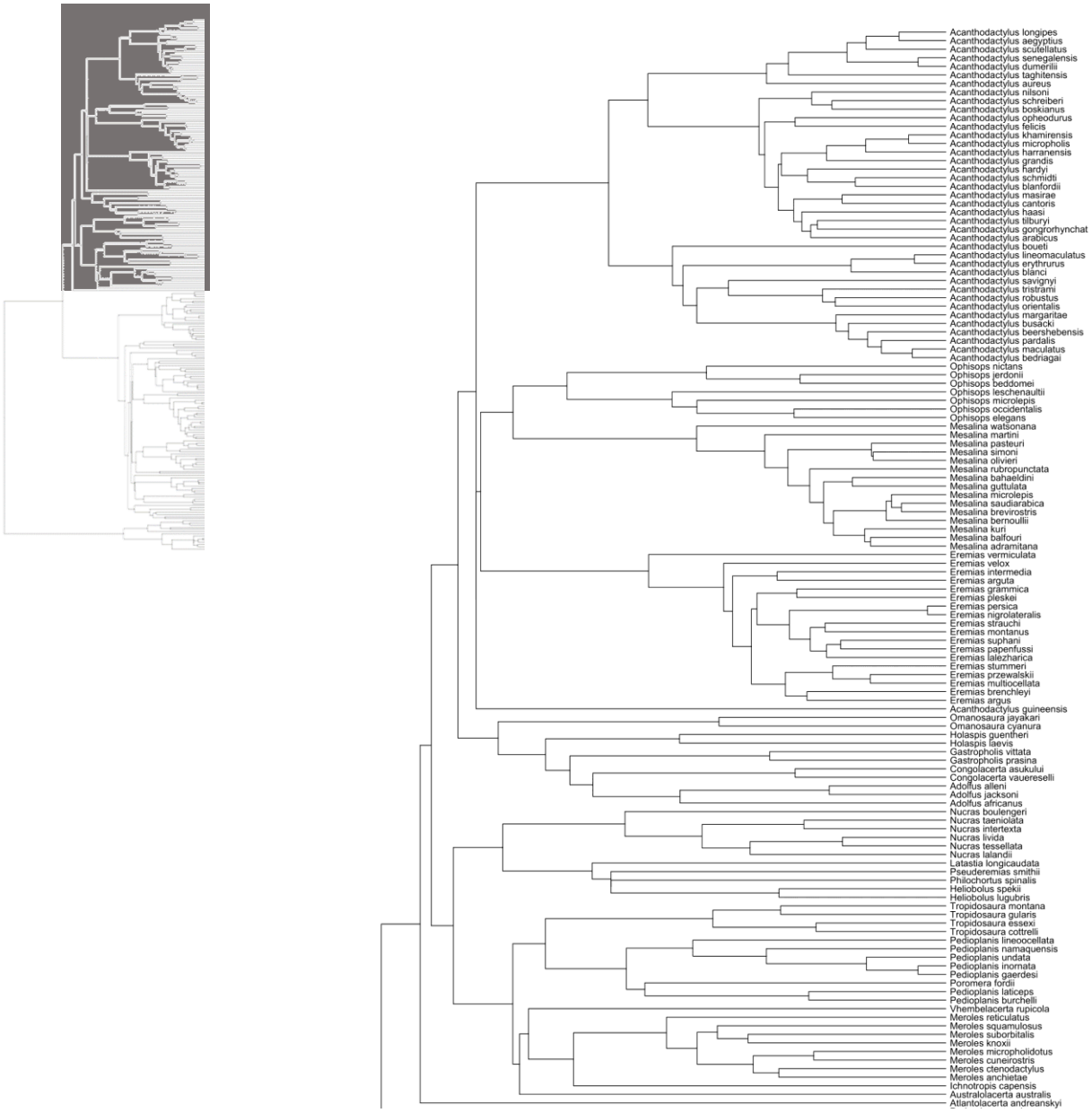

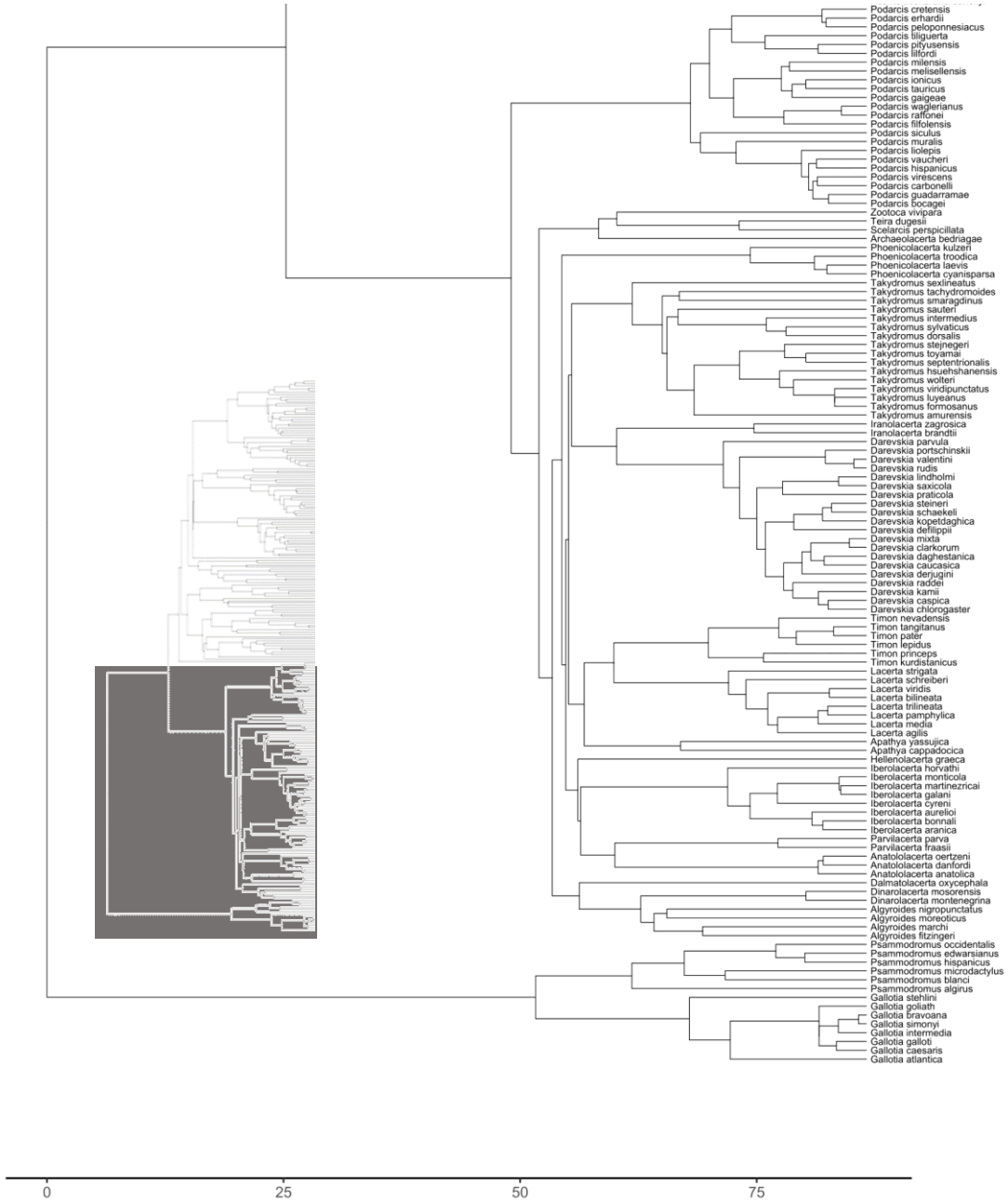

Figure S4.1. Phylogenetic tree used for the phylogenetic comparative analyses. The dated tree was performed by using genomic and genetic data. For further

information about the methodology, node support, divergence dates, etc. see the supplementary material from García-Porta et al. 2019.

Supplementary information for chapter 5

Table S5.1. Summary of the measured and coded variables for each individual in the study. Columns include species (SP), specimen code used in this paper (Code_this paper), original code (CODE_or), sex (SEX), snout–vent length (SVL), parietal length (PL), and mandible length (ML). Measures are in mm.

SP	Code_this paper	CODE_or	SEX	SVL	PL	ML
Acanthodactylus aureus	Acanthodactylus_aureus_01	24Aaur01	M	49.11	13.00	7.54
Acanthodactylus aureus	Acanthodactylus_aureus_02	24Aaur02	M	46.96	12.36	7.46
Acanthodactylus aureus	Acanthodactylus_aureus_03	24Aaur03	M	44.70	11.77	7.24
Acanthodactylus aureus	Acanthodactylus_aureus_04	24Aaur04	M	50.05	12.97	8.65
Acanthodactylus aureus	Acanthodactylus_aureus_05	24Aaur05	M	52.70	14.32	11.26
Acanthodactylus aureus	Acanthodactylus_aureus_06	24Aaur06	M	51.92	12.92	7.66
Acanthodactylus aureus	Acanthodactylus_aureus_07	24Aaur07	M	53.89	12.91	8.01
Acanthodactylus aureus	Acanthodactylus_aureus_08	24Aaur08	M	48.70	13.32	8.19
Acanthodactylus aureus	Acanthodactylus_aureus_09	24Aaur09	M	46.63	11.73	7.22
Acanthodactylus aureus	Acanthodactylus_aureus_10	24Aaur10	M	53.13	13.37	8.41
Acanthodactylus aureus	Acanthodactylus_aureus_11	24Aaur11	M	45.50	12.26	7.61
Acanthodactylus aureus	Acanthodactylus_aureus_12	24Aaur12	M	47.86	12.36	8.25
Acanthodactylus aureus	Acanthodactylus_aureus_13	24Aaur13	M	50.73	12.89	7.63
Acanthodactylus aureus	Acanthodactylus_aureus_14	24Aaur14	M	45.97	11.75	8.31
Acanthodactylus aureus	Acanthodactylus_aureus_15	24Aaur15	M	50.71	12.82	8.32
Acanthodactylus boskianus	Acanthodactylus_boskianus_01	24Abos01	M	65.89	15.78	10.31
Acanthodactylus boskianus	Acanthodactylus_boskianus_02	24Abos02	M	63.74	15.25	10.23
Acanthodactylus boskianus	Acanthodactylus_boskianus_03	24Abos03	M	69.90	16.11	10.72
Acanthodactylus boskianus	Acanthodactylus_boskianus_04	24Abos04	M	65.14	15.07	9.83
Acanthodactylus boskianus	Acanthodactylus_boskianus_05	24Abos05	M	59.93	15.12	9.32
Acanthodactylus boskianus	Acanthodactylus_boskianus_06	24Abos06	M	66.90	16.49	9.77
Acanthodactylus boskianus	Acanthodactylus_boskianus_07	24Abos07	M	59.14	14.14	9.01
Acanthodactylus boskianus	Acanthodactylus_boskianus_08	24Abos08	M	53.64	13.06	9.08
Acanthodactylus boskianus	Acanthodactylus_boskianus_09	24Abos09	M	61.19	14.25	10.24
Acanthodactylus boskianus	Acanthodactylus_boskianus_10	24Abos10	M	60.35	14.47	9.83

Acanthodactylus boskianus	Acanthodactylus_boskianus_11	24Abos11	M	58.23	13.32	8.21
Acanthodactylus boskianus	Acanthodactylus_boskianus_12	24Abos12	M	55.04	13.33	8.56
Acanthodactylus boskianus	Acanthodactylus_boskianus_13	24Abos13	M	57.97	13.75	9.92
Acanthodactylus boskianus	Acanthodactylus_boskianus_14	24Abos14	M	53.33	13.17	8.41
Acanthodactylus dumerilii	Acanthodactylus_dumerilii_01	24Adum01	M	56.91	13.43	8.71
Acanthodactylus dumerilii	Acanthodactylus_dumerilii_02	24Adum02	M	52.53	12.52	7.61
Acanthodactylus dumerilii	Acanthodactylus_dumerilii_04	24Adum04	M	51.91	12.70	7.21
Acanthodactylus dumerilii	Acanthodactylus_dumerilii_05	24Adum05	M	51.65	13.00	7.98
Acanthodactylus dumerilii	Acanthodactylus_dumerilii_06	24Adum06	M	53.64	12.50	6.87
Acanthodactylus dumerilii	Acanthodactylus_dumerilii_07	24Adum07	M	50.52	12.00	7.52
Acanthodactylus dumerilii	Acanthodactylus_dumerilii_08	24Adum08	M	54.44	12.58	8.54
Acanthodactylus dumerilii	Acanthodactylus_dumerilii_09	24Adum09	M	56.17	13.06	8.10
Acanthodactylus dumerilii	Acanthodactylus_dumerilii_10	24Adum10	M	54.45	13.38	8.53
Acanthodactylus dumerilii	Acanthodactylus_dumerilii_11	24Adum11	M	47.58	12.70	7.19
Acanthodactylus erythrurus	Acanthodactylus_erythrurus_01	1932.12.7.4	M	66.25	15.4	12.29
Acanthodactylus erythrurus	Acanthodactylus_erythrurus_02	1982.1180	M	74.62	17.11	13.34
Acanthodactylus erythrurus	Acanthodactylus_erythrurus_03	1982.1183	M	66.45	15.46	13.27
Acanthodactylus margaritae	Acanthodactylus_margaritae_01	24Amarg01	M	70.19	16.34	9.87
Acanthodactylus margaritae	Acanthodactylus_margaritae_02	24Amarg02	M	68.15	15.09	11.15
Acanthodactylus margaritae	Acanthodactylus_margaritae_03	24Amarg03	M	72.37	15.91	10.92
Acanthodactylus margaritae	Acanthodactylus_margaritae_04	24Amarg04	M	78.92	16.79	11.14
Acanthodactylus margaritae	Acanthodactylus_margaritae_05	24Amarg05	M	80.52	16.49	11.77
Acanthodactylus pardalis	Acanthodactylus_pardalis_01	1924.12.8.5	M	55.46	13.73	10.08
Acanthodactylus pardalis	Acanthodactylus_pardalis_02	1893.11.30.11	M	70.8	15.22	12.39
Acanthodactylus pardalis	Acanthodactylus_pardalis_03	1893.11.30.13	M	63.25	14.95	11.96
Acanthodactylus schmidti	Acanthodactylus_schmidti_01	1975.1028	M	62.61	16.53	11.54
Acanthodactylus schmidti	Acanthodactylus_schmidti_02	1975.1029	M	50.58	13.3	10.28
Acanthodactylus schmidti	Acanthodactylus_schmidti_03	1953.1.8.55	M	70.65	17.84	14.67
Archaeolacerta bedriagae	Archaeolacerta_bedriagae_01	1920.1.20.1658a	M	82.13	21.97	16.66
Archaeolacerta bedriagae	Archaeolacerta_bedriagae_02	1928.12.8.546	M	78.42	20.6	15.84
Archaeolacerta bedriagae	Archaeolacerta_bedriagae_03	1928.12.8.547	M	82.37	22.72	16.86
Atlantolacerta andreansky	Atlantolacerta_andreansky_01	24Aand01	M	46.22	10.55	7.46
Atlantolacerta andreansky	Atlantolacerta_andreansky_02	24Aand02	M	43.75	10.27	8.41
Atlantolacerta andreansky	Atlantolacerta_andreansky_03	24Aand03	M	43.64	9.54	7.74
Atlantolacerta andreansky	Atlantolacerta_andreansky_04	24Aand04	M	43.98	9.42	6.22
Atlantolacerta andreansky	Atlantolacerta_andreansky_05	24Aand05	M	43.81	10.25	7.39

Atlantolacerta andreansky	Atlantolacerta_andreansky_06	24Aand06	M	45.91	9.80	7.02
Atlantolacerta andreansky	Atlantolacerta_andreansky_07	24Aand07	M	44.73	9.99	7.76
Atlantolacerta andreansky	Atlantolacerta_andreansky_08	24Aand08	M	45.32	10.33	7.40
Atlantolacerta andreansky	Atlantolacerta_andreansky_09	24Aand09	M	43.50	9.16	7.45
Atlantolacerta andreansky	Atlantolacerta_andreansky_10	24Aand10	M	42.84	11.12	7.43
Atlantolacerta andreansky	Atlantolacerta_andreansky_12	24Aand12	M	42.89	9.63	7.06
Atlantolacerta andreansky	Atlantolacerta_andreansky_13	24Aand13	M	45.23	9.59	6.87
Atlantolacerta andreansky	Atlantolacerta_andreansky_14	24Aand14	M	46.99	9.87	6.71
Atlantolacerta andreansky	Atlantolacerta_andreansky_15	24Aand15	M	48.87	10.11	8.86
Australolacerta australis	Australolacerta_australis_01	1988.296	M	66	15.32	14.3
Dalmatolacerta oxycephala	Dalmatolacerta_oxycephala_01	1928.12.8.501	M	64.66	13.85	10.07
Dalmatolacerta oxycephala	Dalmatolacerta_oxycephala_02	1928.12.8.502	M	58.35	15.11	10.66
Dalmatolacerta oxycephala	Dalmatolacerta_oxycephala_03	1928.12.8.504	M	62.7	15.04	10.96
***Gallotia* atlantica**	*Gallotia*_atlantica_01	1914.6.16.5	M	94.85	23.28	15.93
***Gallotia* caesaris**	*Gallotia*_caesaris_01	1967.1573	M	85.18	22.58	16.71
***Gallotia* caesaris**	*Gallotia*_caesaris_02	1967.1574	M	76.69	21.16	14.36
***Gallotia* caesaris**	*Gallotia*_caesaris_03	1967.1575	M	85.43	22.92	16.53
***Gallotia* galloti**	*Gallotia*_galloti_01	1967.1546	M	112.43	30.25	18.71
***Gallotia* simonyi**	*Gallotia*_simonyi_01	1891.3.3.1	M	222.67	54.37	41.21
Heliobolus lugubris	Heliobolus_lugubris_01	1910.5.30.19	M	55.18	14.7	11.06
Heliobolus lugubris	Heliobolus_lugubris_02	1910.5.30.21	M	53.9	13.66	10.27
Heliobolus lugubris	Heliobolus_lugubris_03	1933.9.9.16	M	51.22	13.33	10.14
Holaspis guentheri	Holaspis_guentheri_01	1946.8.7.25	M	48.98	13.3	9.36
Holaspis guentheri	Holaspis_guentheri_02	1983.1275	M	45.09	10.22	6.85
Holaspis guentheri	Holaspis_guentheri_03	1958.1.2.96	M	49.5	11.63	8.15
Iberolacerta horvathi	Iberolacerta_horvathi_01	1928.12.8.354	M	62.93	13.41	10.37
Iberolacerta horvathi	Iberolacerta_horvathi_02	1928.12.8.353	M	55.87	13.76	10.23
Iberolacerta monticola	Iberolacerta_monticola_02	1973.772	M	67.82	16.65	11.88
Iberolacerta monticola	Iberolacerta_monticola_03		M	66.17	16.98	12.94
Ichnotropis capensis	Ichnotropis_capensis_01	1905.5	M	69.94	17.6	13.52
Ichnotropis capensis	Ichnotropis_capensis_02	1905.5	M	76.36	17.52	15.45
Lacerta agilis	Lacerta_agilis_01	111/1976/1	M	88.16	21.01	19.58
Lacerta agilis	Lacerta_agilis_02	35646	M	84.8	19.19	17.54
Lacerta agilis	Lacerta_agilis_03	1886.1.23.16	M	84.87	18.27	16.62
Lacerta agilis	Lacerta_agilis_04	19116.4.18.2	M	82.59	20.09	18.27
Lacerta agilis	Lacerta_agilis_05	10770.1	M	71.66	17.68	16.05

Lacerta agilis	Lacerta_agilis_06	110/1976/6	M	82.84	19.89	17.65
Lacerta agilis	Lacerta_agilis_07	110/1976/8	M	86.71	19.58	17.16
Lacerta agilis	Lacerta_agilis_08	19116.4.18.3	M	86.6	20.9	18.89
Lacerta agilis	Lacerta_agilis_09	34717/3	M	72.85	18.02	16.31
Lacerta agilis	Lacerta_agilis_10	110/1976/14	M	91.55	20.85	19.25
Lacerta bilineata	Lacerta_bilineata_01	24Lbil01	M	105.90	26.07	23.73
Lacerta bilineata	Lacerta_bilineata_02	24Lbil02	M	120.30	29.55	26.30
Lacerta schreiberi	Lacerta_schreiberi_01	12630	M	113.54	27.55	24.85
Lacerta schreiberi	Lacerta_schreiberi_02	33399	M	94.94	27.98	24.81
Lacerta schreiberi	Lacerta_schreiberi_03	33369	M	104.73	24.09	21.9
Lacerta schreiberi	Lacerta_schreiberi_04	6154	M	111.01	28.61	23.62
Lacerta schreiberi	Lacerta_schreiberi_05	40094	M	109.71	28.45	25.53
Lacerta schreiberi	Lacerta_schreiberi_06	6138	M	104.14	24.22	22.37
Lacerta schreiberi	Lacerta_schreiberi_07	33400	M	112.18	30.24	27.08
Lacerta schreiberi	Lacerta_schreiberi_08	33402	M	103.9	26.26	23.58
Lacerta schreiberi	Lacerta_schreiberi_09	12647	M	107.82	25.46	23.47
Lacerta schreiberi	Lacerta_schreiberi_10	17293	M	93.33	22.73	20.02
Lacerta viridis	Lacerta_viridis_01	10846.9	M	111.16	28.71	25
Lacerta viridis	Lacerta_viridis_02	1965.1307	M	95.9	23.64	21.05
Lacerta viridis	Lacerta_viridis_03	34819.4	M	87.47	21.58	19.46
Lacerta viridis	Lacerta_viridis_04	56764	M	83.2	22.2	20.2
Lacerta viridis	Lacerta_viridis_05	193/1985	M	91.17	22.98	20.9
Lacerta viridis	Lacerta_viridis_06	3225	M	117.72	27.27	24.45
Lacerta viridis	Lacerta_viridis_07	19179.4	M	107.76	27.35	23.98
Lacerta viridis	Lacerta_viridis_08	19179.2	M	120	30.14	26.77
Lacerta viridis	Lacerta_viridis_09	3500	M	103.24	25.2	22.24
Lacerta viridis	Lacerta_viridis_10	19179.5	M	104.88	25.07	21.55
Latastia longicaudata	Latastia_longicaudata_01	1897.10.28.225	M	110.55	25.13	20.03
Latastia longicaudata	Latastia_longicaudata_02	1897.10.28.226	M	103.26	22.31	14.87
Latastia longicaudata	Latastia_longicaudata_03	1897.10.28.227	M	96.89	22.5	19.03
Meroles anchietae	Meroles_anchietae_02	1996.370	M	57.01	14.78	11.21
Meroles ctenodactylus	Meroles_ctenodactylus_01	1905.3.7.123	M	80.02	22.16	17.98
Meroles ctenodactylus	Meroles_ctenodactylus_02	1905.3.7.124	M	74.48	21.51	17.02
Meroles ctenodactylus	Meroles_ctenodactylus_03	1905.3.7.125	M	81.64	22.66	18.48
Meroles cuneirostris	Meroles_cuneirostris_01	1937.4.2.13	M	53.81	14.62	10.41
Meroles cuneirostris	Meroles_cuneirostris_02	1996.373	M	58.28	15.55	13.27

Meroles knoxii	Meroles_knoxii_01	1905.3.7.113	M	54.19	12.53	7.98
Meroles knoxii	Meroles_knoxii_02	1905.3.7.115	M	47.56	12.91	7.05
Meroles knoxii	Meroles_knoxii_03	1988.505	M	52.4	13	9.4
Meroles suborbitalis	Meroles_suborbitalis_01	1910.5.27.9	M	60.74	15.18	11.56
Meroles suborbitalis	Meroles_suborbitalis_02	1998.5.26.31.3	M	62.17	15.49	11.96
Mesalina brevirostris	Mesalina_brevirostris_01	1909.4.20.31	M	52.66	11.3	7.39
Mesalina brevirostris	Mesalina_brevirostris_02	1909.4.20.32	M	49.03	10.06	6.95
Mesalina guttulata	Mesalina_guttulata_01	24Mgut01	M	42.76	10.81	7.19
Mesalina guttulata	Mesalina_guttulata_02	24Mgut02	M	43.15	10.80	7.23
Mesalina guttulata	Mesalina_guttulata_03	24Mgut03	M	43.33	10.64	6.15
Mesalina guttulata	Mesalina_guttulata_04	24Mgut04	M	44.83	11.20	7.43
Mesalina guttulata	Mesalina_guttulata_05	24Mgut05	M	44.38	10.75	7.29
Mesalina guttulata	Mesalina_guttulata_06	24Mgut06	M	48.07	11.47	7.20
Mesalina guttulata	Mesalina_guttulata_07	24Mgut07	M	46.09	10.95	7.84
Mesalina guttulata	Mesalina_guttulata_08	24Mgut08	M	41.93	10.01	7.09
Mesalina guttulata	Mesalina_guttulata_09	24Mgut09	M	40.31	10.56	6.87
Mesalina guttulata	Mesalina_guttulata_10	24Mgut10	M	44.55	10.81	7.03
Mesalina guttulata	Mesalina_guttulata_11	24Mgut11	M	43.12	10.22	6.04
Mesalina guttulata	Mesalina_guttulata_12	24Mgut12	M	42.64	10.52	7.23
Mesalina simoni	Mesalina_simoni_01	24Msim01	M	43.16	9.84	6.69
Mesalina simoni	Mesalina_simoni_02	24Msim02	M	43.22	10.11	6.37
Mesalina simoni	Mesalina_simoni_03	24Msim03	M	47.63	11.17	7.58
Mesalina simoni	Mesalina_simoni_04	24Msim04	M	47.87	11.27	7.14
Nucras intertexta	Nucras_intertexta_01	1937.12.3.90	M	78.64	15.68	11.27
Nucras intertexta	Nucras_intertexta_02	1946.8.6.19	M	54.66	10.95	7.85
Nucras intertexta	Nucras_intertexta_03	1946.8.6.20	M	53.66	11.18	8.21
Nucras taeniolata	Nucras_taeniolata_01	1907.4.17.28	M	91.84	20.35	16.38
Nucras taeniolata	Nucras_taeniolata_02	93.11.20.2	M	85.86	16.88	11.34
Nucras tessellata	Nucras_tessellata_01	1903.4.7.33	M	71.16	14.68	10.28
Nucras tessellata	Nucras_tessellata_02	1907.6.29.11	M	71.08	12.97	9.7
Pedioplanis burchelli	Pedioplanis_burchelli_01	1974.2314	M	64.35	14.19	9.94
Pedioplanis inornata	Pedioplanis_inornata_01	98.5.26.25	M	50.6	12.65	7.86
Pedioplanis laticeps	Pedioplanis_laticeps_01	1879.6.9.15	M	59.55	15.59	10.64
Pedioplanis laticeps	Pedioplanis_laticeps_02	1879.6.9.16	M	65.67	15.52	11.11
Pedioplanis namaquensis	Pedioplanis_namaquensis_01	1936.8.1.491	M	49.92	11.71	8.73
***Podarcis* bocagei**	Mol_A1	Mol_A1	M	59.2	14.51	13.3

***Podarcis* bocagei**	Mol_A10	Mol_A10	M	52.17	12.32	10.92
***Podarcis* bocagei**	Mol_A2	Mol_A2	M	52.61	12.79	11.36
***Podarcis* bocagei**	Mol_A3	Mol_A3	M	59.37	14.8	12.74
***Podarcis* bocagei**	Mol_A5	Mol_A5	M	56.52	13.97	12.7
***Podarcis* bocagei**	Mol_B13	Mol_B13	M	50.18	12.27	11.37
***Podarcis* bocagei**	Mol_B15	Mol_B15	M	48.37	11.8	10.45
***Podarcis* bocagei**	Mol_B20	Mol_B20	M	52.7	12.16	11.26
***Podarcis* bocagei**	Mol_B23	Mol_B23	M	52.91	12.9	11.7
***Podarcis* bocagei**	Mol_B24	Mol_B24	M	42.88	10.39	9.26
***Podarcis* bocagei**	Mol_B25	Mol_B25	M	50.95	11.99	11.04
***Podarcis* bocagei**	Mol_B27	Mol_B27	M	47.23	11.79	10.71
***Podarcis* bocagei**	Mol_B31	Mol_B31	M	55.95	13.89	12.21
***Podarcis* bocagei**	Mol_B34	Mol_B34	M	52.3	12.46	11.27
***Podarcis* bocagei**	Mol_B4	Mol_B4	M	60.04	14.28	12.54
***Podarcis* bocagei**	Mol_B6	Mol_B6	M	53.44	13.38	11.42
***Podarcis* bocagei**	Mol_B9	Mol_B9	M	53.96	13.09	11.53
***Podarcis* bocagei**	Mol_C14	Mol_C14	M	42.52	10.29	8.98
***Podarcis* bocagei**	Mol_C33	Mol_C33	M	55.26	13.69	11.86
***Podarcis* bocagei**	Mol_C34	Mol_C34	M	49.88	11.94	10.82
***Podarcis* bocagei**	Mol_C4	Mol_C4	M	56.24	12.82	11.21
***Podarcis* bocagei**	Mol_C5	Mol_C5	M	55.2	13.98	12.47
***Podarcis* bocagei**	Mol_C6	Mol_C6	M	53.02	13.45	11.47
***Podarcis* bocagei**	Mol_C9	Mol_C9	M	50.63	12.27	11.01
***Podarcis* bocagei**	Mol_F1	Mol_F1	M	53.28	12.84	11.2
***Podarcis* bocagei**	Mol_F3	Mol_F3	M	58.8	14.38	12.96
***Podarcis* bocagei**	Mol_F5	Mol_F5	M	56.1	13.63	12.04
***Podarcis* bocagei**	Mol_F6	Mol_F6	M	56.1	13.32	11.67
***Podarcis* bocagei**	Mol_F9	Mol_F9	M	45.97	11.1	9.85
***Podarcis* bocagei**	Mol_X11	Mol_X11	M	50.52	11.88	10.58
***Podarcis* bocagei**	Mol_X18	Mol_X18	M	58.81	14.21	12.71
***Podarcis* bocagei**	Mol_X33	Mol_X33	M	48.86	12.04	10.77
***Podarcis* carbonelli**	C10	C10	M	46.8	12.03	10.82
***Podarcis* carbonelli**	C14	C14	M	49.47	12.3	10.85
***Podarcis* carbonelli**	C15	C15	M	47.05	11.58	9.98
***Podarcis* carbonelli**	C17	C17	M	48.08	12.09	10.16
***Podarcis* carbonelli**	C2	C2	M	49	12.57	10.43

***Podarcis* carbonelli**	C20	C20	M	46.56	11.56	9.39
***Podarcis* carbonelli**	C21	C21	M	49.05	12.24	10.63
***Podarcis* carbonelli**	C26	C26	M	47.44	12.11	10.51
***Podarcis* carbonelli**	C27	C27	M	49.39	12.06	10.92
***Podarcis* carbonelli**	C28	C28	M	42.35	10.55	9.34
***Podarcis* carbonelli**	C29	C29	M	48.11	11.88	10.6
***Podarcis* carbonelli**	C3	C3	M	49.58	12.58	10.32
***Podarcis* carbonelli**	C32	C32	M	47.97	11.58	10.11
***Podarcis* carbonelli**	C33	C33	M	47.29	11.66	10.05
***Podarcis* carbonelli**	C37	C37	M	48.06	11.66	10.26
***Podarcis* carbonelli**	C4	C4	M	51	12.66	10.36
***Podarcis* carbonelli**	C5	C5	M	49.72	12.01	10.65
***Podarcis* cretensis**	CREM1	CREM1	M	67.78	16.39	14.25
***Podarcis* cretensis**	CREM10	CREM10	M	67.42	15.89	14.04
***Podarcis* cretensis**	CREM11	CREM11	M	69.27	16.01	14.32
***Podarcis* cretensis**	CREM12	CREM12	M	64.86	15.17	12.77
***Podarcis* cretensis**	CREM13	CREM13	M	66.83	15.74	13.49
***Podarcis* cretensis**	CREM14	CREM14	M	67.3	16.41	13.7
***Podarcis* cretensis**	CREM15	CREM15	M	67.19	16.47	13.97
***Podarcis* cretensis**	CREM16	CREM16	M	66.27	15.19	13.3
***Podarcis* cretensis**	CREM17	CREM17	M	64.58	15.71	13.76
***Podarcis* cretensis**	CREM18	CREM18	M	64.18	15.22	12.96
***Podarcis* cretensis**	CREM19	CREM19	M	64.94	15.15	13.09
***Podarcis* cretensis**	CREM2	CREM2	M	66.65	15.44	13.33
***Podarcis* cretensis**	CREM3	CREM3	M	71.5	16.42	14.46
***Podarcis* cretensis**	CREM4	CREM4	M	68.47	15.42	14.12
***Podarcis* cretensis**	CREM5	CREM5	M	67.25	15.8	13.63
***Podarcis* cretensis**	CREM6	CREM6	M	69.31	16.36	14
***Podarcis* cretensis**	CREM7	CREM7	M	67.09	15.48	14
***Podarcis* cretensis**	CREM8	CREM8	M	65.52	15.06	13.23
***Podarcis* cretensis**	CREM9	CREM9	M	66.19	15.67	13.56
***Podarcis* erhardii_Cgreece**	ERHM1	ERHM1	M	74.31	17.7	14.22
***Podarcis* erhardii_Cgreece**	ERHM10	ERHM10	M	67.9	17.03	13.92
***Podarcis* erhardii_Cgreece**	ERHM11	ERHM11	M	68.46	14.89	13.41
***Podarcis* erhardii_Cgreece**	ERHM12	ERHM12	M	74	17.1	14.7
***Podarcis* erhardii_Cgreece**	ERHM13	ERHM13	M	71.97	16.63	14.4

***Podarcis* erhardii_Cgreece**	ERHM14	ERHM14	M	67.27	15.82	13
***Podarcis* erhardii_Cgreece**	ERHM15	ERHM15	M	69.43	16.1	13.65
***Podarcis* erhardii_Cgreece**	ERHM16	ERHM16	M	66.45	15.32	13.03
***Podarcis* erhardii_Cgreece**	ERHM17	ERHM17	M	70.57	16.31	14.25
***Podarcis* erhardii_Cgreece**	ERHM18	ERHM18	M	70.41	17	15.21
***Podarcis* erhardii_Cgreece**	ERHM19	ERHM19	M	73.93	16.69	14.73
***Podarcis* erhardii_Cgreece**	ERHM2	ERHM2	M	65.96	15.45	13.74
***Podarcis* erhardii_Cgreece**	ERHM20	ERHM20	M	71.24	16.31	14.08
***Podarcis* erhardii_Cgreece**	ERHM3	ERHM3	M	71.19	16.55	14.7
***Podarcis* erhardii_Cgreece**	ERHM4	ERHM4	M	73.2	16.83	13.57
***Podarcis* erhardii_Cgreece**	ERHM5	ERHM5	M	66.57	16.63	14.02
***Podarcis* erhardii_Cgreece**	ERHM6	ERHM6	M	64.7	14.75	12.38
***Podarcis* erhardii_Cgreece**	ERHM7	ERHM7	M	71.32	16.11	13.63
***Podarcis* erhardii_Cgreece**	ERHM8	ERHM8	M	65.4	15.94	13.62
***Podarcis* erhardii_Cgreece**	ERHM9	ERHM9	M	69.49	15.5	13.7
***Podarcis* erhardii_islands**	19-ERH-M1	19-ERH-M1	M	77.91	18.05	15.34
***Podarcis* erhardii_islands**	19-ERH-M10	19-ERH-M10	M	70.4	15.75	14.16
***Podarcis* erhardii_islands**	19-ERH-M11	19-ERH-M11	M	67.85	15.64	14.13
***Podarcis* erhardii_islands**	19-ERH-M12	19-ERH-M12	M	75.02	16.31	14.7
***Podarcis* erhardii_islands**	19-ERH-M13	19-ERH-M13	M	75.06	17.82	16
***Podarcis* erhardii_islands**	19-ERH-M14	19-ERH-M14	M	73.14	15.61	13.86
***Podarcis* erhardii_islands**	19-ERH-M15	19-ERH-M15	M	78.01	17.53	14.74
***Podarcis* erhardii_islands**	19-ERH-M16	19-ERH-M16	M	74.5	16.83	14.23
***Podarcis* erhardii_islands**	19-ERH-M17	19-ERH-M17	M	75.44	16.77	14.95
***Podarcis* erhardii_islands**	19-ERH-M18	19-ERH-M18	M	67.85	15.69	13.68
***Podarcis* erhardii_islands**	19-ERH-M19	19-ERH-M19	M	78.44	17.29	14.91
***Podarcis* erhardii_islands**	19-ERH-M2	19-ERH-M2	M	70.6	16.12	13.65
***Podarcis* erhardii_islands**	19-ERH-M20	19-ERH-M20	M	73.76	17.03	14.94
***Podarcis* erhardii_islands**	19-ERH-M3	19-ERH-M3	M	76.34	17.25	15.43
***Podarcis* erhardii_islands**	19-ERH-M4	19-ERH-M4	M	71.92	15.96	13.97
***Podarcis* erhardii_islands**	19-ERH-M5	19-ERH-M5	M	76.44	17.18	13.91
***Podarcis* erhardii_islands**	19-ERH-M6	19-ERH-M6	M	71.76	16.17	13.6
***Podarcis* erhardii_islands**	19-ERH-M7	19-ERH-M7	M	78.51	17.19	15.83
***Podarcis* erhardii_islands**	19-ERH-M8	19-ERH-M8	M	70.31	16.06	13.77
***Podarcis* erhardii_islands**	19-ERH-M9	19-ERH-M9	M	72.75	16.57	14.44
***Podarcis* filfolensis**	19-PFIL-M1	19-PFIL-M1	M	67.1	15.77	13.77

***Podarcis* filfolensis**	19-PFIL-M10	19-PFIL-M10	M	56.1	12.87	11.03
***Podarcis* filfolensis**	19-PFIL-M11	19-PFIL-M11	M	63.44	14.41	12.24
***Podarcis* filfolensis**	19-PFIL-M12	19-PFIL-M12	M	63.45	15.14	13.12
***Podarcis* filfolensis**	19-PFIL-M13	19-PFIL-M13	M	59.32	14.13	12.65
***Podarcis* filfolensis**	19-PFIL-M14	19-PFIL-M14	M	62.56	14.38	11.94
***Podarcis* filfolensis**	19-PFIL-M15	19-PFIL-M15	M	60.73	14.18	12.18
***Podarcis* filfolensis**	19-PFIL-M16	19-PFIL-M16	M	60.2	13.74	12.1
***Podarcis* filfolensis**	19-PFIL-M17	19-PFIL-M17	M	63.91	15.37	13.24
***Podarcis* filfolensis**	19-PFIL-M18	19-PFIL-M18	M	60.77	14.7	12.95
***Podarcis* filfolensis**	19-PFIL-M19	19-PFIL-M19	M	55.6	13.71	11.9
***Podarcis* filfolensis**	19-PFIL-M2	19-PFIL-M2	M	58.56	13.38	11.91
***Podarcis* filfolensis**	19-PFIL-M20	19-PFIL-M20	M	61.37	14.39	12.31
***Podarcis* filfolensis**	19-PFIL-M3	19-PFIL-M3	M	53.15	12.27	10.64
***Podarcis* filfolensis**	19-PFIL-M4	19-PFIL-M4	M	55.59	12.91	10.95
***Podarcis* filfolensis**	19-PFIL-M5	19-PFIL-M5	M	63.32	14.49	12.94
***Podarcis* filfolensis**	19-PFIL-M6	19-PFIL-M6	M	61.23	14.72	13.19
***Podarcis* filfolensis**	19-PFIL-M7	19-PFIL-M7	M	61.56	15.07	12.9
***Podarcis* filfolensis**	19-PFIL-M8	19-PFIL-M8	M	61.86	14.47	12.77
***Podarcis* filfolensis**	19-PFIL-M9	19-PFIL-M9	M	63.68	15.21	13.73
***Podarcis* gaigeae**	GAIM1	GAIM1	M	61.72	13.87	12.21
***Podarcis* gaigeae**	GAIM10	GAIM10	M	64.07	15.44	13.94
***Podarcis* gaigeae**	GAIM11	GAIM11	M	56.19	12.85	11.49
***Podarcis* gaigeae**	GAIM12	GAIM12	M	63.95	14.7	13
***Podarcis* gaigeae**	GAIM13	GAIM13	M	61.38	15.03	13.1
***Podarcis* gaigeae**	GAIM14	GAIM14	M	61.61	14.47	12.92
***Podarcis* gaigeae**	GAIM15	GAIM15	M	51.68	11.72	10.42
***Podarcis* gaigeae**	GAIM16	GAIM16	M	73.12	16.71	14.62
***Podarcis* gaigeae**	GAIM17	GAIM17	M	52.27	11.93	10.46
***Podarcis* gaigeae**	GAIM18	GAIM18	M	52.7	11.9	10.86
***Podarcis* gaigeae**	GAIM19	GAIM19	M	59.74	13.83	12.54
***Podarcis* gaigeae**	GAIM2	GAIM2	M	58.84	13.19	11.22
***Podarcis* gaigeae**	GAIM20	GAIM20	M	55.03	12.32	10.85
***Podarcis* gaigeae**	GAIM3	GAIM3	M	66.47	15.51	13.8
***Podarcis* gaigeae**	GAIM4	GAIM4	M	63.25	14.96	13.34
***Podarcis* gaigeae**	GAIM5	GAIM5	M	55.82	12.46	11.07
***Podarcis* gaigeae**	GAIM6	GAIM6	M	66.36	14.84	12.87

***Podarcis* gaigeae**	GAIM7	GAIM7	M	61.72	13.88	12.62
***Podarcis* gaigeae**	GAIM8	GAIM8	M	57.79	12.94	11.72
***Podarcis* gaigeae**	GAIM9	GAIM9	M	66.39	15.06	13.66
***Podarcis* guadarramae_guadarramae**	19-Pgg-M32	19-Pgg-M32	M	53.51	11.72	10.23
***Podarcis* guadarramae_guadarramae**	19-Pgg-M33	19-Pgg-M33	M	51.36	11	9.34
***Podarcis* guadarramae_guadarramae**	19-Pgg-M34	19-Pgg-M34	M	61.32	13.53	12.62
***Podarcis* guadarramae_guadarramae**	19-Pgg-M35	19-Pgg-M35	M	63.17	14.13	11.69
***Podarcis* guadarramae_guadarramae**	19-Pgg-M36	19-Pgg-M36	M	58.04	13.04	11.62
***Podarcis* guadarramae_guadarramae**	19-Pgg-M37	19-Pgg-M37	M	55.7	12.26	11.09
***Podarcis* guadarramae_guadarramae**	19-Pgg-M38	19-Pgg-M38	M	57.97	12.63	10.91
***Podarcis* guadarramae_guadarramae**	19-Pgg-M39	19-Pgg-M39	M	53.64	11.78	10.58
***Podarcis* guadarramae_guadarramae**	19-Pgg-M40	19-Pgg-M40	M	53.92	11.57	10.28
***Podarcis* guadarramae_guadarramae**	19-Pgg-M41	19-Pgg-M41	M	63.79	14.43	12.87
***Podarcis* guadarramae_guadarramae**	19-Pgg-M42	19-Pgg-M42	M	65.44	14.95	13.03
***Podarcis* guadarramae_guadarramae**	19-Pgg-M43	19-Pgg-M43	M	59.58	13.7	12.07
***Podarcis* guadarramae_guadarramae**	19-Pgg-M44	19-Pgg-M44	M	64.77	15.17	13.34
***Podarcis* guadarramae_guadarramae**	19-Pgg-M45	19-Pgg-M45	M	56.34	12.64	11.43
***Podarcis* guadarramae_guadarramae**	19-Pgg-M46	19-Pgg-M46	M	55.95	12.47	11.07
***Podarcis* guadarramae_guadarramae**	19-Pgg-M47	19-Pgg-M47	M	49.38	10.73	9.64
***Podarcis* guadarramae_guadarramae**	19-Pgg-M48	19-Pgg-M48	M	59.21	13.07	11.72
***Podarcis* guadarramae_guadarramae**	19-Pgg-M49	19-Pgg-M49	M	61.4	13.92	11.64
***Podarcis* guadarramae_guadarramae**	19-Pgg-M50	19-Pgg-M50	M	59.55	12.67	11.67
***Podarcis* guadarramae_guadarramae**	19-Pgg-M51	19-Pgg-M51	M	63.23	14.16	12.35
***Podarcis* guadarramae_guadarramae**	PhT1B1	PhT1B1	M	54.04	12.82	12.45
***Podarcis* guadarramae_guadarramae**	PhT1B10	PhT1B10	M	49.18	12.13	11.31
***Podarcis* guadarramae_guadarramae**	PhT1B2	PhT1B2	M	53.67	13.05	12.2
***Podarcis* guadarramae_guadarramae**	PhT1B3	PhT1B3	M	53.94	13.28	11.54
***Podarcis* guadarramae_guadarramae**	PhT1B4	PhT1B4	M	58.57	13.36	12.8
***Podarcis* guadarramae_guadarramae**	PhT1B5	PhT1B5	M	56.78	13.46	12.33
***Podarcis* guadarramae_guadarramae**	PhT1B6	PhT1B6	M	59.73	14.33	12.97
***Podarcis* guadarramae_guadarramae**	PhT1B7	PhT1B7	M	45.74	11.26	10.37
***Podarcis* guadarramae_guadarramae**	PhT1B8	PhT1B8	M	48.15	11.29	10.41
***Podarcis* guadarramae_guadarramae**	PhT1B9	PhT1B9	M	48.25	11.81	11.23
***Podarcis* guadarramae_lusitanica**	Mol_A11	Mol_A11	M	55.15	13.34	11.57
***Podarcis* guadarramae_lusitanica**	Mol_A6	Mol_A6	M	58.27	13.3	11.38
***Podarcis* guadarramae_lusitanica**	Mol_A7	Mol_A7	M	41.28	10.3	8.6

***Podarcis* guadarramae_lusitanica**	Mol_A8	Mol_A8	M	60.37	14.25	11.95
***Podarcis* guadarramae_lusitanica**	Mol_B1	Mol_B1	M	53	12.57	10.64
***Podarcis* guadarramae_lusitanica**	Mol_B11	Mol_B11	M	54.5	12.8	11.32
***Podarcis* guadarramae_lusitanica**	Mol_B17	Mol_B17	M	47.81	11.43	9.56
***Podarcis* guadarramae_lusitanica**	Mol_B19	Mol_B19	M	49.22	11.34	9.7
***Podarcis* guadarramae_lusitanica**	Mol_B22	Mol_B22	M	46.11	10.71	9.51
***Podarcis* guadarramae_lusitanica**	Mol_B29	Mol_B29	M	57.75	12.95	11.16
***Podarcis* guadarramae_lusitanica**	Mol_B3	Mol_B3	M	52.33	12.32	10.79
***Podarcis* guadarramae_lusitanica**	Mol_B35	Mol_B35	M	56.06	13.11	11.6
***Podarcis* guadarramae_lusitanica**	Mol_B8	Mol_B8	M	53.43	12.53	11.11
***Podarcis* guadarramae_lusitanica**	Mol_C1	Mol_C1	M	46.03	11.05	9.59
***Podarcis* guadarramae_lusitanica**	Mol_C20	Mol_C20	M	43.76	10	9.1
***Podarcis* guadarramae_lusitanica**	Mol_C30	Mol_C30	M	45.26	10.9	9.79
***Podarcis* guadarramae_lusitanica**	Mol_C31	Mol_C31	M	52.25	12.64	10.74
***Podarcis* guadarramae_lusitanica**	Mol_C32	Mol_C32	M	57.98	12.63	11.34
***Podarcis* guadarramae_lusitanica**	Mol_C38	Mol_C38	M	40.74	9.78	8.73
***Podarcis* guadarramae_lusitanica**	Mol_C7	Mol_C7	M	49.75	12	10.4
***Podarcis* guadarramae_lusitanica**	Mol_F4	Mol_F4	M	51.14	11.89	10.49
***Podarcis* guadarramae_lusitanica**	Mol_F7	Mol_F7	M	48.69	11.7	10.08
***Podarcis* guadarramae_lusitanica**	Mol_X12	Mol_X12	M	56.35	12.81	11.31
***Podarcis* guadarramae_lusitanica**	Mol_X17	Mol_X17	M	48.83	11.6	10.06
***Podarcis* guadarramae_lusitanica**	Mol_X20	Mol_X20	M	54.94	12.89	11.7
***Podarcis* guadarramae_lusitanica**	Mol_X25	Mol_X25	M	46.92	11.52	9.86
***Podarcis* guadarramae_lusitanica**	Mol_X30	Mol_X30	M	58.54	12.79	11.13
***Podarcis* guadarramae_lusitanica**	Mol_X32	Mol_X32	M	57.25	13.76	11.82
***Podarcis* guadarramae_lusitanica**	Mol_X34	Mol_X34	M	53.81	12.5	10.82
***Podarcis* guadarramae_lusitanica**	Mol_X35	Mol_X35	M	57.2	13.32	11.81
***Podarcis* guadarramae_lusitanica**	Mol_X5	Mol_X5	M	53.92	12.94	11.55
***Podarcis* guadarramae_lusitanica**	Mol_X6	Mol_X6	M	48.18	10.73	9.84
***Podarcis* guadarramae_lusitanica**	Mol_X8	Mol_X8	M	58.98	13.27	11.39
***Podarcis* hispanica_albacete_murcia**	PhAl1	PhAl1	M	48.95	12.22	10.93
***Podarcis* hispanica_albacete_murcia**	PhAl10	PhAl10	M	42.86	9.72	8.76
***Podarcis* hispanica_albacete_murcia**	PhAl2	PhAl2	M	45.94	11.58	10.47
***Podarcis* hispanica_albacete_murcia**	PhAl3	PhAl3	M	48.53	11.93	9.8
***Podarcis* hispanica_albacete_murcia**	PhAl4	PhAl4	M	40.34	10.05	8.96
***Podarcis* hispanica_albacete_murcia**	PhAl5	PhAl5	M	43.37	10.72	9.93

***Podarcis* hispanica_albacete_murcia**	PhAl6	PhAl6	M	41.44	10.21	8.93
***Podarcis* hispanica_albacete_murcia**	PhAl7	PhAl7	M	41.39	9.66	9.67
***Podarcis* hispanica_albacete_murcia**	PhAl8	PhAl8	M	40.29	9.69	9.11
***Podarcis* hispanica_albacete_murcia**	PhAl9	PhAl9	M	37.79	9.61	8.04
***Podarcis* hispanica_galera**	PhCa1	PhCa1	M	41.02	9.86	8.7
***Podarcis* hispanica_galera**	PhCa10	PhCa10	M	42.89	10.59	9.09
***Podarcis* hispanica_galera**	PhCa14	PhCa14	M	41.32	9.54	8.44
***Podarcis* hispanica_galera**	PhCa3	PhCa3	M	42.31	10.89	9.34
***Podarcis* hispanica_galera**	PhCa4	PhCa4	M	44.14	11.04	9.42
***Podarcis* hispanica_galera**	PhCa5	PhCa5	M	42.1	10.86	10.29
***Podarcis* hispanica_galera**	PhCa6	PhCa6	M	43.33	10.64	10.31
***Podarcis* hispanica_galera**	PhCa7	PhCa7	M	40.37	10.41	9.07
***Podarcis* hispanica_galera**	PhCa8	PhCa8	M	40.42	10.17	9.12
***Podarcis* hispanica_jebelsirwah**	13MS	13MS	M	53.72	13.4	8.53
***Podarcis* hispanica_jebelsirwah**	14MS	14MS	M	50.32	12.52	8.39
***Podarcis* hispanica_jebelsirwah**	15MS	15MS	M	56.01	13.59	9.28
***Podarcis* hispanica_jebelsirwah**	16MS	16MS	M	50.58	12.91	8.31
***Podarcis* hispanica_jebelsirwah**	17MS	17MS	M	54.96	13.65	9.18
***Podarcis* hispanica_jebelsirwah**	18MS	18MS	M	47.87	11.67	8.02
***Podarcis* hispanica_jebelsirwah**	19MS	19MS	M	51.59	12.7	7.93
***Podarcis* hispanica_jebelsirwah**	20MS	20MS	M	49.04	11.94	7.73
***Podarcis* hispanica_jebelsirwah**	24MS	24MS	M	53.29	13.63	8.6
***Podarcis* hispanica_jebelsirwah**	26MS	26MS	M	51.6	12.49	8.88
***Podarcis* hispanica_jebelsirwah**	27MS	27MS	M	50.14	12.54	9.03
***Podarcis* hispanica_jebelsirwah**	28MS	28MS	M	49.03	12.31	7.72
***Podarcis* hispanica_jebelsirwah**	29MS	29MS	M	54.07	12.72	9.03
***Podarcis* hispanica_sensu_stricto**	PHSS1	PHSS1	M	46.42	10.89	9.3
***Podarcis* hispanica_sensu_stricto**	PHSS2	PHSS2	M	46.92	11.7	9.65
***Podarcis* hispanica_sensu_stricto**	PHSS3	PHSS3	M	56.52	12.82	11.71
***Podarcis* hispanica_sensu_stricto**	PHSS4	PHSS4	M	49.64	12.25	10.06
***Podarcis* hispanica_sensu_stricto**	PHSS5	PHSS5	M	53.06	12.56	11.16
***Podarcis* hispanica_sensu_stricto**	PHSS6	PHSS6	M	53.43	12.41	10.79
***Podarcis* levendis**	LEVM1	LEVM1	M	72.4	17.12	14.95
***Podarcis* levendis**	LEVM10	LEVM10	M	75.45	17.18	14.87
***Podarcis* levendis**	LEVM11	LEVM11	M	81.89	18.49	16.26
***Podarcis* levendis**	LEVM12	LEVM12	M	73.04	16.1	14.62

***Podarcis* levendis**	LEVM13	LEVM13	M	79.2	18.12	15.43
***Podarcis* levendis**	LEVM14	LEVM14	M	72.25	16.82	14.62
***Podarcis* levendis**	LEVM2	LEVM2	M	78.01	17.75	15.57
***Podarcis* levendis**	LEVM3	LEVM3	M	75.8	17.93	16
***Podarcis* levendis**	LEVM4	LEVM4	M	76.39	17.89	15.55
***Podarcis* levendis**	LEVM5	LEVM5	M	82.49	18.7	15.94
***Podarcis* levendis**	LEVM6	LEVM6	M	74.81	17.7	16
***Podarcis* levendis**	LEVM7	LEVM7	M	79.52	18.37	15.76
***Podarcis* levendis**	LEVM8	LEVM8	M	62.9	15.3	13.34
***Podarcis* levendis**	LEVM9	LEVM9	M	78.2	18.05	15.8
***Podarcis* lilfordi**	L18	L18	M	68.38	16.59	14.25
***Podarcis* lilfordi**	L2	L2	M	63.74	15.68	13.1
***Podarcis* lilfordi**	L22	L22	M	75.28	18.6	16.17
***Podarcis* lilfordi**	L23	L23	M	74.3	18.93	16.42
***Podarcis* lilfordi**	L24	L24	M	73.47	17.15	15.31
***Podarcis* lilfordi**	L25	L25	M	69.18	16.54	14.42
***Podarcis* lilfordi**	L26	L26	M	69.59	17.26	14.86
***Podarcis* lilfordi**	L27	L27	M	72.38	17.41	15.03
***Podarcis* lilfordi**	L28	L28	M	72.08	17.59	14.76
***Podarcis* lilfordi**	L29	L29	M	74.05	18.37	15.41
***Podarcis* lilfordi**	L30	L30	M	74.01	18.59	15.62
***Podarcis* lilfordi**	L31	L31	M	70.1	17.53	15.05
***Podarcis* lilfordi**	L32	L32	M	74.89	18.5	16.3
***Podarcis* lilfordi**	L33	L33	M	71.16	18.24	15.47
***Podarcis* lilfordi**	L34	L34	M	69.25	17	14.14
***Podarcis* lilfordi**	L35	L35	M	72.18	18.14	15.45
***Podarcis* lilfordi**	L36	L36	M	74.57	18.38	15.24
***Podarcis* lilfordi**	L37	L37	M	69.28	16.82	14.34
***Podarcis* lilfordi**	L38	L38	M	74.84	18.11	15.17
***Podarcis* lilfordi**	L39	L39	M	75.15	17.79	15.17
***Podarcis* liolepis**	LM10	LM10	M	61.32	14.78	12.77
***Podarcis* liolepis**	LM12	LM12	M	59.21	14.67	13.21
***Podarcis* liolepis**	LM13	LM13	M	62.49	15.34	13.75
***Podarcis* liolepis**	LM14	LM14	M	58.9	14.79	12.83
***Podarcis* liolepis**	LM16	LM16	M	56.87	13.96	12.43
***Podarcis* liolepis**	LM18	LM18	M	59.85	14.35	12.52

***Podarcis* liolepis**	LM6	LM6	M	60.07	15.15	13.05
***Podarcis* liolepis**	LM7	LM7	M	63.65	15.47	12.62
***Podarcis* liolepis**	LM9	LM9	M	63.08	15.9	14.17
***Podarcis* liolepis**	24-lio-1	24-lio-1	M	53.91	12.53	10.71
***Podarcis* liolepis**	24-lio-A1	24-lio-A1	M	55.01	12.92	11.21
***Podarcis* liolepis**	24-lio-A10	24-lio-A10	M	47.81	11.7	9.84
***Podarcis* liolepis**	24-lio-A14	24-lio-A14	M	44.71	10.46	8.94
***Podarcis* liolepis**	24-lio-A3	24-lio-A3	M	54.18	13.01	10.94
***Podarcis* liolepis**	24-lio-A4	24-lio-A4	M	45.82	10.8	9.28
***Podarcis* liolepis**	24-lio-A5	24-lio-A5	M	51.13	12.51	11.09
***Podarcis* liolepis**	24-lio-A7	24-lio-A7	M	49.08	12.16	10.31
***Podarcis* liolepis**	24-lio-A8	24-lio-A8	M	50.9	12.82	11.36
***Podarcis* liolepis**	24-lio-C1	24-lio-C1	M	40.61	9.87	9.18
***Podarcis* liolepis**	24-lio-C11	24-lio-C11	M	54.89	12.83	11.26
***Podarcis* liolepis**	24-lio-C12	24-lio-C12	M	51.05	12.31	11.45
***Podarcis* liolepis**	24-lio-C13	24-lio-C13	M	51.62	12.16	10.5
***Podarcis* liolepis**	24-lio-C14	24-lio-C14	M	42.42	10.88	8.76
***Podarcis* liolepis**	24-lio-C15	24-lio-C15	M	53.51	13.35	12.15
***Podarcis* liolepis**	24-lio-C7	24-lio-C7	M	40.64	9.94	8.3
***Podarcis* liolepis**	24-lio-H3	24-lio-H3	M	50.51	12	10.95
***Podarcis* melisellensis_fiumanaS**	Pmel_1	Pmel_1	M	63.69	13.94	12.06
***Podarcis* melisellensis_fiumanaS**	Pmel_11	Pmel_11	M	58.55	12.74	11.8
***Podarcis* melisellensis_fiumanaS**	Pmel_12	Pmel_12	M	55.05	11.94	10.91
***Podarcis* melisellensis_fiumanaS**	Pmel_13	Pmel_13	M	58.53	12.9	11.6
***Podarcis* melisellensis_fiumanaS**	Pmel_15	Pmel_15	M	63.47	13.93	12.49
***Podarcis* melisellensis_fiumanaS**	Pmel_16	Pmel_16	M	51.74	11.68	10.07
***Podarcis* melisellensis_fiumanaS**	Pmel_17	Pmel_17	M	56.47	12.15	10.72
***Podarcis* melisellensis_fiumanaS**	Pmel_18	Pmel_18	M	60.29	13.47	12.1
***Podarcis* melisellensis_fiumanaS**	Pmel_2	Pmel_2	M	54.49	12.1	12.75
***Podarcis* melisellensis_fiumanaS**	Pmel_3	Pmel_3	M	63.76	13.89	12.45
***Podarcis* melisellensis_fiumanaS**	Pmel_31	Pmel_31	M	53.94	11.97	10.18
***Podarcis* melisellensis_fiumanaS**	Pmel_33	Pmel_33	M	51.18	11.51	10.96
***Podarcis* melisellensis_fiumanaS**	Pmel_36	Pmel_36	M	54.94	12.49	10.92
***Podarcis* melisellensis_fiumanaS**	Pmel_38	Pmel_38	M	58.62	13	11.8
***Podarcis* melisellensis_fiumanaS**	Pmel_4	Pmel_4	M	53.99	12.31	10.74
***Podarcis* melisellensis_fiumanaS**	Pmel_5	Pmel_5	M	59.78	13.12	11.77

***Podarcis* melisellensis_fiumanaS**	Pmel_6	Pmel_6	M	58.33	12.54	11.16
***Podarcis* melisellensis_fiumanaS**	Pmel_7	Pmel_7	M	60.14	13.63	11.88
***Podarcis* melisellensis_fiumanaS**	Pmel_8	Pmel_8	M	55.77	12.19	11.2
***Podarcis* melisellensis_fiumanaS**	Pmel_9	Pmel_9	M	55.14	11.89	10.81
***Podarcis* milensis**	MILM11	MILM11	M	61.04	13.67	12
***Podarcis* milensis**	MILM13	MILM13	M	58.36	14.21	12.34
***Podarcis* milensis**	MILM16	MILM16	M	61.29	13.45	11.89
***Podarcis* milensis**	MILM18	MILM18	M	59.82	13.68	12.02
***Podarcis* milensis**	MILM19	MILM19	M	51.31	12.04	10.6
***Podarcis* milensis**	MILM2	MILM2	M	56.39	13.16	12.42
***Podarcis* milensis**	MILM3	MILM3	M	55.62	12.82	11.15
***Podarcis* milensis**	MILM6	MILM6	M	61.48	14.48	12.3
***Podarcis* milensis**	MILMB1	MILMB1	M	54.96	12.4	11.35
***Podarcis* milensis**	MILMB2	MILMB2	M	54.05	11.8	10.7
***Podarcis* milensis**	MILMB3	MILMB3	M	52.74	12.31	10.73
***Podarcis* milensis**	MILMB4	MILMB4	M	50.41	11.64	10.39
***Podarcis* milensis**	MILMB5	MILMB5	M	47.98	11.12	9.5
***Podarcis* muralis_LIN1**	FB010	FB010	M	66.91	16.14	13.99
***Podarcis* muralis_LIN1**	FB012	FB012	M	67.59	16.72	14.5
***Podarcis* muralis_LIN1**	FB013	FB013	M	69.53	17.18	14.2
***Podarcis* muralis_LIN1**	FB015	FB015	M	66.46	16.14	13.78
***Podarcis* muralis_LIN1**	FB017	FB017	M	69.15	16.36	14.79
***Podarcis* muralis_LIN1**	FB019	FB019	M	61.99	15	13.81
***Podarcis* muralis_LIN1**	FB024	FB024	M	71.97	16.86	14.58
***Podarcis* muralis_LIN1**	FB031	FB031	M	68.83	16.53	14.25
***Podarcis* muralis_LIN1**	FB032	FB032	M	64.67	16.57	15
***Podarcis* muralis_LIN1**	FB034	FB034	M	71.76	17.28	14.73
***Podarcis* muralis_LIN1**	FB035	FB035	M	68.96	17.59	15.71
***Podarcis* muralis_LIN1**	FB037	FB037	M	64.26	15.15	12.8
***Podarcis* muralis_LIN1**	FB038	FB038	M	69.44	16.91	15.09
***Podarcis* muralis_LIN1**	FB040	FB040	M	62.55	14.92	13.39
***Podarcis* muralis_LIN1**	FB041	FB041	M	70.73	17.19	14.93
***Podarcis* muralis_LIN1**	FB044	FB044	M	64.7	15.4	14.12
***Podarcis* muralis_LIN1**	FB047	FB047	M	63.38	14.49	12.95
***Podarcis* muralis_LIN1**	FB053	FB053	M	67.91	16.47	14.99
***Podarcis* muralis_LIN1**	FB058	FB058	M	62.17	15.14	13.35

***Podarcis* muralis_LIN1**	FB076	FB076	M	60.88	14.74	13.43
***Podarcis* peloponnesiaca_east**	PELEM1	PELEM1	M	84.8	20.03	17.14
***Podarcis* peloponnesiaca_east**	PELEM10	PELEM10	M	80.35	18.96	17
***Podarcis* peloponnesiaca_east**	PELEM11	PELEM11	M	79.14	18.68	16.65
***Podarcis* peloponnesiaca_east**	PELEM12	PELEM12	M	69.5	17	15.32
***Podarcis* peloponnesiaca_east**	PELEM13	PELEM13	M	69	15.35	14.16
***Podarcis* peloponnesiaca_east**	PELEM14	PELEM14	M	82.5	19.79	17.48
***Podarcis* peloponnesiaca_east**	PELEM15	PELEM15	M	80.24	19.72	17.56
***Podarcis* peloponnesiaca_east**	PELEM16	PELEM16	M	85.07	20.6	17.9
***Podarcis* peloponnesiaca_east**	PELEM17	PELEM17	M	81.6	19.64	17.6
***Podarcis* peloponnesiaca_east**	PELEM18	PELEM18	M	77.62	17.83	16.24
***Podarcis* peloponnesiaca_east**	PELEM19	PELEM19	M	72.69	16.34	15.08
***Podarcis* peloponnesiaca_east**	PELEM2	PELEM2	M	76.16	18.1	16.71
***Podarcis* peloponnesiaca_east**	PELEM21	PELEM21	M	74.72	16.64	15.15
***Podarcis* peloponnesiaca_east**	PELEM3	PELEM3	M	80.87	19.3	16.63
***Podarcis* peloponnesiaca_east**	PELEM4	PELEM4	M	75.61	18.74	16.65
***Podarcis* peloponnesiaca_east**	PELEM5	PELEM5	M	76.84	18.31	17.1
***Podarcis* peloponnesiaca_east**	PELEM6	PELEM6	M	67.38	15.56	14.32
***Podarcis* peloponnesiaca_east**	PELEM7	PELEM7	M	70.66	17.24	15.8
***Podarcis* peloponnesiaca_east**	PELEM9	PELEM9	M	84.6	20.3	18.77
***Podarcis* peloponnesiaca_west**	PELWM1	PELWM1	M	80.71	19.66	18.33
***Podarcis* peloponnesiaca_west**	PELWM10	PELWM10	M	86.14	20.83	19.42
***Podarcis* peloponnesiaca_west**	PELWM11	PELWM11	M	84.9	20.36	17.62
***Podarcis* peloponnesiaca_west**	PELWM12	PELWM12	M	77.16	18.1	16.69
***Podarcis* peloponnesiaca_west**	PELWM13	PELWM13	M	81.12	19.09	17.56
***Podarcis* peloponnesiaca_west**	PELWM15	PELWM15	M	79.57	19.45	16.81
***Podarcis* peloponnesiaca_west**	PELWM16	PELWM16	M	79.71	19.7	17.78
***Podarcis* peloponnesiaca_west**	PELWM17	PELWM17	M	79.67	19.29	17.51
***Podarcis* peloponnesiaca_west**	PELWM18	PELWM18	M	75.63	18.28	17.17
***Podarcis* peloponnesiaca_west**	PELWM19	PELWM19	M	78.03	19.24	17.43
***Podarcis* peloponnesiaca_west**	PELWM2	PELWM2	M	76.29	18.5	16.76
***Podarcis* peloponnesiaca_west**	PELWM20	PELWM20	M	74.95	18.31	15.75
***Podarcis* peloponnesiaca_west**	PELWM21	PELWM21	M	81.95	19.13	17.52
***Podarcis* peloponnesiaca_west**	PELWM3	PELWM3	M	69.75	16.87	14.23
***Podarcis* peloponnesiaca_west**	PELWM4	PELWM4	M	71.11	16.83	16.1
***Podarcis* peloponnesiaca_west**	PELWM5	PELWM5	M	79.07	19.07	17.02

***Podarcis* peloponnesiaca_west**	PELWM6	PELWM6	M	78.2	18.14	17.21
***Podarcis* peloponnesiaca_west**	PELWM7	PELWM7	M	81.14	19.69	17.19
***Podarcis* peloponnesiaca_west**	PELWM8	PELWM8	M	75.97	17.87	16.46
***Podarcis* peloponnesiaca_west**	PELWM9	PELWM9	M	79.18	19.14	18.47
***Podarcis* pityusensis**	P1	P1	M	73.68	17.49	14.77
***Podarcis* pityusensis**	P10	P10	M	69.62	15.79	13.99
***Podarcis* pityusensis**	P12	P12	M	66.81	15.41	13.57
***Podarcis* pityusensis**	P14	P14	M	73.28	17.81	15.58
***Podarcis* pityusensis**	P15	P15	M	72.45	17.15	14.69
***Podarcis* pityusensis**	P16	P16	M	73.09	16.83	13.65
***Podarcis* pityusensis**	P2	P2	M	73.23	16.9	14.73
***Podarcis* pityusensis**	P27	P27	M	65.36	15.95	13.76
***Podarcis* pityusensis**	P3	P3	M	77.86	19.44	16.53
***Podarcis* pityusensis**	P4	P4	M	77.53	17.41	15.65
***Podarcis* pityusensis**	P41	P41	M	60.05	14.44	12.31
***Podarcis* pityusensis**	P44	P44	M	59.36	13.8	11.37
***Podarcis* pityusensis**	P5	P5	M	73.91	17.66	14.29
***Podarcis* pityusensis**	P6	P6	M	75.96	17.9	15.42
***Podarcis* pityusensis**	P7	P7	M	73.27	17.07	14.84
***Podarcis* pityusensis**	P8	P8	M	79.06	18	15.39
***Podarcis* pityusensis**	PX1	PX1	M	73.48	16.39	14.14
***Podarcis* pityusensis**	PX2	PX2	M	73.13	17.43	15.88
***Podarcis* pityusensis**	PX3	PX3	M	77.32	17.93	15.99
***Podarcis* pityusensis**	PX4	PX4	M	75.02	18.83	16.04
***Podarcis* sicula_N**	19PSICNM1	19PSICNM1	M	61.2	14.65	12.92
***Podarcis* sicula_N**	19PSICNM10	19PSICNM10	M	75.23	18.4	15.8
***Podarcis* sicula_N**	19PSICNM11	19PSICNM11	M	62.38	14.9	13.21
***Podarcis* sicula_N**	19PSICNM12	19PSICNM12	M	77.81	18.04	16.07
***Podarcis* sicula_N**	19PSICNM13	19PSICNM13	M	72.34	17.62	15.63
***Podarcis* sicula_N**	19PSICNM14	19PSICNM14	M	75.45	18.26	16.07
***Podarcis* sicula_N**	19PSICNM15	19PSICNM15	M	72.14	17.59	14.47
***Podarcis* sicula_N**	19PSICNM16	19PSICNM16	M	77.75	19.53	17.14
***Podarcis* sicula_N**	19PSICNM17	19PSICNM17	M	73.57	18.05	15.77
***Podarcis* sicula_N**	19PSICNM18	19PSICNM18	M	79.47	18.63	16.21
***Podarcis* sicula_N**	19PSICNM19	19PSICNM19	M	80.33	19.96	17.51
***Podarcis* sicula_N**	19PSICNM2	19PSICNM2	M	63.04	14.48	12.53

***Podarcis* sicula_N**	19PSICNM20	19PSICNM20	M	76.68	17.96	15.54
***Podarcis* sicula_N**	19PSICNM3	19PSICNM3	M	63.47	14.61	12.91
***Podarcis* sicula_N**	19PSICNM4	19PSICNM4	M	75.14	18.58	16.45
***Podarcis* sicula_N**	19PSICNM5	19PSICNM5	M	74.11	18.44	17.02
***Podarcis* sicula_N**	19PSICNM6	19PSICNM6	M	77.86	18.55	15.84
***Podarcis* sicula_N**	19PSICNM7	19PSICNM7	M	64.9	15.25	13.73
***Podarcis* sicula_N**	19PSICNM8	19PSICNM8	M	76.86	17.97	15.46
***Podarcis* sicula_N**	19PSICNM9	19PSICNM9	M	74.75	18.52	16.4
***Podarcis* sicula_S**	A10	A10	M	72.87	18.98	16.79
***Podarcis* sicula_S**	A11	A11	M	71.68	19.15	17.38
***Podarcis* sicula_S**	A12	A12	M	76.61	19.06	17.5
***Podarcis* sicula_S**	A2	A2	M	76.49	19.28	17.57
***Podarcis* sicula_S**	A9	A9	M	79.38	19.79	16.28
***Podarcis* sicula_S**	D3	D3	M	73.23	18.27	16.85
***Podarcis* sicula_S**	D4	D4	M	58.12	14.39	13.1
***Podarcis* sicula_S**	D6	D6	M	72.98	18.38	16.42
***Podarcis* sicula_S**	S15	S15	M	75.05	19.54	16.26
***Podarcis* sicula_S**	S16	S16	M	81.04	19.37	17.77
***Podarcis* sicula_S**	S17	S17	M	79.252	19.33	16.77
***Podarcis* sicula_S**	S18	S18	M	75.89	19.72	17.29
***Podarcis* sicula_S**	S19	S19	M	78.74	19.29	17.42
***Podarcis* sicula_S**	S20	S20	M	73.35	18.88	17.19
***Podarcis* sicula_S**	S21	S21	M	80.13	20.41	17.24
***Podarcis* sicula_S**	S22	S22	M	75.7	19.04	16.51
***Podarcis* sicula_S**	S23	S23	M	76.06	19.7	16.85
***Podarcis* sicula_S**	S24	S24	M	71.87	18.97	16.37
***Podarcis* sicula_S**	S25	S25	M	75.5	19.19	17.15
***Podarcis* sicula_S**	S26	S26	M	73.21	19.54	18.04
***Podarcis* sicula_S**	S27	S27	M	76.76	19.55	17.46
***Podarcis* taurica_ionicus_A**	19-PTIA-M1	19-PTIA-M1	M	72.56	17.39	15.77
***Podarcis* taurica_ionicus_A**	19-PTIA-M10	19-PTIA-M10	M	65.14	15.86	14.16
***Podarcis* taurica_ionicus_A**	19-PTIA-M11	19-PTIA-M11	M	74.06	17.8	16.51
***Podarcis* taurica_ionicus_A**	19-PTIA-M12	19-PTIA-M12	M	73.25	17.89	15.7
***Podarcis* taurica_ionicus_A**	19-PTIA-M13	19-PTIA-M13	M	75.02	18.18	16.67
***Podarcis* taurica_ionicus_A**	19-PTIA-M14	19-PTIA-M14	M	73.5	17.54	15.7
***Podarcis* taurica_ionicus_A**	19-PTIA-M15	19-PTIA-M15	M	66.67	16.12	14.91

***Podarcis* taurica_ionicus_A**	19-PTIA-M16	19-PTIA-M16	M	68.67	16.41	14.81
***Podarcis* taurica_ionicus_A**	19-PTIA-M17	19-PTIA-M17	M	68.58	16.46	14.87
***Podarcis* taurica_ionicus_A**	19-PTIA-M18	19-PTIA-M18	M	65.55	15.35	13.87
***Podarcis* taurica_ionicus_A**	19-PTIA-M2	19-PTIA-M2	M	75.84	17.77	16.31
***Podarcis* taurica_ionicus_A**	19-PTIA-M3	19-PTIA-M3	M	66.24	15.12	14.09
***Podarcis* taurica_ionicus_A**	19-PTIA-M4	19-PTIA-M4	M	71.27	16.94	15.59
***Podarcis* taurica_ionicus_A**	19-PTIA-M5	19-PTIA-M5	M	76.75	17.61	15.31
***Podarcis* taurica_ionicus_A**	19-PTIA-M6	19-PTIA-M6	M	73.8	17.66	15.45
***Podarcis* taurica_ionicus_A**	19-PTIA-M7	19-PTIA-M7	M	72.67	16.75	15.34
***Podarcis* taurica_ionicus_A**	19-PTIA-M8	19-PTIA-M8	M	70.08	16.29	15.12
***Podarcis* taurica_ionicus_A**	19-PTIA-M9	19-PTIA-M9	M	73.3	17.63	16.37
***Podarcis* taurica_ionicus_C**	ionCM1	ionCM1	M	60.3	14.78	13.55
***Podarcis* taurica_ionicus_C**	ionCM10	ionCM10	M	61.24	14.12	12.52
***Podarcis* taurica_ionicus_C**	ionCM11	ionCM11	M	60.48	14.31	13.18
***Podarcis* taurica_ionicus_C**	ionCM12	ionCM12	M	63.11	15.09	14.11
***Podarcis* taurica_ionicus_C**	ionCM13	ionCM13	M	62.4	14.52	13.84
***Podarcis* taurica_ionicus_C**	ionCM14	ionCM14	M	73.25	17.61	15.76
***Podarcis* taurica_ionicus_C**	ionCM15	ionCM15	M	62.07	14.77	13.86
***Podarcis* taurica_ionicus_C**	ionCM16	ionCM16	M	73.2	17.66	16.23
***Podarcis* taurica_ionicus_C**	ionCM17	ionCM17	M	74.11	17.26	16.09
***Podarcis* taurica_ionicus_C**	ionCM18	ionCM18	M	65.26	15.16	14.89
***Podarcis* taurica_ionicus_C**	ionCM19	ionCM19	M	62.39	13.34	13.2
***Podarcis* taurica_ionicus_C**	ionCM2	ionCM2	M	63.57	13.81	13.2
***Podarcis* taurica_ionicus_C**	ionCM3	ionCM3	M	52.61	12.41	11.46
***Podarcis* taurica_ionicus_C**	ionCM4	ionCM4	M	59.84	13.46	12.38
***Podarcis* taurica_ionicus_C**	ionCM5	ionCM5	M	55.21	12.68	11.72
***Podarcis* taurica_ionicus_C**	ionCM6	ionCM6	M	53.57	12.43	11.74
***Podarcis* taurica_ionicus_C**	ionCM7	ionCM7	M	56.07	13.08	11.69
***Podarcis* taurica_ionicus_C**	ionCM8	ionCM8	M	59.37	13.56	12.04
***Podarcis* taurica_ionicus_C**	ionCM9	ionCM9	M	63.44	15.07	13.44
***Podarcis* taurica_ionicus_E**	19-PTIE-M1	19-PTIE-M1	M	75.25	17.28	16.69
***Podarcis* taurica_ionicus_E**	19-PTIE-M10	19-PTIE-M10	M	69.11	15.5	13.76
***Podarcis* taurica_ionicus_E**	19-PTIE-M11	19-PTIE-M11	M	67.77	15.67	14.27
***Podarcis* taurica_ionicus_E**	19-PTIE-M12	19-PTIE-M12	M	69.87	15.66	13.86
***Podarcis* taurica_ionicus_E**	19-PTIE-M13	19-PTIE-M13	M	68.46	15.94	14.5
***Podarcis* taurica_ionicus_E**	19-PTIE-M14	19-PTIE-M14	M	70.37	16.32	14.96

***Podarcis* taurica_ionicus_E**	19-PTIE-M15	19-PTIE-M15	M	72.09	16.55	15.55
***Podarcis* taurica_ionicus_E**	19-PTIE-M16	19-PTIE-M16	M	62.42	14.65	12.94
***Podarcis* taurica_ionicus_E**	19-PTIE-M17	19-PTIE-M17	M	69.98	16.57	14.98
***Podarcis* taurica_ionicus_E**	19-PTIE-M18	19-PTIE-M18	M	74.37	17.52	15.67
***Podarcis* taurica_ionicus_E**	19-PTIE-M2	19-PTIE-M2	M	71.07	15.75	14.81
***Podarcis* taurica_ionicus_E**	19-PTIE-M3	19-PTIE-M3	M	74.86	17.67	16.16
***Podarcis* taurica_ionicus_E**	19-PTIE-M4	19-PTIE-M4	M	79.06	18.32	17.18
***Podarcis* taurica_ionicus_E**	19-PTIE-M5	19-PTIE-M5	M	72.72	16.47	14.71
***Podarcis* taurica_ionicus_E**	19-PTIE-M6	19-PTIE-M6	M	72.41	16.48	14.24
***Podarcis* taurica_ionicus_E**	19-PTIE-M7	19-PTIE-M7	M	66.13	15.08	13.25
***Podarcis* taurica_ionicus_E**	19-PTIE-M8	19-PTIE-M8	M	72.23	16.64	14.55
***Podarcis* taurica_ionicus_E**	19-PTIE-M9	19-PTIE-M9	M	74.65	16.59	15.58
***Podarcis* taurica_tauricus**	19-PTT-M1	19-PTT-M1	M	62.07	13.34	12.02
***Podarcis* taurica_tauricus**	19-PTT-M10	19-PTT-M10	M	69.76	16.18	15.02
***Podarcis* taurica_tauricus**	19-PTT-M11	19-PTT-M11	M	57.77	12.54	11.41
***Podarcis* taurica_tauricus**	19-PTT-M12	19-PTT-M12	M	63.83	14.31	13.15
***Podarcis* taurica_tauricus**	19-PTT-M13	19-PTT-M13	M	60.1	13.42	12.28
***Podarcis* taurica_tauricus**	19-PTT-M14	19-PTT-M14	M	56.41	12.89	11.66
***Podarcis* taurica_tauricus**	19-PTT-M15	19-PTT-M15	M	62.12	13.67	12.16
***Podarcis* taurica_tauricus**	19-PTT-M16	19-PTT-M16	M	60	13.31	11.82
***Podarcis* taurica_tauricus**	19-PTT-M17	19-PTT-M17	M	53.29	11.71	10.48
***Podarcis* taurica_tauricus**	19-PTT-M18	19-PTT-M18	M	60.04	12.78	11.7
***Podarcis* taurica_tauricus**	19-PTT-M19	19-PTT-M19	M	72.36	15.88	14.66
***Podarcis* taurica_tauricus**	19-PTT-M2	19-PTT-M2	M	71.66	16.54	14.69
***Podarcis* taurica_tauricus**	19-PTT-M20	19-PTT-M20	M	56.58	12.41	11.43
***Podarcis* taurica_tauricus**	19-PTT-M21	19-PTT-M21	M	56.51	12.88	11.59
***Podarcis* taurica_tauricus**	19-PTT-M3	19-PTT-M3	M	58.51	12.11	10.81
***Podarcis* taurica_tauricus**	19-PTT-M4	19-PTT-M4	M	65.41	14.47	12.8
***Podarcis* taurica_tauricus**	19-PTT-M5	19-PTT-M5	M	65.09	14.58	13.1
***Podarcis* taurica_tauricus**	19-PTT-M7	19-PTT-M7	M	60.84	14.03	11.82
***Podarcis* taurica_tauricus**	19-PTT-M8	19-PTT-M8	M	62.82	13.97	12.46
***Podarcis* taurica_tauricus**	19-PTT-M9	19-PTT-M9	M	62.23	13.71	12.77
***Podarcis* tiliguerta_Lin1**	19PTIL1M1	19PTIL1M1	M	58.91	13.65	11.55
***Podarcis* tiliguerta_Lin1**	19PTIL1M10	19PTIL1M10	M	59.22	14.11	11.83
***Podarcis* tiliguerta_Lin1**	19PTIL1M11	19PTIL1M11	M	57.97	13.83	11.84
***Podarcis* tiliguerta_Lin1**	19PTIL1M12	19PTIL1M12	M	60.13	14.9	12.74

***Podarcis* tiliguerta_Lin1**	19PTIL1M13	19PTIL1M13	M	62.52	14.84	12.86
***Podarcis* tiliguerta_Lin1**	19PTIL1M14	19PTIL1M14	M	60.69	13.69	12.17
***Podarcis* tiliguerta_Lin1**	19PTIL1M15	19PTIL1M15	M	62.95	14.54	12.4
***Podarcis* tiliguerta_Lin1**	19PTIL1M16	19PTIL1M16	M	58.31	13.65	11.55
***Podarcis* tiliguerta_Lin1**	19PTIL1M17	19PTIL1M17	M	59.88	13.69	11.58
***Podarcis* tiliguerta_Lin1**	19PTIL1M18	19PTIL1M18	M	61.93	14.41	12.55
***Podarcis* tiliguerta_Lin1**	19PTIL1M19	19PTIL1M19	M	56.48	13.46	11.25
***Podarcis* tiliguerta_Lin1**	19PTIL1M2	19PTIL1M2	M	58.71	13.91	12.11
***Podarcis* tiliguerta_Lin1**	19PTIL1M20	19PTIL1M20	M	61.11	14.2	12.41
***Podarcis* tiliguerta_Lin1**	19PTIL1M3	19PTIL1M3	M	61.03	14.82	12.19
***Podarcis* tiliguerta_Lin1**	19PTIL1M4	19PTIL1M4	M	59.74	14.69	12.3
***Podarcis* tiliguerta_Lin1**	19PTIL1M5	19PTIL1M5	M	62.7	14.65	12.79
***Podarcis* tiliguerta_Lin1**	19PTIL1M6	19PTIL1M6	M	64.32	15	12.38
***Podarcis* tiliguerta_Lin1**	19PTIL1M7	19PTIL1M7	M	59.83	14.81	12.32
***Podarcis* tiliguerta_Lin1**	19PTIL1M8	19PTIL1M8	M	60.15	14.17	11.77
***Podarcis* tiliguerta_Lin1**	19PTIL1M9	19PTIL1M9	M	60.74	15.28	12.9
***Podarcis* tiliguerta_Lin2**	19PTIL2M1	19PTIL2M1	M	60.83	14.6	12.75
***Podarcis* tiliguerta_Lin2**	19PTIL2M10	19PTIL2M10	M	60.15	14.47	11.62
***Podarcis* tiliguerta_Lin2**	19PTIL2M11	19PTIL2M11	M	61.23	14.39	11.93
***Podarcis* tiliguerta_Lin2**	19PTIL2M12	19PTIL2M12	M	59.3	14.75	12.73
***Podarcis* tiliguerta_Lin2**	19PTIL2M13	19PTIL2M13	M	59.44	14.94	12.45
***Podarcis* tiliguerta_Lin2**	19PTIL2M14	19PTIL2M14	M	58.35	13.94	11.78
***Podarcis* tiliguerta_Lin2**	19PTIL2M15	19PTIL2M15	M	59.36	14.15	12.5
***Podarcis* tiliguerta_Lin2**	19PTIL2M16	19PTIL2M16	M	59.07	14.4	11.9
***Podarcis* tiliguerta_Lin2**	19PTIL2M17	19PTIL2M17	M	59.38	13.8	12.16
***Podarcis* tiliguerta_Lin2**	19PTIL2M18	19PTIL2M18	M	63.76	14.37	12.38
***Podarcis* tiliguerta_Lin2**	19PTIL2M19	19PTIL2M19	M	62.45	14.94	12.85
***Podarcis* tiliguerta_Lin2**	19PTIL2M2	19PTIL2M2	M	61.65	14.41	12.13
***Podarcis* tiliguerta_Lin2**	19PTIL2M20	19PTIL2M20	M	60.55	14.93	12.3
***Podarcis* tiliguerta_Lin2**	19PTIL2M21	19PTIL2M21	M	59.61	14.02	11.96
***Podarcis* tiliguerta_Lin2**	19PTIL2M3	19PTIL2M3	M	60.4	14.29	12.13
***Podarcis* tiliguerta_Lin2**	19PTIL2M5	19PTIL2M5	M	59.86	14.15	12.45
***Podarcis* tiliguerta_Lin2**	19PTIL2M6	19PTIL2M6	M	60.09	14.22	12.39
***Podarcis* tiliguerta_Lin2**	19PTIL2M7	19PTIL2M7	M	60.11	14.54	12.04
***Podarcis* tiliguerta_Lin2**	19PTIL2M8	19PTIL2M8	M	61.09	14.27	12.3
***Podarcis* tiliguerta_Lin2**	19PTIL2M9	19PTIL2M9	M	57.33	13.59	11.79

***Podarcis* tiliguerta_Lin3**	19PTIL3M1	19PTIL3M1	M	67.01	16.49	13.81
***Podarcis* tiliguerta_Lin3**	19PTIL3M10	19PTIL3M10	M	65.3	16.45	13.56
***Podarcis* tiliguerta_Lin3**	19PTIL3M12	19PTIL3M12	M	61.82	15.17	12.93
***Podarcis* tiliguerta_Lin3**	19PTIL3M13	19PTIL3M13	M	66.11	15.48	13.05
***Podarcis* tiliguerta_Lin3**	19PTIL3M15	19PTIL3M15	M	65.87	15.71	13.81
***Podarcis* tiliguerta_Lin3**	19PTIL3M16	19PTIL3M16	M	62.51	15.37	13.08
***Podarcis* tiliguerta_Lin3**	19PTIL3M17	19PTIL3M17	M	65.91	16.31	13.7
***Podarcis* tiliguerta_Lin3**	19PTIL3M18	19PTIL3M18	M	64.75	15.69	12.29
***Podarcis* tiliguerta_Lin3**	19PTIL3M2	19PTIL3M2	M	64.86	15.84	13.75
***Podarcis* tiliguerta_Lin3**	19PTIL3M20	19PTIL3M20	M	53.78	13.11	11.09
***Podarcis* tiliguerta_Lin3**	19PTIL3M21	19PTIL3M21	M	65.37	15.52	13.38
***Podarcis* tiliguerta_Lin3**	19PTIL3M22	19PTIL3M22	M	56.98	13.95	11.46
***Podarcis* tiliguerta_Lin3**	19PTIL3M3	19PTIL3M3	M	68.26	16.45	13
***Podarcis* tiliguerta_Lin3**	19PTIL3M4	19PTIL3M4	M	64.4	16.1	13.54
***Podarcis* tiliguerta_Lin3**	19PTIL3M5	19PTIL3M5	M	67.54	16.02	13.64
***Podarcis* tiliguerta_Lin3**	19PTIL3M6	19PTIL3M6	M	68.04	16.27	13.9
***Podarcis* tiliguerta_Lin3**	19PTIL3M7	19PTIL3M7	M	65.4	16.2	13.74
***Podarcis* tiliguerta_Lin3**	19PTIL3M9	19PTIL3M9	M	64.28	15.54	13.08
***Podarcis* tiliguerta_Lin4**	19PTIL4M1	19PTIL4M1	M	65.6	15.3	13.23
***Podarcis* tiliguerta_Lin4**	19PTIL4M10	19PTIL4M10	M	65.63	16.02	13.33
***Podarcis* tiliguerta_Lin4**	19PTIL4M11	19PTIL4M11	M	65.21	16.4	13.51
***Podarcis* tiliguerta_Lin4**	19PTIL4M12	19PTIL4M12	M	65.85	15.53	13.47
***Podarcis* tiliguerta_Lin4**	19PTIL4M13	19PTIL4M13	M	62.63	16.09	13.9
***Podarcis* tiliguerta_Lin4**	19PTIL4M14	19PTIL4M14	M	66.78	16.89	14.12
***Podarcis* tiliguerta_Lin4**	19PTIL4M15	19PTIL4M15	M	65.83	15.23	13.15
***Podarcis* tiliguerta_Lin4**	19PTIL4M16	19PTIL4M16	M	66.01	15.29	12.96
***Podarcis* tiliguerta_Lin4**	19PTIL4M17	19PTIL4M17	M	67.39	16.19	13.9
***Podarcis* tiliguerta_Lin4**	19PTIL4M18	19PTIL4M18	M	64.54	16.01	13.15
***Podarcis* tiliguerta_Lin4**	19PTIL4M19	19PTIL4M19	M	66.5	15.87	13
***Podarcis* tiliguerta_Lin4**	19PTIL4M2	19PTIL4M2	M	63.57	14.97	12.94
***Podarcis* tiliguerta_Lin4**	19PTIL4M20	19PTIL4M20	M	67.2	15.96	13.93
***Podarcis* tiliguerta_Lin4**	19PTIL4M3	19PTIL4M3	M	68.77	17	14.28
***Podarcis* tiliguerta_Lin4**	19PTIL4M4	19PTIL4M4	M	66.09	15.79	12.9
***Podarcis* tiliguerta_Lin4**	19PTIL4M5	19PTIL4M5	M	65.05	15.45	13.28
***Podarcis* tiliguerta_Lin4**	19PTIL4M6	19PTIL4M6	M	65.52	15.55	13.08
***Podarcis* tiliguerta_Lin4**	19PTIL4M7	19PTIL4M7	M	65	15.46	12.81

***Podarcis* tiliguerta_Lin4**	19PTIL4M8	19PTIL4M8	M	70.98	17.01	14.68
***Podarcis* tiliguerta_Lin4**	19PTIL4M9	19PTIL4M9	M	64.63	14.9	13.33
***Podarcis* vaucheri**	V10	V10	M	55.9	13.54	11.46
***Podarcis* vaucheri**	V11	V11	M	53.33	13.15	10.47
***Podarcis* vaucheri**	V13	V13	M	54.64	13.51	11.53
***Podarcis* vaucheri**	V16	V16	M	52.07	12.97	10.51
***Podarcis* vaucheri**	V2	V2	M	63.42	15.34	12.91
***Podarcis* vaucheri**	V22	V22	M	49.68	12.49	10.92
***Podarcis* vaucheri**	V24	V24	M	53.78	13.33	11.66
***Podarcis* vaucheri**	V26	V26	M	58.27	14.57	12.08
***Podarcis* vaucheri**	V27	V27	M	57.96	14.6	13.17
***Podarcis* vaucheri**	V3	V3	M	59.21	14.29	12.53
***Podarcis* vaucheri**	V30	V30	M	57.41	13.92	11.61
***Podarcis* vaucheri**	V35	V35	M	58.37	14.49	11.82
***Podarcis* vaucheri**	V39	V39	M	56.73	13.92	12.16
***Podarcis* vaucheri**	V4	V4	M	65.26	16.11	13.28
***Podarcis* vaucheri**	V40	V40	M	53.29	13.56	12.09
***Podarcis* vaucheri**	V5	V5	M	60.98	14.49	12.98
***Podarcis* vaucheri**	V6	V6	M	59.12	14.2	11.68
***Podarcis* vaucheri**	V7	V7	M	60.74	14.72	12.93
***Podarcis* vaucheri**	V9	V9	M	50.47	11.68	10.01
***Podarcis* vaucheri_Mor_Alg**	PVMAM1	PVMAM1	M	58.74	13.94	12.21
***Podarcis* vaucheri_Mor_Alg**	PVMAM10	PVMAM10	M	52.55	12.26	10.63
***Podarcis* vaucheri_Mor_Alg**	PVMAM11	PVMAM11	M	52.07	12.36	10.68
***Podarcis* vaucheri_Mor_Alg**	PVMAM12	PVMAM12	M	54.37	12.73	10.82
***Podarcis* vaucheri_Mor_Alg**	PVMAM13	PVMAM13	M	53.1	12.42	10.66
***Podarcis* vaucheri_Mor_Alg**	PVMAM14	PVMAM14	M	54.61	12.37	11.04
***Podarcis* vaucheri_Mor_Alg**	PVMAM15	PVMAM15	M	46.88	10.75	9.67
***Podarcis* vaucheri_Mor_Alg**	PVMAM16	PVMAM16	M	47.39	11	9.48
***Podarcis* vaucheri_Mor_Alg**	PVMAM17	PVMAM17	M	52.14	12.41	11.08
***Podarcis* vaucheri_Mor_Alg**	PVMAM18	PVMAM18	M	54.33	12.85	10.69
***Podarcis* vaucheri_Mor_Alg**	PVMAM19	PVMAM19	M	57.27	13.25	11.98
***Podarcis* vaucheri_Mor_Alg**	PVMAM2	PVMAM2	M	53.9	12.54	10.83
***Podarcis* vaucheri_Mor_Alg**	PVMAM20	PVMAM20	M	50.75	11.7	9.95
***Podarcis* vaucheri_Mor_Alg**	PVMAM3	PVMAM3	M	53.45	12.64	10.34
***Podarcis* vaucheri_Mor_Alg**	PVMAM4	PVMAM4	M	49.48	11.37	9.9

***Podarcis* vaucheri_Mor_Alg**	PVMAM5	PVMAM5	M	57.26	12.91	10.52
***Podarcis* vaucheri_Mor_Alg**	PVMAM6	PVMAM6	M	46.93	10.61	9.21
***Podarcis* vaucheri_Mor_Alg**	PVMAM7	PVMAM7	M	47.73	11.91	10.19
***Podarcis* vaucheri_Mor_Alg**	PVMAM8	PVMAM8	M	48.18	11.18	9.8
***Podarcis* vaucheri_Mor_Alg**	PVMAM9	PVMAM9	M	50.69	12.15	11.12
***Podarcis* virescens**	PH2_20	PH2_20	M	61.5	14.77	13.45
***Podarcis* virescens**	PH2_21	PH2_21	M	58.81	14.45	12.87
***Podarcis* virescens**	PH2_22	PH2_22	M	50.54	11.83	10.14
***Podarcis* virescens**	PH2_51	PH2_51	M	61.86	14.76	12.93
***Podarcis* virescens**	PH2_52	PH2_52	M	60.28	14.72	12.48
***Podarcis* virescens**	PH2_53	PH2_53	M	52.62	12.49	10.76
***Podarcis* virescens**	PH2_54	PH2_54	M	60.04	14.21	12.23
***Podarcis* virescens**	PH2_55	PH2_55	M	52.36	12.84	11.13
***Podarcis* virescens**	PH2_8	PH2_8	M	65.81	15.59	13.37
***Podarcis* virescens**	PH2_9	PH2_9	M	53.2	12.92	11.29
***Podarcis* wagleriana**	W1	W1	M	67.14	16.26	14.92
***Podarcis* wagleriana**	W10	W10	M	72.79	16.69	14.94
***Podarcis* wagleriana**	W11	W11	M	69.54	17.2	15.64
***Podarcis* wagleriana**	W12	W12	M	73.21	17.52	16.56
***Podarcis* wagleriana**	W13	W13	M	69.56	16.47	15.15
***Podarcis* wagleriana**	W14	W14	M	63.35	13.71	12.35
***Podarcis* wagleriana**	W18	W18	M	72.38	18.05	15.78
***Podarcis* wagleriana**	W2	W2	M	62.45	14.76	14.06
***Podarcis* wagleriana**	W20	W20	M	68.41	16.9	15.05
***Podarcis* wagleriana**	W21	W21	M	59	13.94	12.49
***Podarcis* wagleriana**	W23	W23	M	69.34	16.4	14.47
***Podarcis* wagleriana**	W29	W29	M	70.11	16.79	15.6
***Podarcis* wagleriana**	W33	W33	M	65.18	15.84	14.95
***Podarcis* wagleriana**	W34	W34	M	67.05	16.34	15.5
***Podarcis* wagleriana**	W37	W37	M	69.2	16.92	14.88
***Podarcis* wagleriana**	W4	W4	M	69.92	16.56	15.19
***Podarcis* wagleriana**	W6	W6	M	72.83	17.67	16.01
***Podarcis* wagleriana**	W7	W7	M	72.17	17.15	15.71
***Podarcis* wagleriana**	W8	W8	M	72.4	17.17	15.5
***Podarcis* wagleriana**	W9	W9	M	68.75	17.27	15.48
Psammodromus algirus	Psammodromus_algirus_01	1905.11.28.40	M	75.76	19.05	14.12

Psammodromus hispanicus	Psammodromus_hispanicus_01	1894.6.1.19	M	41.43	10.17	6.8
Scelarcis perspicillata	Scelarcis_perspicillata_01	24Sper01	M	48.61	19.93	8.76
Takydromus septentrionalis	Takydromus_septentrionalis_01	1888.1.30.10	M	63.43	15.51	9.96
Takydromus septentrionalis	Takydromus_septentrionalis_02	1888.1.30.11	M	62.89	15.54	10.54
Takydromus sexlineatus	Takydromus_sexlineatus_01	1995.5.6	M	56.85	13.51	10.51
Takydromus sexlineatus	Takydromus_sexlineatus_02	72.2.14.2	M	58.76	14.69	10.48
Teira dugesii	Teira_dugesii_01	24Tdug01	M	72.11	17.79	11.63
Teira dugesii	Teira_dugesii_03	24Tdug03	M	68.79	16.19	10.44
Teira dugesii	Teira_dugesii_04	24Tdug04	M	70.61	16.56	9.55
Teira dugesii	Teira_dugesii_06	24Tdug06	M	67.54	16.67	10.56
Teira dugesii	Teira_dugesii_07	24Tdug07	M	71.43	17.55	11.32
Teira dugesii	Teira_dugesii_12	24Tdug12	M	68.55	17.22	10.63
Teira dugesii	Teira_dugesii_13	24Tdug13	M	72.80	17.74	11.40
Teira dugesii	Teira_dugesii_14	24Tdug14	M	69.19	16.07	10.94
Teira dugesii	Teira_dugesii_16	24Tdug16	M	67.29	17.15	10.20
Teira dugesii	Teira_dugesii_17	24Tdug17	M	69.24	16.13	10.73
Teira dugesii	Teira_dugesii_18	24Tdug18	M	74.65	18.49	11.42
Timon lepidus	Timon_lepidus_01	3558	M	207	65.5	54.38
Timon lepidus	Timon_lepidus_02	3560	M	209	58.78	56.44
Timon lepidus	Timon_lepidus_03	6120	M	248	71.22	63.38
Timon lepidus	Timon_lepidus_04	32686	M	215	58.45	54.33
Timon lepidus	Timon_lepidus_05	36043	M	205	53.11	50.49
Timon lepidus	Timon_lepidus_06	37277	M	205	58.95	53.45
Timon lepidus	Timon_lepidus_07	40524	M	206	55.95	50.19
Timon lepidus	Timon_lepidus_08	67/1976	M	208	58.9	53.85
Timon lepidus	Timon_lepidus_09	69/1976/1	M	221	60.5	55.97
Timon tangitanus	Timon_tangitanus_01	24Ttan01	M	155.92	40.22	33.40
Tropidosaura essexi	Tropidosaura_essexi_01	1976.1819	M	45	9.99	8.68
Zootoca vivipara	Zootoca_vivipara_01	92.2.11.2	M	43.05	9.79	7.75
Zootoca vivipara	Zootoca_vivipara_02	1940.2.21.11	M	46.44	11.28	8.47
Zootoca vivipara	Zootoca_vivipara_03	86.9.9.3	M	52.48	11.56	8.87

Table S5.2. Results of the phylogenetic signal analysis of allometric corrected lateral and dorsal shape, bite force, and snout-to-vent length. Significant p-values (at α = 0.05) are highlighted in bold.

Trait	K	p-val	Z	K≠1 (p-val)	Z	trace(K)	p-val	Z	det(K)	p-val	Z	Kmult	p-val	Z
Lateral shape	0.515	**0.001**	11.589	**0.001**	-5.165	6.219	**0.001**	13.807	3.863e-07	**0.001**	8.713	0.215	**0.001**	7.863
Dosal shape	0.505	**0.001**	31.591	**0.001**	-5.767	3.270	**0.001**	9.438	1.289E-04	**0.001**	7.847	0.152	**0.001**	5.495
Bite force	0.329	**0.002**	3.090	**0.001**	-3.41									
Snout-vent length	0.625	**0.001**	7.929	0.175	-0.982									

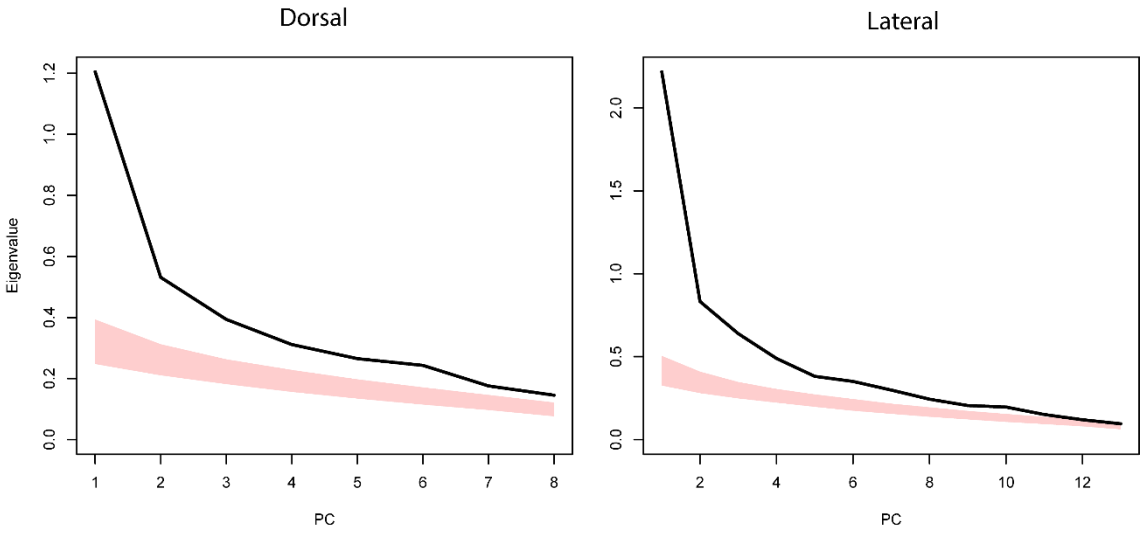

Figure S1. Eigenvalues of K for the dorsal and lateral shape data (black line) represents the relative strength of phylogenetic signal for each K-component. The red polygon represents the 95% interval from 1000 random permutations.

Table S5.3. Results of regressions conducted to test for differences in dorsal allometry at different biological levels: using *Podarcis* individuals, *Podarcis* species and all Lacertidae species in this study. d.f.: degrees of freedom; R2: R squared; F: F-value; Z: Z-score. P-values are based on 1000 residual permutations and significant p-values (at α = 0.05) are highlighted in bold.

	Df	*SS*	*MS*	*Rsq*	*F*	*Z*	*Pr(>F)*
***Podarcis* individuals**							
Dorsal shape ~ SVL							
SVL	1	0.082	0.082	0.099	73.287	10.865	**0.001**
Residuals	668	0.746	0.001	0.901			
Total	669	0.828					
***Podarcis* species**							
Dorsal shape ~ SVL							
	Df	SS	MS	Rsq	F	Z	Pr(>F)
SVL	1	0.003	0.003	0.247	6.573	3.568	**0.001**
Residuals	20	0.008	0.000	0.753			
Total	21	0.011					
Lacertidae species							
Dorsal shape ~ SVL							
	Df	SS	MS	Rsq	F	Z	Pr(>F)
SVL	1	0.051	0.051	0.134	10.675	3.496	**0.001**
Residuals	69	0.330	0.005	0.866			
Total	70	0.381					

Table S5.4. Results of regressions conducted to test for differences in lateral allometry at different biological levels: using *Podarcis* individuals, *Podarcis* species and all Lacertidae species in this study. d.f.: degrees of freedom; R2: R squared; F: F-value; Z: Z-score. P-values are based on 1000 residual permutations and significant p-values (at α = 0.05) are highlighted in bold.

	Df	*SS*	*MS*	*Rsq*	*F*	*Z*	*Pr(>F)*
***Podarcis* individuals**							
Lateral shape ~ SVL							
SVL	1	0.087	0.087	0.048	33.268	9.829	**0.001**
Residuals	661	1.734	0.003	0.952			
Total	662	1.821					
***Podarcis* species**							
Lateral shape ~ SVL							
	Df	SS	MS	Rsq	F	Z	Pr(>F)
SVL	1	0.003	0.003	0.099	2.201	1.654	0.054
Residuals	20	0.023	0.001	0.901			
Total	21	0.026					
Lacertidae species							
Lateral shape ~ SVL							
	Df	SS	MS	Rsq	F	Z	Pr(>F)
SVL	1	0.028	0.028	0.060	4.384	2.823	**0.002**
Residuals	69	0.436	0.006	0.940			
Total	70	0.464					

Table S5.5. Results of regressions conducted to test for differences in bite force allometry. d.f.: degrees of freedom; R2: R squared; F: F-value; Z: Z-score. P-values are based on 1000 residual permutations and significant p-values (at α = 0.05) are highlighted in bold.

	Df	*SS*	*MS*	*Rsq*	*F*	*Z*	*Pr(>F)*
SVL	1	50.089	50.089	0.759	217.710	7.126	**0.001**
Residuals	69	15.875	0.230	0.241			
Total	70	65.963					

Table S5.6. Results of phylogenetic regressions conducted to test for differences in raw dorsal shape and bite force relationship at different biological levels: using *Podarcis* individuals, *Podarcis* species and all Lacertidae species in this study. d.f.: degrees of freedom; R2: R squared; F: F-value; Z: Z-score. P-values are based on 1000 residual permutations and significant p-values (at α = 0.05) are highlighted in bold.

	Df	SS	MS	Rsq	F	Z	P-val
***Podarcis* individuals**							
Dorsal shape ~ Bite force * species I *Podarcis* phylogeny							
bite	1	0.023	0.023	0.027	29.485	5.752	**0.001**
sp	21	0.237	0.011	0.286	14.703	20.513	**0.001**
bite:sp	21	0.036	0.002	0.044	2.243	6.260	**0.001**
Residuals	626	0.480	0.001	0.579			
Total	669	0.828					
***Podarcis* species**							
Dorsal shape ~ Bite force I *Podarcis* phylogeny							
bite	1	1.37E-04	1.37E-04	0.134	3.085	1.946	**0.026**
Residuals	20	0.001	4.43E-05	0.866			
Total	21	0.001					
Lacertidae species							
Dorsal shape ~ Bite force I Lacertidae phylogeny							
bite	1	1.82E-04	1.82E-04	0.018	1.261	0.624	0.281
Residuals	69	0.010	1.44E-04	0.982			
Total	70	0.010					

Table S5.7. Results of phylogenetic regressions conducted to test for differences in raw lateral shape and bite force relationship at different biological levels: using *Podarcis* individuals, *Podarcis* species and all Lacertidae species in this study. d.f.: degrees of freedom; R2: R squared; F: F-value; Z: Z-score. P-values are based on 1000 residual permutations and significant p-values (at α = 0.05) are highlighted in bold.

	Df	SS	MS	Rsq	F	Z	P-val
***Podarcis* individuals**							
Lateral shape ~ Bite force * species I *Podarcis* phylogeny							
bite	1	0.026	0.026	0.014	14.896	6.569	**0.001**
sp	21	0.581	0.028	0.319	15.869	22.298	**0.001**
bite:sp	21	0.063	0.003	0.035	1.730	4.278	**0.001**
Residuals	619	1.080	0.002	0.593			
Total	662	1.821					
***Podarcis* species**							
Lateral shape ~ Bite force I *Podarcis* phylogeny							
bite	1	0.000	0.000	0.037	0.772	-0.372	0.628
Residuals	20	0.002	0.000	0.963			
Total	21	0.002					
Lacertidae species							
Lateral shape ~ Bite force I Lacertidae phylogeny							
bite	1	0.001	0.001	0.043	3.081	2.422	**0.009**
Residuals	69	0.013	0.000	0.957			
Total	70	0.014					

Table S5.8. Results of phylogenetic regressions conducted to test for differences in allometric-corrected dorsal shape and bite force relationship at different biological levels: using *Podarcis* individuals, *Podarcis* species and all Lacertidae species in this study. d.f.: degrees of freedom; R2: R squared; F: F-value; Z: Z-score. P-values are based on 1000 residual permutations and significant p-values (at α = 0.05) are highlighted in bold.

	Df	SS	MS	Rsq	F	Z	P-val
***Podarcis* individuals**							
Dorsal shape ~ Bite force * species I *Podarcis* phylogeny							
bite	1	0.003	0.003	0.004	3.772	2.704	**0.005**
sp	21	0.250	0.012	0.323	15.717	17.473	**0.001**
bite:sp	21	0.045	0.002	0.057	2.795	8.193	**0.001**
Residuals	626	0.475	0.001	0.612			
Total	669	0.776					
***Podarcis* species**							
Dorsal shape ~ Bite force I *Podarcis* phylogeny							
bite	1	1.04E-04	1.04E-04	0.108	2.410	1.647	0.055
Residuals	20	0.001	4.33E-05	0.892			
Total	21	0.001					
Lacertidae species							
Dorsal shape ~ Bite force I Lacertidae phylogeny							
bite	1	0.001	0.001	0.111	8.577	2.729	**0.003**
Residuals	69	0.010	1.43E-04	0.889			
Total	70	0.011					

Table S5.9. Results of phylogenetic regressions conducted to test for differences in allometric-corrected lateral shape and bite force relationship at different biological levels: using *Podarcis* individuals, *Podarcis* species and all Lacertidae species in this study. d.f.: degrees of freedom; R2: R squared; F: F-value; Z: Z-score. P-values are based on 1000 residual permutations and significant p-values (at α = 0.05) are highlighted in bold.

	Df	SS	MS	Rsq	F	Z	P-val
***Podarcis* individuals**							
Lateral shape ~ Bite force * species I *Podarcis* phylogeny							
bite	1	0.010	0.010	0.006	5.626	3.857	**0.001**
sp	21	0.615	0.029	0.344	16.761	21.347	**0.001**
bite:sp	21	0.068	0.003	0.038	1.842	5.475	**0.001**
Residuals	619	1.081	0.002	0.605			
Total	662	1.785					
***Podarcis* species**							
Lateral shape ~ Bite force I *Podarcis* phylogeny							
bite	1	1.25E-04	1.25E-04	0.056	1.185	0.505	0.316
Residuals	20	0.002	1.06E-04	0.944			
Total	21	0.002					
Lacertidae species							
Lateral shape ~ Bite force I Lacertidae phylogeny							
bite	1	0.001	0.001	0.083	6.236	2.925	**0.001**
Residuals	69	0.013	0.000	0.917			
Total	70	0.014					

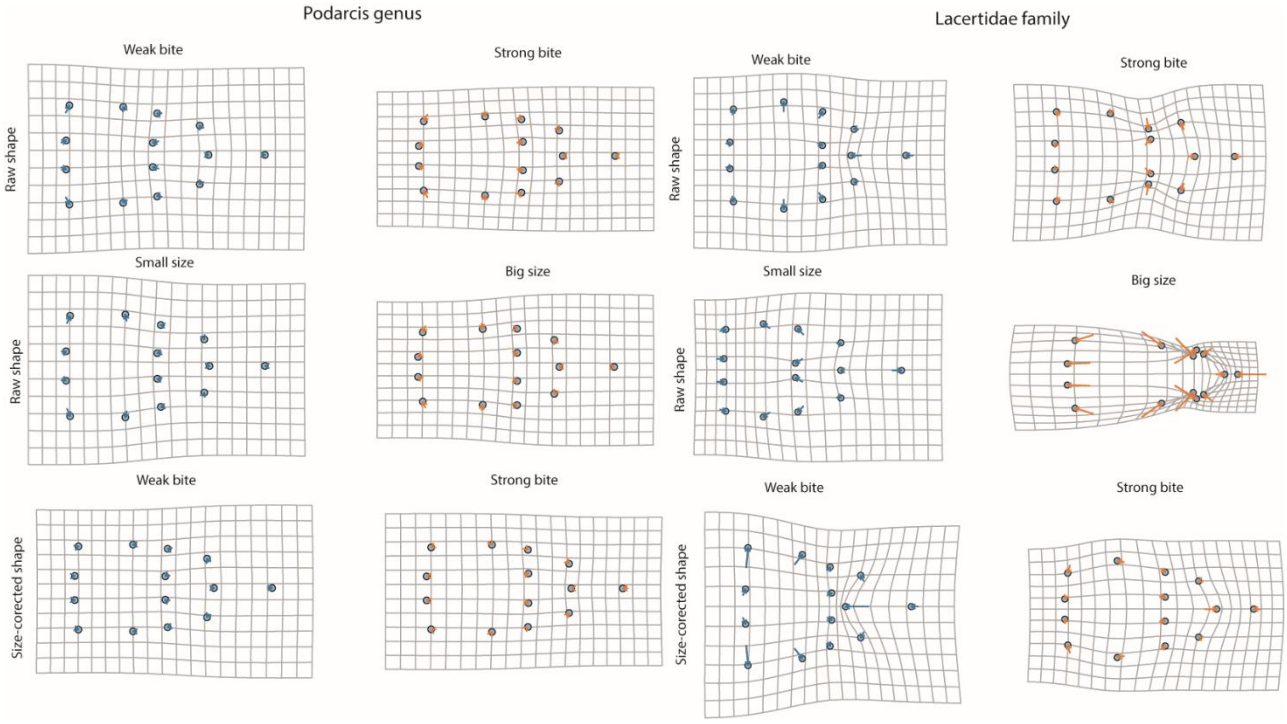

Figure S5.2. Deformation grids (3x) of dorsal shape showing the different biological scales, and with different data.

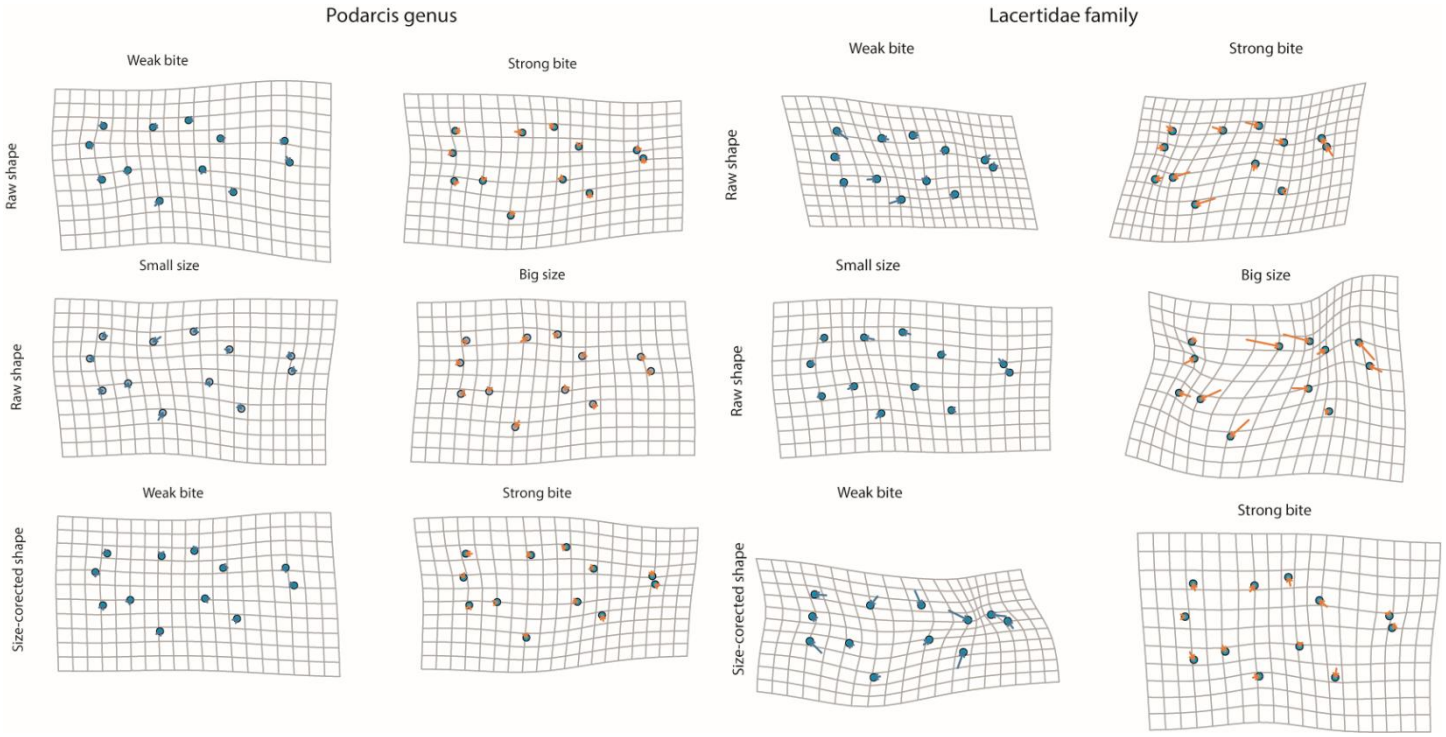

Figure S5.3. Deformation grids (3x) of lateral shape showing the different biological scales and with different data.

Table S5.10. Comparison of form-function slopes for head shape relative to bite force across biological levels. Slopes were estimated using raw dorsal shape data. Individual-level regressions for each *Podarcis* species were compared to genus- and family-level trends by calculating angular differences in morphospace, with significance assessed via permutation tests (999 iterations) following RRPP procedures. Angle deg: represents the observed angle between species and genus/family; Z score; p-value (at α = 0.05) are highlighted in bold.

Species	Individual vs genus			Individual vs family		
	angle deg	**Z**	**p value**	**angle deg**	**Z**	**p value**
Podarcis bocagei	52.052	-0.404	0.650	85.491	0.016	0.498
Podarcis carbonelli	119.729	0.416	0.339	81.519	-0.257	0.577
Podarcis cretensis	116.615	0.165	0.440	82.852	-0.053	0.533
Podarcis erhardii	107.665	0.182	0.428	93.514	0.083	0.478
Podarcis filfolensis	98.019	0.072	0.478	95.031	0.138	0.476
Podarcis gaigeae	73.633	-0.199	0.577	52.484	-0.804	0.771
Podarcis guadarramae	66.711	-0.169	0.561	53.947	-0.567	0.675
Podarcis hispanicus	92.231	0.063	0.470	91.611	0.001	0.489
Podarcis ionicus	96.903	0.006	0.491	61.631	-0.864	0.795
Podarcis lilfordi	73.104	-0.163	0.559	73.901	-0.219	0.552
Podarcis liolepis	86.192	-0.039	0.514	77.268	-0.326	0.605
Podarcis melisellensis	96.474	0.150	0.454	115.122	0.584	0.287
Podarcis milensis	84.624	-0.026	0.514	76.307	-0.235	0.571
Podarcis muralis	53.388	-0.305	0.614	70.497	-0.185	0.548
Podarcis peloponnesiacus	57.292	-0.435	0.672	56.940	-0.508	0.652
Podarcis pityusensis	72.861	-0.177	0.567	90.802	0.070	0.476
Podarcis siculus	105.802	0.168	0.449	74.624	-0.458	0.666
Podarcis tauricus	78.534	-0.086	0.519	53.738	-1.038	0.855
Podarcis tiliguerta	60.848	-0.272	0.593	51.040	-0.793	0.781
Podarcis vaucheri	89.939	0.015	0.492	77.333	-0.229	0.571
Podarcis virescens	94.682	0.064	0.482	123.890	0.914	0.189
Podarcis waglerianus	63.291	-0.189	0.561	91.138	0.081	0.477

Table S5.11. Comparison of form-function slopes for head shape relative to bite force across biological levels. Slopes were estimated using raw lateral shape data. Individual-level regressions for each *Podarcis* species were compared to genus- and family-level trends by calculating angular differences in morphospace, with significance assessed via permutation tests (999 iterations) following RRPP procedures. Angle deg: represents the observed angle between species and genus/family; Z score; p-value (at α = 0.05) are highlighted in bold.

Species	Individual's vs genus			Individual's vs family		
	angle deg	**Z**	**p value**	**angle deg**	**Z**	**p value**
Podarcis bocagei	57.369	-0.851	0.791	43.310	-1.939	0.980
Podarcis carbonelli	115.737	0.732	0.243	125.951	0.893	0.194
Podarcis cretensis	63.120	-0.423	0.656	88.815	-0.043	0.513
Podarcis erhardii	88.659	-0.005	0.509	121.661	0.517	0.327
Podarcis filfolensis	122.919	0.846	0.201	135.783	1.350	0.083
Podarcis gaigeae	114.359	0.755	0.231	119.071	1.025	0.159
Podarcis guadarramae	85.754	-0.038	0.517	104.187	0.430	0.338
Podarcis hispanicus	98.543	0.273	0.400	116.745	0.649	0.258
Podarcis ionicus	118.128	0.807	0.220	117.734	0.983	0.161
Podarcis lilfordi	62.492	-1.384	0.910	74.539	-0.134	0.551
Podarcis liolepis	101.418	0.410	0.343	121.976	0.894	0.196
Podarcis melisellensis	126.013	0.868	0.208	148.851	2.177	**0.011**
Podarcis milensis	112.302	0.805	0.236	126.233	1.302	0.099
Podarcis muralis	110.635	0.690	0.258	123.807	1.148	0.120
Podarcis peloponnesiacus	75.617	-0.496	0.683	101.737	0.202	0.432
Podarcis pityusensis	87.988	0.080	0.477	87.367	-0.093	0.528
Podarcis siculus	53.111	-1.199	0.876	48.710	-1.280	0.901
Podarcis tauricus	106.646	0.675	0.260	124.605	1.515	0.064
Podarcis tiliguerta	110.912	0.607	0.268	140.291	1.685	0.042
Podarcis vaucheri	124.356	0.747	0.249	122.973	1.089	0.140
Podarcis virescens	114.698	0.787	0.230	110.625	0.696	0.234
Podarcis waglerianus	79.401	-0.205	0.575	94.242	0.038	0.487

Table S5.12. Comparison of form-function slopes for head shape relative to bite force across biological levels. Slopes were estimated using allometric-corrected dorsal shape data. Individual-level regressions for each *Podarcis* species were compared to genus- and family-level trends by calculating angular differences in morphospace, with significance assessed via permutation tests (999 iterations) following RRPP procedures. Angle deg: represents the observed angle between species and genus/family; Z score; p-value (at α = 0.05) are highlighted in bold.

Species	Individual's vs genus			Individual's vs family		
	angle deg	**Z**	**p value**	**angle deg**	**Z**	**p value**
Podarcis bocagei	87.386	-0.096	0.525	78.578	-0.191	0.592
Podarcis carbonelli	126.791	0.455	0.347	104.203	0.095	0.478
Podarcis cretensis	140.570	1.004	0.174	98.413	0.072	0.481
Podarcis erhardii	90.983	0.076	0.469	60.545	-0.400	0.644
Podarcis filfolensis	118.364	0.448	0.364	137.371	0.356	0.399
Podarcis gaigeae	121.870	0.466	0.335	79.404	-0.122	0.537
Podarcis guadarramae	43.984	-0.723	0.768	78.157	-0.089	0.531
Podarcis hispanicus	65.595	-0.349	0.634	112.043	0.330	0.376
Podarcis ionicus	120.455	0.586	0.295	114.018	0.333	0.360
Podarcis lilfordi	81.709	-0.092	0.529	101.590	0.046	0.485
Podarcis liolepis	89.245	0.031	0.489	117.531	0.620	0.261
Podarcis melisellensis	84.423	-0.073	0.540	119.565	0.724	0.221
Podarcis milensis	123.440	0.426	0.353	131.631	0.329	0.406
Podarcis muralis	127.457	0.642	0.270	123.050	0.550	0.310
Podarcis peloponnesiacus	99.581	0.129	0.462	66.866	-0.383	0.650
Podarcis pityusensis	75.405	-0.243	0.586	125.457	0.411	0.340
Podarcis siculus	117.742	0.399	0.366	101.352	0.057	0.486
Podarcis tauricus	62.731	-0.493	0.678	101.611	0.105	0.466
Podarcis tiliguerta	113.024	0.283	0.400	84.103	-0.149	0.560
Podarcis vaucheri	64.586	-0.328	0.645	119.224	0.278	0.408
Podarcis virescens	70.081	-0.346	0.625	99.733	0.109	0.450
Podarcis waglerianus	90.151	0.008	0.499	119.241	0.484	0.323

Table S5.13. Comparison of form-function slopes for head shape relative to bite force across biological levels. Slopes were estimated using allometric-corrected lateral shape data. Individual-level regressions for each *Podarcis* species were compared to genus- and family-level trends by calculating angular differences in morphospace, with significance assessed via permutation tests (999 iterations) following RRPP procedures. Angle deg: represents the observed angle between species and genus/family; Z score; p-value (at α = 0.05) are highlighted in bold.

Species	Individual's vs genus			Individual's vs family		
	angle deg	**Z**	**p value**	**angle deg**	**Z**	**p value**
Podarcis bocagei	81.519	-0.248	0.603	109.317	0.324	0.388
Podarcis carbonelli	97.643	0.212	0.409	63.591	-0.720	0.758
Podarcis cretensis	73.496	-0.252	0.589	67.073	-0.481	0.683
Podarcis erhardii	76.463	-0.260	0.593	56.989	-0.742	0.773
Podarcis filfolensis	104.901	0.439	0.327	84.164	-0.099	0.523
Podarcis gaigeae	94.412	0.179	0.436	85.176	-0.094	0.547
Podarcis guadarramae	64.474	-0.719	0.764	94.240	0.056	0.485
Podarcis hispanicus	73.619	-0.333	0.628	67.661	-0.420	0.666
Podarcis ionicus	103.781	0.483	0.314	87.423	-0.045	0.528
Podarcis lilfordi	70.751	-0.801	0.781	84.842	-0.091	0.541
Podarcis liolepis	76.000	-0.386	0.653	85.237	-0.073	0.532
Podarcis melisellensis	96.322	0.156	0.441	76.388	-0.175	0.572
Podarcis milensis	125.430	1.844	**0.033**	90.789	-0.046	0.518
Podarcis muralis	128.959	1.578	0.056	80.627	-0.242	0.582
Podarcis peloponnesiacus	67.374	-0.694	0.750	105.641	0.133	0.471
Podarcis pityusensis	94.145	0.080	0.491	71.971	-0.364	0.653
Podarcis siculus	90.440	0.022	0.495	81.189	-0.215	0.574
Podarcis tauricus	94.021	0.087	0.468	73.900	-0.621	0.728
Podarcis tiliguerta	92.667	0.142	0.442	66.746	-0.416	0.648
Podarcis vaucheri	105.260	0.272	0.393	80.409	-0.204	0.582
Podarcis virescens	80.215	-0.286	0.598	77.444	-0.308	0.622
Podarcis waglerianus	97.284	0.176	0.451	74.461	-0.318	0.642

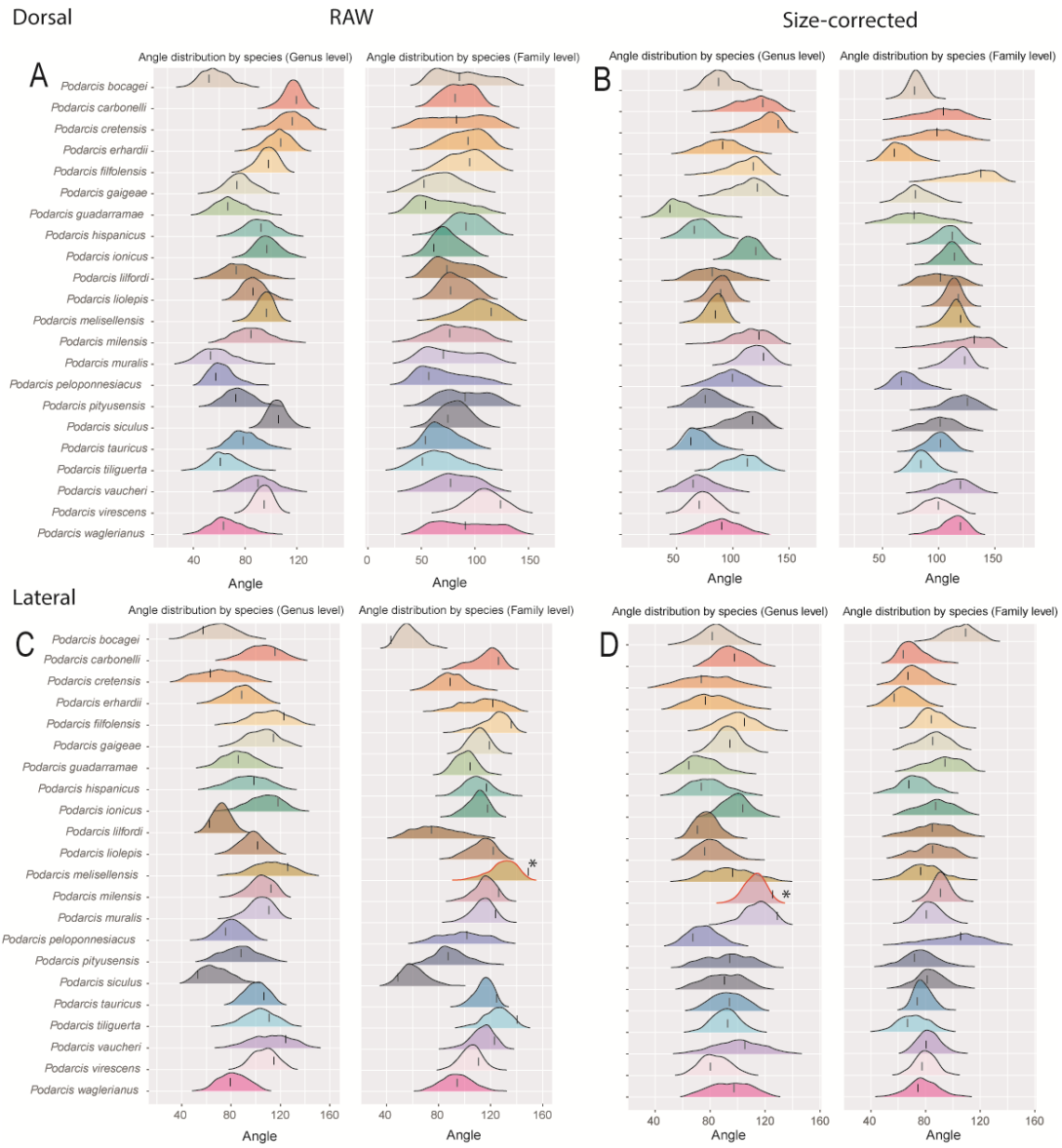

Figure S5.4. Graphic representation of the null distributions of pairwise angular differences among regression vectors, with observed mean angles indicated by dashed lines; red outlines and asterisks denote significant departures from random expectations. A: Dorsal raw data. B: Dorsal allometric corrected data. C: Lateral raw data. D: Lateral allometric corrected data.